

Simultaneous Binding and Toughening Concept for
an Efficient and Qualified Manufacturing of
Textile Reinforced pCBT Composites

D i s s e r t a t i o n

to be awarded the degree
Doctor of Engineering (Dr.-Ing.)

submitted by

M.Sc. Wangqing Wu
from Anhui, P.R.China

approved by the Faculty of Natural and Materials Science
Clausthal University of Technology

Date of oral examination

25.07.2013

Chairperson of the Board of Examiners:

Prof. Dr. rer. nat. Albrecht Wolter

Chief Reviewer:

Prof. Dr.-Ing. Gerhard Ziegmann

Reviewer:

Prof. Dr. rer. nat. Alfred Weber

Reviewer:

Prof. Dr. Bingyan Jiang

School of Aeronautics and Astronautics

Central South University, Changsha, P.R.China

Eidesstattliche Erklärung

Hiermit erkläre ich an Eides Statt, dass ich die bei der Fakultät für Natur- und Materialwissenschaften der Technischen Universität Clausthal eingereichte Dissertation selbständig und ohne unerlaubte Hilfe verfasst und die benutzten Hilfsmittel vollständig angegeben habe.

Clausthal-Zellerfeld, den

Wangqing Wu

Eidesstattliche Erklärung

Hiermit erkläre ich an Eides Statt, dass die eingereichte Dissertation weder in Teilen noch in Ihrer Gesamtheit einer anderen Hochschule zur Begutachtung vorliegt oder vorgelegen hat und dass ich bisher noch keinen Promotionsversuch unternommen habe.

Clausthal-Zellerfeld, den

Wangqing Wu

Acknowledgment

I would like to express my sincere gratitude to all the colleagues, friends and my family who supported, encouraged and guided me through all the duration of my doctoral research and study in Institute of Polymer Materials and Plastics Engineering, Clausthal University of Technology, Germany.

Especially, I would like to express my deepest gratitude to my advisor, Prof. Dr.-Ing. Gerhard Ziegmann, for his constant guidance and encouragement throughout my graduate studies, as well as, Prof. Dr. rer. nat. Alfred Weber and Prof. Dr. Bingyan Jiang, for their constructive suggestions and insightful comments. I would like to extend the thanks to Prof. Dr. rer. nat. Albrecht Wolter for serving as the chairperson of my promotion commission.

I am also really appreciated for the invaluable helps and supports from all the scientific and technical co-workers in the institute. Special thanks go to Dr.-Ing. Lei Xie, Dr.-Ing. Florian Klunker, Dr.-Ing. Stefan Kirchberg, Dr.sc.nat. Leif Steuernagel, Dipl.-Wirt.-Ing. David Christian Berg, Dipl.-Ing. Matthias Dickert, Dipl.-Ing. Santiago Aranda, Dipl.-Ing. Widyanto Surjoseputro, M.Sc. Dilmurat Abliz, Dipl.-Ing. Sonja Niemeyer, Dipl.-Ing. Janina Reimers, Dipl.-Ing. (FH) Tamara Florian, Dipl.-Ing. Paula Brunotte, etc. for the many interesting discussions and for their friendship and support in the years that I have come to know them at the Clausthal University of Technology. It is my great pleasure that I have such a chance to be able to work together with those wonderful persons. Without their support, this dissertation cannot be finished so smoothly.

Many thanks also go to Mr. Tim Blackmore and Mr. Andriy Tymoshenko from Cyclics Europe GmbH for supplying research materials and the state-of-art information about the CBT[®] Technology in the Europe market. The companies DOW Chemicals Germany and Arkema France are appreciated for kindly supporting the impact modifier system. Thanks would like to be given further to Mrs. Dröttboom for the extensive thermal and rheological analysis and Mr. Reinhard Görke from Institute of Nonmetallic Materials for SEM test. I would also like to thank the ma-

ny talented student members in Institute who I was fortunate enough to supervise: Qiang Lei, Hailin Sun, Tianxiao Yu, Jing Guo, Zhe liu, Chao Liu, Songshan Gao, Wenzheng Liang and Qinxin Li (Clausthal University of Technology); Jehad El-Demellawi (Ain Shams University, Cairo); Fernando Pitelli do Nascimento (University of Sao Paulo); Vincent Antonie, Christophe Piedagnel and Matthieu Demoulin (Institute of Materials and Advanced Mechanics (ISMANS), France)

In addition, I want to thank the financial support from Chinese Scholarship Council (CSC) and Forschungskuratorium Textil (FKT). A word of thanks also goes to the Institute of Textile Technology RWTH Aachen for supplying the textile reinforcement in the frame of scientific research project DFG-AiF-Cluster Leichtbau und Textilien". The co-workers, especially Ms. Lianping Huang, in the department of education of the Chinese Embassy in the Federal Republic of Germany are greatly appreciated for their considerate help and support during my stay in Germany.

Last but not least I would like to express my deepest gratitude especially to my parents and my sister for their always supports and encouragements. My wife Ms. Wenjuan Hu owns my greatest appreciation for her unconditional support during the PhD study.

Thanks every one,

Wangqing Wu

May 2013, Clausthal-Zellerfeld, Germany

Abstract

In situ polymerization of Cyclic Butylene Terephthalate (CBT) is a new and promising manufacturing technology developed for production of textile reinforced thermoplastics in Liquid Composite Molding (LCM) processes such as Thermoplastic Vacuum Assisted Resin Infusion (T-VARI). The application of in-situ polymerized CBT (pCBT), however, is greatly impeded due to the relatively high brittleness of pCBT from isothermal polymerization and crystallization. Therefore, in this dissertation, a new concept consisting of binding and toughening has been proposed for an efficient and qualified manufacturing of textile reinforced pCBT composites. Specifically, textile preforms with preforming binder are prepared for enhanced handling stability and improved process efficiency. After impregnation of the bindered textile preforms with liquid catalyzed CBT oligomers melt, the textile reinforced pCBT composites were manufactured successfully under isothermal conditions. The unique of this process is that the textile reinforced pCBT composites can be efficiently manufactured and qualifiedly toughened simultaneously due to the applied preforming binder. In the present dissertation, research emphasis have been put on the following three key aspects: (1) Materials characterization focusing on the effect of preforming binder on the material behavior of textile preforms and catalyzed CBT oligomers; (2) Process development including T-VARI manufacturing process and single factor analysis on the process parameters; and (3) Process optimization in terms of the performance of various preforming binders and the toughening concept. The results from the material characterization indicate that the material properties, e.g. the compaction behavior of bindered textile preforms as well as the thermal and rheological properties of the catalyzed CBT oligomers, were significantly influenced due to the presence of the preforming binder. Based on the results of material characterization, T-VARI manufacturing process has been developed successfully for production of textile reinforced pCBT composites. The composite laminates manufactured according to the proposed concept results a great improvement of flexural strain at break and flexural strength without impairing other flexural properties such as flexural modulus, indicating a very good toughening potential of the proposed concept for textile reinforced pCBT composites. According to the single factor analysis of the production process, it was con-

firmed that the process parameters including catalyst amount, preforming binder, processing temperature and vacuum pressure have significant influences on the flexural properties of the textile reinforced pCBT composite. Furthermore, to assess the toughening performance of various preforming binders, inter-laminar fracture properties of textile reinforced pCBT composite were investigated under mode I and mode II deformation. A standard Double Cantilever Beam (DCB) test and an End Notched Flexure (ENF) test based on a three-point bending test were applied to evaluate the inter-laminar fracture toughness in mode I and mode II respectively. The effect of binder type, filling content and toughening concept on the fracture properties under the mentioned two deformation modes were discussed on the basis of morphology analysis of fracture sections with Scanning Electron Microscopy. By comparison, the preforming binder, which is based on the acrylic toughening agent, is the optimum in terms of inter-laminar fracture properties and flexural properties. The results obtained illustrate that the toughening of textile reinforced pCBT composites has been successfully achieved with simultaneously improved process efficiency by introducing simultaneous binding and toughening concept.

Keywords: Textile Reinforced Thermoplastics; Binded Textile Preforms; Cyclic Butylene Terephthalate; Polymerization and Crystallization; Toughening; Fracture Toughness; Flexural Properties

Zusammenfassung

Die in-situ-Polymerisation von Cyclic Butylene Terephthalat (CBT) ist eine neue und vielversprechende Fertigungstechnologie für die Herstellung von textilverstärkten Thermoplasten durch Liquid Composite Molding (LCM) Prozesse, wie z.B. Thermoplastic Vacuum Assisted Resin Infusion (T-VARI). Ein erheblicher Nachteil bei der Applikation von in-situ polymerisiertem CBT (pCBT) ist die relativ hohe Sprödigkeit nach der isothermen Polymerisation und Kristallisation. Daher wurde in dieser Doktorarbeit ein neues Fertigungskonzept einschließlich Bebindung und Schlagzähmodifizierung für eine effiziente und qualifizierte Fertigung von textilverstärkten pCBT-Komposite konzipiert. Zunächst wird durch Bebindung der Textilien eine verbesserte Preformhandhabung und erhöhte Prozesseffizienz erzielt. Bei der anschließenden Imprägnierung der bebinderten Textilpreforms wird durch den Binder gleichzeitig deutliche Erhöhung der Schlagzähmodifizierung von textilverstärkten pCBT bei Schubbeanspruchung erreicht. In der vorliegenden Arbeit wurden die folgenden drei Aspekte betrachtet: (1) Materialcharakterisierung mit Fokus auf den Einfluss von Binder auf das Materialverhalten von textilen Preforms und katalysierten CBT Oligomeren; (2) Prozessentwicklung einschließlich T-VARI Fertigungsverfahren und parametrische Analyse der Verarbeitungsbedingungen; und (3) Prozessoptimierung im Hinblick auf die Leistungsfähigkeit verschiedener Binder und das Fertigungskonzept. Die Ergebnisse aus den Materialcharakterisierungen zeigen, dass die Anwesenheit des Binders einen signifikanten Einfluss auf die Materialeigenschaften, wie z.B. das Kompaktierungsverhalten von bebinderten Textilpreforms sowie die thermischen und rheologischen Eigenschaften der katalysierten CBT Oligomer, hat. Basierend auf den Ergebnissen der Materialcharakterisierung wurde das T-VARI Fertigungsverfahren erfolgreich für die Fertigung von textilverstärkten pCBT-Kompositen entwickelt. Die mit dem vorgeschlagenen Fertigungskonzept hergestellten Kompositlamine zeichnen sich durch eine deutliche Verbesserung der Biegebruchdehnung und Biegefestigkeit ohne Beeinträchtigung anderer mechanischen Eigenschaften, wie z.B. Biegesteifigkeit, aus. Hierdurch konnte ein sehr hohes Schlagzähmodifizierungspotential der textilverstärkten pCBT-Komposite nachgewiesen werden. Durch die Einzelfaktor-Analyse des o.g. Herstellungsverfahrens wurde bestätigt, dass die Prozessparameter Kataly-

satormenge, Binder, Verarbeitungstemperatur und Vakuum einen signifikanten Einfluss auf die Biegeeigenschaften der textilverstärkten pCBT-Komposite haben. Ferner wurde die interlaminare Bruchzähigkeit der textilverstärkten pCBT-Komposite unter Mode I und Mode II untersucht, um die Leistungsfähigkeit verschiedener Binder hinsichtlich der Schlagzähmodifizierung zu beurteilen. Ein standardisierter Double-Cantilever-Beam (DCB) Test und ein End-Notched-Flexure (ENF) Test auf Basis einer Drei-Punkt-Biegung wurden durchgeführt, um jeweils die interlaminare Bruchzähigkeit in Mode I und Mode II auszuwerten. Der Einfluss von Bindertyp, Füllgrad und Fertigungskonzept auf die Bruchzähigkeiten wurde unter den o.g. Deformationsmodi mittels Morphologieanalyse der Bruchfläche anhand Raster-Elektronenmikroskopie diskutiert. Im Vergleich zeigt der Binder mit acrylischem Schlagzähmodifikator die beste Performance hinsichtlich interlaminarer Bruchzähigkeiten und Biegeeigenschaften. Die erzielten Ergebnisse zeigen, dass die Schlagzähmodifizierung der textilverstärkten pCBT-Komposite bei gleichzeitig erhöhter Prozesseffizienz durch das simultane Bebinderungs- und Schlagzähmodifizierungskonzept erfolgreich umgesetzt werden konnte.

Stichwörter: textilverstärkte Thermoplaste; bebinderte Textilpreforms; Cyclic Butylene Terephthalate; Polymerisation und Kristallisation; Schlagzähmodifizierung; Bruchzähigkeit; Biegeeigenschaften.

Contents

List of Tables	xv
List of Figures	xvii
Nomenclature	xxiii
1 Introduction	1
1.1 Background	1
1.1.1 CBT technology for textile reinforced thermoplastics	4
1.1.2 Binding technology for automated textile preforming	7
1.2 Motivation	9
1.3 State of the science, research and technology	11
1.3.1 Processing of textile reinforced thermoplastics	11
1.3.2 Toughening of in-situ polymerized pCBT composites	20
1.3.3 Toughening concept for thermosets resin composites	22
1.4 Problem statement	24
1.5 Research objectives	26
1.6 Organization of the dissertation	27
2 Theoretical background and characterization techniques	31
2.1 Reactive processing of textile reinforced thermoplastics	31
2.1.1 Polymerization reaction	31
2.1.2 Reactive processing of pCBT	33

2.1.3	Processing characteristics	34
2.1.4	Crystallization structures of thermoplastics	36
2.1.5	Toughening mechanisms	38
2.2	Thermal and rheological analysis of matrix system	41
2.2.1	Differential Scanning Calorimetry (DSC)	42
2.2.2	Thermogravimetric Analysis (TGA)	43
2.2.3	Dynamic Mechanical Analysis (DMA)	45
2.2.4	Rheological analysis	46
3	Materials and methodology	49
3.1	Materials	49
3.1.1	Textile	49
3.1.2	Matrix systems	51
3.1.3	Preforming binders	52
3.2	Methodology for key aspect I: Characterization of the processing materials	54
3.2.1	Compaction behavior of bindered textile preforms	54
3.2.2	Thermal and rheological properties of processing materials	63
3.3	Methodology for key aspect II: Development of the manufacturing process	66
3.3.1	Thermoplastic Vacuum Assisted Resin Infusion (T-VARI)	66
3.3.2	Thermal and mechanical behavior of composite system	67
3.3.3	Simultaneous binding and toughening concept	68
3.3.4	Influence of process parameters	71
3.4	Methodology for key aspect III: Optimization of the manufacturing process	72
3.4.1	Influence of preforming binders and toughening concepts	72
3.4.2	Verification and further optimization trials	79
4	Key aspect I: Characterization of the processing materials	81
4.1	Compaction behavior of bindered textile preforms	83
4.1.1	Fiber Volume Fraction (FVF)	83
4.1.2	Residual Preform Thickness (RPT)	91
4.1.3	Significant sequence analysis	99

4.1.4	Verification experiments	100
4.2	Thermal and rheological behavior of matrix system	102
4.2.1	Conversion rate analysis	102
4.2.2	Melting and crystallization analysis	106
4.2.3	Thermal stability analysis	120
4.2.4	Rheological analysis	122
5	Key aspect II: Development of the manufacturing process	129
5.1	Realization of the manufacturing concept	131
5.1.1	Thermoplastic Vacuum Assisted Resin Infusion (T-VARI) . .	131
5.1.2	Characterization of the manufactured pCBT composites . . .	133
5.1.3	Simultaneous binding and toughening concept	138
5.2	Influence of process parameters	142
5.2.1	Analysis of related process parameters	142
5.2.2	Effect of catalyst amount	148
5.2.3	Effect of binder content	150
5.2.4	Effect of processing temperature	151
5.2.5	Effect of vacuum pressure	153
6	Key aspect III: Optimization of the manufacturing process	155
6.1	Mode I inter-lamianr fracture properties	157
6.1.1	Effect of binder type and filling content	157
6.1.2	Fracture morphology of mode I deformation	165
6.2	Mode II inter-laminar fracture properties	170
6.2.1	Effect of binder filling content	170
6.2.2	Fracture morphology of mode II deformation	175
6.3	Verification experiments	180
6.3.1	Verification of the optimized preforming binder	180
6.3.2	Further optimization trials	182
7	Conclusions and future work	187
7.1	Conclusions	187
7.2	Future works	191

A Curriculum Vitae	195
---------------------------	------------

Bibliography	197
---------------------	------------

List of Tables

1.1	Comparison of glass fiber-reinforced laminated based on pCBT and PA6 [30]	4
1.2	Typical physical and mechanical properties of representative unreinforced thermoplastic polymers used in structural applications (adapted from [102]	14
2.1	Mechanical properties of injection mold PBT with various mold temperatures [116]	41
3.1	Effect of different catalysts on the pot life time and polymerization time of CBT500 [27].	53
3.2	Compaction and preforming parameters used in the experiments . .	62
3.3	Experimental design using the L_{16} orthogonal array	63
3.4	Dimension of DCB and ENF specimens	73
4.1	Experimental results for FVF	84
4.2	Response table mean signal-to-noise (S/N) ratio for FVF factor and significant interaction	85
4.3	Experimental results for RPT	91
4.4	Response table mean signal-to-noise (S/N) ratio for RPT factor and significant interaction	92
4.5	Results of ANOVA for FVF	99
4.6	Results of ANOVA for RPT	100

4.7	Results of the confirmation experiment for FVF	101
4.8	Results of the confirmation experiment for RPT	101
4.9	Effect of binder on the thermal transition parameters of CBT500 (Catalyzed with FASCAT4102)	114
4.10	The physical interpretation of the Avrami parameters for different crystallization mechanisms of polymers [37, 87]	117
5.1	Effect of simultaneous binding and toughening concept on the flex- ural properties of textile reinforced pCBT composite	140
5.2	Process parameters for single factor experiment analysis	148
5.3	Effect of catalyst amount on the flexural properties of textile rein- forced pCBT composite	149
5.4	Effect of binder content on the flexural properties of textile rein- forced pCBT composite	151
5.5	Effect of processing temperature on the flexural properties of textile reinforced pCBT composite	152
5.6	Effect of vacuum pressure on the flexural properties of textile rein- forced pCBT composite	154
6.1	Effect of binder type on the flexural properties of textile reinforced pCBT composite	181
6.2	Effect of PARALOID® binder content on the flexural properties of textile reinforced pCBT composite	182
6.3	Effect of simultaneous binding and toughening concept variants on the flexural properties of textile reinforced pCBT composite	184

List of Figures

1.1	CBT granulate [30]	5
1.2	Principle of CBT technology	6
1.3	Instantaneous crystallization vs. consecutive crystallization	7
1.4	Auto-preforms concept [38]	9
1.5	Simultaneous binding and toughening concept	10
1.6	Material forms of thermoplastic composites [102]	12
1.7	Ability of thermoplastic to elongate and absorb energy [102]	12
1.8	Effect of cooling path on the mechanical properties of pCBT composites [9]	21
1.9	Effect of addition of carbon nanotubes on the mechanical properties of pCBT composites [11]	22
1.10	Ex-situ concept for composites toughening [47]	24
1.11	RTM processing with integrated ex-situ toughening [60]: (a) insertion of a TP film in between fiber plies, (b) dissolution of the TP film and polymerization process and (c) generation of a TP-dispersed phase from a reaction-induced phase separation and final curing of the epoxy matrix	25
1.12	Solution strategy and organization of this dissertation	29
2.1	Ring-opening polymerization of PBT [75]	34
2.2	The arrangement of molecular chains in amorphous and semi-crystalline polymers [55]	36

2.3	Overview of organizational level in semi-crystalline polymers [115]	37
2.4	Schematic representation of the DSC curve with the appearance of several common transitions	43
2.5	Schematic representation of the TGA curve and the method of evaluation of T_d	44
2.6	Schematic representation of the DMA curve	46
2.7	Measurement of the viscosity of a polymerizing thermoplastic prepolymer	47
3.1	PANEX 35 uni-directional fabrics	50
3.2	Saertex $\pm 45^\circ$ bi-axial carbon fiber non crimp fabric	50
3.3	Tri-axial glass fiber non crimp fabric	50
3.4	Effect of catalyst and reaction temperature on the reaction time of CBT500 [27]	52
3.5	Molecular structure of the various catalysts for CBT oligomers: (I) FASCAT4101, (II) TEGOCAT 256 and (III) FASCAT4102	53
3.6	Lab based binding process	56
3.7	Compression test	57
3.8	Typical compression procedure	58
3.9	Typical stress-strain curves during three point bending test, where σ_f is the flexural stress, ϵ_f is the flexural strain, σ_{fM} is the flexural strength, σ_{fB} is the flexural stress at break, σ_{fC} is the flexural stress at 5 % strain limit. ϵ_{fM} is the flexural strain corresponding to flexural strength, ϵ_{fB} is the flexural strain at break [8].	70
3.10	Mode I and mode II specimens	73
3.11	Modified compliance calibration	75
3.12	Load displacement trace from the DCB test	76
3.13	Thin binder film made from LOTADEL [®] AX8900 granulate prepared by compression molding	78
4.1	Solution strategy: Cornerstone	82
4.2	Comparison of actual and predicted S/N ratios of FVF using regression analysis	85

4.3	Comparison of residual and predicted S/N ratios of FVF using regression analysis	86
4.4	Effect of compaction temperature on the FVF	86
4.5	Fitting of compaction curve of textile preforms with three parameters power law model	88
4.6	Fitting of compaction curve of bindered textile preforms at room temperature (25 °C) with proposed model	88
4.7	Fitting of compaction curve of bindered textile preforms at elevated temperatures with proposed model	89
4.8	Comparison of actual and predicted S/N ratios of RPT using regression analysis	92
4.9	Comparison of residual and predicted S/N ratios of RPT using regression analysis	93
4.10	Effect of compaction temperature on the RPT	94
4.11	Weight Change of both fabric layers after compression at 190 °C and burn down at 500 °C	95
4.12	Fitting of release curve of bindered textile preforms	95
4.13	Comparison of the RPT from the experiment and the model	96
4.14	Surfaces morphology of the resultants from CBT500 and CBT160	104
4.15	Effect of catalyst amount on the conversion rate of CBT500 comparison with CBT160 at 190 °C	105
4.16	Effect of polymerization temperature on the conversion rate of CBT160	105
4.17	Typical DSC heating and cooling trace of CBT500 without any catalyst	106
4.18	Polymerization and crystallization behavior of CBT500 (Catalyzed with FASCAT4102) and CBT160	111
4.19	PLM morphology of pCBT crystallized at 195 °C shows inner positive/outer negative spherulites (circled) and boundary crystals (pointed by arrow) [108]. (a) image with quartz plate, (b) image without quartz plate.	112
4.20	Effect of preforming binder on the melting and crystallization behavior of FASCAT4102 catalyzed CBT500	113

4.21	Effect of preforming binder on the simultaneous polymerization and crystallization of FASCAT4102 catalyzed CBT500 at 190 °C	116
4.22	An Avrami plot for the simultaneous polymerization and crystallization of CBT500 (Catalyzed with FASCAT4102)	118
4.23	Effect of binder on the relative crystallinity of FASCAT4102 catalyzed CBT500 during simultaneous polymerization and crystallization	119
4.24	Instantaneous variation of Avrami exponent n value for FASCAT4102 catalyzed CBT500 at 190 °C	120
4.25	Dynamic thermal stability of processing materials	121
4.26	Thermal stability of processing materials at isothermal processing temperature	122
4.27	Typical viscosity variation behavior of CBT500 during isothermal processing conditions	123
4.28	Effect of binder on the processing time of CBT500 with various catalysts	124
5.1	Solution strategy: First milestone	130
5.2	Development of T-VARI processing system	132
5.3	Melting behavior of unidirectional carbon fiber reinforced pCBT laminate	133
5.4	Thermal stability of unidirectional carbon fiber reinforced pCBT laminate	134
5.5	Dynamic mechanical properties of a bi-axial carbon fiber fabric reinforced pCBT laminate	135
5.6	Impregnation quality of unidirectional carbon fiber reinforced pCBT laminate	137
5.7	Typical flexural stress-strain relations of textile reinforced pCBT laminate prepared with simultaneous binding and toughening concept	139
5.8	Various preforming binder states under different activation temperatures according to Dickert et al. [29]	141
5.9	Schematic description of the influence of preforming binder on the matrix system, textile preforms and manufacturing process	143

5.10 Thermoplastic fleece binder [5]	145
5.11 Influence of binder on the dynamic mechanical properties of textile reinforced pCBT laminate	146
6.1 Solution strategy: Second milestone	156
6.2 Load displacement trace from DCB test	157
6.3 The final mode I fracture toughness and thickness of all the tested specimens	159
6.4 Relation between mode I fracture toughness and the increment of crack length for textile reinforced reference laminate	161
6.4 Relation between mode I fracture toughness and the increment of crack length for textile reinforced reference laminate	162
6.5 Effect of binder content on the mode I fracture toughness of textile reinforced pCBT laminate	163
6.6 Effect of the toughening concept on the mode I fracture toughness .	164
6.7 Scanning electron micro-graphs of the fracture surface under mode I loading of textile fiber reinforced pCBT laminates	166
6.7 Scanning electron micro-graphs of the fracture surface under mode I loading of textile fiber reinforced pCBT laminates	167
6.8 Scanning electron micro-graphs of the fracture surface under mode I loading of pCBT/ PARALOID EXL [®] 2314 laminate	168
6.8 Scanning electron micro-graphs of the fracture surface under mode I loading of pCBT/ PARALOID EXL [®] 2314 laminate	169
6.9 Intra-ply delamination behavior of pCBT laminate under mode II deformation	171
6.10 Load vs. displacement curves of textile reinforced pCBT laminate obtained by ENF tests	171
6.11 Effect of binder content on the mode II fracture toughness of textile reinforced pCBT laminate	172
6.12 Effect of the toughening concept on the mode II fracture toughness	173
6.13 Effect of the impregnation length on mode II fracture toughness of in-situ toughened laminate	175

6.14	Scanning electron micro-graphs of the fracture surface under mode II loading of textile fiber reinforced pCBT laminates	176
6.14	Scanning electron micro-graphs of the fracture surface under mode II loading of textile fiber reinforced pCBT laminates	177
6.15	Scanning electron micro-graphs of the fracture surface under mode II loading of pCBT/ PARALOID EXL [®] 2314 laminate	178
6.15	Scanning electron micro-graphs of the fracture surface under mode II loading of pCBT/ PARALOID EXL [®] 2314 laminate	179
7.1	Future works for serial production of high performance textile reinforced pCBT composites	191

Nomenclature

\bar{y}	The average of the observed data
ΔH	Enthalpy of transition
ΔP	Pressure difference
δ_{exp}	Crack opening displacement determined at the loading point
ϵ_f	Flexural strain
ϵ_{fB}	Flexural strain at break
ϵ_{fM}	Flexural strain corresponding to flexural strength
η	Apparent viscosity
η^*	Complex viscosity
ρ_f	Fiber density
σ_B	Brittle strength
σ_e	Effective (deviatoric) stress
σ_{fB}	Flexural stress at break
σ_{fC}	Flexural stress at 5 % strain limit
σ_{fM}	Flexural strength
σ_f	Flexural stress
φ	Porosity

A	Area of the cross section of fiber preforms
a_0	Initial crack length
A_t	Area under the transition curve
A_1	Approximated linear coefficient
A_f	Fabric areal density
b	Width of the specimen
C	Calorimetric constant
c	Initial FVF under 0 compaction pressure
c_b	Binder content
C_d	Compliance of the crack opening displacement
C_e	Compliance in ENF test
D	Deflection of the center-line of the specimen at the middle of the support span
d_n	Constant thickness of discs
DOC	Degree of Conversion
E_1	Flexural modulus of composites
G	Shear modulus of matrix system
g	Crystal growth
G_{13}	Shear modulus of composites
G_∞	Shear modulus of cured/polymerized matrix system
G_{II}	Energy release rate for mode II deformation
G_I	Energy release rate for mode I deformation
h	Depth of the specimen
h_p	Preform thickness
K	Temperature dependent rate constant, $K = K(T)$, reflecting nucleation and growth characteristics

k	Test length
K_p	Permeability
L	Half of support span
l	Flow distance
L_D	Length of DCB specimens
L_E	Length of ENF specimens
L_n	Density of nuclei
l_n	Nucleation rate
m_{pol}	Weight of polymerized portion
m_{tol}	Total weight of the reactant
N	Number of fabric layers
n	Avrami exponent
n_o	The number of observations
P	Applied load at a given point on the load-deflection curve
P_c	Compaction pressure
P_d	Load applied on the end section of the DCB specimen
P_m	Maximum load when the delamination extends from the initial point during ENF test
P_{cont}	Percent contribution
Q	Volume flow rate
r	Constant radius of rods
s	Compaction stiffness index
SS_A	Variation due to factor A
SS_B	Variation due to factor B
SS_e	The error sum of squares
SS_m	The mean sum of squares

SS_T	Total variation
SS_{AB}	Variation due to interaction of factors A and B
t	Impregnation time
T_c	Crystallization Temperature
T_d	Degradation temperature
T_g	Glass transition temperature
T_m	Melting temperature
T_{act}	Binder activation temperature
t_{act}	Binder activation time
T_{comp}	Compaction temperature
t_{gel}	Resin gel time
u	Volume fraction of the stack at unit compaction pressure
v	Apparent velocity
V_f	Fiber Volume Fraction
$X(t)$	Fractional crystallinity at time t
Y	Plastic resistance
y	The observed data
y_i	The i th observation
S/N_{HB}	S/N ratio, larger is the better
S/N_{NB}	S/N ratio, nominal is the best
S/N_{SB}	S/N ratio, smaller is the better
s_y^2	The variance of the observed data
$\widehat{\eta}_{FVF}$	Predicted S/N ratio for FVF
$\widehat{\eta}_{RPT}$	Predicted S/N ratio for RPT
ANOVA	<u>A</u> nalysis of <u>v</u> ariance
APA6	<u>A</u> nionic <u>P</u> olyamide 6

ASTM	American Standard Test Method
BMI	Bismaleimide
CAS	Chemical Abstracts Service
CBT	Cyclic Butylene Terephthalate
CF	Carbon fiber
CL	ϵ - caprolactone
CNT	Carbon Nanotube
COD	Crack Opening Displacement
DCB	Double Cantilever Beam
DMA	Dynamic Mechanical Analysis
DSC	Differential Scanning Calorimetry
ENF	End Notched Flexure
FVF	Fiber Volume Fraction
GF	Glass fiber
GPC	Gel Permeation Chromatography
ILSS	Interlaminar shear strength
LCM	Liquid Composite Molding
LFT	Long fiber reinforced thermoplastics
LL	Lauryllactam
NCF	Non Crimp Fabric
PA	Polyamide
PA12	Polyamide 12
PA6	Polyamide 6
PAEK	Polyaryletherketone
PBT	Polybutyleneterephthalate
pCBT	polymerized Cyclic Butylene Terephthalate

PE	<u>P</u> oly <u>e</u> thylene
PEI	<u>P</u> oly <u>e</u> ster <u>i</u> mi <u>d</u> e
PEKK	<u>P</u> oly <u>e</u> ther <u>k</u> etone <u>k</u> etone
PES	<u>P</u> oly <u>e</u> ther <u>s</u> ulphone
PET	<u>P</u> oly <u>e</u> ther <u>t</u> erephthalate
PP	<u>P</u> olypropylene
PPS	<u>P</u> oly <u>p</u> heylene <u>s</u> ulphide
PU	<u>P</u> oly <u>u</u> rethane
ROP	<u>R</u> ing- <u>o</u> pening polymerization
RPT	<u>R</u> esidual <u>P</u> reform <u>T</u> hickness
RTM	<u>R</u> esin <u>T</u> ransfer <u>M</u> olding
SEM	<u>S</u> canning <u>E</u> lectron <u>M</u> icroscopy
SRIM	<u>S</u> tructural <u>R</u> eaction <u>I</u> njection <u>M</u> olding
T-VARI	<u>T</u> hermoplastic <u>V</u> acuum <u>A</u> ssisted <u>R</u> esin <u>I</u> nfusion
TGA	<u>T</u> hermogravimetric <u>A</u> nalysis
THF	<u>T</u> etrahydro <u>f</u> uran
VARI	<u>V</u> acuum <u>A</u> ssisted <u>R</u> esin <u>I</u> nfusion
VARTM	<u>V</u> acuum <u>A</u> ssisted <u>R</u> esin <u>T</u> ransfer <u>M</u> olding
wf	<u>w</u> eight <u>f</u> raction

Chapter 1

Introduction

In this chapter, scientific background on the composite materials and their manufacturing processes is introduced firstly, focusing on the CBT technology for textile reinforced thermoplastics and binding technology for automated textile preforming. Secondly, the motivation for the proposed solution strategy in this dissertation for an efficient and qualified manufacturing of textile reinforced pCBT composite is explained. Thirdly, the state of science, research and technology related to the proposed solution strategy are discussed for the problem statement. In the end, the research objectives of this dissertation is defined, followed by the organization details of this dissertation.

1.1. Background

Composites materials are engineered materials consisting of two or more constituent materials with significant different physical or chemical properties. The constituents that do not dissolve nor merge into a single material chemically contribute their properties to the unique properties of composites. The mechanical performance of a composite, e.g. the Fiber Reinforced Plastics (FRP), depends greatly on the selection of reinforcement, matrix, manufacturing process and a host of other variables such as Fiber Volume Fraction (FVF) and fiber orientation.

Compared with other conventionally used materials to meet the particular requirements, composites have more flexibility because they can be designed to provide a variety of properties through the selection of appropriate components. Due to these characteristics, composites can be applied to a wide range of industrial applications. Furthermore, the high ratio of stiffness and strength to weight is another great advantage of the fiber reinforced plastic composites. These features make, e.g. carbon fiber composites, very attractive for application in the aerospace, automobile and sporting goods industries.

The widespread growth of composites materials, however, has been stunted due to the higher cost of raw materials such as carbon fibers and production process compared to other materials. One of the common manufacturing method is using prepreg, which is a single ply of textile structure saturated with liquid matrix. Prepreg is stacked as the basic building block, and cured at an elevated temperature in an autoclave while being pressed by vacuum and additional pressure to achieve the desired fiber volume fraction. Then, post-assembly is required to produce an integrated structure. With the use of prepreg, the fiber wetting can be greatly improved because resin infiltration takes place only across one ply [15]. Unfortunately, the total cost of the composites part manufactured with prepreg process is very high due to the significantly increased process time. Hence, the cost can be significantly reduced if the preparation of prepreg or the post-assembly procedure is eliminated.

In this context, Liquid Composite Molding (LCM) processes, which are the methods to inject the liquid resin directly into the fiber preform by hydraulic pressure, can be taken into consideration. The mold, in which the fiber preform is placed, is prepared according to the designed part configuration [86]. By using the mold, it becomes easier to manufacture the complex composites structures in mass production. In addition, a post-assembly process which is otherwise required can be eliminated. Additionally, the process variables must be optimized to satisfy the effective wetting condition and cycle time. For instance, the injection pressure has to be adapted to have an appropriate injection velocity so that lower void fraction can be obtained by equilibrating the wetting in macro- and micro scale [32, 86]. On the other hand, the mold temperature has a close relation to the resin viscosity. Due to the issues of resin viscosity and impregnation, the resin used in LCM processes is

commonly limited to thermoset resins. Those resins are less viscous (Viscosity < 1 Pa s) than thermoplastic melts (Viscosity usually higher than 100 Pa s), and their rheology is more suitable for the proper impregnation requirements.

One of the main disadvantages of the composites based on the thermoset resins is their limited recycling options. Therefore, the thermoplastic composites have drawn increasing attention for their unique properties in the last decades. For examples, the textile reinforced thermoplastics, which have higher fiber volume fraction and controllable fiber orientation, have improved stiffness and strength compared with its short/long fiber reinforced variants. Especially, their environmental resistance and reformability, higher fracture toughness and impact strength compared with their thermoset counterparts make these materials more attractive for the future. The high viscous nature of the thermoplastic materials, however, is a great challenge encountered in LCM processes. Therefore, these composites are commonly manufactured using the prepreg or tape laying methods, which are used to overcome the high viscosity caused wetting problems. However, those two-stage processes (preparation of prepreg or tape, and the production of composite structure/laminate) inevitably hampers productivity and increases the production cost, which are the main reasons for a limited application of textile reinforced thermoplastic composite materials.

With the advent of thermoplastic oligomers having low melt viscosity like thermosetting resins [66, 69, 79], the possibility has arisen to manufacture textile reinforced thermoplastic composite materials with LCM processes. Low initial viscosity (below 0.03 Pa s) of the thermoplastic oligomers could facilitate an excellent impregnation of the preforms. Subsequently, in-situ polymerization would lead to a matrix material with thermoplastic properties of in the finished product. Presently, anionic ring-opening polymerization of polyamides [79] and in-situ polymerization of Cyclic Butylene Terephthalate (CBT) [66] get mostly interests because of their higher possibility that can be adapted to LCM processes. They start both with solid granulate and need heating equipment for the un-reacted resin mixture. The mold temperature is about 140 °C to 230 °C. Depending on the matrix system, the production can be tailored as isothermal or non-isothermal depending on the processing constraints.

Table 1.1 shows the comparison of the glass fiber reinforced laminate based on in-situ polymerized Cyclic Butylene Terephthalate (pCBT) and Polyamide 6 (PA6) matrix. It is obvious that the properties of laminate base on pCBT matrix have distinct advantages over PA6 in terms of mechanical properties, moisture resistance and production cycle. Therefore, this research will focus on the pCBT based composite materials.

Table 1.1.: Comparison of glass fiber-reinforced laminated based on pCBT and PA6 [30]

Properties	Unit	GF/pCBT (55% wf) PPG plain weave 320 gsm	GF/PA6 (55% wf) PPG plain weave 320 gsm
Tensile	MPa	370	319
Tensile Modulus	GPa	20.7	20.1
Flexural strength	MPa	556	383
ILSS (ASTM D2344)	MPa	45	35
Moisture content after 2h in boiling water	%	0.2	3.1
Process details: Compression molding, 0/90° lay-up			
GF/pCBT plate: 190 °C isothermal molding			
GF/PA plate: At 230 °C molded, then cooled down to 120 °C			

1.1.1. CBT technology for textile reinforced thermoplastics

CBT technology is a new manufacturing technology developed for production of textile reinforced thermoplastics. CBT is usually available in granulate form at room temperature as shown in Figure 1.1. It is a mixture of oligomers of butyleneterephthalate in a cyclic form. After melting around 150 °C, CBT exhibits a very low viscosity of 0.15 Pa s, which decreases even further to about 0.03 Pa s when CBT is heated to 190 °C, indicating a very suitable matrix resin for LCM processes [31]. Especially, in an entropically driven ring-opening process with trans-esterification tin- or titanium-based catalyst [21, 23, 94], the cyclic oligomer CBT is polymerized rapidly into a better known engineering thermoplastic polybutyleneterephtha-

late (PBT) without evolution of low-molecular-weight byproducts, as shown in Figure 1.2. The polymer resulting from this polymerization is usually hereafter referred to as pCBT. The integration of low viscosity and its thermoplastic characteristics makes the CBT resin based technology a very promising solution for production of textile reinforced thermoplastic composites.



Figure 1.1.: CBT granulate [30]

The fast crystallization nature of pCBT during in-situ polymerization, however, is one of the major disadvantages of CBT resin [65]. For the in-situ polymerization of CBT, the crystallization process can be tailored as instantaneous or consecutive crystallization according to the process conditions as shown in Figure 1.3. The instantaneous crystallization takes place when the reaction temperature is below the melting temperature of pCBT (about 225 °C). Hakme et al. [34] studied the instantaneous crystallization of CBT by dielectric sensing. It was found that, for CBT, simultaneous polymerization and crystallization occurs below 200 °C, polymerization is followed by crystallization above 200 °C, and only polymerization occurs above 220 °C. Thus, the process condition is believed to affect the crystal morphology and influence the final properties of the polymer.

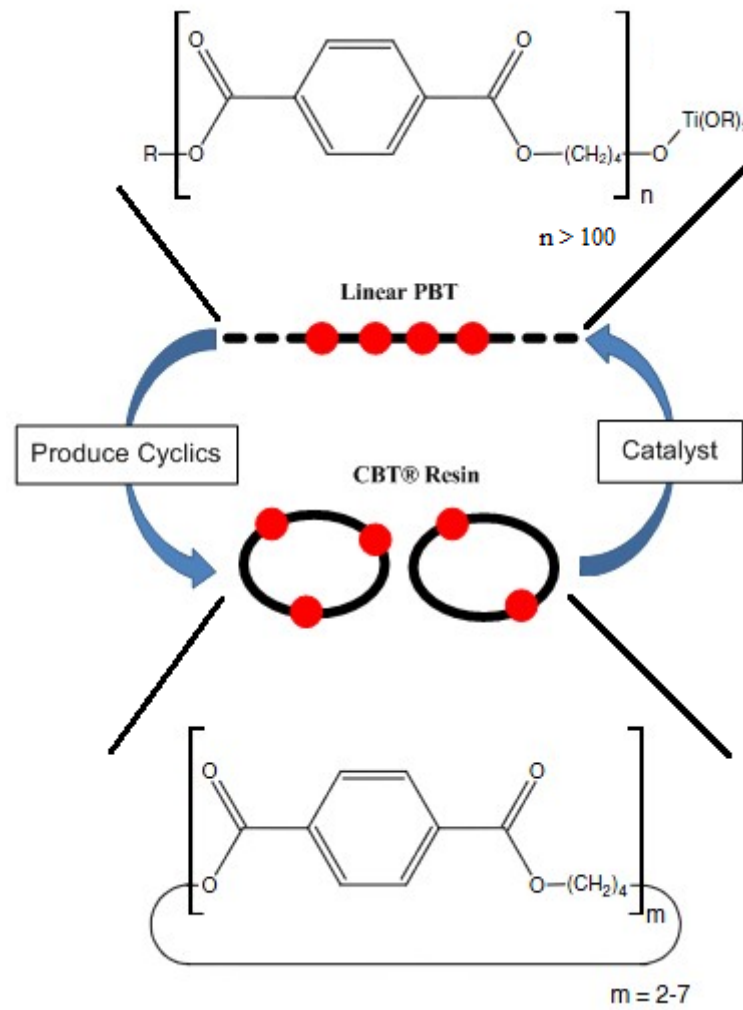


Figure 1.2.: Principle of CBT technology

The consecutive crystallization occurs when the pCBT is polymerized at temperatures higher than the melting point and then cooled down to temperatures lower than the melting point. The crystallinity of pCBT polymer is dependent on the cooling rate. The higher the cooling rate, the lower the crystallinity [12]. As the non-isothermal production process is usually accompanied by a large amount of energy consumption due to the unavoidable thermal cycles [65], isothermal production of pCBT with temperatures below the melting point of pCBT is usually preferred by CBT from the economical point of view. Therefore, it is of practical importance to find a solution so that the brittleness problem of pCBT can be eliminated without impairing its other characteristics.

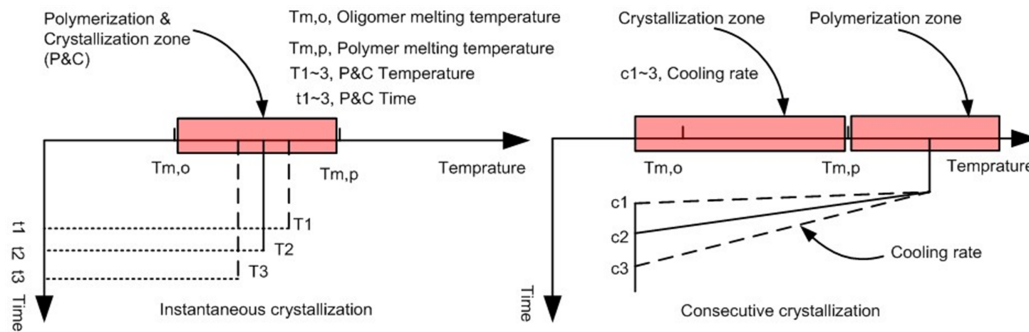


Figure 1.3.: Instantaneous crystallization vs. consecutive crystallization

1.1.2. Binding technology for automated textile preforming

Textile reinforced plastic composites have a high potential for lightweight construction and have been increasingly used in highly loaded structures. The production of those materials, however, is still dominated by manual steps in many areas, leading to limited marketable options. In order to improve the process efficiency and preforms handling stability, binder technology has been widely applied during textile preforming process. At room temperatures the binders are usually in a solid state with powder or granulate form, which will melt at the so called activation temperatures so that the textile plies can be bonded together after a preforming cycle. In this way, the bindered textile preform can be transported or handled without

damaging its textile structure such as fiber orientations. For instance, Henning et al. [38] studied the manufacturing of textile reinforced composite parts with automated fabricated preforms in the scientific research project "AutoPreforms¹". It has been shown that a high degree of automation can be achieved through the use of adhesive preforming binders as well as innovative handling technology (Figure 1.4). Based on this project, Greb et al [33] developed further an automated preforming center, where the whole process chain starting from textile cutting to binder activation has been integrated with a high degree of automation.

In the presence of the preforming binder the material behavior of both the single component such as the textile preforms and the composite system can be changed. For instance, the compaction behavior of textile preforms which contain thermoplastic toughening fleece as inter-layer between fabrics was studied by Aranda et al. [5] under different pre-heating conditions. It has been observed that the thermoplastic toughening fleece undergoes a geometry change after heat treatment, leading to a contractive and wavy preform with increased initial preform thickness and therefore lower fiber volume fraction. The effects of binder type and binder content at higher temperatures on fiber volume fraction, deformation and compaction pressure were analyzed by Aranda et al. [6] in a further study where the influence of preforming binder on the compaction behavior of textile preforms was investigated. The results indicate that the compressibility is improved in the case of bindered textile preforms. For the same compaction pressure higher fiber volume fraction can be obtained with bindered textile preforms as compared to the dry textile preforms without binder.

As for the effect of preforming binder on the mechanical properties, Tanoglu and Seyhan [96] investigated the effects of a preforming binder on the mechanical properties and ballistic performance of E-glass fiber reinforced polyester composite systems. Bindered textile preforms were prepared and consolidated by application of heat and pressure over plies of the glass fabrics coated with various concentrations of a thermoplastic polyester binder. Although the flexural strength and mode I inter-laminar fracture toughness were found being decreased by 15 % and 40 %

¹AiF-Projekt 14420 N: Wirtschaftliche Herstellung von Faserverbundbauteilen mit Hilfe automatisiert hergestellter textiler Preforms

respectively in the presence of 3 wt.% of the binder, the results showed that the preforming binder has significant potential for tailoring of the properties of textile reinforced composites.

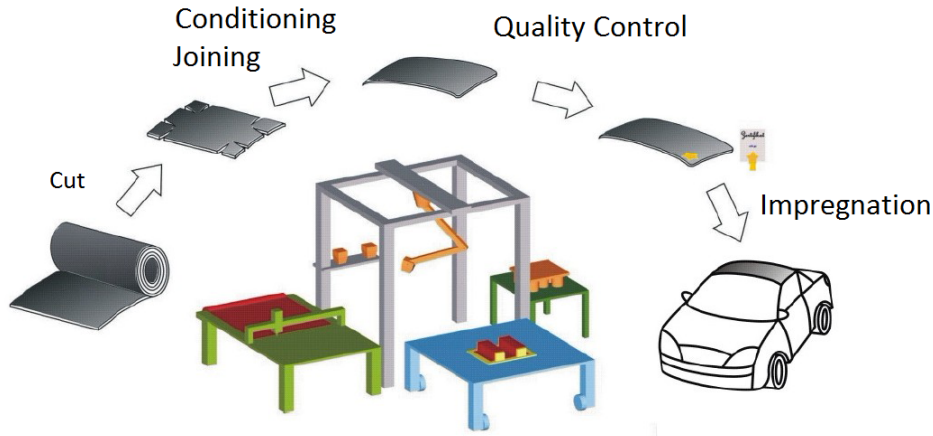


Figure 1.4.: Auto-preforms concept [38]

1.2. Motivation

The growing interest in textile reinforced thermoplastic composites have made considerable improvements, which have been devoted on the manufacturing technology based on in-situ polymerized Cyclic Butylene Terephthalate (pCBT). The brittleness problem of pCBT, however, is a significant disadvantage that hinders the application of CBT technology for production of textile reinforced thermoplastic composites. The research results that the preforming binder has significant potential to tailor composite properties may open a new door for the brittleness problem of pCBT based textile composites. With appropriate preforming binder, an efficient and qualified manufacturing process for textile reinforced pCBT composites could be realized by a new concept consisting of binding and toughening simultaneously, as shown in Figure 1.5.

For efficient manufacturing, bindered textile preform, as shown in Figure 1.5(a), is prepared by applying preforming binder (green) between textile fabrics layers.

The shape and especially the fiber orientations can be maintained during preform handling, which is essential for an automated manufacturing process. For qualified manufacturing, as shown Figure 1.5(c), the composite toughness is improved because of the toughening effect contributed by the preforming binder. In-situ copolymerization of CBT and preforming binder is expected to occur under isothermal processing conditions during/after impregnation of matrix resin (purple). The gradual change from purple to green in the composite system is supposed to be the pCBT matrix toughened with different concentration of preforming binder. Because the preforming binder in the inter-ply region could be melted (re-activation) at the processing temperature (about 185-205 °C) and decentralized unevenly in the transverse direction of the bindered textile preform (re-distribution) due to the flow of the binder melts under compaction pressure applied by the compression mold (Figure 1.5(b)).

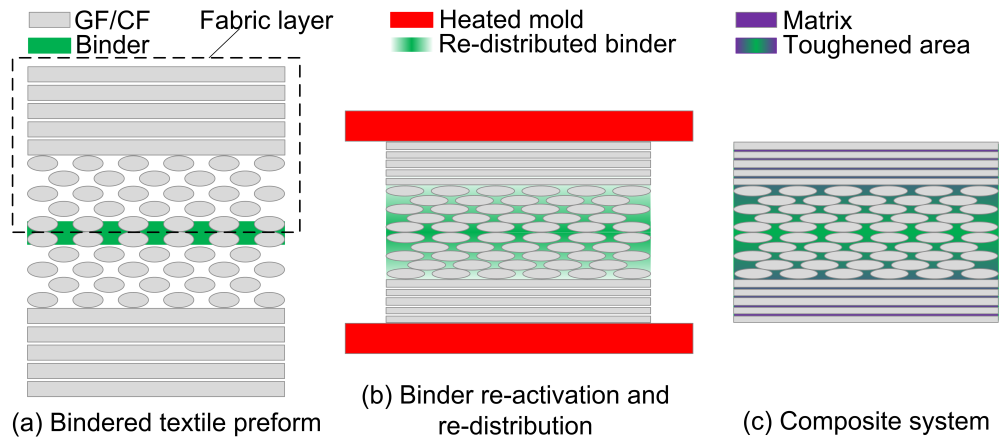


Figure 1.5.: Simultaneous binding and toughening concept

As the toughening effect contributed by preforming binder is mainly occurred locally at the inter-ply regions, the inter-laminar properties such as the fracture toughness in mode I and mode II of the composite system, which are mainly matrix dominant, are expected to be improved by applying appropriate preforming binder. In addition, other mechanical properties like stiffness and strength of the composite system, which are mainly dependent on the fiber reinforced intra-plys, are supposed to be not significantly influenced. However, the introduction of preforming binder brings about a number of changes in the traditional composites manufacturing pro-

cess as well, especially the change of material properties and the resulting impact on the manufacturing process parameters. For instance, the changed compaction behavior of bindered textile preforms can influence the resin infusion pressure needed for a complete impregnation. In addition, the presence of preforming binder may also change the thermal rheological properties of the catalyzed CBT resin. Those changes are of great importance to be understood to achieve an effective production of textile reinforced composites. Therefore, the state of science, research and technology related to the above mentioned motivation are discussed in the coming section and summarized as a problem statement which is to be addressed in this dissertation research.

1.3. State of the science, research and technology

1.3.1. Processing of textile reinforced thermoplastics

Thermoplastic composites

With the advent of high performance thermoplastic polymers, structural applications of thermoplastic composites are increasing rapidly. Since 1990s, the number of material forms and combinations in fiber reinforced thermoplastic polymers has increased exponentially, thereby expanding application avenues in transportation, automotive, mass transit, marine, aerospace, military and construction sectors [102].

The range of thermoplastic composites material forms is quite wide as illustrated in Figure 1.6. The classification may be based on the aspect ratio (length/diameter) as short and long fiber, or based on the orientation and/or fiber architecture such as unidirectional and fabric reinforced. In this part, a brief description of thermoplastic polymers used in structural applications will be summarized firstly, which is then followed by the description of the impregnation strategies of continuous fiber reinforced composites.

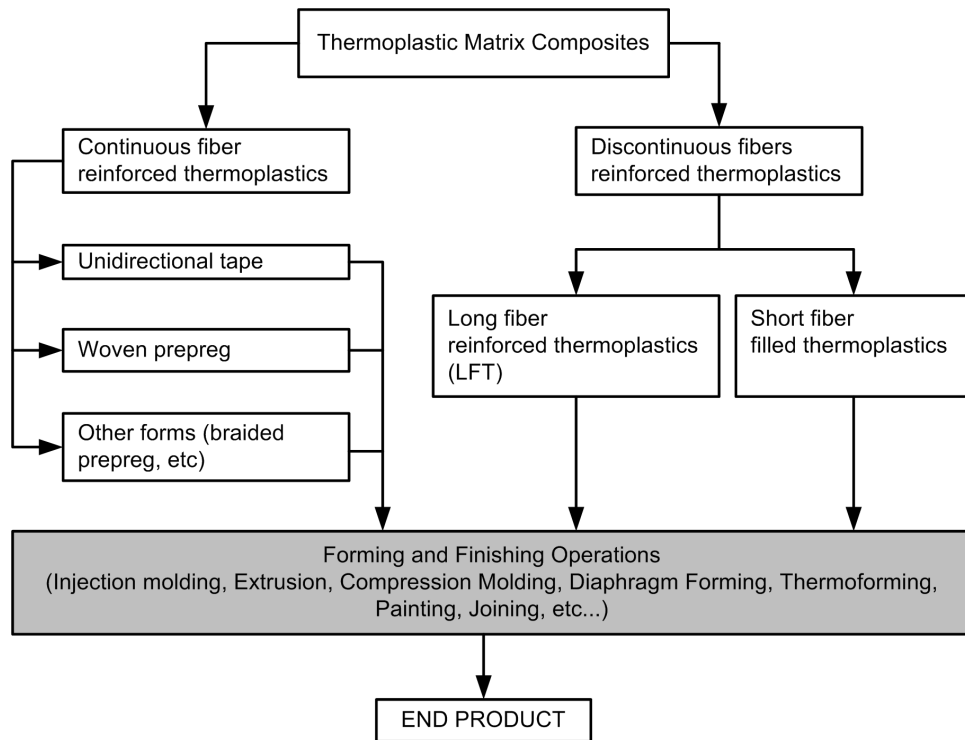


Figure 1.6.: Material forms of thermoplastic composites [102]

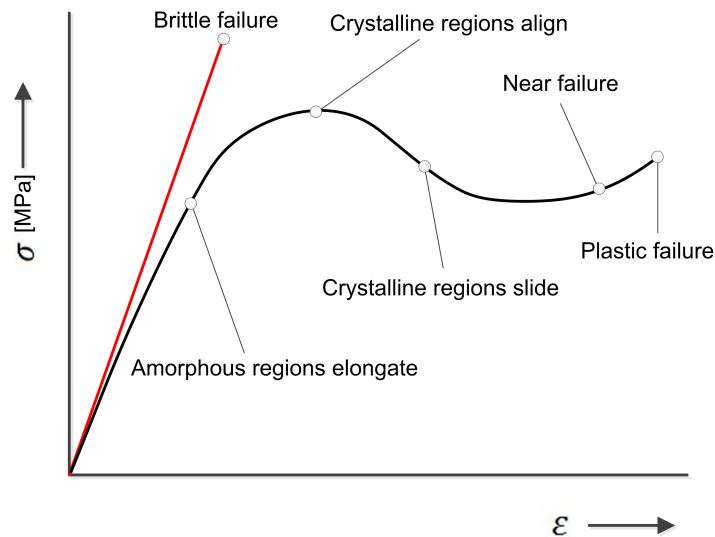


Figure 1.7.: Ability of thermoplastic to elongate and absorb energy [102]

Matrix System

Thermoplastic polymers exhibit elastic plastic behavior through the morphology of the polymer chains and their rearrangement during loading and unloading. Those polymers can stretch considerably before rupturing as illustrated in Figure 1.7. The toughness of these materials is superior to that of thermosetting polymers and therefore can sustain extensive damage without cracking or failing [102]. Table 1.2 summarizes typical physical, thermal and mechanical properties that are used as matrix materials in composites for structural applications. Some of them are described in detail as follows:

1. Polypropylene (PP) [102]: PP is a commodity polymer being unusually resistant to most solvent and chemicals. It exhibits high toughness, medium stiffness and strength. PP allows for simple fabrication techniques to be used because of its limited thermal behavior (relatively low melting point of 180 °C). PP based composites are commonly made with short and long fibers in injection and extrusion/compression molding.
2. Polyamides or nylons (PA) [102]: PA is superior to PP in stiffness, strength as well as thermal stability, but maintains adequate ductility and flexibility. When reinforced with reinforcing fibers, it is used in load bearing applications and structural components. PA has excellent temperature performance up to 200 °C. The melting point of standard PA is in the range of 215 to 220 °C.
3. Polybutylene Terephthalate (PBT) [102]: PBT is a thermoplastic semi-crystalline polymer, and a type of polyester. It is resistant to solvents, offering a low shrinkage during forming and cooling, and is mechanically strong. The heat-resistance of PBT is up to 150 °C (or 200 °C with glass fiber reinforcement).

Table 1.2.: Typical physical and mechanical properties of representative un-reinforced thermoplastic polymers used in structural applications (adapted from [102])

Materials	Tensile modulus Gpa	Tensile strength (yield), MPa	Melt flow g/10 min	Melting point °C	Density g/cm ³
Polypropylene (PP)	1.5-1.75	28-39	0.47-350	134-165	0.89-0.91
Polyethylene (PE)	0.15	10-18	0.25-2.6	104-113	0.918-0.919
Polyurethane (PU)	0.028-0.72	5-28	4-49	220-230	1.15-1.25
Polyamide (PA)	0.7-3.3	40-86	15-75	211-265	1.03-1.16
Poly pheyene sulphide (PPS)	3.4-4.3	28-93	75	280-282	1.35-1.43
Polybutylene terephthalate (PBT)	1.75-2.5	40-55	10	230	1.24-1.31
Poly ether ketone ketone (PEKK)	4.4	110	30	360	1.31
Poly ether ether ketone (PEEK)	3.1-8.3	90-110	4-49.5	340-344	1.31-1.44
Poly ether imide (PEI)	2.7-6.4	100-105	2.4-16.5	220	1.26-1.7
Poly ether sulphone (PES)	2.4-8.62	83-126	1.36-1.58	220	1.36-1.58
Poly ether terephthalate (PET)	2.47-3	50-57	30-35	243-250	1.3-1.33

Impregnation strategies

It is well known that molten thermoplastics with a high viscosity ranging from 100 up to 10 000 Pa s that are very difficult to be applied for impregnation of textile preforms when compared with un-cured thermosets that usually offer a viscosity lower than 1 Pa s. Different impregnation strategies hereby have been developed to adapt the high viscosity of molten thermoplastic for textile reinforced thermoplastic composites.

To obtain a high performance of textile reinforced thermoplastics, a good and complete impregnation of the fiber bundles with the matrix is necessary. In this way not only a void free composite system, but also a good stress transfer between fiber and matrix can be achieved. Therefore, every fiber should be surrounded by matrix after the impregnation. According to Darcy's law, the impregnation of the fiber preforms in the case of the flow front is unidirectional can be described as:

$$v = \frac{Q}{A} = \phi \cdot \frac{dx}{dt} = \frac{K_p}{\eta} \cdot \frac{\Delta P}{l} \quad (1.1)$$

In which v (m/s) is the apparent velocity of the matrix, Q (m³/s) is the volume flow rate, A (m²) is the area of the cross section of fiber preforms, ϕ (-) is the porosity which is the fraction of the cross section available to flow, K_p (m²) is the permeability of the fabric, η (Pa s) is the apparent viscosity of the resin, ΔP (Pa) is the pressure difference and l (m) is the flow distance. When the permeability K_p and the viscosity η are constant, this equation can be integrated, resulting the necessary time for complete impregnation is:

$$t = \frac{\phi \eta l^2}{2K_p \Delta P} \quad (1.2)$$

The total time for impregnation is a function of the viscosity and of the flow distance according to the equation 1.2. To minimize the impregnation time and therefore the production cost, the viscosity and/or the flow distance should be as low as possible. The other parameters can only be changed in a very limited way: the permeability

is a property of the fabric that is used and the pressure cannot be increased too much due to the possible distortion of the fiber orientation and the more expensive molds to be used.

The impregnation strategies that are commonly used for continuous fiber reinforced thermoplastic composites can be divided into two categories based on the two variable parameters in equation 1.2 [13, 103]. One of them makes the time of impregnation shorter by using a lower distance (e.g. Powder impregnated tows [36], film stacking [62], melt impregnated prepreg tapes [68] and commingled or co-weaved shapeable fabric [107]), the other one by lowering the viscosity (e.g. Solution impregnated tows [109], in-situ polymerization of low molecule pre-polymers [84]). As the research interest of this dissertation is textile reinforced pCBT composites, in-situ polymerization of low molecule pre-polymers will be discussed in depth in the following section.

In-situ polymerization of low molecule pre-polymers

Rosso et al. [84] investigate the scope of a new developed polymerization molding system for polyamide 12 (PA12), especially with respect to the formation of carbon fiber reinforced PA12 composites. Initial screening of PA12 composite was performed by means of an internal mixer in order to identify the suitable type of surface-treated carbon fiber (CF). The fraction of residual lauryllactam (LL) monomer reflected the influence of the CF-treatment on the polymerization process involved in anionic in-situ polymerization of LL. The cryogenic fracture surfaces were analyzed by Scanning Electron Microscopy (SEM) in order to evaluate the adhesion quality between the components. Finally, a bench-scale polymerization molding process was established successfully for the fabrication of multi-axial laminates. The results indicate that the anionic LL polymerization by means of the Atofina initiator/activator system can be characterized as reliable and with rather good reproducibility. At a polymerization of 270 °C, the polymerization reaction is completed within some minutes and the composite materials obtained possess a high molecular weight PA12 matrix, having only a very small fraction of residual monomer. Compared to the EMS in-situ PA12 systems, an immense advantage is

that the polymerization mixture is stable at the melting temperature of the LL for prolonged periods of time. Due to this fact, only one storage tank is sufficient and no mixing devices are needed. Therefore, this system is much more attractive from an engineering point of view because it requires less maintenance and offers an easier handling. The produced composite materials show similar mechanical properties as known from commercially available systems. Moreover, the new PA12 system is less sensitive to fillers in general, which could be investigated by inspection of the adhesion quality and compatibility to differently sized carbon fibers [84].

To accommodate the differences of the thermoplastic resin, the conventional Vacuum Assisted Resin Transfer Molding (VARTM) process was significantly modified by Pillary et al. [69]. The process was developed involving various parameters such as resin, catalyst, activator, and temperature control etc. to maintain a low resin viscosity for sufficient time to wet out the preform fully, attaining good fibre impregnation and optimizing polymerization of the resin. APA6 was chosen for PA6 matrix composites produced by VARTM. Microscopic studies for the impregnation quality, the effect of temperature and flow distance on the fiber weight fraction and crystallinity of the PA6 resin and the degree of conversion from monomer to polymer were investigated. The method of infusion the resin at 100 °C and ramping in the temperature to 150 °C, compared to infusing the resin at 150 °C was proved effective in achieving the flow of the resin through entire preform. The optical and SEM images show that macroscopic and microscopic fiber impregnation was achieved. The fiber weight percentage was fairly uniform in the panel infused at 100 °C, which also had a higher fiber weight percentage than the panel infused at 150 °C. The results from DSC measurement show an average melt temperature for the neat polymer and the panels infused at 150 °C and 100 °C of 220.06, 214.9 and 218.2 °C, respectively. The panel infused at 100 °C has a crystallinity that is about 5 % higher than the panel infused at 150 °C. The increase in crystallinity is a reasonable trade-off for the longer infusion time and effectiveness of the process, and also can be a benefit with respect to modulus and moisture absorption. The process also yields a relatively high degree of conversion from monomer to polymer, about 98 % for both of the processing conditions.

In order to manufacture thicker, larger and more integrated thermoplastic parts than currently can be achieved by melt processing, a VARI process also based on APA6 was developed at the Delft University of Technology by Rijswijk et al. [73, 74, 76, 77, 78, 79, 97, 98]. In their serial studies, mechanical properties of APA6, fiber matrix interactions, effect of textile fiber reinforcement and polymerization temperature on the composites properties were investigated. It has been shown that the APA6 resin has excellent mechanical properties. The addition of pre-heated fibers not only shortens the infusion window, but also influences the matrix properties by reducing the exothermic heat production. In addition, the low in-plane permeability of the textile preforms influences the infusion time and causes the entrapment of voids. The reactions between the matrix and the fibers surface can lead to deactivation of the initiator and bond formation with the activator. Generally, a higher mold temperature results in a stronger interface, but at the same time a reduction in crystallinity weakens the matrix, which makes a compromise inevitable. In order to improve the interface strength at lower processing temperatures, the use of (i) activators that are capable of inter-facial bonding at lower temperatures, and (ii) mixtures containing various activators are explored. It has been demonstrated that stronger bonding of the activators on the fiber surface does not automatically improve the mechanical properties of the composite.

Besides the aforementioned PA12 and APA6 resin systems used for reactive processing of thermoplastic composite, Parton et al. [65, 66] and Steeg et al. [40, 88, 90, 91] studied the in-situ polymerization of thermoplastic composite based on CBT technology.

Process conditions of RTM like processes and the properties of poly(butylene terephthalate) polymerized from cyclic oligomers and its composites were investigated in [65, 66]. The process window for fiber impregnation was found to be small and strongly dependent on the process parameters due to the high reaction speed of the cyclic oligomers. Therefore, process parameters need to be well-controlled in order to achieve reproducible parts. The presence of the fibers reduces the degree of conversion of pCBT. The value obtained from the GPC measurements for reinforced samples, however, is the lower boundary due to the interference of the fiber sizing in the measurements. There is a small decrease in molecular weight

in the composite specimens; nevertheless, the molecular weight is still comparable to that of commercially available PBT Twintex. Partially cross-linked PBT, showing as a very high molecular weight fraction in the chromatograms, is formed due to side reactions of the cyclic oligomers with epoxied functional groups presented in the fiber sizing. Due to the processing route and more specifically the time-temperature profile, inherent to the RTM process, the crystals of the matrix consist out of well-defined, thick and well-oriented crystal lamellae. Together with a high overall degree of crystallinity and a low density of tie molecules, these large and perfect crystals cause polymer brittleness. Matrix brittleness lowers the transverse strength of unidirectional composites even below the matrix strength, but leaves the mechanical properties in the fiber direction unaffected.

Shahzad et al. [88] demonstrate the potential of CBT technology for a successful production of pCBT matrix composites by LCM in the work on the development and characterization of glass fiber reinforced in-situ polymerized pCBT composite. The low molecular weight cyclic oligomers facilitated good impregnation and wetting-out of the preform. Subsequently, the precursor oligomers were converted to high molecular weight thermoplastic matrix successfully inside the mold by in-situ polymerization. Study of the micro-structure of the developed composite material elucidated good impregnation quality, fiber wet-out, and an excellent fiber to matrix adhesion. Besides, the partially ductile nature of the fracture of the thermoplastic matrix was noticed. It is noteworthy that the industrial scale manufacturing of the pCBT matrix composite materials requires suitable equipments and consumables that are chemically resistant to CBT oligomers and catalysts and withstand higher processing temperatures. Reaction kinetics of in-situ polymerization of the oligomers toward high molecular weight thermoplastic material depends critically on parameters like reaction time, molding temperature, and catalyst amount. The robust and reliable development of composite structures by in-situ polymerization of the thermoplastics requires that equipments are sensorized to control the related process parameters.

1.3.2. Toughening of in-situ polymerized pCBT composites

Various potential toughening approaches have been attempted to overcome the brittleness problem of pCBT. In general, there have been three basic routes being investigated to increase the toughness of pCBT composites: (1) by using non-isothermal production process [9], (2) by co-polymerization with soft polymers [2, 3, 10, 12, 14, 101], and (3) by incorporation of nano particles [11].

Toughening of pCBT with non-isothermal production process was reported in [9]. Intensive drying and a temperature of 240 °C are found necessary for the complete polymerization to increase the molecular weight. For the non-isothermal production two different cooling rates after complete polymerization are used: a slow cooling rate and quenching. An increase in toughness of the composites can be concluded for the quenched samples due to the greatly improved failure strain as shown in Figure 1.8. And the fracture toughness in Mode II test even indicates a crack propagation energy which is twice as high for the quenched samples as compared to the slowly cooled samples [9]. The higher toughness after quenching can be found in the crystal perfection. The slowly cooled as well as the quenched composites contain the same amount of crystals, but in the case of the quenched samples the crystals contain a lot more defects. These defects are in fact some amorphous material present in between the crystals. Therefore a higher amount of defects will give a higher toughness.

Toughening of pCBT with chemical modification process have been done by co-polymerization with polycaprolactone [10], polytetrahydrofuran [12], poly(vinyl butyral) [99], ϵ -caprolactone [101], poly [ethylene-co-(vinyl acetate)] [14], tetrahydrofuran (THF) [3] and low molecular weight bi-functional epoxy resin [2]. The resulting co-polyesters showed increased toughness in the case of co-polymerization with polycaprolactone [10], ϵ -caprolactone [101] and poly[ethylene-co-(vinyl acetate)] [14]. The stiffness and strength, however, were found to decrease in these co-polyesters due to the properties of the co-polymers used. In the case of THF [3] and low molecular weight bi-functional epoxy resin [2], the resultant pCBT showed an increased ductility, while other important properties such as tensile strength, tensile modulus and glass transition temperature were not significantly altered.

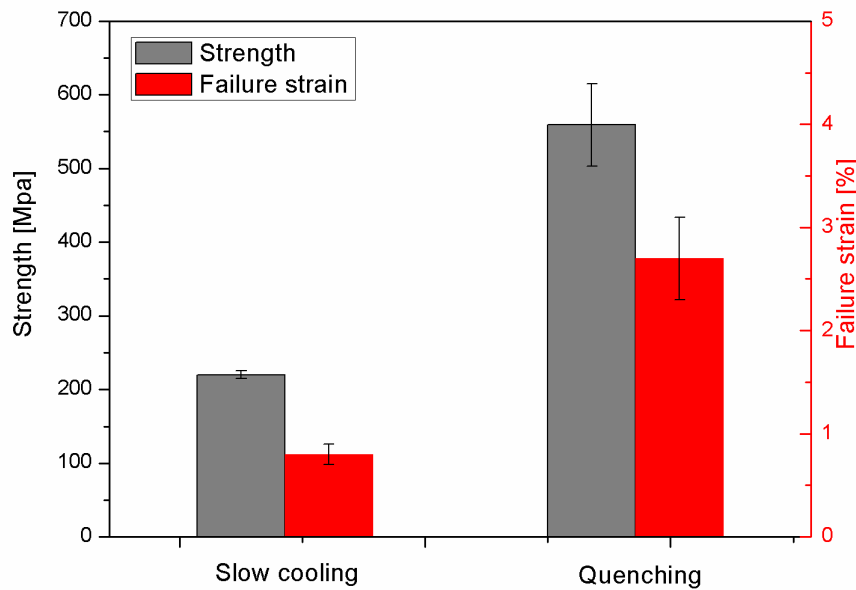


Figure 1.8.: Effect of cooling path on the mechanical properties of pCBT composites [9]

In a further attempt, **physical modification was attempted by adding carbon nanotubes (CNTs)** [11]. The dispersion of CNTs in CBT oligomers melt up to 0.1 wt.% is achieved by rotational mixing. It was demonstrated that the CBT is a material in which the dispersion of CNTs seems quite easy. The CNTs can be finely dispersed in a multilevel manner with both micron and sub-micron sized agglomerates of CNTs. The addition of CNTs leads to an increase in stiffness, strength and energy to failure, however, the failure strain slightly decreases. The CNTs-filled pCBT showed a failure strain of about 4 % as shown in Figure 1.9, well below that of commercial PBT (>50 %) [3]. In addition, thermal measurements indicate that the CNTs have no influence on the crystallinity. The limitation of this method is that the CNTs show a tendency of filtration through the fabric when the mixture of CBT oligomers melt and CNTs is processed in vacuum infusion processes, which is commonly applied for manufacturing of textile reinforced composites.

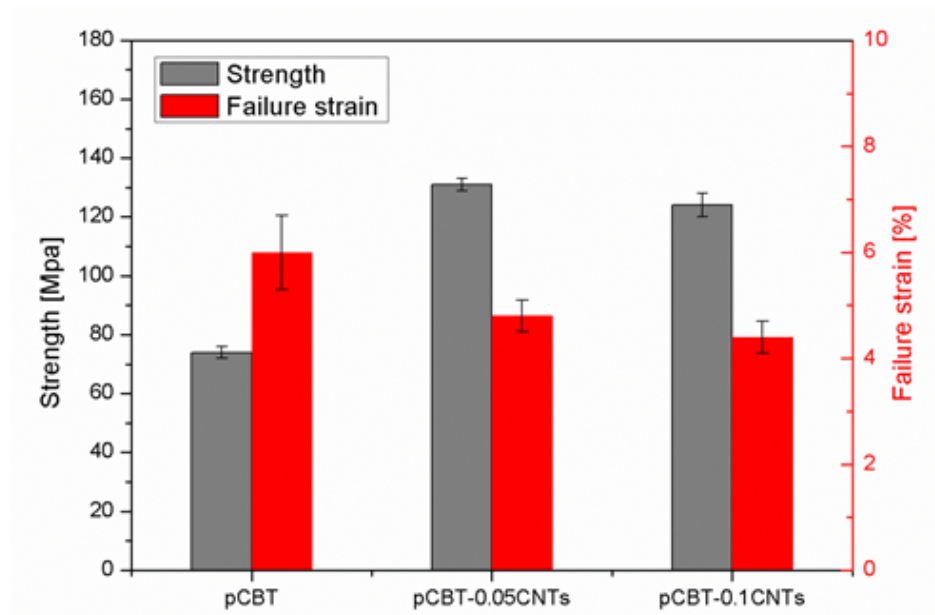


Figure 1.9.: Effect of addition of carbon nanotubes on the mechanical properties of pCBT composites [11]

1.3.3. Toughening concept for thermosets resin composites

Thermosetting resins such as epoxy resins have been used within the last decades as the matrix resins of composites rather than thermoplastic resins, due to their better processability. The low fracture toughness of thermoset resin matrix composites compared with metals, however, is one of the factors which limits their application as primary structural materials. Therefore, improvement of fracture toughness has been a hot topic of the composite industry. With this background, toughening technologies have been extensively researched by many people. In general, those researches can be classified into two categories. One of them is in-situ toughening by blending thermoset resin with elastomer particles or thermoplastic resin [24, 54, 67]. The other category to enhance the toughness of the composite laminate is ex-situ toughening (also called inter-leaf concept) by placing a toughening agent such as a thermoplastic film at the inter-ply region, which is the weakest portion of the laminate [25, 60, 106, 114].

In-situ toughening

Elastomer particles were used for in-situ toughening of epoxy resin in [67]. The toughening effect depends very much on the shear deformation capacity of the matrix resin itself which includes elastomer particles. They indicated the importance of the cross-link density of the matrix epoxy resins. Comparatively lightly cross-linked epoxy was easily toughened by elastomer addition, but highly cross-linked epoxy was not. For thermoplastic resin blended thermoset resins [24, 54], a micro-phase separated morphology is formed during the curing process of the resin blend. The toughness of the cured resins depends on the phase separated morphology. The problem of those toughening methods is the dramatic increase in matrix viscosity because of the addition of the toughening agents with high molecular weight, leading to a poor impregnation of textile reinforcements.

Ex-situ toughening

Ex-situ toughening concept, which was first point out by Yi et al. [25, 106, 114] to increase the impact damage resistance of thermoset matrix composites used for aerospace, was inspired by natural laminates e.g., shells and woods with typically periodic layered structures. In this concept, solid thermoplastic thin layers were periodically inserted as inter-layer between the fabric layers. After impregnation of the dry fabric with thermosets resin, an interaction between the thermoplastic thin layer and the thermosets resin occurs at elevated temperatures during the curing reaction (Figure 1.10). As a successful example, during the investigation of the interaction between toughening polymer (PAEK) and the BMI resin, the aerospace-grade RTM composite panels were fabricated based on the ex-situ RTM technique. The results indicate that, compared with reference samples, the mode I inter-laminar fracture toughness of the composites is increased by a factor of four when the ex-situ RTM technique is applied.

In order to overcome the high viscosity of the thermoset resin mixture from in-situ toughening process, Naffakh et al. [60] developed a toughening process which has almost the same principle as ex-situ toughening concept. The thermoplastics tough-

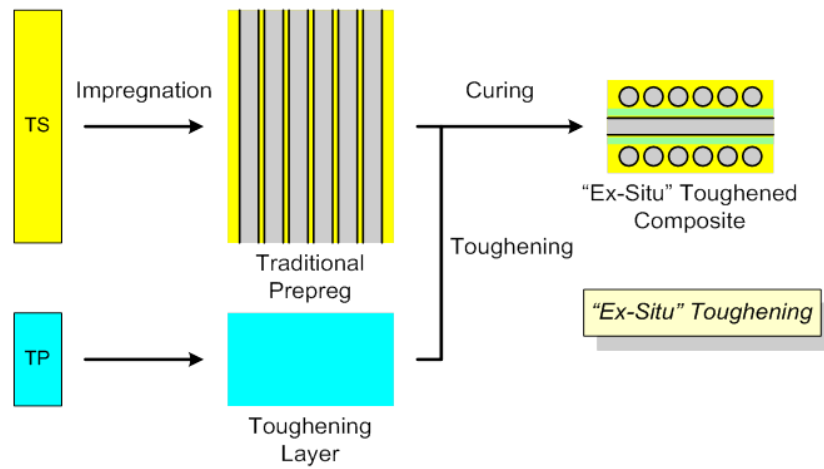


Figure 1.10.: Ex-situ concept for composites toughening [47]

ening agent, in the form of films, was placed between layers of fiber glass in the mold. A reactive solvent composed of an epoxy resin and a liquid amine hardener was used to dissolve thermoplastic films in-situ and produce composites modified by thermoplastics via RTM. In this manner, a thermoplastic/thermoset blend which will be generated in the inter-ply regions after the following events take place: impregnation, dissolution of the films and a reaction induced phase separation of the thermoplastic (namely, polyether imide, PEI) (Figure 1.11). Investigation into the blend morphology shown that the PEI nodules were dispersed between the fiber glass layers. This morphology may be compared to that observed in other thermoplastic/thermoset blend, i.e. "conventional" blends formed either from epoxy-amine/thermoplastic films (without glass fibers) or epoxy-amine/thermoplastic solutions at fixed concentration.

1.4. Problem statement

After reviewing the current state of the science, research and technology, it can be seen that the textile reinforced thermoplastic materials have great opportunity for future light weight solutions. In-situ polymerization technology with pre-polymers has aroused more and more research interests for its potential of improved effi-

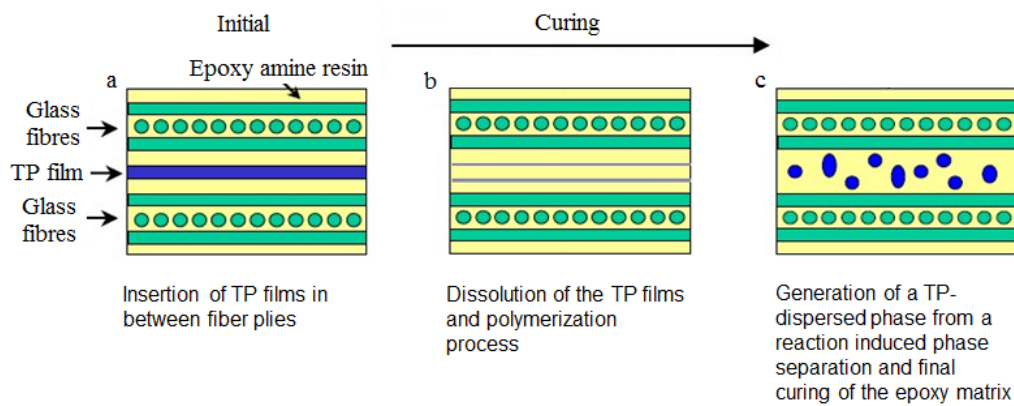


Figure 1.11.: RTM processing with integrated ex-situ toughening [60]: (a) insertion of a TP film in between fiber plies, (b) dissolution of the TP film and polymerization process and (c) generation of a TP-dispersed phase from a reaction-induced phase separation and final curing of the epoxy matrix

ciency and reduced production cost. CBT technology is one of the strong competitive solution for processing of textile reinforced thermoplastic composites. However, the brittleness problem of pCBT is a significant disadvantage that greatly impedes further application of CBT technology for manufacturing of textile reinforced thermoplastic composites. According to the three different toughening methods (section 1.3.2) that have been tried out on un-reinforced and reinforced pCBT and the toughening concept developed for thermosets resin matrix composites (section 1.3.3), the following opening problems could be summarized after the literature review:

1. Non isothermal toughening process can make pCBT tougher. However, with introduced thermal cycle and further the production cost, it **sacrifices one of the biggest advantages of CBT technology , which is that the pCBT can be produced isothermally.**
2. Toughening with chemical and physical modification process may either **sacrifice the mechanical properties of pCBT** (e.g. co-polymerization with Polytetrahydrofuran [12]) and **the working environment** (e.g. co-polymeri-

zation with organic solvent like THF [3]) or the flow properties of CBT (e.g. addition of fine particles like CNTs [11])

3. The **synergistic relationship between manufacturing and toughening** for textile reinforced pCBT composite are usually ignored. Toughening processes are usually taken as a separate step during manufacturing. As a result, the toughening effectiveness (e.g. improved toughness) and the manufacturing issues (e.g. costs, working environment etc.) cannot be satisfied simultaneously.

Since nowadays the research on toughening of pCBT and manufacturing of textile reinforced pCBT composites are still not enough adequate, the dissertation focusing on exploring a new concept consisting binding and toughening simultaneously as stated in section 1.2 for efficient and qualified manufacturing of textile reinforced thermoplastic composites is necessary and emergent.

1.5. Research objectives

According to the statement in section 1.2 and section 1.4, the objective of this research is to provide:

1. Material characterization method focusing on the effect of introduced pre-forming binder on the material behavior of textile preforms and CBT resin matrix system.
2. An experimental approach for preparing of in-situ polymerized textile reinforced pCBT composites according to simultaneous binding and toughening concept;
3. The knowledge on the effect of processing conditions and the introduced binder systems on the thermal and mechanical properties of textile reinforced pCBT composites;

4. The mechanism of simultaneous binding and toughening concept and its effect on the inter-laminar fracture properties of in-situ polymerized textile reinforced pCBT composites;
5. An engineering design approach for manufacturing of textile reinforced pCBT composites according to simultaneous binding and toughening concept.

1.6. Organization of the dissertation

Figure 1.12 shows the solution strategy and detailed tasks of this dissertation research. Starting from the single material component to the final textile reinforced pCBT composites part, the whole research can be classified into three key aspects, namely characterization of the materials, development of the manufacturing process and optimization of the manufacturing process.

In Chapter 2 the general theoretical background and characterization techniques are explained for the research tasks of this dissertation research, which is followed by the materials and methodology illustrated in Chapter 3. The clarified methodology is divided into three parts which are corresponding to the above mentioned three key aspects respectively. The systematic way to achieve the proposed concept will be discussed comprehensively in Chapter 4- 6.

In chapter 4 is the results and discussions regarding to the first key aspect, which is the characterization of the processing materials including the compaction behavior of bindered textile preforms and the thermal and rheological properties of catalyzed CBT oligomers. Effect of preforming and compaction parameters on the compaction performance such as the fiber volume fraction are investigated and described mathematically with a proposed four parameter compaction model. Furthermore, the focus of this research is also extended to the influence of preforming binder on the melting and crystallization behavior, the isothermal simultaneous polymerization and crystallization phenomenon, and the processing window of the catalyzed CBT resin system as well. The results of this chapter is the basis for further development of the manufacturing process.

In chapter 5 is the results and discussions regarding to the second key aspect, which concentrate on the development of the manufacturing process for textile reinforced pCBT composites according to the proposed concept. Thermoplastic Vacuum Assisted Resin Infusion (T-VARI) manufacturing process is developed according to the processing characteristics and the isothermal production requirements of pCBT. After that, the thermal mechanical properties of the manufactured pCBT composites are characterized to evaluate the performance of the T-VARI manufacturing process. At the end, the single factor analysis is performed to study the influence of process parameters on the manufacturing process and the flexural properties of pCBT composites.

In chapter 6 is the results and discussions regarding to the third key aspect, which are the optimization of the toughening performance of textile reinforced pCBT composite and T-VARI manufacturing process and focus on the influence of various preforming binder types, filling contents and toughening concepts. Inter-laminar fracture toughness in mode I and mode II of specimens prepared with various binder are characterized to optimize the preforming binder. Flexural properties of the specimens fabricated with the optimized preforming binder are studied to verify the optimization, where flexural strain is taken for assessing toughening performance, and the flexural modulus and strength are taken for evaluating mechanical properties. A modification of the proposed concept is tried for further optimization possibilities.

Chapter 7 summarizes the uniqueness, contributions and perspectives of this research.

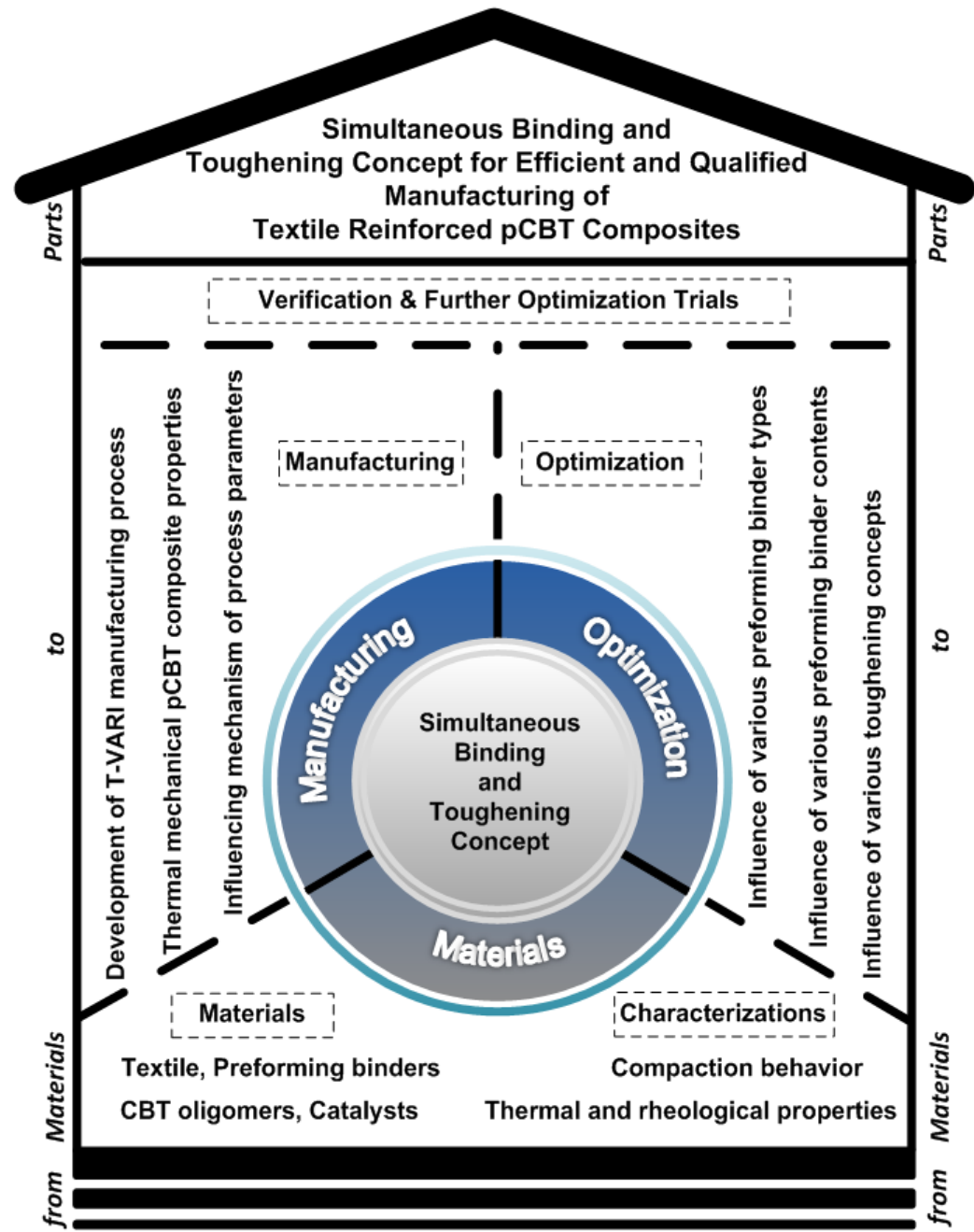


Figure 1.12.: Solution strategy and organization of this dissertation

Chapter 2

Theoretical background and characterization techniques

In this chapter, the theoretical background and characterization techniques related to the research tasks in this dissertation are elaborated. Specifically, theoretical aspects in reactive processing of textile reinforced thermoplastics and design of experiment are discussed firstly, followed by the description of the characterization techniques for thermal and rheological analysis of matrix system.

2.1. Reactive processing of textile reinforced thermoplastics

2.1.1. Polymerization reaction

For reactive processing of textile reinforced thermoplastic composites, the in-situ polymerization of low molecule pre-polymers has to meet the following requirements: (1) the resulted linear polymer has to have a high molecular weight, (2) the conversion rate from pre-polymers to high molecular polymer should be sufficiently high and reproducible and (3) The polymerization reaction process is rapid and generates no low-molecular-byproducts. According to those requirements, vinyl

polymerization and ring-opening polymerization are the two commonly used appropriate polymerization reactions for textile reinforced thermoplastics.

Vinyl polymerization

Vinyl polymers are polymers made from vinyl monomers, which is a small molecule containing carbon-carbon double bonds. The double bonds are broken into single bonds during polymerization reaction, resulting in two free electrons. The free electrons are used to join monomer units to form a long chain of many thousand of carbon atoms containing only single bonds between atoms.

There are a variety of ways to make vinyl polymers from vinyl monomers like, free radical vinyl polymerization, anionic vinyl polymerization, cationic vinyl polymerization, Ziegler-Natta catalysis, and metallocene catalysis polymerization. The free radical vinyl polymerization is one of the most common and useful polymerization reaction for making polymers. Polymers made by free radical polymerization include polystyrene, poly(methyl methacrylate), poly(vinyl acetate) and branched polyethylene.

Ring-opening polymerization (ROP)

Ring-opening polymerization (ROP) is a form of chain-growth polymerization, in which the terminal end of a polymer acts as a reactive center, where further cyclic monomers join to form a larger polymer chain through ionic propagation. It has received attention for its potential as clean alternative for polymerization reaction that results in the generation of nasty by-products or require the use of large amounts of hazardous solvents. For instance, the production of PEEK and PPS makes use of high-boiling solvents such as diphenyl sulfone and dichlorobenzene [71, 105].

The molecular weight of polymers acquired through ROP are generally higher than the same polymer acquired through polycondensation reactions. Exemplary polymers produced by this method include: (a) Polyamides, such as polycaprolactame (PA 6) from caprolactam and polylauroamide (PA 12) from lauryllactam; (2)

Polyesters, such as polycaprolactone (PCL) from caprolactone and poly(butylene terephthalate) (PBT) from cyclic butylene terephthalate; and (3) Polyethers, such as poly(ethylene oxide) (PEO) from ethylene oxide and polytetrahydrofuran (PTHF) from tetrahydrofuran.

2.1.2. Reactive processing of pCBT

For reactive processing of textile reinforced thermoplastic composites, there are several matrix systems such as PA 6, PA 12 and PBT. As stated in 1.1, the focus of this research are pCBT based composite materials. Therefore, the details of reactive processing of pCBT will be given here.

As the principle of CBT technology shown in Figure 1.2, de-polymerization of linear PBT yields a macro-cyclic oligomer mixture. The mixture can be re-polymerized directly into solid semi-crystalline PBT with an average molecular weight of 445,000. The polymerization reaction usually can take place at 180 - 200 °C by addition of a titanium initiator [20, 22], as shown in Figure 2.1. Depending on the reaction temperature and the applied catalyst, the polymerization CBT to pCBT may range from a few minutes to several hours.

The properties of the pCBT depend strongly on the polymerization temperature. When isothermally polymerized below its melting point ($T_m = 220\text{-}267$ °C), the pCBT is highly crystalline and tends to become brittle due to a phenomena called cold-crystallization [63], as described in section 1.1.1. A subsequent melting and cooling brings back the more ductile behavior. The properties of initially reactively processed pCBT are largely unaffected after mechanical-thermal recycling (i.e. re-grinding followed by injection molding) [92]. Additionally, as shown in Figure 1.2, chemically recycling of pCBT is possible by de-polymerization into the cyclic oligomers or all the way into its monomers dimethylterephthalate and butanediol [39].

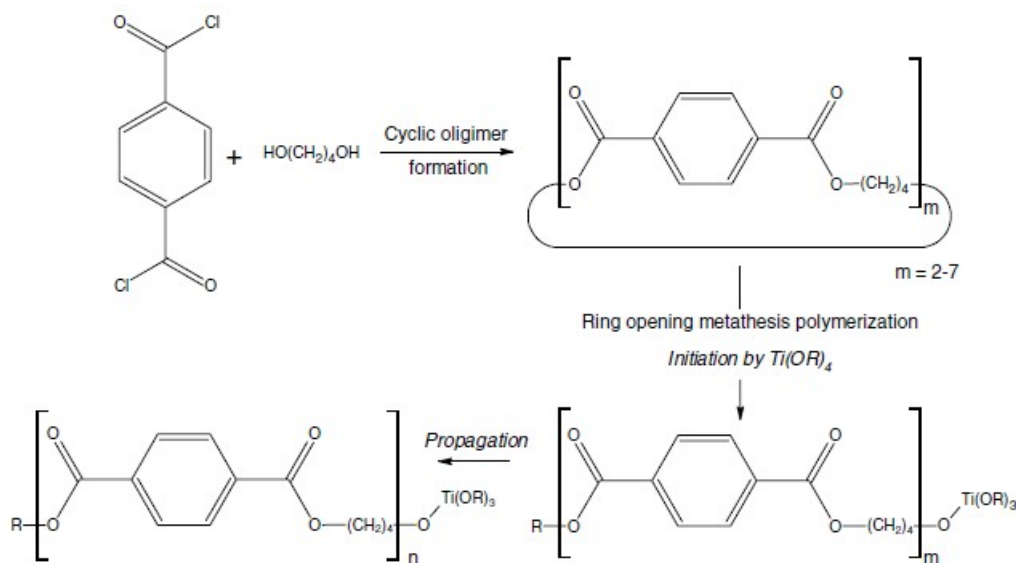


Figure 2.1.: Ring-opening polymerization of PBT [75]

2.1.3. Processing characteristics

Reactive processing of textile reinforced thermoplastics, has a lot in common with manufacturing of thermoset composites: a low viscosity mono- or oligomeric precursor is used to impregnate the fibers, followed by in-situ polymerization. After a certain degree of polymerization, the composite product is de-molded. With this method, textile reinforced thermoplastics can be manufactured through low pressure infusion processes such as Resin Transfer Molding (RTM), Structural Reaction Injection Molding (SRIM) and Vacuum Assisted Resin Infusion (VARI) which incorporates reactive processing with additional advantages like [102]:

1. Larger, thicker and more integrated product can be obtained than what is currently achievable with melt processing and,
2. A thermoplastic composite with a chemical fiber-to-matrix bond can be obtained, due to the fact that polymerization takes place around the fibers.

A few significant differences, however, should be considered first when applying the current production technology to in-situ polymerization of low molecule pre-polymers:

1. Simultaneous polymerization and crystallization is normally the case when processing of reactive thermoplastic materials with a semi-crystalline nature. The processing temperature has to be chosen such that polymerization and crystallization are well balanced because the crystallization in this case is adversely affected by temperature. When the temperature is too low, crystallization will be too fast so that the reactive chain ends with monomer get trapped inside crystals before they can polymerize. On the other hand, when the temperature is too high, the final degree of crystallinity will be reduced, which further decreases the strength, stiffness and chemical resistance of the polymer [65, 66, 76, 100].
2. Some reactive thermoplastic pre-polymers of PA6, PA12 and PBT have a melt viscosity about 0.01 Pa s [56, 79, 104], which is an order of magnitude lower than of common thermoset resins. As a consequence, the capillary forces occurring during impregnation of the fiber preform are significant and form a potential source for voids formation which is the direct cause to reduced moisture resistance of textile reinforced thermoplastics [79].
3. Heating equipment is necessary to keep the un-reacted mixture in the molten state, because at room temperature most thermoplastic precursors are solid granulate, whereas most thermoset resins are liquid.
4. Thermoplastic resin waste during processing such as reacted and un-reacted resin in tubes as well as waste from mechanical trimming such as flashes can be fully recycled when compared with thermoset resin.
5. As thermoset composites, the performance of thermoplastic composites also dependent on the fiber-to-matrix interface. Coupling agents have been developed for numerous thermoset composites resin to improve this bond. However, coupling agents specifically for reactive processing of thermoplastic

composites have not been developed yet, but have recently become a topic of interest [75].

6. The processing consumables such as the vacuum bagging films, resin transport tubes and sealant for VARI process are not commercially tailored for higher temperature applications as compared to the case for reactive processing of thermoset composites.

2.1.4. Crystallization structures of thermoplastics

Thermoplastics exhibit two types of morphology in the solid state: amorphous and semi-crystalline. As we can see in Figure 2.2, the molecules in an amorphous polymer are usually oriented randomly and are intertwined. Thermoplastics with ordered chains can only crystallize to a certain extent due to the high molecular weights and are therefore called semi-crystalline, meaning that some amorphous regions are always remain in a semi-crystalline polymer [55].

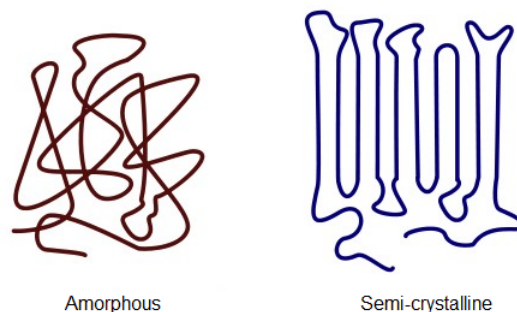


Figure 2.2.: The arrangement of molecular chains in amorphous and semi-crystalline polymers [55]

According to [115], the crystallization of thermoplastics occurs by insertion of chain units into a crystal unit cell (Figure 2.3(c)). Due to their length (up to 1000 nm) chains are never fully included into one unit cell, they belong to several successive ones as well. Therefore some adjacent unit cells are linked through covalent bonds,

while others are linked only by secondary forces. This is very different from metals where bonding forces in all directions are similar (metallic bonds).

Also due to their length, chains are almost never fully extended, even in crystalline phase. For this reason and also due to the kinetics of chain mobility, chains undergo folding after 10-100 nm, leading to the formation of lamellae about this thickness (Figure 2.3(b)). It is possible that polymer chains crystallize into two or more lamellae. These polymer chains, called tie-molecules, connect the different lamellae to each other by the amorphous phase and are very important for the mechanical properties of a semi-crystalline polymer. Stacks of lamellae linked by tie-molecules are often called fibrils.

Lamellae and fibrils grow from a stable nucleus and rapidly branch and buckle filling in the space all around. Their growth becomes radial from the nucleus leading to spherulites. Finally the spherulites impinge each other, resulting in a spherulitic superstructure, filling in the full sample (Figure 2.3(a)). It should however be remembered that there is always a quite large amount of material remains amorphous with lower density in between lamellae (tie-molecules), fibrils and at the border of spherulites.

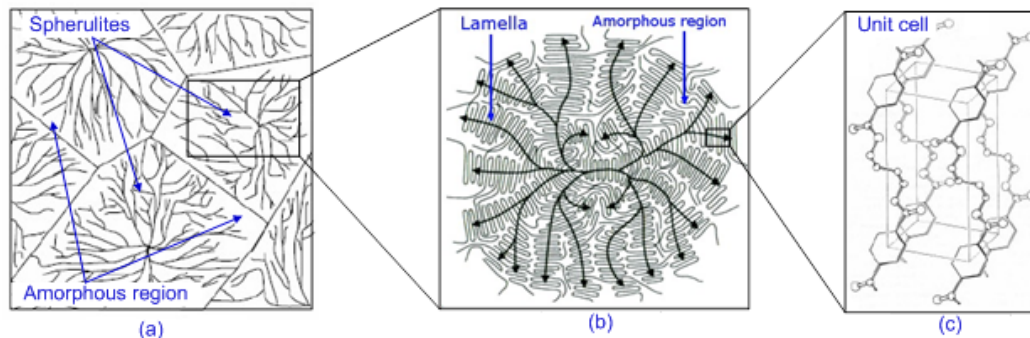


Figure 2.3.: Overview of organizational level in semi-crystalline polymers [115]

Most thermoplastics have crystalline regions alternating with amorphous regions. The amorphous regions contribute elasticity and the crystalline regions contribute strength and rigidity. Crystallinity, which is the fraction of the ordered molecules in polymer, is an important factor that can influence the main mechanical properties of

the polymer like the modulus, strength and toughness. Higher crystallinity results in a harder and more stable, but also more brittle material, whereas the amorphous regions provide certain elasticity and impact resistance [18].

2.1.5. Toughening mechanisms

Many semi-crystalline engineering polymers including PA, PBT and linear polyethylene exhibit very attractive strength and ductility at room temperature and under moderate rates of deformation. However, they become brittle under severe conditions of deformation such as low temperature or high strain rates, and can undergo a sharp ductile-to-brittle transition. In the brittle regime a crack can propagate with little resistance. Because of this poor performance at extreme conditions there has been considerable commercial and scientific interests in the toughening of semi-crystalline engineering thermoplastic [9, 11, 17, 16, 28, 59, 95]. In general, there are three basic routes of increasing toughness of semi-crystalline polymeric materials:

1. **By using non-isothermal production process** [9, 95]: The mechanical properties of a semi-crystalline polymer are influenced by the degree of crystallization and the size of the crystals, which both are determined by the thermal history of the polymer during processing. As a typical example, there is an effect of mold temperature on the mechanical properties of injection molded PBT as shown in Table 2.1 [116]. It is obvious that with increasing mold temperature the failure strain and the Izod impact strength decreases, however the tensile strength and the tensile modulus are increasing. This can be attributed to the crystal structure of PBT [9]. A higher mold temperature leads to a slower cooling and therefore longer time for crystallization, while the crystallization at lower mold temperatures is too fast to have crystal perfection. The crystals formed include a lot more defects which is in fact some amorphous materials present in between the crystals. Therefore, a higher amount of defects at lower mold temperatures will give a higher toughness, meaning a higher failure strain and Izod impact strength.

2. **By blending with soft particles and co-polymerization with soft polymer which changes the intrinsic properties of polymer** [28]: Blending with the soft particles is one of the most popular toughening mechanisms for brittle matrices. The soft particles, which can on one hand take up a lot of energy during loading and could on the other hand hinder the crystallization, have a great potential to influence the toughness of the brittle matrices. Typical examples of this toughening mechanism can be found in the research from Bartczak et al. [17], where high-density polyethylene (HDPE) was toughened by blending with rubber particles in the form of finely dispersed spherical inclusions with sizes well below 1 μm [17]. The incorporation of rubber into HDPE does not substantially change its crystallinity, but produces special forms of preferential crystallization around the rubber particles. As a result, the notch toughness of the rubber-modified HDPE increases by more than 16-fold [17]. As for the toughening mechanism by co-polymerization with soft polymers, the toughness of the brittle matrices will be influenced by either the introduced soft polymer chains or the hindered crystallization due to the non-regular polymer chains formed by co-polymerization. For instance, in-situ co-polymerization of CBT oligomers and ϵ - caprolactone (CL) was studied by Tripathy et al. [101]. The result indicates that the typical brittle nature of pCBT polymer can be eliminated by the incorporation of a small amount of CL. The stress-strain curve of pCBT/CL co-polymers shows a typical ductile behavior - a yield point, necking, and strain hardening until fracture. All of the co-polymers (pCBT/CL with weight mixing ratio of 50/50, 60/40, 70/30, 80/20) failed in a ductile manner with yielding and a high elongation at break. pCBT rich co-polymer (pCBT/CL with weight ratio of 70/30) shows yield and a maximum stress at break along with a high elongation.
3. **By reinforcing them with long and high-strength fibers, or by incorporation of fine particles** [11, 16, 17]: Both methods can reduce the overall plastic resistance of the polymers and are frequently used in engineering practice. The mechanism of those two toughening methods is the influence of structural imperfections and foreign particles size on the ductile - brittle transition which can be attributed to a competition between the brittle behav-

ior and the plastic response [17]. The brittle behavior is characterized by a brittle strength (σ_B) and considered to be nearly temperature independent and flaw-governed. While the plastic resistance, (Y), characterizing the ductile response, has substantial temperature and strain rate dependence. Therefore, for a given strain rate a ductile to brittle transition can be expected to occur at a temperature where Y rises above σ_B . This transition temperature increases with increasing strain rate due to the sensitivity of Y on strain rate. Furthermore, while σ_B relates to a tensile response, the plastic behavior responds to only a critical level of the effective (deviatoric) stress, σ_e . In the presence of sharp notches or cracks, individual stress components can be substantially augmented by a negative pressure in the notch field, while the effective stress producing plastic flow remains equal to Y . This, plus the significant elevation of Y itself due to the severe strain rate concentration around notches will lead to a remarkable increase in the brittle-to-ductile transition temperature. Consequently, when structural imperfections, such as notches, crack-like flaws or poorly adhering large foreign particles, are present in the material in the size range of about 10 μm , they will result in a brittle response of the material. However, if the structural imperfections are well controlled and foreign particles are only in the sub-micron range, the brittle strength of polymer can be increased somewhat to suppress the ductile-to-brittle transition to lower temperatures. Thus, when the yield strength falls below the brittle strength and plastic response is initiated, it often results in neutralization of the effect of some of the imperfections by molecular alignment or texture development that can significantly elevate the fracture stress across the principal direction of extension.

Table 2.1.: Mechanical properties of injection mold PBT with various mold temperatures [116]

Mold temperature	Tensile strength	Tensile modulus	Failure strain	Izod impact strength
[°C]	[MPa]	[GPa]	[%]	[J/mm ²]
20	53.8	2.53	197.7	55
40	55.4	2.60	167.3	48
60	56.8	2.69	70.4	44
80	57.5	2.72	45.3	39
120	58.1	2.69	31.8	40

2.2. Thermal and rheological analysis of matrix system

Thermal analysis is a branch of material science where the properties of materials are studied as they change with temperature. For polymeric composites manufacturing processes, it is extremely important that the thermal behavior of the resin matrix system should be understood thoroughly. For instance, the thermal analysis with Differential Scanning Calorimetry (DSC) can determine the curing properties of the resins used in composite materials, and confirm whether a resin can be cured and how much heat is evolved during that process as well. Another example is that the Thermogravimetric analysis (TGA) can be applied to measure the fiber fraction of composites by heating a sample up to the degradation temperature of the resin to remove it and then determining the mass remaining.

For in-situ polymerization of thermoplastic pre-polymers, the thermal analysis equipment such as DSC is also indispensable for analyzing polymerization and crystallization behavior. For this dissertation research, DSC, TGA and Dynamic Mechanical Analysis (DMA) were applied to study the thermal behavior of CBT resin matrix system and textile reinforced pCBT composites. The principle of those equipments are described in the following sections.

2.2.1. Differential Scanning Calorimetry (DSC)

DSC is a thermoanalytical technique in which the difference in the amount of heat required to increase the temperature of a sample and reference is measured as a function of temperature. Both the sample and the reference are maintained at nearly the same temperature throughout the experiment. Generally, the temperature program for a DSC analysis is designed such that the sample holder temperature increases linearly as a function of time. The reference sample should have a well-defined heat capacity over the range of temperature to be scanned.

The result of a DSC experiment is a curve of heat flux versus temperature or versus time as shown in Figure 2.4. Glass transitions may occur as the temperature of an amorphous solid is increased. These transitions appear as a step in the baseline of the recorded DSC signal. This is due to the sample undergoing a change in heat capacity; no formal phase change occurs. As the temperature increases, an amorphous solid will become less viscous. At some point the molecules may obtain enough freedom of motion to spontaneously arrange themselves into a crystalline form. This is known as crystallization temperature (T_c). This transition from amorphous solid to crystalline solid is an exothermic process, and results in a peak in the DSC signal. As the temperature increases the sample eventually reaches its melting temperature (T_m). The melting process results in an endothermic peak in the DSC curve.

The curve can be used to calculate enthalpies of transitions by integrating the endothermic/exothermic peaks (i.e. the crystallization transition as shown in Figure 2.4). It can be shown that the enthalpy of transition can be expressed using the following equation:

$$\Delta H = CA_t \quad (2.1)$$

where ΔH is the enthalpy of transition, C is the calorimetric constant, and A_t is the area under the transition curve. The calorimetric constant is a dependent variable on

the instrument, which can be determined by analyzing a well-characterized sample with known enthalpies of transition [70].

In this research, the DSC measurement was applied to determine the thermal behavior of CBT resin matrix and the CBT/binder blends. The melting of CBT resin, simultaneous polymerization and crystallization phenomenon, and the influence of binder on these behavior was studied. The apparatus used was DSC Q2000 from TA Instrument.

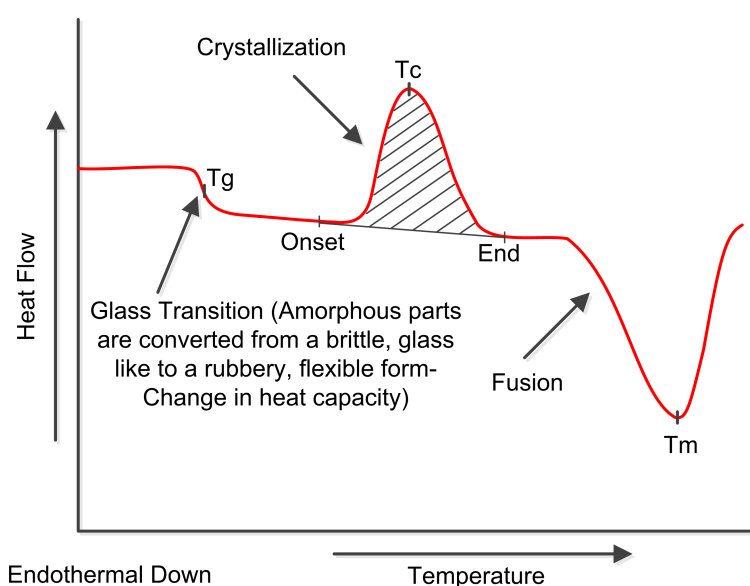


Figure 2.4.: Schematic representation of the DSC curve with the appearance of several common transitions

2.2.2. Thermogravimetric Analysis (TGA)

TGA is commonly used to determine selected characteristics of materials that exhibit either mass loss or gain due to decomposition, oxidation, or loss of volatiles (such as moisture). Common applications of TGA are (1) materials characterization through analysis of characteristic decomposition patterns, (2) studies of degradation mechanisms and reaction kinetics, (3) determination of organic content in a sample, and (4) determination of inorganic (e.g. ash) content in a sample, which may be

useful for corroborating predicted material structures or simply used as chemical analysis. It is an especially useful technique for the study of polymeric materials, including thermoplastics, thermosets, elastomers, composites, fibers and so on.

TGA relies on a high degree of precision in three measurements: mass change, temperature, and temperature change. Therefore, the basic instrumental requirements for TGA are a precision balance with a pan loaded with the sample, and a programmable furnace. The furnace is usually programmed for a constant heating rate. The sample is placed in a small, electrically heated furnace equipped with a thermocouple to monitor accurate measurements of the temperature by comparing its voltage output with that of the voltage-versus-temperature table stored in the computer's memory. A reference sample may be placed on another balance in a separate chamber. The atmosphere in the sample chamber may be purged with an inert gas to prevent oxidation or other undesired reactions.

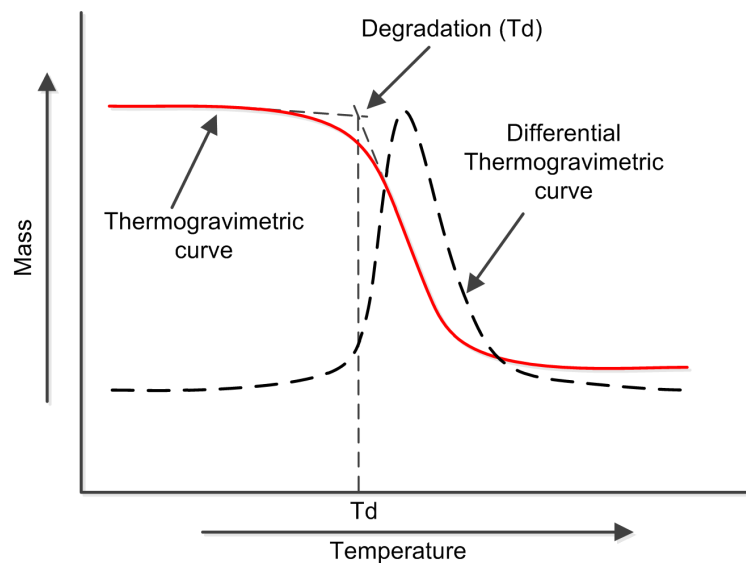


Figure 2.5.: Schematic representation of the TGA curve and the method of evaluation of T_d

The results from TGA may be presented by (1) mass versus temperature (time) curves, referred to as the Thermogravimetric curve, or (2) rate of mass loss versus temperature curve, referred to as the differential Thermogravimetric curve as shown

in Figure 2.5. The onset of intense thermal degradation T_d determined by the point of intersection of tangents to two branches of the thermogravimetric curve.

TGA measurement was used in this dissertation to determine the degradation temperature of processing materials and the thermal stability of processing materials at processing temperatures. The applied instrument is TGA Q5000 from TA Instrument.

2.2.3. Dynamic Mechanical Analysis (DMA)

DMA is a powerful analytical technique for studying the temperature and frequency-dependent behavior of polymeric materials. DMA can be used to determine fundamental transition temperatures, such as glass transition, and how that value changes with material formulation and conditioning. The mechanical response of different materials being considered for an application can be compared over the temperature range anticipated in service. More advanced applications for the DMA include stress-relaxation behavior and creep testing.

DMA measures the modulus (stiffness) and damping (energy dissipation) of materials as they are deformed under a small, usually sinusoidal, oscillating force. The sample is clamped into a frame of measurement heat and is heated by the furnace. The deformation amount generated by the sinusoidal force is detected. Viscoelastic values such as elasticity and viscosity are calculated from the applied stress and the strain, which is then plotted as a function of temperature or time as show in Figure 2.6. A wide range of materials can be characterized by DMA using the different deformation modes. DMA deformation mode has tension, compression, dual cantilever bending, 3-point-bending, and shear mode. The deformation mode is selected dependent on the specimen shape and modulus, and the measurement purpose.

DMA measurement is applied in this research to investigate the effect of the pre-forming binder on the dynamic mechanical properties of textile reinforced pCBT composites. The equipment applied was DMA Q800 from TA Instrument.

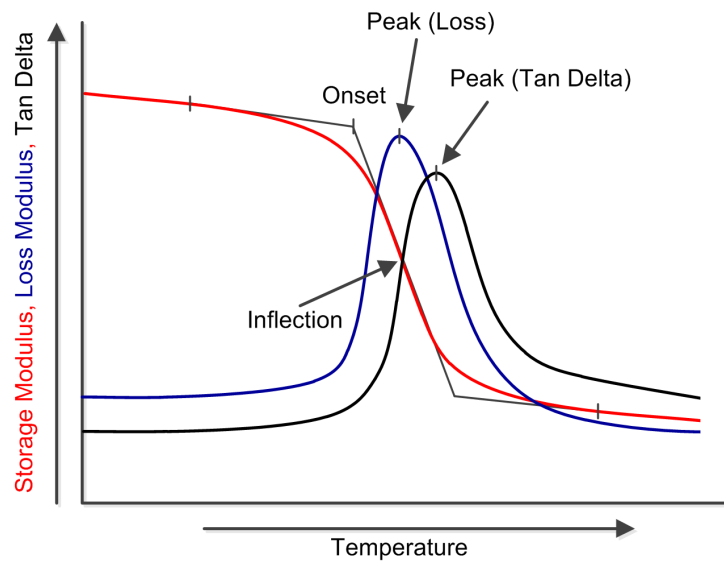


Figure 2.6.: Schematic representation of the DMA curve

2.2.4. Rheological analysis

For the technology of in-situ polymerization of low molecule pre-polymers for reactive processing of textile reinforced thermoplastic composites, the thermoplastic structure development is accompanied by enormous rheological changes: The resin changes from a thermoplastic solid to a low viscosity liquid, to a gel, and then to a stiff solid. Thus, the rheological properties are vitally important to successful processing. For instance, in structural laminate, resin flow properties influences void formation, manufactured part dimensional uniformity, and process economics. Therefore, it is essential that the rheological state at each stage of the process should be known to employ these materials effectively and economically.

The rheology of reactive thermoplastic pre-polymers can be studied using both steady shear and dynamical oscillatory tests. Steady shear measurements can characterize only the initial portion of a reactive thermoplastic pre-polymer's viscosity range. Near the gel point the steady shear viscosity increases rapidly and becomes unmeasurable. Eventually the stiffening sample fractures or tears. On the contrary, dynamic oscillatory measurements of the resin's viscosity can be made as the reaction proceeds through the gel point - and beyond - until the resin becomes a stiff

solid. This is possible because the measurements can be made at a strain amplitude low enough to prevent disruption of the gel structure as it is being formed. The comparison between steady shear viscosity data and dynamic viscosity data for a polymerizing pre-polymer is as show in Figure 2.7.

In this research, the viscosity of polymerizing CBT was studied by a rheometer AR2000 ex from TA Instrument. The effect of binder filling content on the processing window (processing time needed to reach the maximum process viscosity which is usually 1 Pa s) of CBT/binder blend system was investigated.

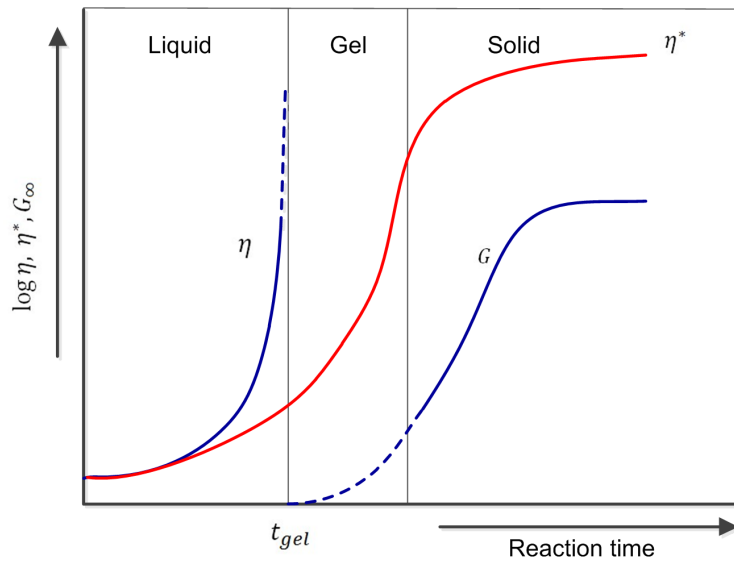


Figure 2.7.: Measurement of the viscosity of a polymerizing thermoplastic prepolymer

Chapter 3

Materials and methodology

In this chapter, the materials applied in this dissertation research are introduced, followed by the methodology which is taken to achieve the research objectives. The methodology is divided into three parts corresponding to the three key aspects as described in section [1.6](#)

3.1. Materials

3.1.1. Textile

Three kinds of textile reinforcements with epoxy sizing were used in this dissertation research. The first one, as shown in Figure [3.1](#), is a uni-directional fabrics PANEX 35 from ZOLTEK which has an average areal weight of 333 g/m². The second one, as shown in Figure [3.2](#), is a standard bi-axial carbon fiber non crimp fabric manufactured by Saertex GmbH, which has an areal weight of 530 g/m². The third one, whose fiber orientations, glass roving and area weight information are illustrated in Figure [3.3](#), is a tri-axial glass fiber non crimp fabric, provided by Institute of Textile Technology, RWTH Aachen, in the frame of scientific cooperation project DFG-AiF-Cluster "Leichtbau und Textilien".



Figure 3.1.: PANEX 35 uni-directional fabrics



Figure 3.2.: Saertex $\pm 45^\circ$ bi-axial carbon fiber non crimp fabric

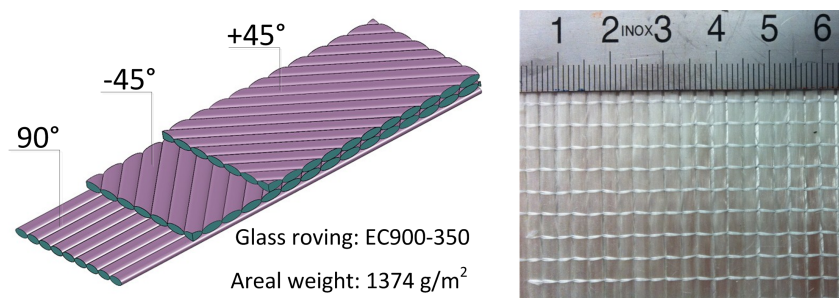


Figure 3.3.: Tri-axial glass fiber non crimp fabric

3.1.2. Matrix systems

A single component matrix system CBT160 and a two component matrix system CBT500, both in granular shape (Figure 1.1), were provided and purchased from Cyclic Corporation (Schwarzheide, Germany). The catalyst contained in CBT160 is FASCAT4101 (butyltinchloride dihydroxide, CAS 13355-96-9) which is pre-mixed in CBT500 for production of a single component product. Both CBT160 and CBT500 are low melt viscosity thermoplastic polyester resins that can be processed in typical composite processes including pultrusion, compression molding, Resin Transfer Molding (RTM), and Vacuum Assisted Resin Infusion (VARI). Through a reaction with the contained or introduced catalyst, both of them can be converted into pCBT with the same molecular structure as the engineering thermoplastic polyester polybutylene terephthalate (PBT). With extremely lower viscosity and good compatibility with all fiber types that are epoxy sized, CBT500 offers superior wet out and higher fiber loading with lower void content. These advantages provide better mechanical properties, and enhanced fatigue life, which makes CBT500 an excellent thermoplastic solution for the impending restrictions on the thermoset market.

As show in Figure 1.2, the number of butyl groups in the CBT oligomer mixture varies from two to seven, resulting in a melting range from 130 - 160 °C. Before processing, the oligomers should be dried at least 18 hours at 80 - 100 °C to remove residual moisture, which could interfere with the polymerization reaction according to the processing guide provided by Cyclics.

Most commonly, there are another two kinds of tin-catalysts, that is, FASCAT 4102 (butyltin tris-2-ethylhexanoate, CAS 23850-94-4) and TEGOCAT 256 (butyl(oxo)tin, CAS 51590-67-1), are used for polymerization of CBT500 besides FASCAT 4101 contained in CBT160. The reaction time required, for example, to reach 90 % conversion of CBT to pCBT, is different for the three catalysts and depends on the reaction temperature as shown in Figure 3.4. It is clear to see that the reaction speed of the three catalyst systems can be ordered as FASCAT 4101 > TEGOCAT 256 > FASCAT 4102 and the higher the temperature the faster the conversion to pCBT. The different performance of the catalyst can be attributed to the different

Sn concentration in the molecular structure of the three catalyst system as shown in Figure 3.5. Table 3.1 gives further information of pot life time and polymerization time of CBT500 with different catalysts.

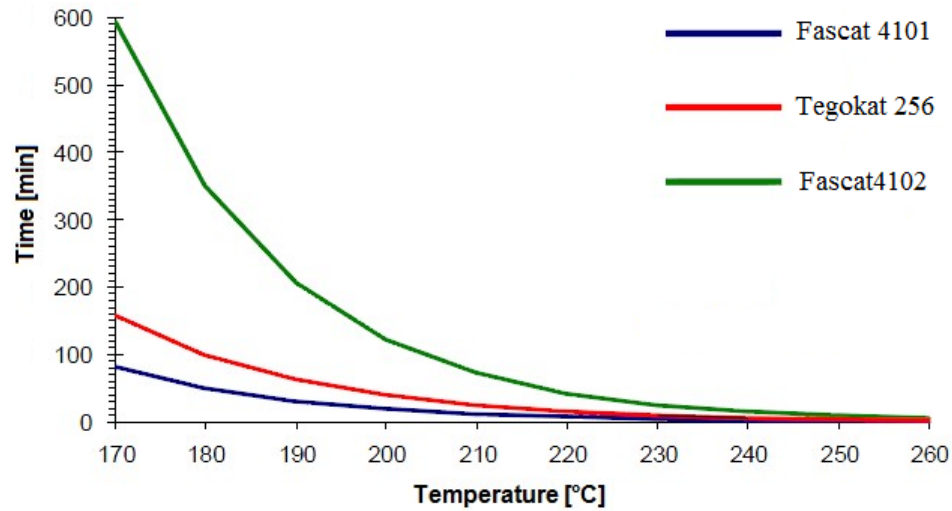


Figure 3.4.: Effect of catalyst and reaction temperature on the reaction time of CBT500 [27]

3.1.3. Preforming binders

To achieve an efficient and qualified manufacturing of textile reinforced pCBT composites with simultaneous binding and toughening concept, the application of appropriate preforming binder is the key factor that should be paid a special attention. A binder system, which has good adhesive properties and in the mean time good toughening potential, should be found out. In this dissertation, an epoxy powder binder EPIKOTE[®] Resin 05390 from HEXION special chemicals, was considered first due to the fact that pCBT can be toughened with a bi-functional epoxy resin described in [2] and the possible reaction between PBT and epoxy resin system reported in [111].

On the other hand, two additional commercial impact modifier systems were also applied as preforming binder for a better toughening performance. One of them is

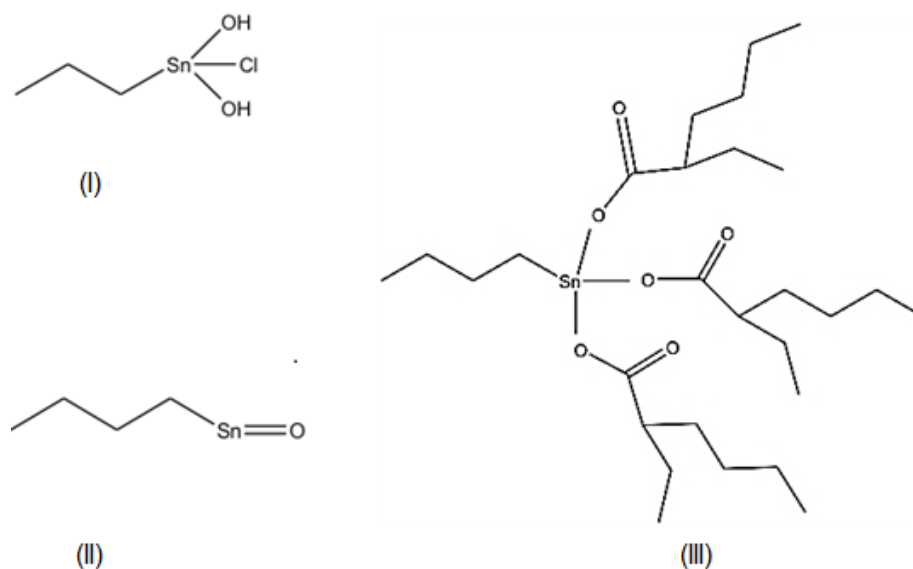


Figure 3.5.: Molecular structure of the various catalysts for CBT oligomers: (I) FASCAT4101, (II) TEGOCAT 256 and (III) FASCAT4102

Table 3.1.: Effect of different catalysts on the pot life time and polymerization time of CBT500 [27].

Catalysts	Pot life time	Form	Polymerization time
	185 °C, 0.3 mol % Sn*		200 °C, 0.3 mol % Sn
FASCAT 4101	10 min	Solid powder	45 min
TEGOCAT 256	30 min	Solid powder	4 hours
FASCAT4102	15 min	Liquid	6 hours

* % based on CBT. For the three catalyst 0.3 mol % Sn means about 0.2 wt.% for FASCAT4101, 0.1 wt.% for TEGOCAT 256, and 0.9 wt.% for FASCAT4102

LOTADEL[®] AX8900 resin (a random terpolymer of ethylene (E), methyl acrylate and glycidyl methacrylate (GMA)) in granulate form provided by Arkema France. Due to its reactive and soft properties, LOTADEL[®] AX8900 is a toughener of choice in order to improve the impact strength of engineering thermoplastics like PA, Polyesters (i.e. PBT, PET), PPS, etc. It can also be used as a compatibilizer for Polyesters/Polyolefins blends and as an adhesive for some laminate structures, which is exactly the case for bindered textile preforms.

The other one is a high efficiency acrylic toughening agent PARALOID EXL[®] 2314 in powder form supported by DOW Germany. Compared with the well established PARALOID EXL[®] 2000 and 3000 families of modifier for the engineering thermoplastics, PARALOID EXL[®] 2314 offers improvement in both efficiency and overall cost performance. Among its properties is a well defined rubber particle size which is not influenced by compounding conditions. With reactive functionality in the shell that reacts with polyesters, nylons, and epoxy resins, PARALOID EXL[®] 2314 can significantly improve the toughening performance. The specific shell chemistry allows the modifier particles to remain homogeneously distributed during the crystallization of semi-crystalline thermoplastics and therefore provides moldings with fully ductile behavior.

3.2. Methodology for key aspect I: Characterization of the processing materials

3.2.1. Compaction behavior of bindered textile preforms

Application background

For composites manufacturing processes, in particular Liquid Composites Molding (LCM) like Resin Transfer Molding (RTM) and Vacuum Assisted Resin Infusion (VARI), it is of great importance to understand the compaction behavior which describes the response of textile reinforcement under normal loading conditions. This compaction response of the textile reinforcement can affect both the manufacturing

parameters like permeability and the mechanical properties of the final product due to the variation of Fiber Volume Fraction (FVF).

In a typical RTM process a representation of the reinforcement stress profile, which can be obtained during a compaction experiment, is required in order to predict the distribution of forces applied to the RTM mold and thus to optimize the dimensioning of the tooling. Additionally, the Residual Preform Thickness (RPT), which is the difference between the initial preforms thickness and the permanent deformation after compaction, is also of great interest. This is because net shape preforms, which have nearly the same thickness as the impregnated parts, are essentially required in the cases where the cavity height can only be fixed so as to avoid complex mold design. In resin infusion processes like VARI, the permeability of the textile reinforcement is changing with the deformation of the textile reinforcement due to the use of flexible tooling. The impregnation of the textile reinforcement is then influenced by the variable permeability as a result of the variation of the FVF, which can be expressed as a function of the compaction pressure.

Several factors that influence the compaction and relaxation behavior such as preforming binder [5], saturated conditions [81], textile structure [49, 82], compaction temperature [112], etc. have been extensively investigated for the compaction behavior of traditional textile preforms under normal loading conditions. However, the influences from the preforming parameters (i.e. binder filling content, activation temperature and time) on the compaction behavior of bindered textile preforms under various processing conditions, which can be simulated in compaction experiments with various compaction temperatures, have been concentrated not enough adequate. It is extremely important that their compaction behavior should be understood thoroughly to achieve an effective process design. Therefore, in this dissertation research the effect of various compaction and preforming parameters on the interested performances such as Fiber Volume Fraction (FVF) and Residual Preform Thickness (RPT) were studied.

Characterization method

A lab based binding process as shown in Figure 3.6 was developed to prepare bindered textile preforms. With the help of an analysis (ISO 3310-1, 100 μm) sieve the required amount of binder was uniformly applied on the surface of the reinforcement. The amount of the binder is calculated as weight percentage referring to the weight of a single fabric layer. After applying binder, the other layer of reinforcement was put on the first layer with binder in between, leading to a symmetric preform configuration of $(+45/-45/90)_s$. Then the preform was laid carefully in a heated plate mold which was placed between two heated press plates to activate the applied binder with an activation temperature of 90 °C. The samples were cut and tested according to the characterization as described in section 3.2.1.

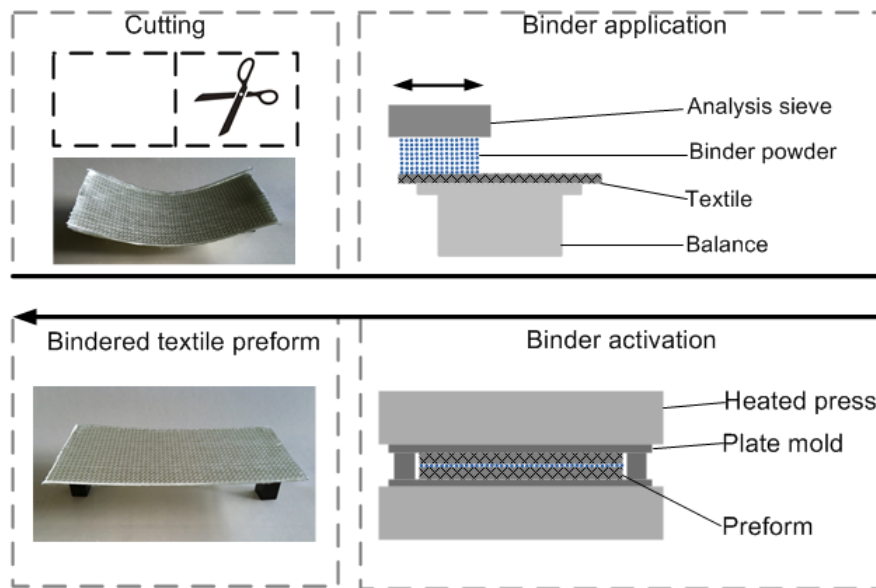


Figure 3.6.: Lab based binding process

To characterize the compaction behavior of textile preforms, one of the methods is to perform a compression test with an universal test machine such as ZMART.PRO from Zwick GmbH. The textile preforms are cut into compression test sample with a dimension of 70 mm \times 70 mm. A schematic description of the compaction equipment is shown in Figure 3.7. The samples can be tested under controlled tempera-

ture conditions. The compaction area is defined by the size of the steel plated (50 mm \times 50 mm) under the preforms. A pre-load of 400 Pa is usually used for the compaction experiment. The whole compaction process is divided into three stages which are compaction, holding deformation and release based on position control as shown in Figure 3.8. The FVF is calculated from the thickness data recorded during compaction experiment with the formula:

$$V_f = \frac{NA_f}{\rho_f h_p} \quad (3.1)$$

where N is the number of fabric layers, A_f is the fabric areal density, ρ_f is the fiber density and h_p is the preform thickness. The Residual Preform Thickness is the last data point recorded from the compaction experiment.

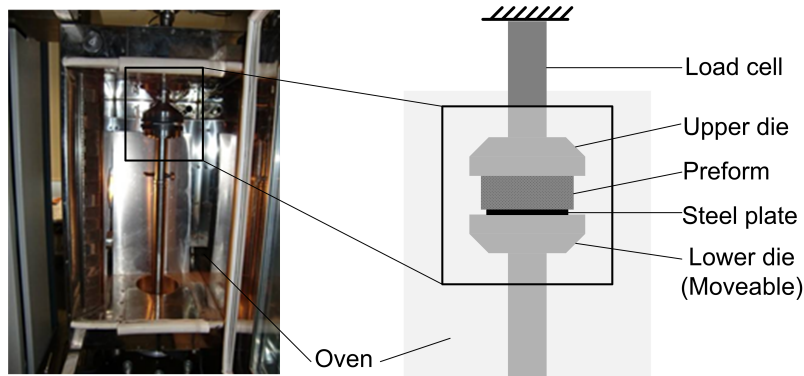


Figure 3.7.: Compression test

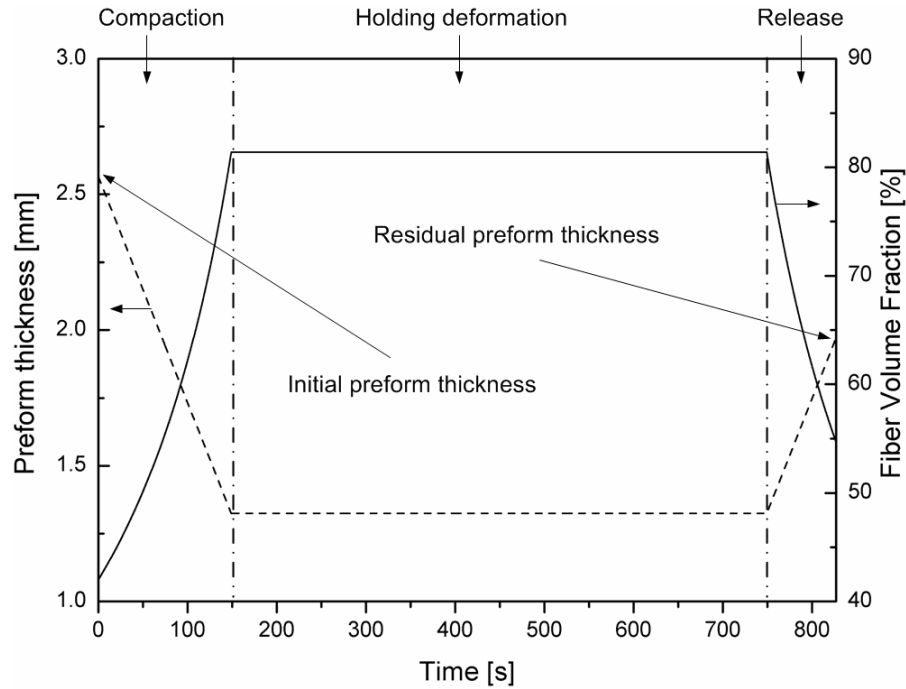


Figure 3.8.: Typical compression procedure

Numerical modeling

To identify the relationship between FVF and compaction pressure, a two parameter power law model was usually used to fit the experimental data [80]. During the investigation on a new sandwich textile reinforcement preforms developed for LCM processes, Luo et al. [49] used the two parameters power law model [80] and a dissipated energy method to model the compaction and relaxation behavior respectively. It was found that when evaluating the compressibility of the multi-mat, mat, and woven fabrics, it is necessary to take the relaxation into account. The fabric relaxation behavior can be understood in terms of volumetric dissipation energy and fabric stiffness. In order to create a model for inclusion in flow simulations of LCM processes, Kelly et al. [44] and Bickerton et al. [19] investigated the viscoelastic compaction behavior of textile preforms. The studied textile preforms have displayed complex time-dependent response, including loading hysteresis, stress relaxation, and strain rate dependent loading behavior under no resin

conditions. The significant influence of preform viscoelasticity was demonstrated by mold filling experiments [44]. The viscoelastic response and the difference in behavior between the dry and wet samples observed were incorporated into a model of textile reinforcement deformation in [19]. The sample model is then used for both compaction and relaxation phases, and matches well experimental data over a range of FVFs and compression speeds. Furthermore, a three parameter power law model applied in [45, 112] for modeling the compaction behavior of textile reinforced reinforcement in VARI process (compaction pressure lower than 0.1 MPa) was found to be better than the two parameter power law model used in [49, 80].

Design of experiment

1. Taguchi's method

Generally, a lot of experiments have to be carried out when the number of parameters increase [48, 113]. The traditional experimental design methods are too complex and difficult to use. In this context, Taguchi's experimental design method was adopted in this research to provide a simple, efficient and systematic approach for optimization of experimental design for performance quality and cost [89, 93]. In the theory of Taguchi, the deviations between the experimental value and the desired value can be calculated by a loss function, which can be further transferred into a signal-to-noise (S/N) ratio, η . Depending on the type of characteristics, there are usually three S/N ratios available: the nominal the better (NB), the higher the better (HB), and the smaller the better (SB). The S/N ratios for each type of characteristic can be calculated as follows [61]:

Nominal is the best:

$$S/N_{NB} = 10 \log \left(\frac{\bar{y}}{s_y^2} \right) \quad (3.2)$$

Larger is the better (maximize):

$$S/N_{HB} = -10 \log \left(\frac{1}{n} \sum_{i=1}^n \frac{1}{y_i^2} \right) \quad (3.3)$$

Smaller is the better (minimize):

$$S/N_{SB} = -10 \log\left(\frac{1}{n} \sum_{i=1}^n y_i^2\right) \quad (3.4)$$

where \bar{y} is the average of the observed data, s_y^2 is the variance of y , n is the number of observations, and y is the observed data. Regardless of the category of the performance characteristics, the greater S/N ratio corresponds to the better performance. Therefore, the optimal level of the process parameters is the highest S/N ratio.

2. Analysis of variance (ANOVA)

ANOVA is a powerful statistical tool that can be used to analyze the variations of the test results into components that are contributed by the different sources. It involves partitioning the total experiment variance to different factors, and even to combinations of different factors. Total sum of squares term can be defined as:

$$SS_T = \sum_{i=1}^n y_i^2 = SS_m + SS_e \quad (3.5)$$

where y_i is the i th observation, SS_m is the mean sum of squares and SS_e is the error sum of squares respectively.

SS_m and SS_e can be further calculated with Eq. 3.6 and 3.7:

$$SS_m = n_o \bar{y}^2 \quad (3.6)$$

$$SS_e = \sum_{i=1}^{n_o} (y_i - \bar{y})^2 \quad (3.7)$$

where n_o is the number of observations and \bar{y} is the mean of the n_o observations.

In case of ANOVA with two factors, when interaction effect of main factors affects output values, total variation may be decomposed into more component as:

$$SS_T = SS_A + SS_B + SS_{AB} + SS_e \quad (3.8)$$

where $SS_A = (A1 - A2)$ and $SS_B = (B1 - B2)$ are variations due to factors A and B , respectively. While SS_{AB} is the variation due to interaction of factors A and B .

While performing ANOVA, degree of freedom should be considered together with each sum of squares as well. In ANOVA studies with certain test error, error variance determination is very important. Obtained data are used to estimate F value of Fisher test (F -test). Total variation observed in an experiment attributed to each significant factor or interaction is reflected in percent contribution (P_{cont}), which shows relative power of a factor or interaction to reduce variation. Factors and interactions with substantial P_{cont} play an important role.

3. Experimental plan

Taguchi method was applied for planning the experiment in order to reduce the experimental effort. Experimental data during the compaction and release process were analyzed and modeled for correlation between the compaction and preforming parameters and the FVF and RPT. The analysis of signal-to-noise (S/N) ratio and variance (ANOVA) were performed to specify the relevance of compaction and preforming parameters according to their importance on the FVF and the residual preforms thickness. For the analysis of S/N ratio, the "HB" (Equ. 3.3) and "SB" (Equ. 3.4) ratios were selected respectively for FVF and RPT to obtain optimum compaction performance because higher FVF at specified compaction pressure and lower RPT after a compaction cycle are indications of better performance during compaction of textile preforms.

Table 3.2 indicates the compaction and preforming parameters (factors) and their values (levers). The factors chosen for the compaction experiments were: (1) compaction temperature (A), T_{comp} , (2) binder activation temperature (B), T_{act} , (3) binder content (C), c_b , and (4) binder activation time (D), t_{act} . Each parameter has

four levels, denoted 1, 2, 3 and 4 . Worth to mention is, a wider range of compaction temperatures starting from 25 °C up to 190 °C were considered for the corresponded four different material states of the binder including solid (25 °C), partly melted (60 °C), fully melted higher viscous (125 °C) and fully melted lower viscous (190 °C). The compaction behavior of bindered textile preforms was studied under the four material states of binder which can be further corresponded to different applications such as the highest level of 190 °C is considered for the in-situ polymerization of textile reinforced pCBT composites.

Table 3.2.: Compaction and preforming parameters used in the experiments

Levels	Factors			
	Compaction temperature	Binder activation temperature	Binder content	Binder activation time
	T_{comp} [°C]	T_{act} [°C]	c_b [wt.%]	t_{act} [min]
1	25	90	1	0.5
2	60	100	3	1.0
3	125	110	5	1.5
4	190	120	7	2.0

To reduce the experimental effort, orthogonal arrays, in which the columns for the independent variables are orthogonal to one another, are often employed in industrial experiments to study the effect of several control factors. In this study, an L_{16} orthogonal array with four columns and sixteen rows was used as shown in Table 3.3, where the FVF results were taken when the compaction pressure increases up to 0.2 bar, the RPT results were taken after one compaction cycle. Each experiment was conducted at least three times in order to ascertain the effect of material and test system variability. Since the influence of the interaction between the preforming parameters such as the activation temperature and the activation time on the results was not clear, a more complex interactive experimental design was not considered in the present study.

Table 3.3.: Experimental design using the L_{16} orthogonal array

Exp. No.	T_{comp} [°C]	T_{act} [°C]	c_b [wt.%]	t_{act} [min]
1	1 (25)	1 (90)	1 (1)	1 (0.5)
2	1	2 (100)	2 (3)	2 (1.0)
3	1	3 (110)	3 (5)	3 (1.5)
4	1	4 (120)	4 (7)	4 (2.0)
5	2 (60)	1	2	3
6	2	2	1	4
7	2	3	4	1
8	2	4	3	2
9	3 (125)	1	3	4
10	3	2	4	3
11	3	3	1	2
12	3	4	2	1
13	4 (190)	1	4	2
14	4	2	3	1
15	4	3	2	4
16	4	4	1	3

3.2.2. Thermal and rheological properties of processing materials

Conversion rate measurement

Polymerization experiments of CBT160 and CBT500 with the three catalysts were performed to study the conversion rate of CBT to pCBT. The effects from factors like polymerization temperature, applied catalyst type and its filling content on the conversion rate were investigated. The experiment was conducted with the reactant in a glass tube heated by oil bath under isothermal conditions. The polymerization process was interrupted after various time by quenching in ice water. The resultant was taken out of the glass tube after cooling and weighed to get the total weight (m_{tot}). The un-reacted CBT was removed by dissolving the resultant in 1,2-dichlorobenzene and filtrating the solution with filter paper. Insoluble substance

(pCBT) left on the filter paper was collected, dried and weighed (m_{pol}). Then the conversion rate can be calculated with:

$$DOC = \frac{m_{pol}}{m_{tot}} \times 100\% \quad (3.9)$$

For the solid powder catalyst, powder blends were prepared by mixing CBT500 powder with the catalyst powder (Fastcat4101 and Tegokat256) according to the defined weight ratios. For the liquid catalyst (Fastcat4102), the CBT500 powder was fully melted in the glass tube and then the amount of catalyst was added to initiate the polymerization reaction.

Differential Scanning Calorimetry (DSC)

DSC measurements were performed on DSC Q2000 device from TA Instrument. Experiments were run with samples ranging from 7 to 10 mg under nitrogen to prevent moisture and oxidative degradation. The aim of the measurements and the corresponding procedure are as follows:

1. To study the thermal behavior of materials (i.e. CBT500, FASKAT4102, EPIKOTE[®] 05390, PARALOID EXL[®] 2314 and LOTADEL[®] AX8900), the samples were first heated at a heating rate of 10 °C/min up to 250 °C and kept for 1 minute. Then the samples were cooled to 30 °C at a cooling rate of 10 °C/min .
2. To study the effect of binder content on the thermal behavior of reactive CBT500 system, the samples were heated at a 5 °C/min heating rate to 250 °C and kept for 1 minute. Then the samples were cooled down to 30 °C at a 10 °C/min cooling rate. In the end, the samples were reheated to 250 °C at a 10 °C/min heating rate.
3. To study the effect of binder system on simultaneous polymerization and crystallization process which occur after the melting of reactive CBT500, the sam-

ples were heated rapidly to 190 °C at a heating rate of 100 °C/min and held at this temperature until the trace back to baseline. Then the sample were cooled to 30 °C at a cooling rate of 10 °C/min. At the end, the samples were reheated to 250 °C at a heating rate of 10 °C/min.

Thermogravimetric analysis (TGA)

TGA measurements were performed on TGA Q5000 device from TA Instrument. Experiments were run with samples ranging from 7 to 10 mg under air environment to study the stability of materials under processing conditions. The aim of the measurements and the corresponding procedure are as follows:

1. To determine the degradation temperature of processing and composite materials the samples were heated in the dynamic mode from 30 °C to 600 °C at a heating rate of 10 °C/min. The weight of the sample as a function of temperature was recorded during the experiment.
2. To study the thermal stabilities of materials at processing temperature (i.e. 190 °C) the material was heated from 30 °C to the target temperature at a heating rate of 10 °C/min. The sample was then held in isothermal mode for 60 minutes. The weight of the sample as a function of time was recorded during the experiment.

Rheological analysis

Viscosity measurements were performed on AR2000ex plate-plate rheometer from TA Instruments to investigate the processing window (processing time needed to reach the maximum process viscosity which is usually 1 Pa s) of CBT/binder blends. Experiments were conducted with sample plates which have a diameter of 25 mm and a thickness of about 1 mm were prepared with a mixture of CBT500 and additives including catalyst and preforming binder. After drying at 80 °C over night to remove moisture, the rheological measurements were accomplished as follows:

1. The chamber of the rheometer was preheated to target temperature such as 185 °C. After equilibrating for 5 min the zero reference between the two plates was set. The distance of the two plates (geometry gap) was then defined for a gap height of 1 mm for the measurement;
2. Before inserting the dried sample, the gap was raised up (e.g. 4 mm) without opening the chamber so that the sample can be inserted easily and the time needed for going to the measurement geometry (1 mm) and the temperature stabilization can be synchronized as much as possible. In this way, the measurement can be started at the target temperature with small deviations ($< \pm 1$ °C) after performing a pre-shear and equilibrium for 30 seconds respectively.
3. The complex viscosity and its changes as a function of a time and temperature was recorded under time sweep step with a frequency of 1 Hz and a strain of 0.5 %.

3.3. Methodology for key aspect II: Development of the manufacturing process

3.3.1. Thermoplastic Vacuum Assisted Resin Infusion (T-VARI)

To manufacture textile reinforced pCBT composites, the traditional VARI process for thermoset resins should be modified according to the processing characteristics of reactive processing of thermoplastics described in section 2.1.3. The modified VARI for thermoplastic pre-polymers should include following features:

1. A resin melting, mixing, and transfer unit with a heating capacity up to 250 °C. The catalyst should be mixed with CBT500 homogeneously without dramatic temperature fluctuation before resin infusion. The transfer unit should provide a constant temperature environment so that the resin can not be cooled down or overheat during transfer;

2. A heated molding plate with a heating capacity up to 250 °C, which can be used for isothermal processing conditions;
3. A suitable mold release agent or de-molding concept for nondestructive and easy de-molding and good surface finish;
4. A temperature resistant (at least until 205 °C) and economical flexible mold (vacuum bag), if possible, also reusable.
5. A controlled reaction environment for polymerization;

With these features the T-VARI manufacturing process was successfully developed for textile reinforced pCBT composites. Unidirectional carbon fabric and bi-axial non crimp carbon fabric reinforced pCBT laminate were manufactured for characterization of the developed production process. Typical properties of the composite system such as thermal and mechanical properties were presented to study the performance of the developed T-VARI manufacturing process.

In addition, impregnation quality of the composite laminate was studied by the cross section morphology of textile reinforced pCBT composites. The microscopical information was captured with digital microscope VHX-500F from Keyence. The specimens were cut, mounted and polished before investigation.

3.3.2. Thermal and mechanical behavior of composite system

Thermal analysis

Textile reinforced pCBT composite samples were prepared and characterized with DSC and TGA to investigate the melting/crystallization behavior and thermal decomposition of the composite system.

Dynamic Mechanical Analysis (DMA)

DMA measurements were performed on DMA Q800 device from TA Instrument. Experiments were run with samples which have a size of about 20 mm \times 10 mm \times 2 mm (Single cantilever) and 50 mm \times 10 mm \times 2 mm (Three point bending). The aim of the measurements is to study the effect of the preforming binder and the processing parameters on the dynamic mechanical properties of textile reinforced pCBT composites. The samples are subjected to a temperature scan from -25 °C to 220 °C with a ramp of 2 °C/min. A fixed strain of 5 μ m and frequency of 1 Hz were used in the measurement.

3.3.3. Simultaneous binding and toughening concept

Preparation of the composite laminates

According to the description in section 1.2 and 1.3.3, the proposed simultaneous binding and toughening concept is actually an ex-situ toughening process with textile preforming binder. When an appropriate binder was applied, the toughness of textile reinforced pCBT composite laminate could definitely be improved as a result of the local toughening effect contributed by ex-situ toughening. To validate this expectation, i.e. the effectiveness of simultaneous binding and toughening concept, the epoxy powder preforming binder EPIKOTE[®] Resin 05390 was applied first as binding and toughening agent (section 3.1.3). In the mean time the same binder was applied as toughening agent for in-situ toughening process, where the binder was directly mixed with molten CBT resin before infiltration. According to the procedure illustrated in Figure 3.6, the bindered textile preforms were prepared by the glass fiber tri-axial non crimp fabric with the symmetric stacking sequence of [90/ - 45/ + 45]_s.

Characterization of the flexural properties

Flexural testing is an important part of the characterization process of any material because the test results provide relevant information for how the material will behave under real-world conditions. Especially for composite materials, which are often used in aerospace, automotive and energy applications, it is critical to understand how much flexure the material has and maintain its strength.

Most commonly a bar of rectangular cross section rests on two supports and the load is applied to the center by the loading nose between the supports, producing a three point bending at a specified rate. The parameters for this test are the support span, the speed of the loading, and the maximum deflection for the test. These parameters are based on the thickness of the test specimen and are defined in a standard such as ASTM D 790 where the test is defined to stop when the specimen reaches 5 % deflection or the specimen breaks before 5 %.

The flexural stress, σ_f , is the stress in the outer fibers at midpoint. It can be calculated by solving the following equation when the support span-to-depth ratio greater than 16 to 1 (in this research, 32 to 1) according to [8]:

$$\sigma_f = \left(\frac{3PL}{bh^2}\right)\left[1 + \frac{3}{2}\left(\frac{D}{L}\right)^2 - \left(\frac{h}{L}\right)\left(\frac{D}{L}\right)\right] \quad (3.10)$$

where P in N is the applied load at a given point on the load-deflection curve, L in mm is the half of support span, b in mm is the width of the specimen, h in mm is the depth of the specimen, and D in mm is the deflection of the center-line of the specimen at the middle of the support span.

The flexural strain, ϵ_f , is the nominal fractional change in the length of an element of the outer surface of the test specimen at mid-span, where the maximum strain occurs. It may be calculated for any deflection with [8]:

$$\epsilon_f = \frac{3Dd}{2L^2} \quad (3.11)$$

where D , d , and L has the same meaning as state in Eq. 3.10.

Figure 3.9 shows typical stress-strain curves during a three point bending test for a) a brittle material that breaks before yielding, b) a ductile material that yields and then breaks before the 5 % strain limit, and c) shows a strong material that is not ductile that neither yields nor breaks before 5 % strain.

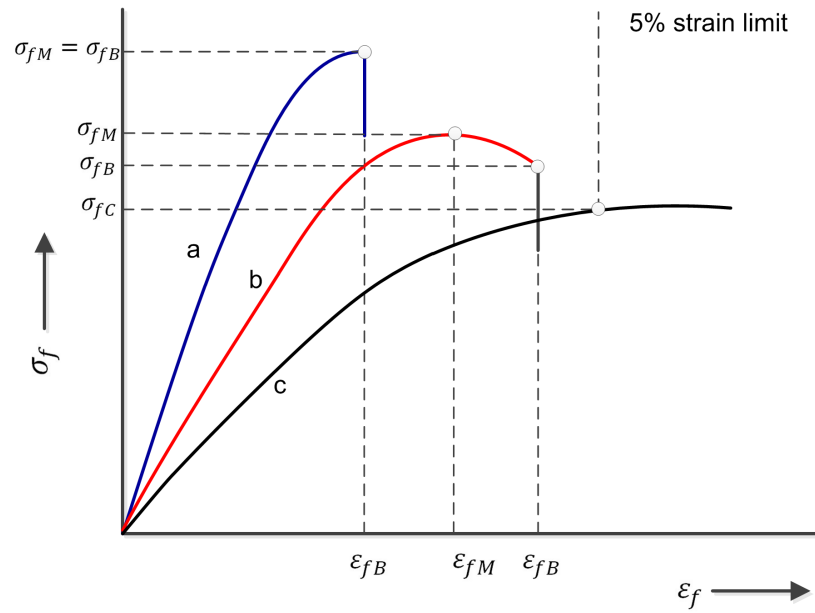


Figure 3.9.: Typical stress-strain curves during three point bending test, where σ_f is the flexural stress, ϵ_f is the flexural strain, σ_{fM} is the flexural strength, σ_{fB} is the flexural stress at break, σ_{fC} is the flexural stress at 5 % strain limit. ϵ_{fM} is the flexural strain corresponding to flexural strength, ϵ_{fB} is the flexural strain at break [8].

Flexural properties of the composite laminates prepared with the two concepts were determined on a universal material testing machine (Zwick GmbH Co. KG, Ulm) using three point bending test according to ASTM D790. A 2.5 kN load cell was integrated to measure the flexural force at a loading speed of 3.41 mm/min. The flexural modulus, the flexural strength, and especially the flexural strain at break which indicates the toughness of the laminate were investigated.

3.3.4. Influence of process parameters

For the simultaneous binding and toughening concept, the introduction of preforming binder leads to a more complicate manufacturing process. Because the preforming binder has an influence on the material properties such as compaction behavior of the textile preforms (section 4.1), and thermal and rheological behavior of matrix system (section 4.2). As a result, the composites mechanical properties will be changed as well due to the different infiltration behavior and different polymerization and crystallization conditions. Therefore, it is necessary to study the influence of process parameters for a better process design.

Generally, scientific experiments can be classified into two broad categories, namely, single factor experiments and multi-factor experiment. In a single factor experiment, only one factor varies while others are kept constant. In these experiments, the treatments consists solely of different levels of the single variable factor, which is very helpful to determine the influence of the single variable factor. In this part process parameters that have a possible effect on the composites flexural properties were first analyzed. Then the single factor design method was applied to study the influencing mechanism of a single process parameter on the flexural properties while other parameters being held constant. A higher flexural strain at break while the flexural modulus and flexural strength are not significantly changed is considered as the optimal performance for the textile reinforced pCBT composites. The flexural properties were determined according to the procedure in section 3.3.3.

3.4. Methodology for key aspect III: Optimization of the manufacturing process

3.4.1. Influence of preforming binders and toughening concepts

Inter-laminar fracture properties

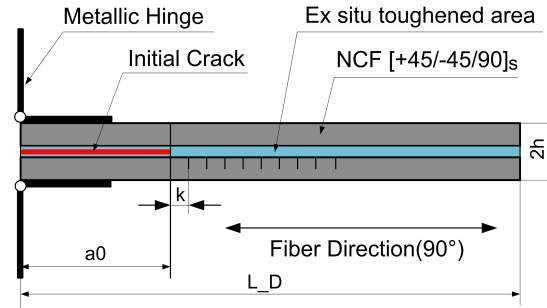
Inter-laminar fracture (delamination) is a serious failure mode for laminated composite structures. Delamination occurs due to high out of plane loads where no fibers are present to resist loading. Delamination can occur from tensile, shear loads, or a combination of the two. Accordingly, the methods developed to characterize the inter-laminar fracture properties of composite laminate including mode I (tensile), mode II (shear) and the mixture of mode I and mode II.

In this research, the inter-laminar fracture toughness of textile reinforced pCBT laminates was investigated under mode I and mode II deformation. The related testing specimens and procedure and the results evaluation involved in the two deformation modes are hereby described as follows:

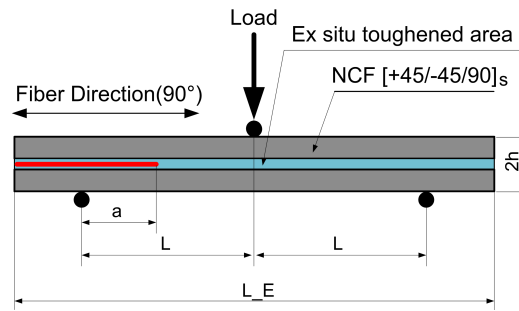
1. Testing specimens and procedure

Double Cantilever Beam (DCB) specimen and End Notch Flexure (ENF) specimen were employed for inter-laminar fracture under mode I and mode II deformation, respectively. The specifications and dimensions of the DCB and ENF specimens are shown in Figure 3.10 and Table 3.4. The initial crack formed in the middle plane of the laminate was made by inserting a Teflon film with a thickness of 25 μm into the stacking process of the laminate.

The universal material testing machine was also applied for the DCB and ENF test with the same load cell to measure the applied load. The DCB and ENF tests were performed with a cross-head speed of 3 mm/min and 3.41 mm/min, respectively. For each type of laminate, three specimens for the DCB test and five specimens for the ENF test were conducted to ascertain the effect of material and test system variability.



(a) Specimens for DCB test



(b) Specimens for ENF test

Figure 3.10.: Mode I and mode II specimens

Table 3.4.: Dimension of DCB and ENF specimens

DCB specimens	Value	ENF specimens	Value
Length: L_D (mm)	150	Length: L_E (mm)	80
Width: b (mm)	20	Span length $2L$ (mm)	60
Depth: h (mm)	1.80-1.99	Width: b (mm)	10
Crack length: a_0 (mm)	40	Depth: h (mm)	1.80-1.99
Test length: k (mm)	5	Crack length: a_0 (mm)	15

2. Calculation of fracture toughness for the DCB test

The energy release rate for mode I deformation of the DCB specimen is given by the following equation according to the modified compliance calibration method [4, 7]:

$$G_I = \frac{3P_d^2 C_d^{2/3}}{2A_1 b h} \quad (3.12)$$

where C_d is the compliance of the crack opening displacement (COD) and h and b are the depth and width of the specimen, respectively. P_d is the load applied on the end section of the DCB specimen. A_1 is the coefficient derived by the linear approximation of following equation:

$$\frac{a}{h} = A_1 C^{1/3} + A_0 \quad (3.13)$$

where a is the crack length. A typical example of this linear approximation was shown in Figure 3.11. Therefore, mode I fracture toughness of the glass fiber non-crimp fabric reinforced pCBT specimen can be estimated from measurement of the applied load, COD compliance, and crack length in the DCB test.

Experimental values of the compliance were determined using the following equation:

$$C = \frac{\delta_{exp}}{P_d} \quad (3.14)$$

where P_d is the critical load associated with the crack arrest, and δ_{exp} is the crack opening displacement determined at the loading point.

The crack length was determined visually by observing the crack growth along the edge, on which key points were marked every 5 mm from the end of the initial crack until the crack length reaches a pre-defined length which is 40 mm in this research. When the delamination front reaches the key points, the corresponding COD was

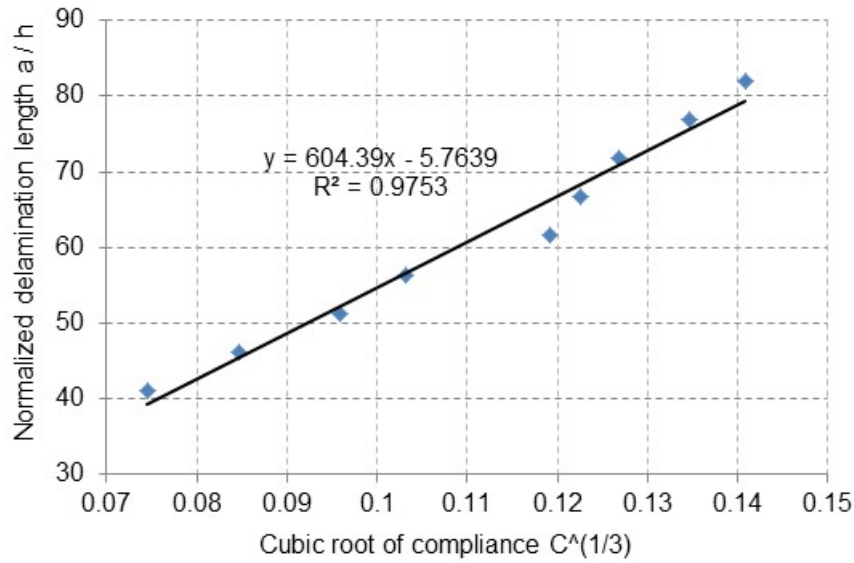


Figure 3.11.: Modified compliance calibration

marked on the load versus opening displacement trace in the sequence a_1, a_2, \dots, a_N as shown in Figure 3.12.

3. Calculation of fracture toughness for the ENF test

When a crack extension from an initial crack length of length a to a final length $a + \delta_a$ occurs in mode II loading condition, the Mode II strain energy release rate, G_{II} , is given by [52], as Equ. 3.15:

$$G_{II} = \frac{P^2}{2b} \frac{dC_e}{da} \quad (3.15)$$

The relationship between the compliance C_e , and the delamination length a is:

$$C_e = \frac{2L^3 + 3a^3}{8E_1bh^3} + \frac{1.2L + 0.9a}{4bhG_{13}} \quad (3.16)$$

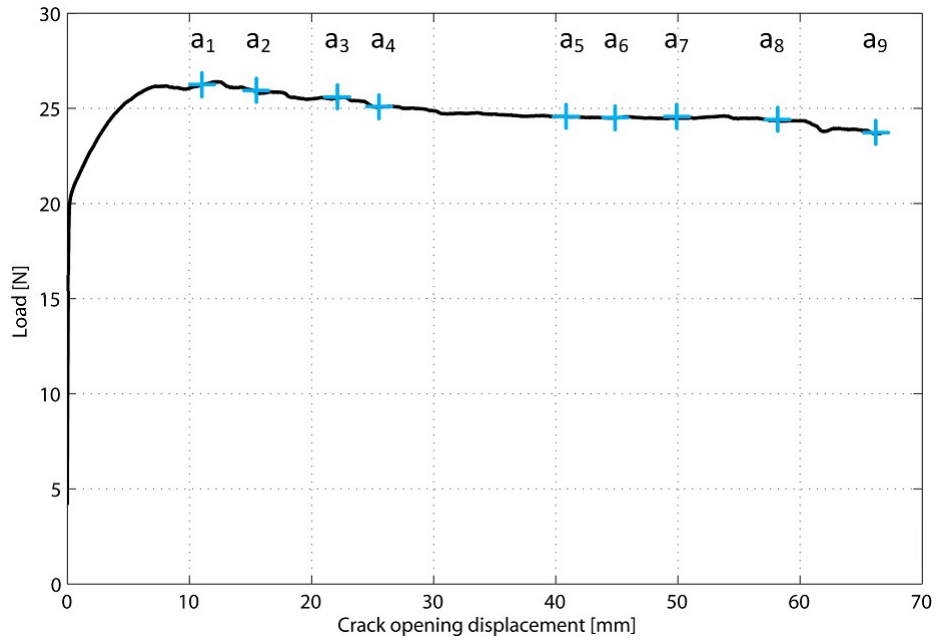


Figure 3.12.: Load displacement trace from the DCB test

Where L is the half span, and E_1 and G_{13} are the flexural and inter-laminar shear modulus, respectively. Substitution of Equation 3.16 into Equation 3.15 yields:

$$G_{II} = \frac{9a^2P^2}{16E_1b^2h^2} \left[1 + 0.2 \left(\frac{E_1}{G_{13}} \right) \left(\frac{h}{a} \right)^2 \right] \quad (3.17)$$

According to [50, 51, 52], the contribution of the inter-laminar shear stresses on the G_{II} is of the order of 2 %. Therefore, the second term in Equation 3.17 can be neglected and the simplified expression for the Mode II fracture toughness is:

$$G_{II} = \frac{9a^2P^2C_e}{2b(2L^3 + 3a^2)} \quad (3.18)$$

Together with the experimentally determined values of the load P , and the compliance C_e , the G_{II} can be calculated with Equ. 3.18. According to the theory of linear fracture mechanics [52] the load P can be substituted with the critical load P_m

which is the maximum load when the delamination extends from the initial point. The compliance C_e can be determined with the displacement at the central loading pin divided by the critical load P_m rather than estimated from the first term of Equ. 3.16. In this way, the error, which is because of neglecting the inter-laminar shear stress, is further reduced.

Optimization scheme

For further improvement of flexural strain at break, it is necessary that the binder should be optimized for the proposed simultaneous binding and toughening concept. Therefore, two additional impact modifiers (subsection 3.1.3) usually applied for toughening of polyester resins were selected in this study for a better toughening performance.

The three binders were used for preparing bindered textile preforms with various filling contents. Powder binders were applied according to the procedure in Figure 3.6. For the granulate binder LOTADEL[®] AX8900, a thin binder film (Figure 3.13) with define area weight was prepared first by compression molding, which was then insert between the symmetrically configured tri-axial textile fabrics. Especially, the silicon paper was applied here to enable a successful preparation of the binder film.

Worth to mention is, an isothermal processing temperature of 205 °C was chosen for this investigation so that the binder could have enough interaction time with pCBT before crystallization. This is because semi-crystalline polymers tend to crystallize slower at the temperatures in the vicinity of melting point (The melting point of pCBT is about 225 °C). Compared with the isothermal processing temperature of 185 °C applied in section 5.2), the polymerization from CBT to pCBT is faster at 205 °C but the crystallization of polymerized pCBT slows down [87]. As a result, the pure pCBT matrix polymerized at 205 °C is usually tougher than the one polymerized at 185 °C [65]. For the textile reinforced pCBT composites manufactured isothermally at 205 °C with simultaneous binding and toughening concept, a binder which can further improve the toughness of composite laminate com-

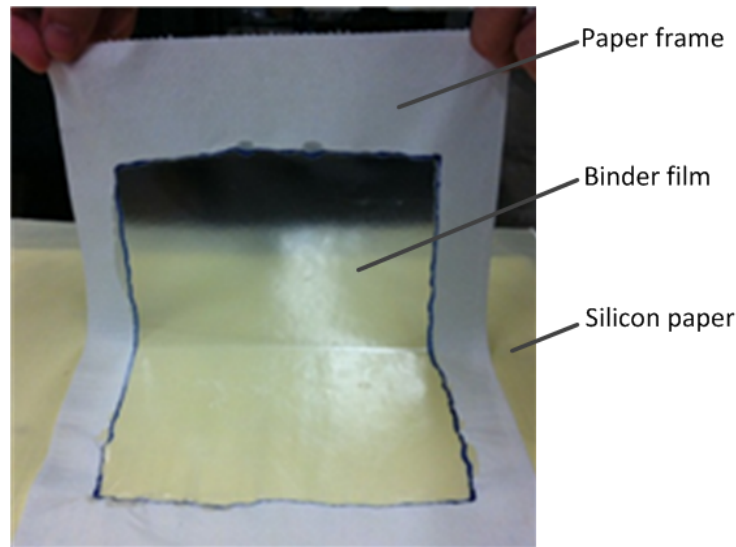


Figure 3.13.: Thin binder film made from LOTADEL[®] AX8900 granulate prepared by compression molding

pared with the reference one without filling binder can be considered as an effective toughening agent for pCBT. This is due to the fact that the binder is not only limited as a filler for hindering the molecular alignment and therefore the crystallization process, but a co-polymerization with pCBT is possible that irregular side chains might be formed.

Inter-laminar fracture properties were characterized to examine the toughening performance of the three binders. The one with the best toughening performance was validated in the optimum processing conditions. Experimental details are given in the following text.

As described in section 3.4.1, the inter-laminar fracture properties of textile reinforced pCBT laminates were investigated under mode I and mode II deformation. Inter-laminar fracture toughness in Mode I and mode II were evaluated by a standard double cantilever beam (DCB) test and an end notched flexure (ENF) test based on a three-point bending test, respectively.

Mode I and mode II specimens of textile reinforced pCBT laminates were prepared with the developed T-VARI system. For each test mode, three kinds of laminates were prepared:

1. The first one is **the reference laminate with no binder** both in the textile preforms and in the molten resin.
2. The second one is **the laminate with binder in the inter-ply region** (simultaneous binding and toughening concept).
3. The third one is the laminate with **binder not in textile preforms but pre-mixed in molten resin before impregnation** of dry textile preforms (in-situ toughening concept).

The fracture surface after fracture tests was analyzed by SEM to consider the fracture mechanism of crack propagation in textile reinforced pCBT laminates. Samples were cut from the fracture surface in size of 10 mm \times 5 mm. After cleaning with pressure air the samples were mounted on aluminum stubs. The fracture surfaces of the samples were then sputter coated with a thin layer of gold to avoid electrical charging. The micro-graphs were taken at a 15 kV acceleration voltage at various magnifications using a REM CamScan CS4 scanning electron microscope. The effect of binder type, filling content and manufacturing concept on fracture properties under mode I and mode II deformation mode were studied.

3.4.2. Verification and further optimization trials

According to the results from mode I and mode II measurements, the PARALOID EXL[®] 2314 binder, which has the best toughening performance among the studied three binders, was verified with the processing conditions according to section 5.2. Flexural properties were determined for the samples from the verification experiment and compared with the results from section 5.2.

Additionally, a variant of simultaneous binding and toughening concept, where the binder is not only used for bindered textile preforms but also mixed with CBT500

resin, was attempted for further improvement of composite toughness. The purpose of this experiment is to combine the advantages of in-situ and ex-situ toughening concept. The advantage of in-situ concept is global toughening that the matrix of the whole laminate can be toughened. The problem is the increase of the matrix viscosity and the decrease of mechanical properties [12]. The ex-situ toughening is local toughening that specially applied for the weakest inter-ply regions of the laminate. The mechanical properties of the laminate can not be significantly altered due to the matrix of the intra-laminate regions is not greatly influenced, which is also the reason for limited toughening. The experiment according the variant was performed with a small amount of in-situ toughening binder mixed in the molten CBT500 resin and the bindered textile preforms. Composite laminates were manufactured and the flexural properties were determined according to the method detailed in section 3.3.3.

Chapter 4

Key aspect I: Characterization of the processing materials

Simultaneous binding and toughening has been proposed for an efficient and qualified manufacturing of textile reinforced pCBT composites, which is supposed to be achieved in Thermoplastic Vacuum Assisted Resin Infusion manufacturing process with bindered textile preforms. Therefore, it is extremely important that influence of the preforming binder on the compaction behavior of the bindered textile preforms and the thermal and rheological properties of the catalyzed CBT oligomers should be studied. The effect of compaction and preforming parameters on the Fiber Volume Fraction (FVF) and the Residual Preform Thickness (RPT) of bindered textile preforms during a compaction experiment was investigated by using Taguchi method. Four compaction and preforming parameters of compaction pressure, binder activation temperature, binder content and binder activation time were selected and optimized with respect to the FVF at specified compaction pressure and RPT after compaction. Thermal and rheological investigations were conducted respectively with Differential Scanning Calorimetry (DSC) and plate-plate rheometry. The results from this chapter can be taken as the cornerstone for the entire solution strategy as shown in Figure [4.1](#).

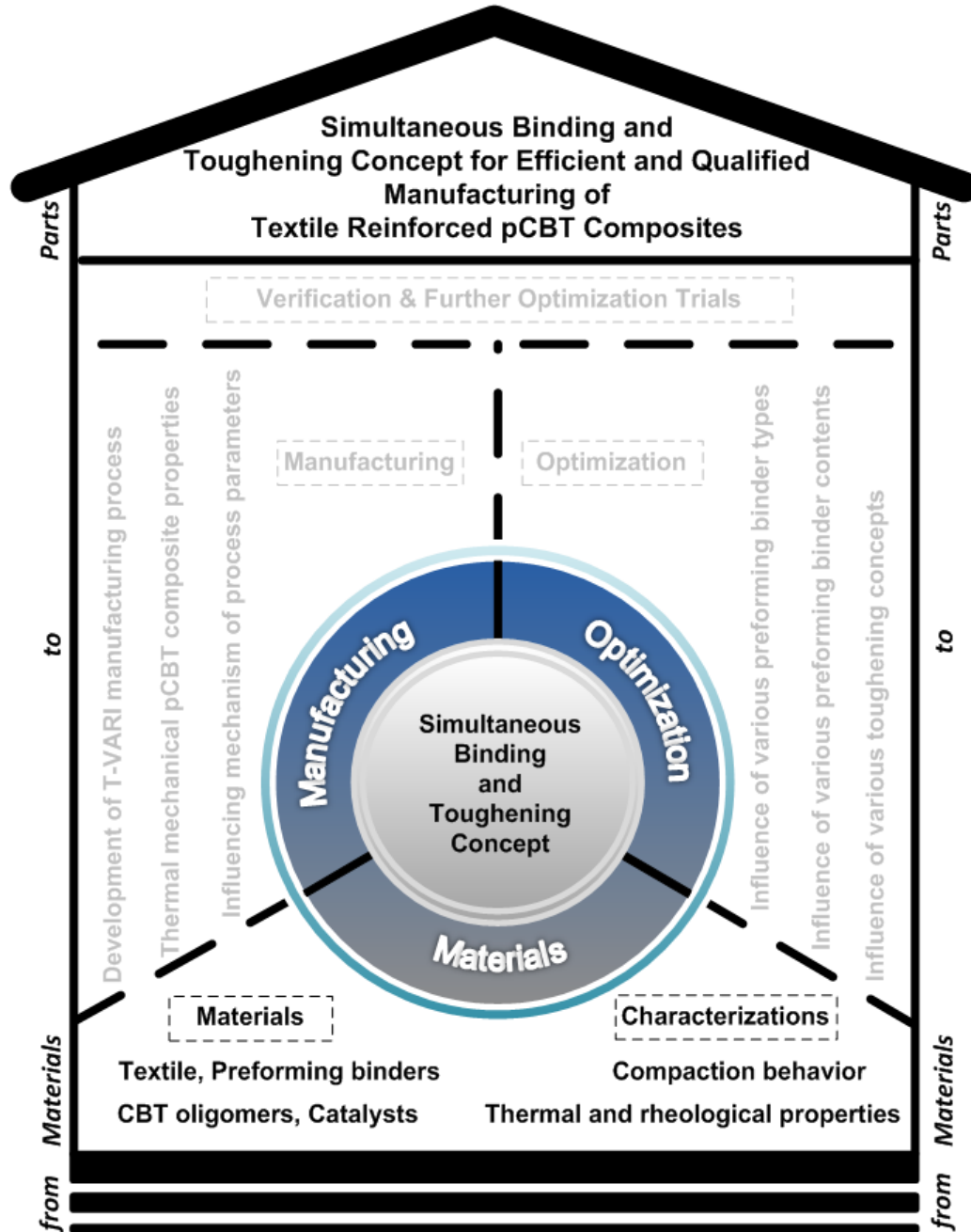


Figure 4.1.: Solution strategy: Cornerstone

4.1. Compaction behavior of bindered textile preforms

4.1.1. Fiber Volume Fraction (FVF)

The experimental results for the FVF, corresponding standard deviation and S/N ratios are as shown in Table 4.1. The mean S/N ratio for each level of the parameters was calculated and summarized in Table 4.2. Additionally, the total mean S/N ratio is computed by averaging the total mean S/N ratios. Based on the data presented in Table 4.2, the optimal compaction performance for FVF was obtained at 190 °C compaction temperature (Level 4), 90 °C binder activation temperature (Level 1), 3 % binder content (Level 2) and 0.5 min binder activation time (Level 1) settings. Figure 4.2 and 4.3 shows the comparison of the predicted and actual as well as residual S/N ratios for the FVF using regression analysis. Most of the points are close to the line and the deviations are very small and negligible. With respect to the coefficient of multiple determinations (R^2) of the fitted model, also known as R^2 -statistics, the value of R^2 obtained for the FVF is 0.989. This means that the model as fitted explains 98.9 % of the variability of FVF.

The compaction temperature represents a positive effect on the FVF. The average value of S/N ratio of compaction temperature increases with increasing compaction temperature as shown in Table 4.2. This result means that higher FVF can be achieved with higher compaction temperature. The positive effect from the compaction temperature can be further confirmed in Figure 4.4, where the relationship between FVF and compaction pressure was recorded under various compaction temperatures (Exp. No. 2, 5, 12, 15). As shown in Figure 4.4, although there are meanwhile effects from preforming parameters (Binder activation temperature and binder activation time), the FVF indicates an obvious increase with increasing compaction temperature under the same compaction pressure. This can be attributed to the higher range of S/N ratio of compaction temperature (0.72), which is about 2.6-3.2 times higher than the range of the other two preforming parameters (Tab. 3). The higher range of S/N ratio from compaction temperature means more significant influence on the FVF so that the effects from the two preforming parameters cannot readily be shown up. It is believed that the effect of compaction temper-

ature on the FVF can be related to the four material state of the binder. Because the four selected levels of compaction temperature correspond to the four material states of the binder, which is solid (level 1, 25 °C), partly melted (level 2, 60 °C), fully melted higher viscous (level 3, 125 °C) and fully melted lower viscous (level 4, 190 °C). The compressibility of the bindered textile preforms can be tailored by the compaction temperature due to the fact that the re-organization of the fibers can be facilitated by the lubricating effect from the melted preforming binder.

Table 4.1.: Experimental results for FVF

Exp. No.	FVF [%]	Std. of FVF	S/N for FVF
1	64.65	0.28	36.21
2	64.35	0.33	36.17
3	62.83	0.72	35.96
4	61.75	0.43	35.81
5	65.10	0.66	36.27
6	63.30	0.89	36.03
7	63.25	0.38	36.02
8	63.61	0.34	36.07
9	67.13	0.53	36.54
10	66.78	0.36	36.49
11	66.44	0.66	36.45
12	67.74	0.15	36.62
13	69.33	0.13	36.82
14	69.56	0.59	36.85
15	67.66	1.67	36.61
16	68.83	1.12	36.76

Table 4.2.: Response table mean signal-to-noise (S/N) ratio for FVF factor and significant interaction

Symbol	Average of value of S/N				Range (Max-Min)
	Level 1	Level 2	Level 3	Level 4	
T_{comp}	36.04	36.10	36.52	36.76 ^a	0.72
T_{act}	36.46 ^a	36.38	36.26	36.32	0.20
c_b	36.36	36.42 ^a	36.36	36.29	0.13
t_{act}	36.42 ^a	36.38	36.37	36.25	0.17
Total mean S/N = 36.35; ^a Optimum level					

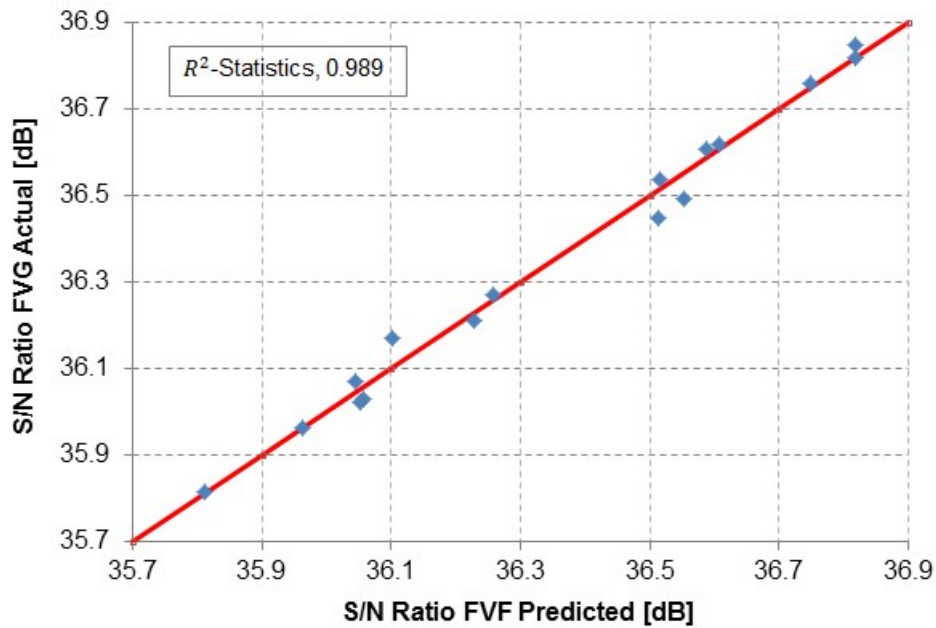


Figure 4.2.: Comparison of actual and predicted S/N ratios of FVF using regression analysis

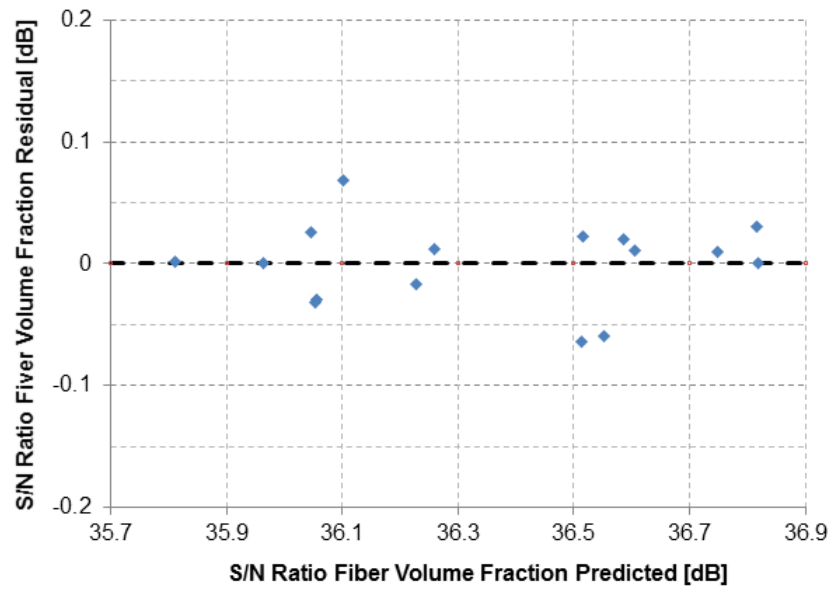


Figure 4.3.: Comparison of residual and predicted S/N ratios of FVF using regression analysis

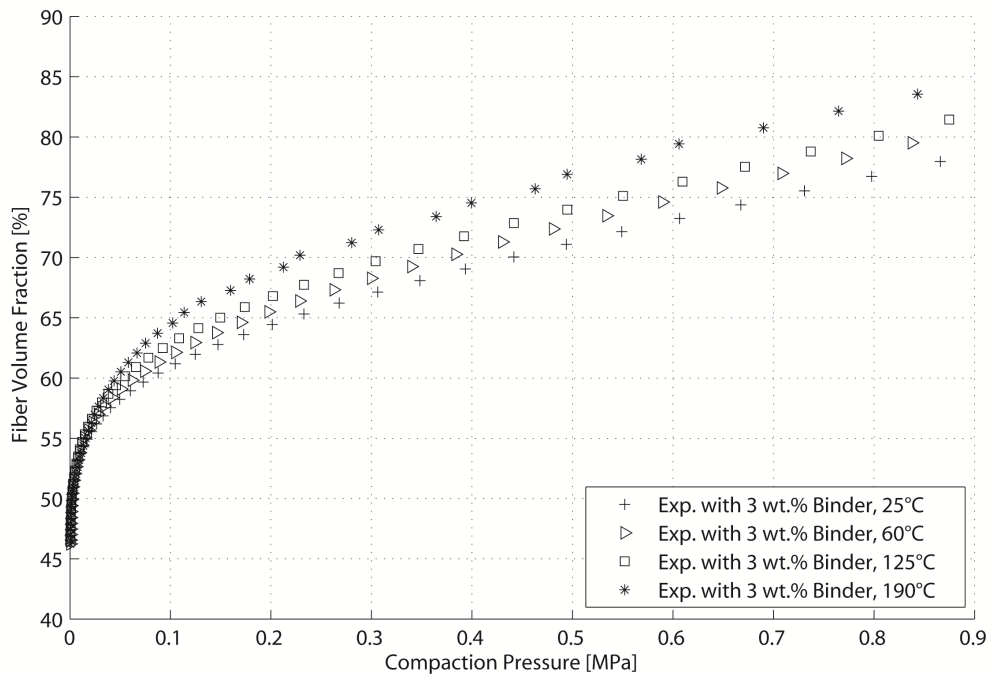


Figure 4.4.: Effect of compaction temperature on the FVF

As stated in section 3.2.1, several studies have been shown that the compaction response of fabrics can be expressed by a three parameter power law model representing the FVF as a function of the compaction pressure [45, 112]:

$$V_f = u \cdot P_c^s + c \quad (4.1)$$

where V_f is FVF, P_c is the compaction pressure, u is the volume fraction of the stack at unit compaction pressure, s is the compaction stiffness index and c is referred to the initial FVF under 0 MPa.

As for the non-crimped fabrics preforms with or without binder used in this study, the three parameters model can only express the compaction response in a limited range (<0.1 MPa) as shown in Figure 4.5. To approximate the FVF with more accuracy, an improved model must be developed for bindered textile preforms. Therefore, the author [110] has proposed a modified four parameters model by multiplying Equ. 4.1 with an exponential function as:

$$V_f = (u \cdot P_c^s + c) \cdot \exp(d \cdot P) \quad (4.2)$$

where V_f and P_c have the same meaning as Equ. 4.1, and u , s , c , and d are material constants. The fitting results with modified four parameter model are as shown in Figure 4.6. As we can see the modified four parameters model can make a better prediction of compaction response of bindered textile preforms. To show the modeling ability of the proposed model in higher compaction temperatures, further attempts to fit the experiments data with 60 °C, 125 °C and 190 °C were performed. Again good agreement between the experimental data and the fitted results is as shown in Figure 4.7. Therefore, this model will be adopted to correlate the FVF and the compaction and preforming parameters as shown in Table 3.2.

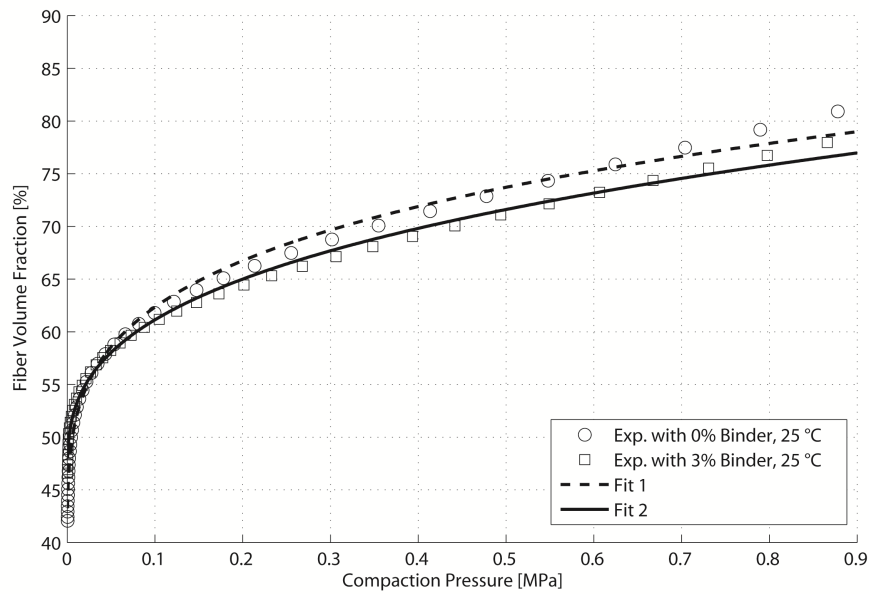


Figure 4.5.: Fitting of compaction curve of textile preforms with three parameters power law model

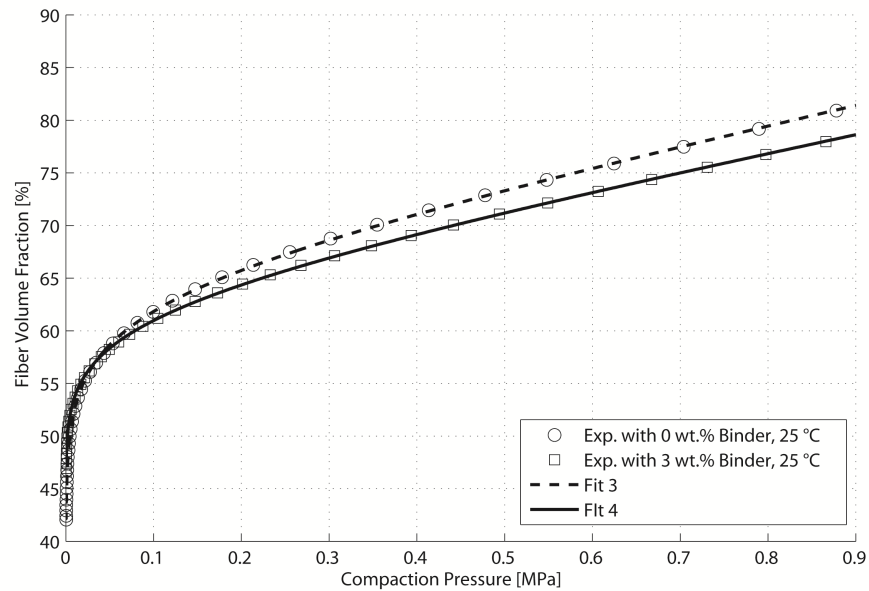


Figure 4.6.: Fitting of compaction curve of bindered textile preforms at room temperature (25 °C) with proposed model

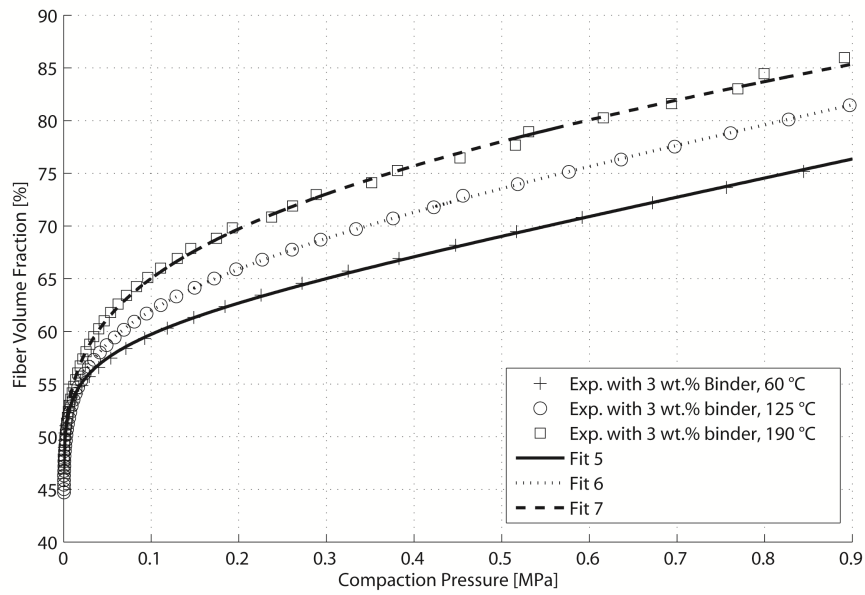


Figure 4.7.: Fitting of compaction curve of bindered textile preforms at elevated temperatures with proposed model

The equation of the model proposed for correlation between the FVF and the compaction and preforming parameters is according to Equ. 4.2 by correlating its four parameters with compaction temperature, binder activation temperature, binder content and binder activation time using linear regression as shown in Equ. 4.3. The FVF at specified compaction pressure can be estimated by Equ. 4.2 with the four parameters calculated with Equ. 4.3¹ and the compaction pressure equals to 0.2 MPa in the present study.

¹The unit of the variables can be found in Table 3.2

$$\begin{bmatrix} u \\ s \\ c \\ d \end{bmatrix} = \begin{bmatrix} 259.43 & 0.627 & -105.278 & -0.153 \\ -0.915 & -9.21E-03 & 0.211 & 5.43E-03 \\ -2.336 & -3.74E-03 & 1.468 & 2.45E-03 \\ -4886.541 & 14.158 & 3980.552 & -10.819 \\ -49.439 & -0.708 & 8.292 & 0.364 \\ 0.01 & 7.83E-05 & -3.31E-03 & -4.87E-05 \\ 22.059 & -0.045 & -16.801 & 0.016 \\ 0.051 & 0.006 & 0.172 & -4.39E-03 \\ 48.971 & -0.174 & -43.192 & 0.121 \\ 0.414 & 0.007 & -0.018 & -3.48E-03 \\ 1161.298 & -2.318 & -794.078 & 5.762 \\ -0.235 & 8.88E-04 & 0.209 & -3.79E-04 \\ -1E-04 & -6.39E-05 & -2.234E-03 & 4.279E-05 \\ -11.396 & 0.023 & 8.47 & -0.055 \end{bmatrix}^T \cdot \begin{bmatrix} 1 \\ T_{comp} \\ T_{act} \\ c_b \\ t_{act} \\ T_{comp} \times T_{act} \\ T_{comp} \times c_b \\ T_{comp} \times t_{act} \\ T_{act} \times c_b \\ T_{act} \times t_{act} \\ c_b \times t_{act} \\ T_{comp} \times T_{act} \times c_b \\ T_{comp} \times T_{act} \times t_{act} \\ T_{act} \times c_b \times t_{act} \end{bmatrix}. \quad (4.3)$$

4.1.2. Residual Preform Thickness (RPT)

The experimental results for the RPT, corresponding standard deviation and S/N ratios are also as shown in Table 4.3. The mean S/N ratio for each level of the parameters was calculated and summarized in Table 4.4. Additionally, the total mean S/N ratio is computed by averaging the total mean S/N ratios. Based on the data presented in Table 4.4, the optimal compaction performance for RPT was obtained at 190 °C compaction temperature (Level 4), 90 °C binder activation temperature (Level 1), 5 % binder content (Level 3) and 0.5 min binder activation time (Level 1) settings. In Figure 4.8 and 4.9 the actual and predicted S/N ratios and residual and predicted S/N ratios for RPT were compared using linear regression analysis. Here, R^2 of the model is 0.999.

Table 4.3.: Experimental results for RPT

Exp. No.	RPT [%]	Std. of RPT	S/N for RPT
1	1.94	0.03	-5.75
2	1.93	0.01	-5.71
3	1.94	0.02	-5.75
4	1.99	0.02	-6.02
5	1.84	0.02	-5.31
6	1.93	0.04	-5.69
7	1.85	0.01	-5.33
8	1.85	0.01	-5.34
9	1.88	0.03	-5.49
10	1.87	0.02	-5.45
11	1.89	0.01	-5.54
12	1.85	0.01	-5.35
13	1.85	0.01	-5.32
14	1.81	0.01	-5.18
15	1.89	0.05	-5.53
16	1.87	0.04	-5.41

As the FVF, the performance of higher mold temperature is positive for RPT as expected as shown in Table 4.4. The range of S/N ratio of compaction temperature results a maximum of 0.45, indicating that the compaction temperature has the most significant influence on the RPT. Figure 4.10 shows the effect of the com-

Table 4.4.: Response table mean signal-to-noise (S/N) ratio for RPT factor and significant interaction

Symbol	Average of value of S/N				
	Level 1	Level 2	Level 3	Level 4	Range (Max-Min)
T_{comp}	-5.81	-5.42	-5.46	-5.36 ^a	0.7
T_{act}	36.46 ^a	36.38	36.26	36.32	0.20
c_b	36.36	36.42	-5.44 ^a	-5.53	0.16
t_{act}	-5.40 ^a	-5.48	-5.48	-5.68	0.28
Total mean S/N = -5.51; ^a Optimum level					

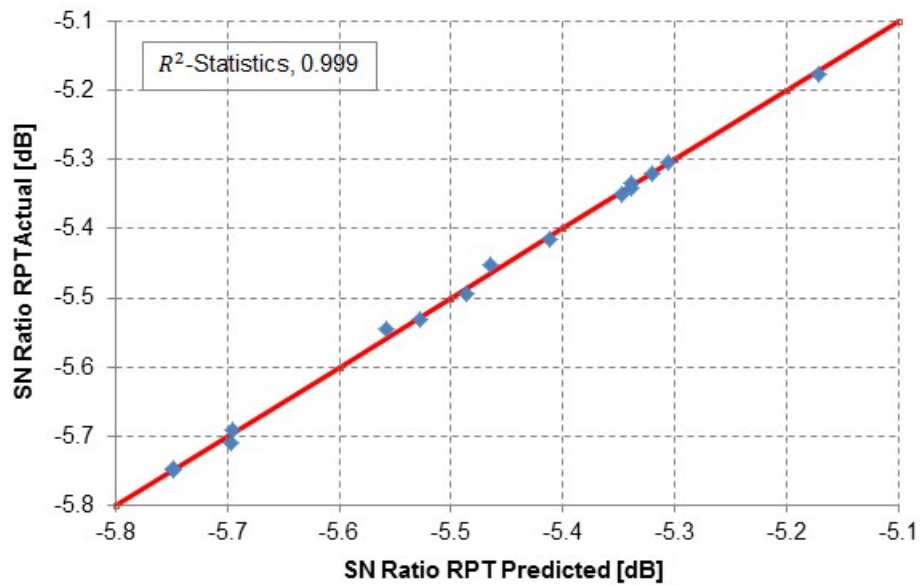


Figure 4.8.: Comparison of actual and predicted S/N ratios of RPT using regression analysis

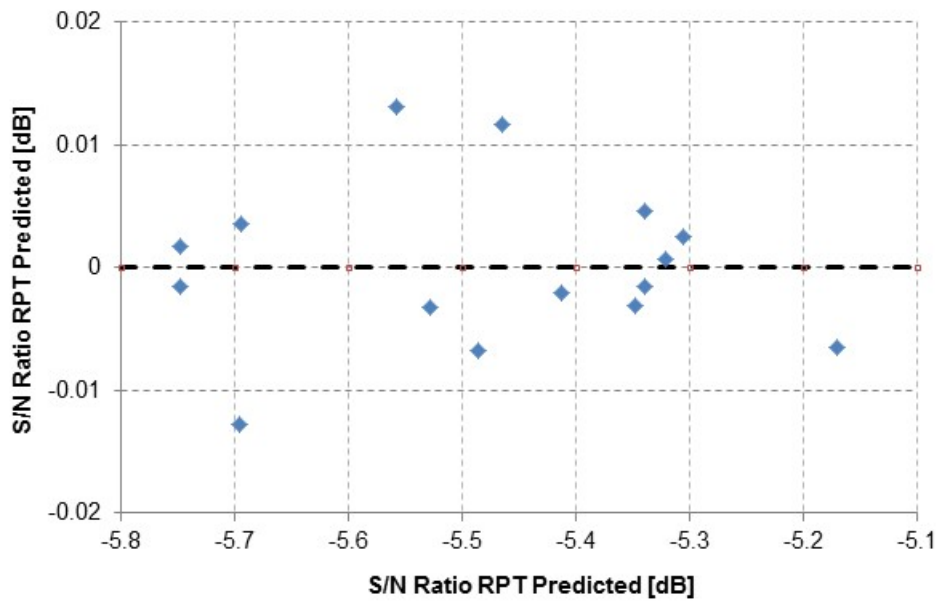


Figure 4.9.: Comparison of residual and predicted S/N ratios of RPT using regression analysis

paction temperature and the binder content on the RPT after a compaction cycle. It is obvious to see that the RPT was influenced by the compaction temperature and this influence is further strengthened for the bindered textile preforms. For each compaction temperature, the RPT of the bindered textile preform is smaller than the one without binder. This may be attributed to the limited relaxation because of the bindered fiber bundles. Starting with a lower compaction temperature of 25 °C, the RPT of bindered textile preform undergoes first a decrement when the compaction temperature increases up to 60 °C. This phenomenon can be explained that the partly melted inter-layer of binder is compressed into the fiber bundles of both upper and lower fabric layer and acts as binder so that the relaxation of fiber bundles is greatly limited. However, at higher compaction temperatures where the binder is fully melted, instead of decrement the RPT compressed at 125 °C shows a slight increment which becomes more remarkable at 190 °C. It is believed that the increment of RPT may be attributed to the inertial effect of the binder melt with lower viscosity. Large amounts of binder melt flow into the lower fabric layer, leading to a reduced binding effect of the upper fabric layer with larger relaxation because

of the released fiber bundles. As shown in Figure 4.11 the weight change of lower fabric layer is obviously higher than the upper fabric layer when both of them were placed in the oven with 500 °C for 1 hour, which further shows that there are more residual binder in lower fabric layer.

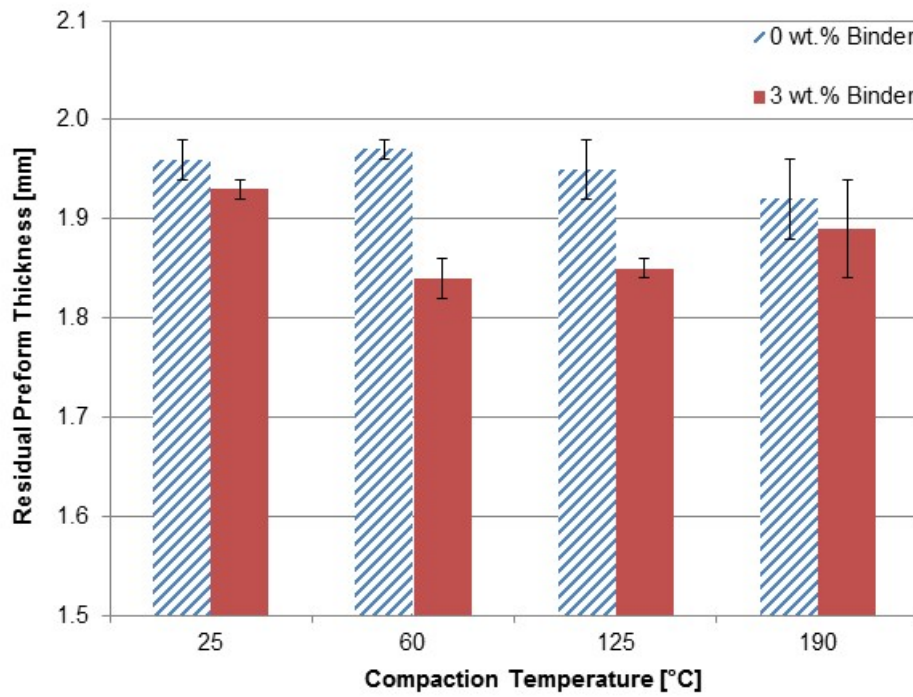


Figure 4.10.: Effect of compaction temperature on the RPT

During the release process the correlation between the preform thickness and the compaction pressure can be derived from Equ. 3.1:

$$h_p = \frac{NA_f}{V_f \rho} \quad (4.4)$$

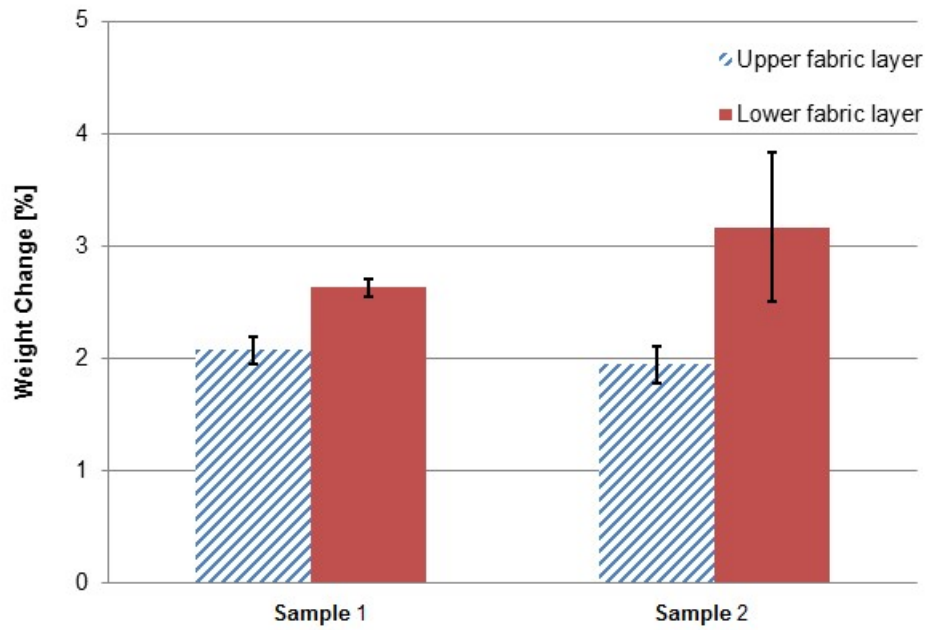


Figure 4.11.: Weight Change of both fabric layers after compression at 190 °C and burn down at 500 °C

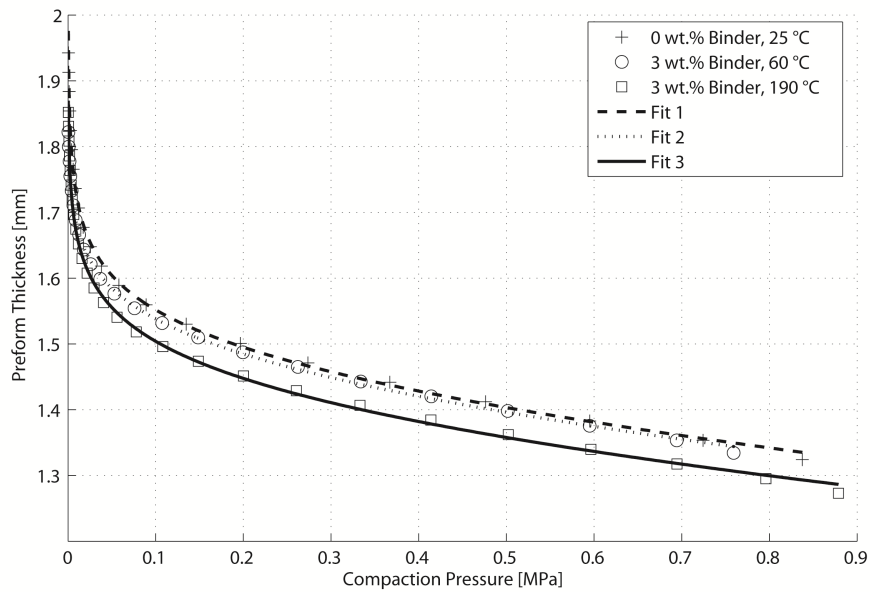


Figure 4.12.: Fitting of release curve of bindered textile preforms

Substituting Equ. 4.2 into Equ. 4.4 with consideration of the density of glass fibers and the preform configuration, the preform thickness h_p as a function of the compaction pressure P_c during the release process is:

$$h_p = \frac{1.0776}{(u \cdot P_c^s + c) \cdot \exp(d \cdot P)} \quad (4.5)$$

where u , s , c and d have the same meaning as Equ. 4.2. The RPT is obtained when the compaction pressure equals released back to the pre-load. Fitting trials with Equ. 4.5 to the release curves of compaction experiment are as shown in Figure 4.12. The fitted results show good agreement with the experimental results. The RPT from the experiment and calculated with Equ. 4.5 are compared in Figure 4.13. These results confirm that the proposed model can make a good prediction of the RPT. Therefore, the model will be further applied to correlate the RPT and the process variables.

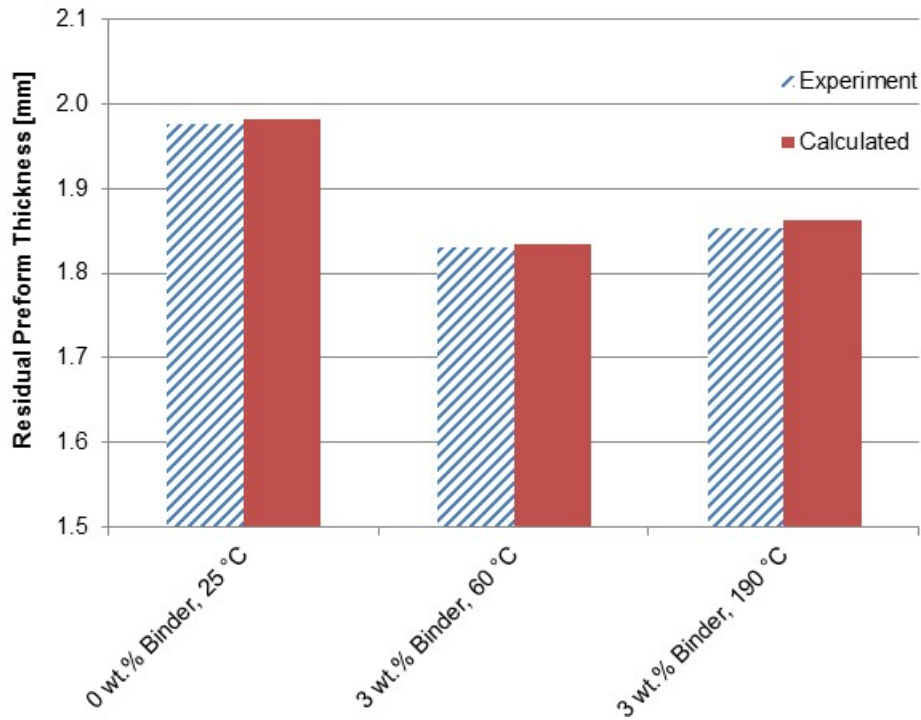


Figure 4.13.: Comparison of the RPT from the experiment and the model

The equation of the model proposed for the RPT is according to Equ. 4.5 by correlating its four parameters with compaction temperature, binder activation temperature, binder content and binder activation time as shown in Equ. 4.6. The RPT after a compaction cycle can be estimated by Equ. 4.5 with the four parameters calculated by Equ. 4.6² and the compaction pressure equals to the pre-load.

²The unit of the variables can be found in Table 3.2

$$\begin{bmatrix} u \\ s \\ c \\ d \end{bmatrix} = \begin{bmatrix} 0 & 0 & 0 & 0 \\ 6.59E-05 & 0.0034 & 0.0077 & -0.0008 \\ 0.0045 & 0.0009 & 0.0035 & -0.0007 \\ 58.7168 & -28.2973 & -68.7473 & 6.5201 \\ -1.0823 & 0.6539 & 2.12 & -0.0326 \\ 3.75E-06 & -3.39E-05 & -7.58E-05 & 8.23E-06 \\ -0.2995 & 0.1327 & 0.3606 & -0.01777 \\ 0.0109 & -0.0071 & -0.0199 & 0.0011 \\ -0.5817 & 0.2638 & 0.6519 & -0.0581 \\ 0.0093 & -0.0061 & -0.0199 & 0.0003 \\ -11.3902 & 6.2629 & 10.7919 & -1.9508 \\ 0.0028 & -0.0012 & -0.0034 & 0.0001 \\ -0.0001 & 6.63E-05 & 0.0002 & -1.02E-05 \\ 0.1204 & -0.0574 & -0.0978 & 0.018 \end{bmatrix}^T \cdot \begin{bmatrix} 1 \\ T_{comp} \\ T_{act} \\ c_b \\ t_{act} \\ T_{comp} \times T_{act} \\ T_{comp} \times c_b \\ T_{comp} \times t_{act} \\ T_{act} \times c_b \\ T_{act} \times t_{act} \\ c_b \times t_{act} \\ T_{comp} \times T_{act} \times c_b \\ T_{comp} \times T_{act} \times t_{act} \\ T_{act} \times c_b \times t_{act} \end{bmatrix} \quad (4.6)$$

4.1.3. Significant sequence analysis

The statistical analysis of variance (ANOVA) was conducted to determine more accurately the optimum combination of the experiment parameters and to specify the relative importance of the design parameters on the FVF and RPT. The analysis is carried out for the level of significance of 1 % (the level of confidence is 99 %) [85, 83]. Table 4.5 and 4.6 show the results of the ANOVA analysis for the experiment output, respectively. The last columns of Table 4.5 and 4.6 indicate the percentage contribution of each factor on the total variation, indicating their degree of influence on the results. The greater the percentage contribution, the greater the influence a factor has on the performance. According to Table 4.5, the compaction temperature was found to be the major factor affecting the FVF (88.17 %), whereas the binder activation temperature, binder content and binder activation time affect the FVF by 5.33 %, 1.77 % and 4.09 %, respectively. The change of preforming parameters in the range given in Tab. 1 has an insignificant effect on the FVF. Table 4.6 shows the results of the ANOVA for RPT, it can be found that the compaction temperature again is the most significant design parameter for affecting RPT (65.67 %). The binder activation time affects the RPT by 23.24 %. The binder activation temperature and binder content has an insignificant effect on the RPT (1.32 % and 7.32 %, respectively).

Table 4.5.: Results of ANOVA for FVF

Parameter	Degree of freedom	Sum of square	Mean square	F ratio	Contribution [%]
T_{comp}	3	82.02	27.34	690.34	88.17
T_{act}	3	5.07	1.69	42.67	5.33
c_b	3	1.77	0.59	14.88	1.77
t_{act}	3	3.92	1.31	32.96	4.09
Error	3	0.12	0.04	-	-
Total	15	92.89	-	-	-

Table 4.6.: Results of ANOVA for RPT

Parameter	Degree of freedom	Sum of square	Mean square	F ratio	Contribution [%]
T_{comp}	3	0.0233	0.0078	134.59	65.67
T_{act}	3	0.0006	0.0002	3.68	1.32
c_b	3	0.0027	0.0009	15.88	7.32
t_{act}	3	0.0084	0.0028	48.28	23.24
Error	3	0.0002	0.00006	-	-
Total	15	0.0352	-	-	-

4.1.4. Verification experiments

To validate the conclusions drawn from the analysis phase verification experiments were performed to predict and verify the improvement of the performance characteristics using the optimal level of the experiment parameters. The predicted S/N ratio $\hat{\eta}$ using the results of regression analysis can be calculated with Equ. 4.7³:

$$\begin{bmatrix} \widehat{\eta_{FVF}} \\ \widehat{\eta_{RPT}} \end{bmatrix} = \begin{bmatrix} 6.47 & -10.789 \\ -0.006 & 0.062 \\ -0.002 & 0.052 \\ 14.284 & -168.588 \\ 0.108 & 9.052 \\ 0.0001 & -0.0006 \\ 0.0195 & 0.675 \\ -0.0008 & -0.076 \\ -.205 & 1.527 \\ -0.003 & -0.091 \\ 4.861 & 30.117 \\ 0 & 0.0065 \\ 0 & 0.0007 \\ 0 & -0.194 \end{bmatrix}^T \cdot \begin{bmatrix} 1 \\ T_{comp} \\ T_{act} \\ c_b \\ t_{act} \\ T_{comp} \times T_{act} \\ T_{comp} \times c_b \\ T_{comp} \times t_{act} \\ T_{act} \times c_b \\ T_{act} \times t_{act} \\ c_b \times t_{act} \\ T_{comp} \times T_{act} \times c_b \\ T_{comp} \times T_{act} \times t_{act} \\ T_{act} \times c_b \times t_{act} \end{bmatrix} \quad (4.7)$$

³The unit of the variables can be found in Table 3.2

Table 4.7 shows the results of the confirmation experiments using the optimal experimental parameters for FVF. The increase of S/N ratio from the initial experimental parameters to the level of optimal experimental parameters is 0.40 dB. The FVF is improved by 4.7 percent. Table 4.8 shows the results of the confirmation experiments using the optimal experimental parameters for RPT. The increase of S/N ratio from the initial experimental parameters to the level of optimal experimental parameters is 0.32 dB. The RPT is reduced by 3.6 percent. Good agreement between the predicted experimental performance and actual experimental performance was observed. The FVF and RPT are both improved by using the approach.

Table 4.7.: Results of the confirmation experiment for FVF

	Initial parameters	Optimized parameters	
		Predicted	Experiment
Level	A1B2C1D1	A4B1C2D1	A4B1C2D1
FVF [%]	64.88	-	67.95
S/N ratio [dB]	36.24	36.72	36.64
Improvement of S/N ratio	-	0.40	-

Table 4.8.: Results of the confirmation experiment for RPT

	Initial parameters	Optimized parameters	
		Predicted	Experiment
Level	A1B2C1D1	A4B1C3D1	A4B1C3D1
RPT [mm]	1.93	-	1.86
S/N ratio [dB]	-5.71	-4.94	-5.39
Improvement of S/N ratio	-	0.32	-

The experimental results confirmed the validity of the applied Taguchi method for enhancing the experimental performance and optimizing compaction and preforming parameters. However, the FVF (67.95 %) with optimal experimental parameters is about 2.3 % lower than the value (69.56 %) from experiment number 14 and the

difference for residual preforms thickness is 2.7 % (1.86 mm vs. 1.81 mm). It is believed that the concluded optimal experiment parameters combination in this research should be further improved. Because the interactions among the experiment parameters like the binder activation temperature and binder activation time were not considered in the current study due to the complicate experimental design. Moreover, there are a great number of steps in the serious experiments starting from the bindered preforms preparation to the compaction experiment. There could be in each of the steps a human error source that could have an influence on the final results. Therefore, it is necessary to consider the parameter interaction and the accumulating human error effect for further research to acquire a better optimal experiment parameter combination.

4.2. Thermal and rheological behavior of matrix system

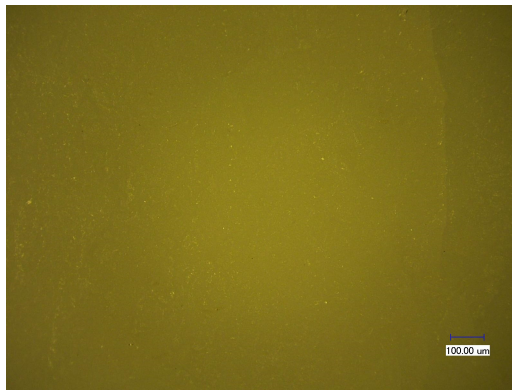
4.2.1. Conversion rate analysis

The quality of pCBT product polymerized with CBT160 and CBT500 with three catalysts was observed first with optical microscope. As shown in Figure 4.14(a) and 4.14(d), the polymerized pCBT samples from single component matrix system CBT160 and CBT500 with FASCAT4102 show a more homogeneous quality than the other two variants (Figure 4.14(b) and 4.14(c)). This may be attributed to the mixing quality of the matrix system. CBT160 is a commercial single component system produced with CBT oligomers and FASCAT4101 catalyst by Cyclics Corporation. The mixing quality is good because of the mature and reproducible production process. A good mixing quality can be obtained for the liquid catalyst FASCAT4102 as well when it is added into the molten CBT resin. However, the mixing quality of the powder blend made from CBT500 powder and the two powder catalysts FASCAT4101 and TEGOCAT256 can not be guaranteed with the applied lab based rotational mixing setup. This is because that the CBT500 powder ground from CBT500 granulate has a large visible distribution of particle size. The powder blending process can only make a limited mixing degree of the CBT500 powder and the catalyst powder due to the different particle size. Therefore, further

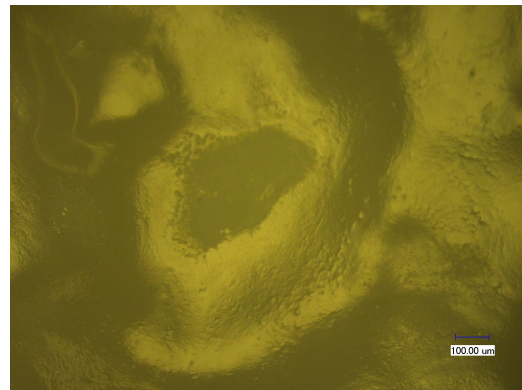
thermal investigations on the effect of catalyst and polymerization temperature are mainly based on the single component CBT160 and the two components system including CBT500 and FASCAT4102 for a better results.

The effect of catalyst amount on the polymerization of CBT500 is shown in Figure 4.15. At the very beginning (until 1 min), no significant difference of the conversion rate was observed for the reactive system with different amount of catalyst. However, there is a clear increase of conversion rate from 1 min to 5 min. for all the three catalyzed systems. The one with the highest amount of catalyst (0.9 wt.%) shows the fastest conversion. The conversion rate increases generally with the catalyst amount, which is very helpful for tailoring CBT500 for different applications. Additionally the results indicate that the polymerization from CBT500 to pCBT can be finished in about 20 min with only 0.9 wt.% FASCAT4101 catalyst, which is a distinct advantage over most of the thermoset resin systems that have long curing cycle of several hours. The conversion curve of CBT500 with 0.6 wt.% FASCAT4101 catalyst is in a narrow range overlapping with the conversion curve from CBT160. This result confirms that the CBT160 system was produced with about 0.6 wt.% FASCAT4101 catalyst and that the polymerization from CBT to pCBT can be tailored by adjusting the amount of catalyst according to the desired conversion rate.

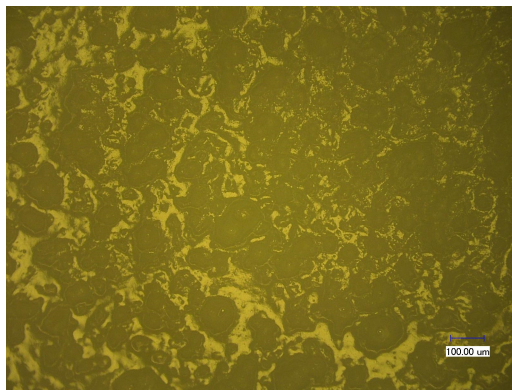
Instead of the FASCAT4102 catalyzed CBT500 system, which may introduce several errors such as metering, the effect of temperature on the polymerization of CBT to pCBT was investigated using the single component CBT160 system for an accurate results. As shown in Figure 4.16, with the same amount of catalyst the polymerization of CBT to pCBT can be affected by the temperature as well. The conversion rate shows an obvious increasing trend with increasing temperature. Compared with the conversion degree of about 80 % at 190 °C, the polymerization process can be finished in 20 min at 200 °C. The temperature is another influencing factor that should be taken into consideration when processing CBT resin matrix system.



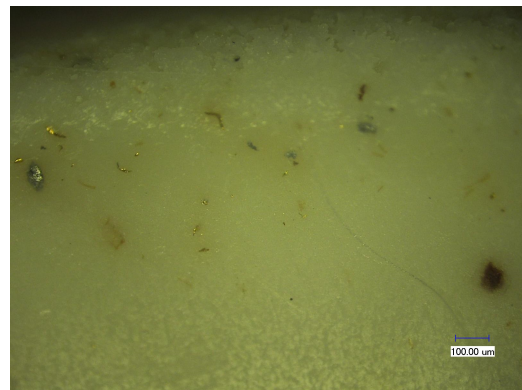
(a) CBT160



(b) CBT500 with FASCAT4101



(c) CBT500 with TEGOCAT 256



(d) CBT500 with FASCAT4102

Figure 4.14.: Surfaces morphology of the resultants from CBT500 and CBT160

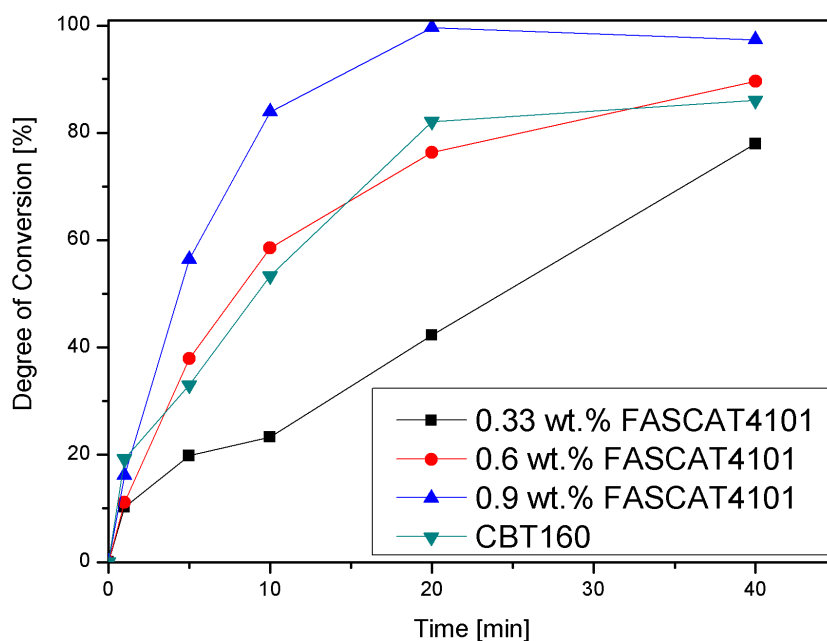


Figure 4.15.: Effect of catalyst amount on the conversion rate of CBT500 compared with CBT160 at 190 °C

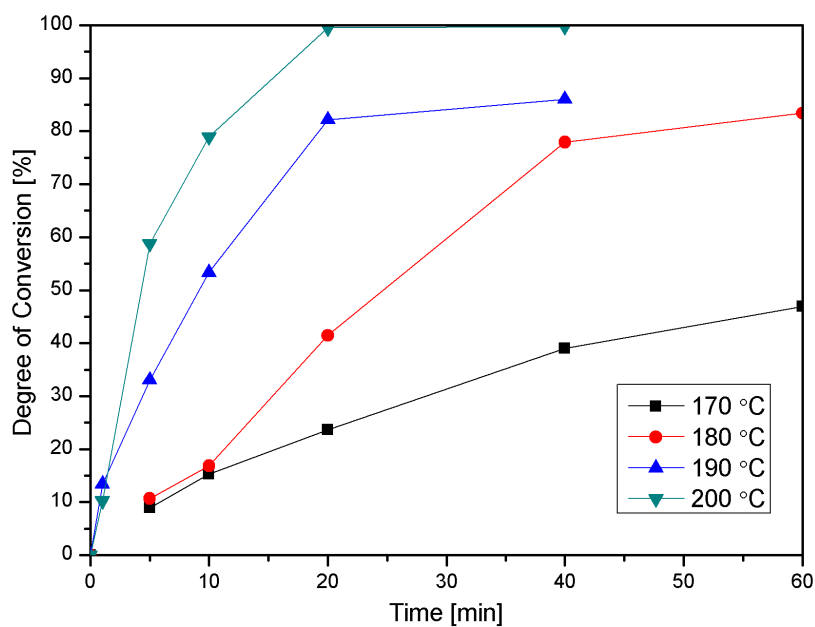


Figure 4.16.: Effect of polymerization temperature on the conversion rate of CBT160

4.2.2. Melting and crystallization analysis

Thermal behavior of CBT based resin matrix

Figure 4.17 shows the heating trace of CBT500 without any catalyst at a rate of 10 °C/min. A melting peak was observed at 140 °C, which can attribute to the melting of CBT oligomers. This is in accordance with earlier investigations reported by other researchers [40, 87]. The melting peak of CBT500 is sandwiched between two broad shoulders, leading to a broad range of melting point of CBT500 from 110 °C to 172 °C. The broadening of the shoulder may be ascribed to the different melting temperatures of the oligomers present in the CBT [40]. Because CBT produced via de-polymerization from PBT contains different proportions of oligomers that have different melting temperatures [20] due to the different molecular weight as shown in Figure 1.2. There is no crystallization peak in the cooling trace of CBT500 as shown in Figure 4.17, meaning the CBT500 matrix is a fully de-polymerized oligomer system from PBT.

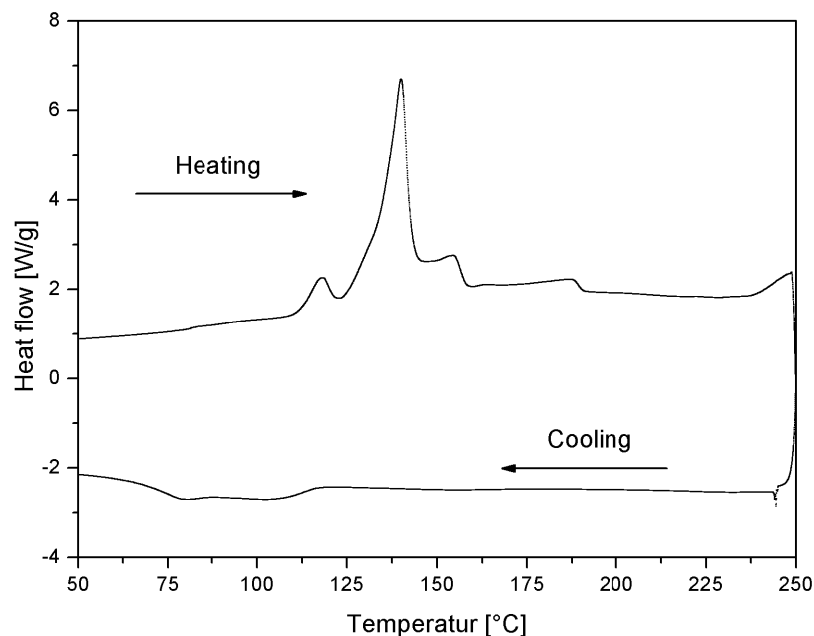


Figure 4.17.: Typical DSC heating and cooling trace of CBT500 without any catalyst

The typical DSC heating/cooling/heating trace of CBT500 with the catalyst FASCAT4102 and CBT160 at a rate of 5 °C/min, is shown in Figure 4.18. For the catalyzed CBT500 system only one melting peak was observed during the first heating trace, which is the melting of CBT oligomers. Compared with the melting peak as shown in Figure 4.17, the melting peak of the FASCAT4102 catalyzed CBT500 is shifted toward to a lower temperature of 127 °C. This may be attributed to the presence of FASCAT4102 which has a liquid state at room temperatures. For the single component CBT160, two melting peaks were observed during the first heating trace. The first melting peak at 141 °C is the melting of CBT oligomers, which is in accordance with Figure 4.17. The integration of powder catalyst FASCAT4101 in CBT oligomers has no significant influence on the melting of CBT oligomers. The second melting peak of 226 °C is the melting of pCBT polymers which is polymerized from CBT during the heating process. This is in agreement with Miller who studied the simultaneous polymerization and crystallization phenomenon at 190 °C and concluded that the isothermal polymerization pCBT has a 50 % crystalline structure which consists of lamellae and exhibits a single melting peak at 225 °C [57].

Before the second melting peak of pCBT polymers an exothermic peak at 195 °C was detected due to the simultaneous polymerization of CBT and crystallization of pCBT [87]. This is believed to occur over the temperature range of 172 °C to 216 °C. As the polymerization of CBT is a thermoneutral reaction, the exothermic peak at 195 °C is mainly because of the crystallization of pCBT [40, 43, 87]. For the FASCAT4102 catalyzed CBT500 system neither crystallization peak nor melting peak of pCBT was observed during the first heating trace. This may be ascribed to the fact that the FASCAT4102 catalyzed CBT500 has a relatively slow conversion rate compared with the fast heating rate. Because the CBT must be converted to a polymer of sufficiently high molecular weight before crystallization can commence [34, 65, 87]. The liquid catalyst FASCAT4102 is the slowest catalyst for polymerization of CBT (Figure 3.4, Table 3.1). There is not enough time for CBT500 that polymerizes to pCBT polymer with sufficiently high molecular weight and crystallizes before the melting point of pCBT at a heating rate of 5 °C/min during the first heating trace.

On the cooling of the two reactants both of them indicate a re-crystallization peak of the polymerized pCBT polymers as shown in Figure 4.18. The re-crystallization process of pCBT polymer from FASCAT4102 catalyzed CBT500 occurred in the region 210 °C to 170 °C. The crystallization temperature is 200 °C and the crystallization enthalpy is 56 J/g. While the pCBT polymer from CBT160 re-crystallizes in the region 200 °C to 160 °C. The crystallization temperature is 188 °C and the crystallization enthalpy is 44.3 J/g. The difference of the re-crystallization behavior of the polymerization of pCBT polymers could be contributed by the different molecular structure of catalyst FASCAT4101 and FASCAT4102 (Figure 3.5). Besides the pCBT molecular chains, the resulted pCBT polymer based on FASCAT4102 chains may have more side chains due to the more complex molecular structures. Therefore, the pCBT polymer from FASCAT4102 catalyzed CBT500 illustrates an earlier crystallization during cooling and generates more heat.

The third part of Figure 4.18 is the second heating trace of the two samples with the same heating rate as the first heating. For both samples a broad endotherm with two melting peaks of re-crystallized pCBT polymers is observed. The shifting of melting peak of pCBT polymers of CBT160 between the first and the second heating could be caused by the different crystalline structures, which means that some small and defective crystals (boundary crystals [108], pointed by the arrow as shown in Figure 4.19) are formed in the re-crystallization of pCBT polymers during cooling. On heating the sample containing boundary crystals, Polarized Light Microscope (PLM) showed that the boundary crystals melted first, followed by the coexisting spherulites, meaning that the boundary crystals are less perfect crystalline [108]. Therefore, during the second heating, it is that the boundary crystals are melted first, followed by their immediate re-crystallization into more stable structures and their subsequent melting. This is in agreement with the earlier MDSC investigations from Righetti and Lorenzo [72] and Ishak [41] as well.

In addition, regarding the enthalpy area, the melting peak of small and defective crystals in the case of pCBT polymers from FASCAT4102 catalyzed CBT500 is smaller than the one from CBT160. This may be attributed to the difference of the re-crystallization process of the two kinds of pCBT polymers. The pCBT polymer from FASCAT4102 catalyzed CBT500 started to crystallize at a higher tempera-

ture and has a higher crystallization temperature (200 °C), because the molecules of pCBT polymer have a higher mobility and can organize easily at higher temperatures during cooling and a highly regular crystalline structures could be formed quickly (steep increase of the crystallization peak during cooling) and only a little amount of small and defective crystals could be formed.

Effect of preforming binder

For LCM processing with CBT resin matrix system, CBT500 with FASCAT4102 is more attractive than the single component system CBT160 due to the easier resin preparation. The integrated fast catalyst FASCAT4101 in CBT160 make the resin a highly reactive system with a very short pot life (about 5 min at 180 °C). For a certain amount of resin need for infusion process, the resin may start to polymerize at un-fully melted status, which won't happen in case of FASCAT4102 catalyzed CBT500. Therefore, the CBT500 with FASCAT4102 was chosen for LCM processes and studied in this research (section 4.2.1).

Figure 4.20 indicates the effect of preforming binder (EPIKOTE[®] Resin 5390) on the melting and crystallization behavior of FASCAT4102 catalyzed CBT500. The upper part of the figure shows the first heating trace of FASCAT4102 catalyzed CBT500 filled with various binder contents. The presence of 2 wt.% preforming binder leads to a reduced melting enthalpy from 38.15 J/g to 30.72 J/g as shown in Table 4.9. Further addition of preforming binder up to 6 wt.% binder has no further significant influence on the melting transition of CBT oligomers.

The middle part of Figure 4.20 indicates the cooling trace of FASCAT4102 catalyzed CBT500 after polymerization in the presence of various binder content. It is obvious to see that the re-crystallization of pCBT polymer was influenced by the presence of preforming binder. The crystallization temperature was shifted from 199.85 °C to 185.74 °C and the crystallization enthalpy decreases from 52.63 J/g to 42.39 J/g with the filling content of preforming binder increases from 0 wt.% to 6 wt.% as shown in Table 4.9, which is corresponding to the fact of decreased crystallinity of CBT matrix by adding preforming binders. This means the selected

EPIKOTE[®] Resin 5390 preforming binder shows the potential as an appropriate toughening agent for pCBT polymers.

The lower part of Figure 4.20 presents the second heating trace of FASCAT4102 catalyzed CBT500 after re-crystallization during previous cooling. Double melting peaks were observed in all of the four samples. The filling of preforming binder seems to have an influence on the size of the first melting peak of small and defective crystals. An increased size of the first melting peak in comparison with the second melting peak could be observed due to the addition of preforming binder. This can be resulted from the crystallization temperature which was shifted to lower temperature in the presence of the preforming binder. More small and defective crystals could be formed and lower regularity of crystalline structure was conformed during re-crystallization process.

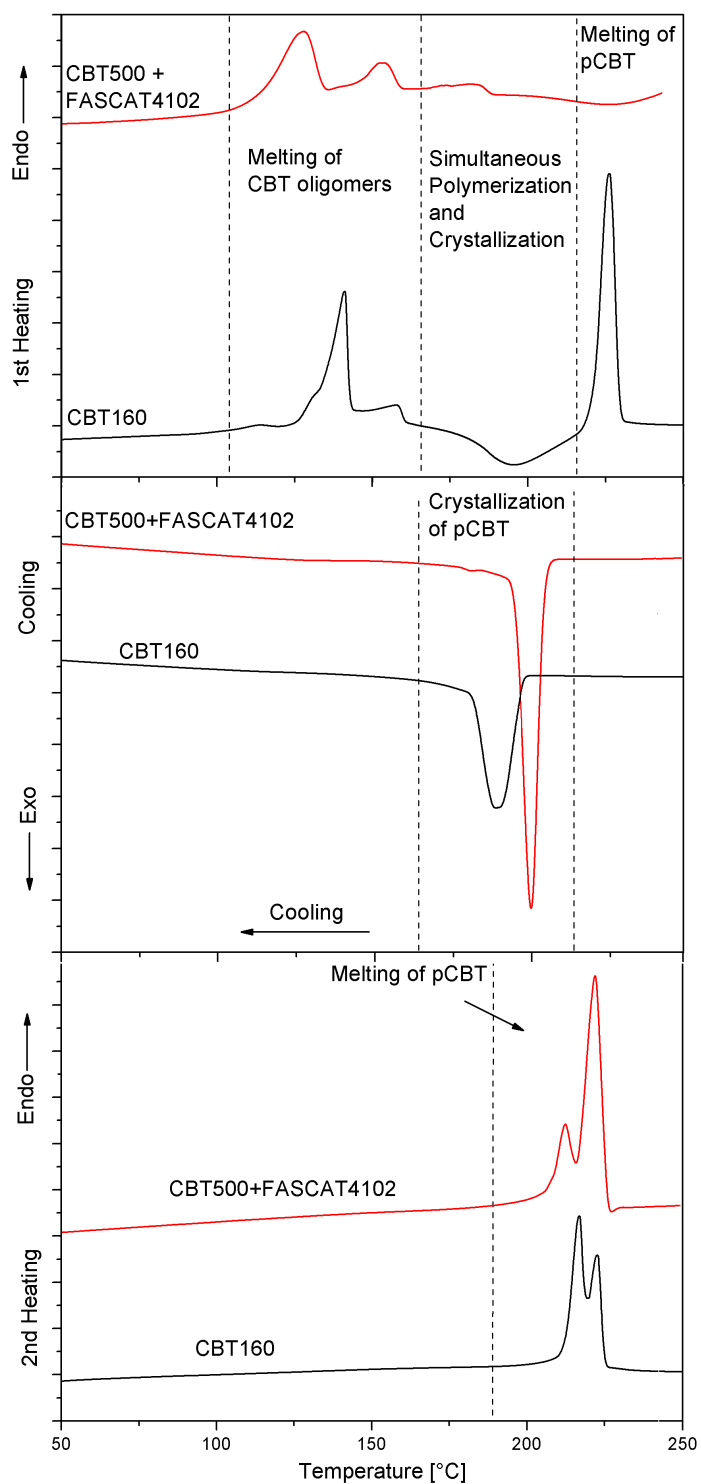


Figure 4.18.: Polymerization and crystallization behavior of CBT500 (Catalyzed with FASCAT4102) and CBT160

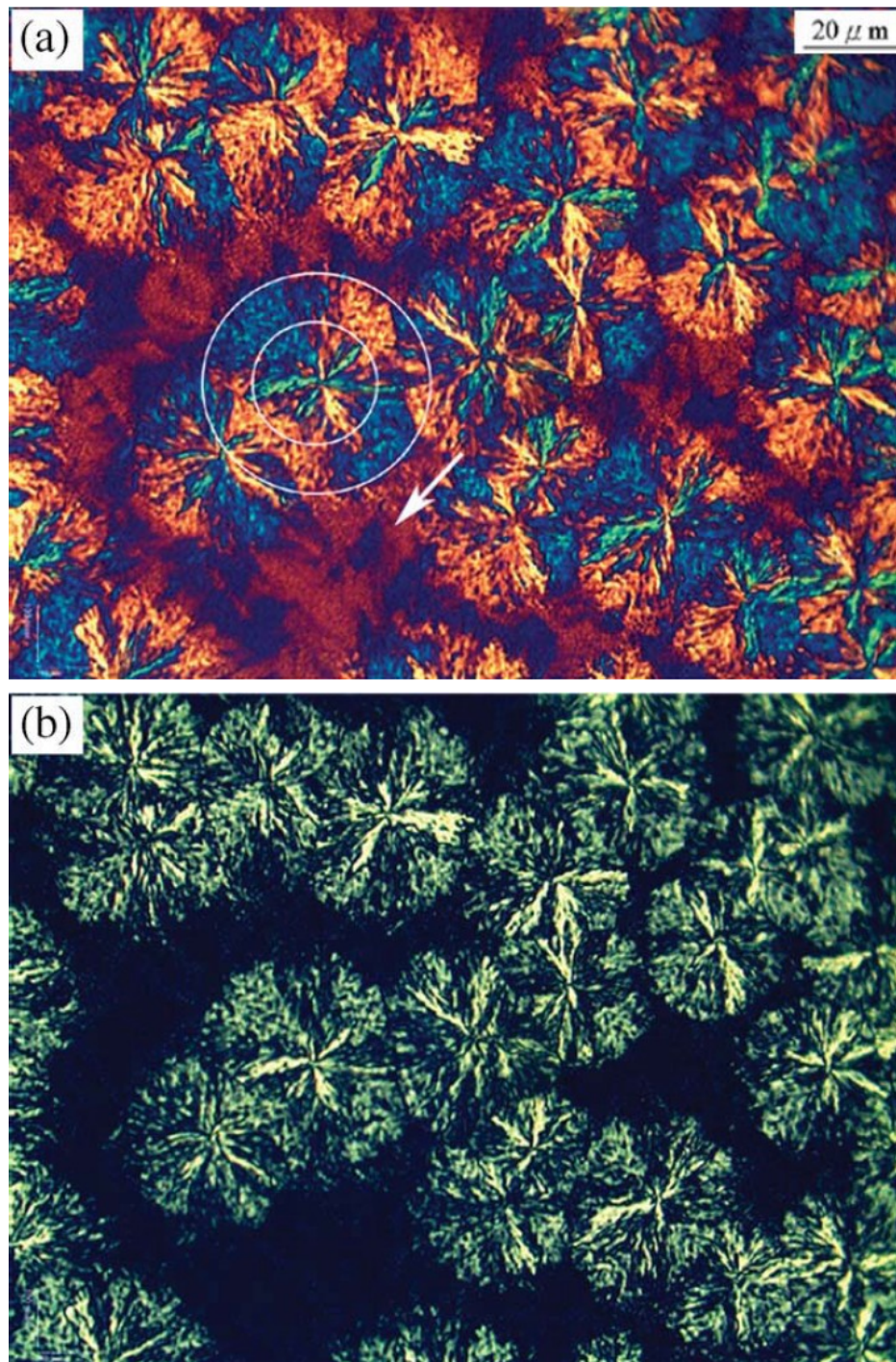


Figure 4.19.: PLM morphology of pCBT crystallized at 195 °C shows inner positive/outer negative spherulites (circled) and boundary crystals (pointed by arrow) [108]. (a) image with quartz plate, (b) image without quartz plate.

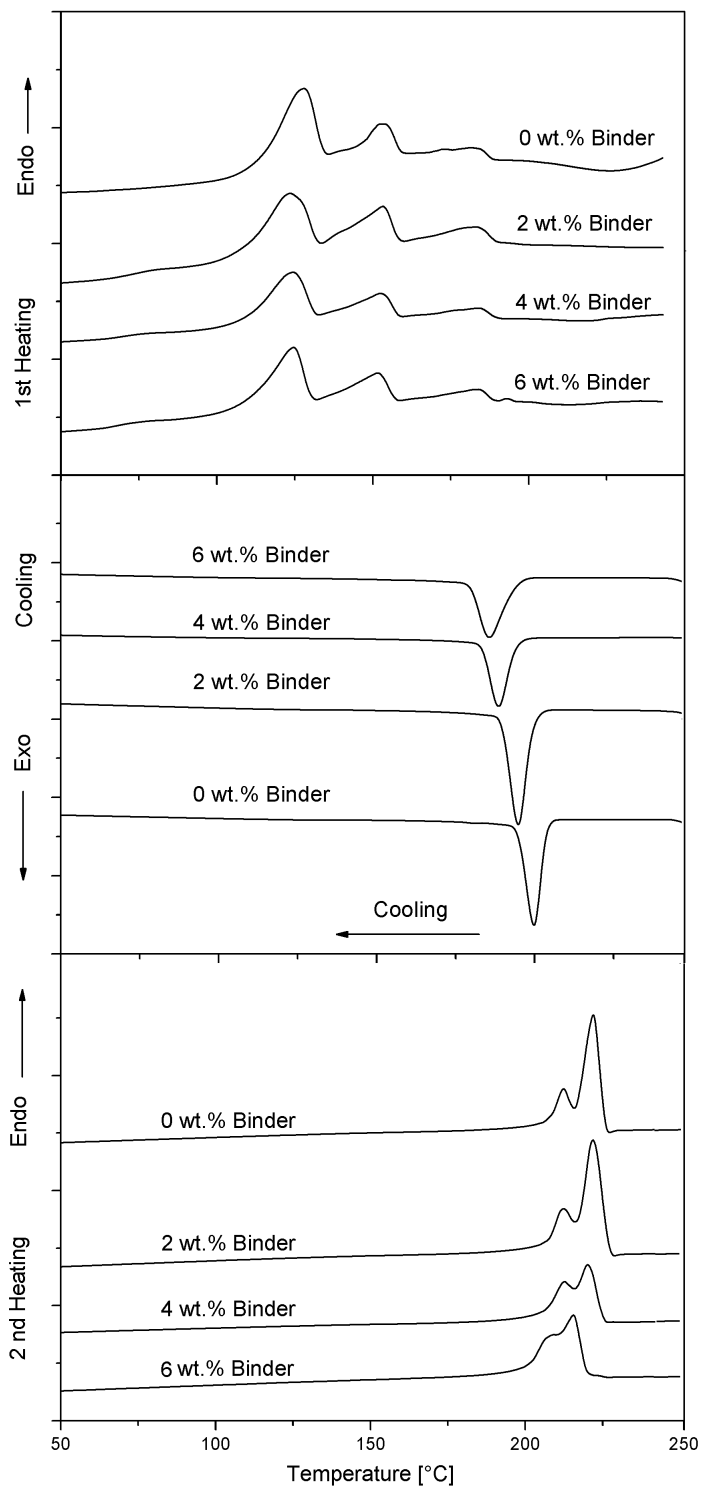


Figure 4.20.: Effect of preforming binder on the melting and crystallization behavior of FASCAT4102 catalyzed CBT500

Table 4.9.: Effect of binder on the thermal transition parameters of CBT500 (Catalyzed with FASCAT4102)

Binder wt. %	First heat			Cooling		Second heat	
	T_{m1} [°C]	T_{m2} [°C]	ΔH_m [J/g]	T_c [°C]	ΔH_c [J/g]	T_m [°C]	ΔH_m [J/g]
0	127.08	153.21	38.15	199.85	52.63	222	54.04
2	122.97	153.01	30.72	194.85	49.50	221.89	47.10
4	124.00	152.12	30.18	188.62	45.30	220.16	44.47
6	124.44	151.64	30.11	185.74	42.39	215.51	38.83

Simultaneous polymerization and crystallization

One of the advantages of CBT resin based technology for textile reinforced thermoplastics is that the production process can be isothermal at temperatures lower than the melting point of pCBT (about 225 °C) without any thermal cycle. Therefore, the simultaneous polymerization and crystallization phenomenon during isothermal production process is of great importance that should be studied.

The effect of preforming binder on the simultaneous polymerization and crystallization of FASCAT4102 catalyzed CBT500 at 190 °C is shown in Figure 4.21. For all of the tested samples only one exothermic crystallization peak was observed during the isothermal stage of about 30 min. The presence of preforming binder significantly changes the simultaneous polymerization and crystallization phenomenon of FASCAT4102 catalyzed CBT500 system. One of the distinct influence due to the addition of preforming binder is the starting time of crystallization of FASCAT4102 catalyzed CBT500 at 190 °C. Compared with the sample without addition of preforming binder (0 wt.%) the addition of 2 wt.% to 6 wt.% leads to an earlier crystallization. The polymerization of CBT oligomers to pCBT polymer with sufficient high molecular weight seems to be accelerated due the presence of preforming binder (EPIKOTE® Resin 05390) including epoxied functional groups which can react with pCBT [64].

The isothermal crystallization with the influence of preforming binder was further studied by Avrami analysis which is the most widely used means of describing the overall bulk isothermal crystallization of polymers. According to the Avrami model [35], isothermal crystallization kinetics can be described as:

$$X(t) = 1 - \exp(-Kt^n) \quad (4.8)$$

where $X(t)$ is the fractional crystallinity at time t , n is Avrami exponent whose value depends on the crystallization mechanism and geometry growth and K is temperature dependent rate constant, $K = K(T)$, reflecting nucleation and growth charac-

teristics. The interpretation and corresponding expressions for n and K values are summarized in Table 4.10.

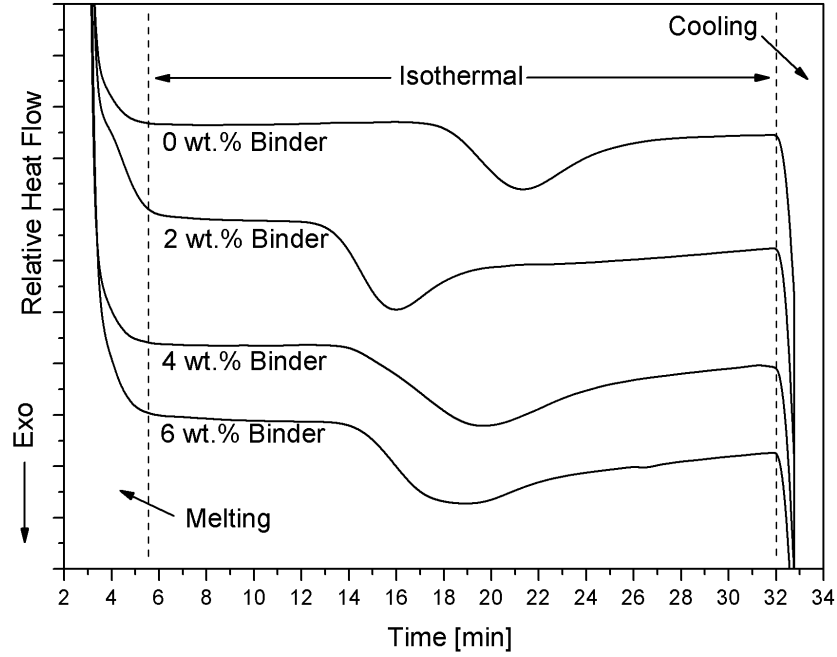


Figure 4.21.: Effect of preforming binder on the simultaneous polymerization and crystallization of FASCAT4102 catalyzed CBT500 at 190 °C

The Avrami parameters K and n in Equation 4.8 are usually determined by taking the double logarithm and expressing in the form:

$$\ln[-\ln(1 - X(t))] = \ln K + n \ln t \quad (4.9)$$

At a given temperature, values of n and K are determined from the isothermal DSC curves (Figure 4.21) using Equation 4.10 by least-squares fitting of $\ln[-\ln(1 - X(t))]$ versus $\ln t$ as shown in Figure 4.22. The fractional crystallinity of the isothermal crystallization $X(t)$ developed at time t was defined as the ratio of the two areas

Table 4.10.: The physical interpretation of the Avrami parameters for different crystallization mechanisms of polymers [37, 87]

Crystallization mechanism		n	K	Geometry
Spheres	Sporadic	4.0	$2/3\pi g^3 l_n$	3 dimensions
	Predetermined	3.0	$4/3\pi g^3 L_n$	3 dimensions
Discs	Sporadic	3.0	$1/3\pi g^3 l_n d_n$	2 dimensions
	Predetermined	2.0	$\pi g^3 L_n d_n$	2 dimensions
Rods	Sporadic	2.0	$1/4\pi g l_n r^2$	1 dimensions
	Predetermined	1.0	$1/2\pi g L_n r^2$	1 dimensions

g is crystal growth, l_n is nucleation rate, L_n is density of nuclei
 d_n is constant thickness of discs, r constant radius of rods

between the heat flow–time curve and baseline, from $t = 0$ to $t = t$ and from $t = 0$ to $t = \text{infinity}$ [87]:

$$X(t)^4 = \frac{\int_0^t (dH_t/dt) dt}{\int_0^\infty (dH_t/dt) dt} \quad (4.10)$$

Figure 4.23 shows the overall development of relative crystallinity with time in the presence of various filling content of preforming binder at 190 °C. The same trend of the development of relative crystallinity with time at various isothermal crystallization temperatures was also reported by Samsudin [87]. It is believed that the isothermal crystallization process represents two stages, a primary and secondary process. The primary process consists of the radial growth of the crystallites until impingement and the secondary process involves the growth of subsidiary lamellae or lamella thickening within the crystallites [42, 87]. In this research, an obvious dependence of crystallization rate on the filling content of preforming binder was observed besides isothermal temperature. This may be explained by the different primary crystallization process indicated by different n values due to the presence of preforming binder (Figure 4.22).

⁴ $X(t)$ is the fractional part of the overall crystallization peak, which is developed at time t .

The value of the Avrami exponent n for the investigated four samples is between 2 and 3, which is in accordance with the results from Karger-Kocsis [46]. According to the Avrami theory, the n value between 2 to 3 means the nucleation of spherulites is heterogeneous and the growth of spherulites was between two-dimensional and three-dimensional [26, 87]. The presence of 2 wt.% preforming binder leads to a n value of about 3, indicating either athermal nucleation with three dimensional spherulitic growth or thermal nucleation with two dimensional disk growth.

According to the determined n and K values as indicated in Figure 4.22, Avrami model was applied to fit the relative crystallinity versus time curve as shown in Figure 4.23. Good agreement was found between the experiment and the fitted results. The small deviation between the experiment and fitted results may be related to the fact that the Avrami model takes only the primary crystallization process into consideration with the assumption that the secondary crystallization process does not occur [87].

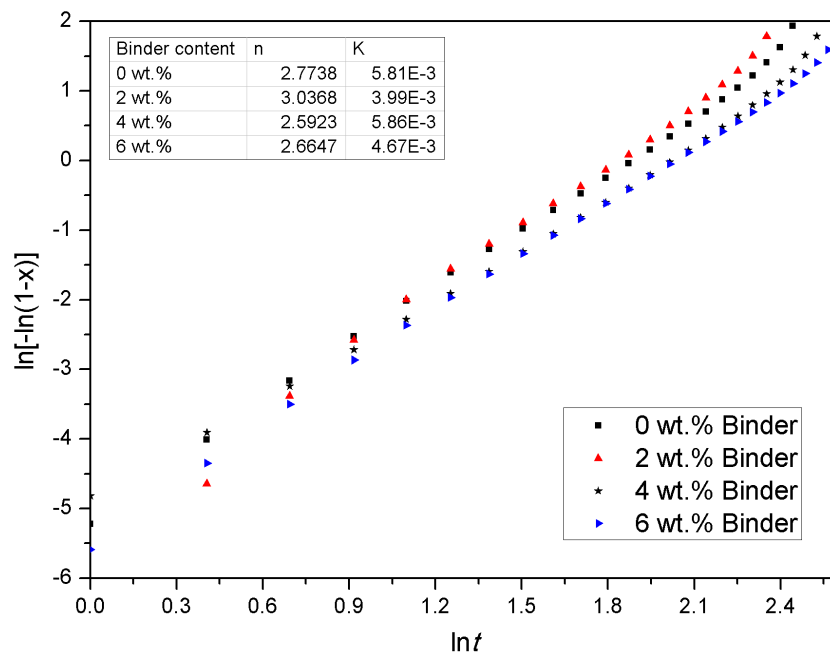


Figure 4.22.: An Avrami plot for the simultaneous polymerization and crystallization of CBT500 (Catalyzed with FASCAT4102)

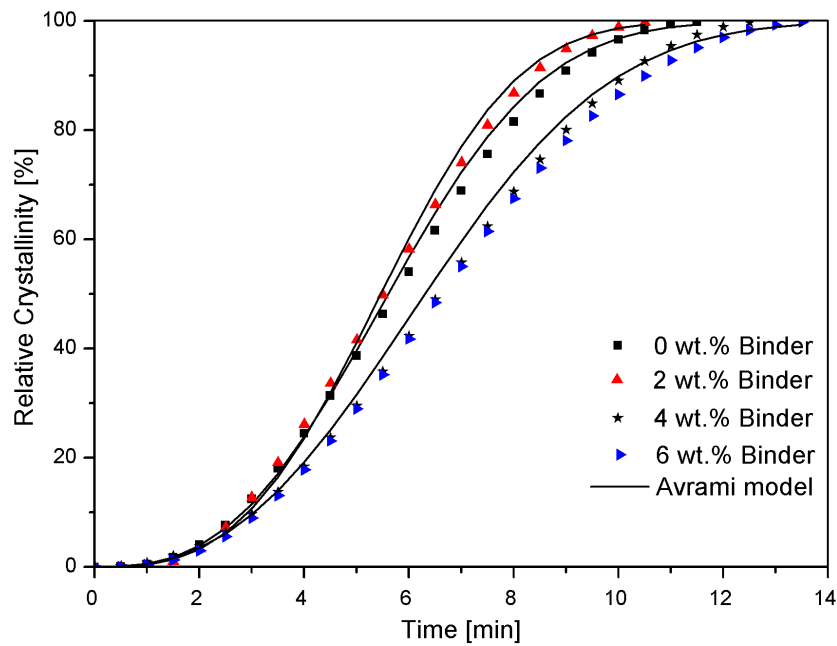


Figure 4.23.: Effect of binder on the relative crystallinity of FASCAT4102 catalyzed CBT500 during simultaneous polymerization and crystallization

Figure 4.24 shows the instantaneous variation of Avrami exponent n with relative crystallinity for FASCAT4102 catalyzed CBT500 during simultaneous polymerization and crystallization. This can be applied to predict the change in crystallization mechanism such as primary to secondary because the n value remains essentially constant during the primary crystallization [42, 87]. Thus, the instantaneous n values can be used to distinguish secondary crystallization from primary crystallization with a sudden change, indicating that the primary process is completed and the secondary process starts [42, 87]. The presence of preforming binder leads to a different instantaneous variation trend of n values at the initial stage of crystallization. Instead of starting with a n between 3 and 4, the preforming binder filled samples starts with a n value between 1 and 2. This is an indication that in the preforming binder filled samples heterogeneous nucleation of disks occurred and the growth of disks was between one-dimensional and two-dimensional [26, 87]. This may be the explanation that the preforming binder filled sample have more small and defective crystals than the one without preforming binder as shown in the previous DSC investigations (section 4.2.2).

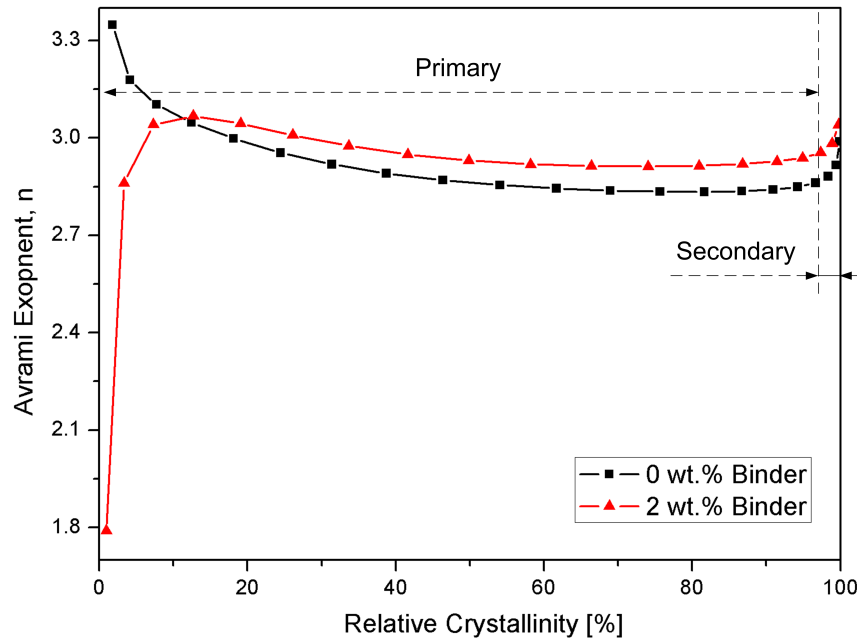


Figure 4.24.: Instantaneous variation of Avrami exponent n value for FASCAT4102 catalyzed CBT500 at 190 °C

4.2.3. Thermal stability analysis

Dynamic thermal stability of processing materials

Dynamic thermal stability of processing materials was investigated in TGA with a temperature scanning from 25 °C up to 600 °C at a rate of 10 °C/min is illustrated in Figure 4.25. The onset points of the processing materials was considered and summarized in Figure 4.25. The liquid catalyst FASCAT4102 has the minimal onset temperature of 258.47 °C. This is in agreement with the manufacturer recommended processing conditions that the FASCAT can be used at temperatures up to 250 °C. Thus, the selected processing materials, which were planned to be used for isothermal production of textile reinforced pCBT composites at temperatures below 225 °C, should be completely in order without any danger of thermal degradation.

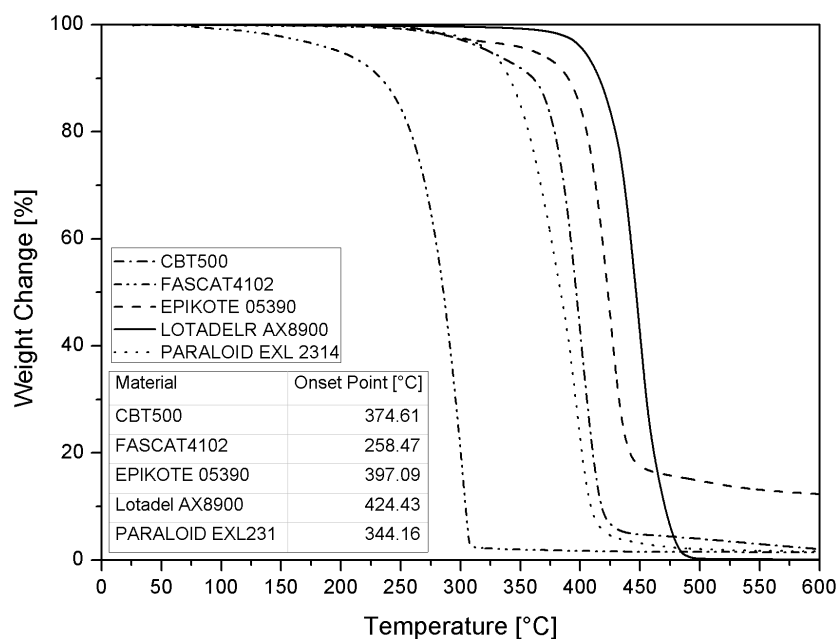


Figure 4.25.: Dynamic thermal stability of processing materials

Thermal stability of materials at processing temperature

The thermal stability of materials was further investigated under processing conditions such as 190 °C for an hour as shown in Figure 4.26. After 60 min the weight loss of the processing materials were examined and summarized in the link table in Figure 4.26. Nearly all processing materials investigated show an ignorable weight loss which is smaller than 1 % except the liquid catalyst FASCAT4102. A huge amount of weight loss up to 44 % was observed in 60 min for FASCAT4102 sample. This may be ascribed to the volatilization of the liquid system at high temperatures. As the pot life of the FASCAT4102 catalyzed CBT500 at 180 °C is usually shorter than 20 min and the weight loss at 190 °C in 20 min is only 7.5 %, suggesting that the infusion with a resin catalyst mixture temperature of 180 °C should be in a "safe" region.

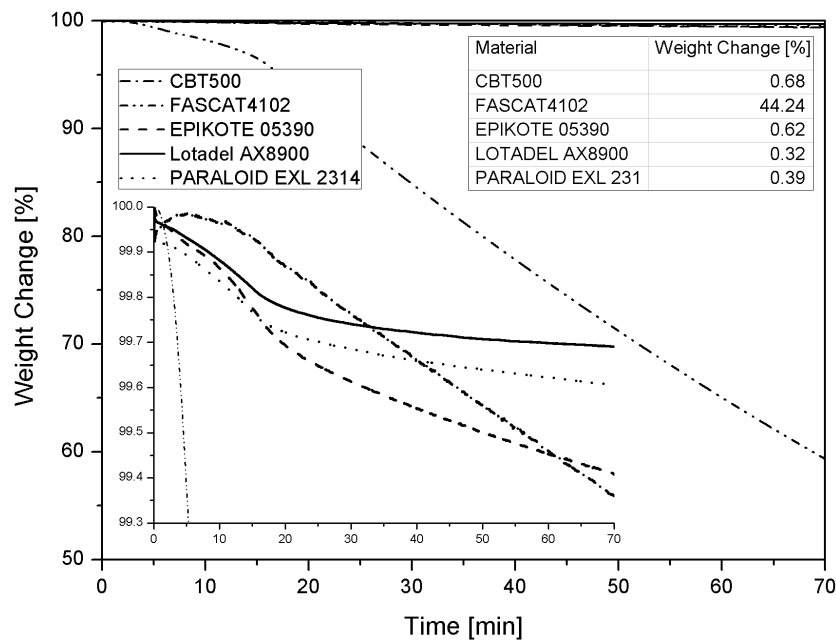


Figure 4.26.: Thermal stability of processing materials at isothermal processing temperature

4.2.4. Rheological analysis

For the rheological analysis the TEGOCAT256 (0.4 wt.%) catalyzed CBT500 matrix system was used for its medium reaction rate and easy sampling. Figure 4.27 illustrates the typical variation of viscosity and phase angle with time for the selected matrix system measured isothermally at 190 °C. The curves can be classified into four typical zones according to the phase transition depicted by the phase angle curve. Zone I in the first 25 min indicates the melting and stabilizing of the matrix system. The scattered phase angles in this zone can be attributed to the different portion of CBT oligomers in the matrix system as observed in the DSC investigations (section 4.2.2). The melted portion of CBT oligomers indicates a very low average complex viscosity of 0.05 Pa s. Zone II between 25 min and 31 min is the stabilized matrix system with a phase angle of 90 °C, indicating a purely viscous (Newtonian) fluid nature. The processing window indicated in the Figure across Zone I and Zone II is usually defined for resin infusion processes for evaluation of the processability of the applied resin system. This is according to the fact that a resin viscosity lower

1 Pa s is generally taken as the appropriate processing viscosity for good impregnation of textile fibers [53, 66]. Zone III between 31 min and 50 min reflects an abrupt phase change from a purely viscous (Newtonian) fluid to a nearly elastic solid with a phase angle of about 2° , indicating a drastic change in viscoelastic behavior in the matrix system. Along with the abrupt phase change, the viscosity of the matrix system increases rapidly from 10 Pa s up to 10^6 Pa s due to the fast ring-opening polymerization. Zone IV between 50 min and 60 min illustrates the end stage of the reaction, where both the phase angle and the complex viscosity remain fairly stable as a result of the completely consolidated sample in the measurement geometry.

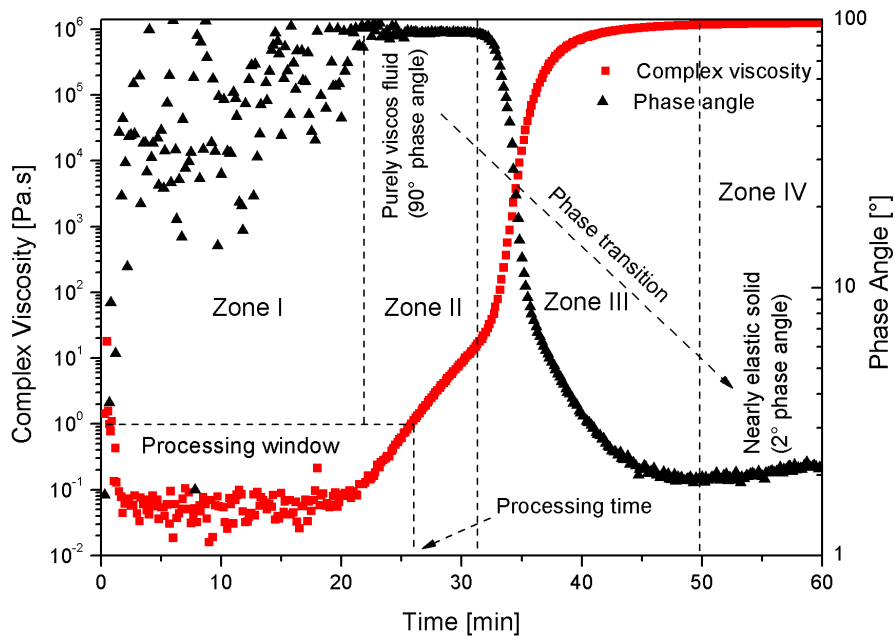


Figure 4.27.: Typical viscosity variation behavior of CBT500 during isothermal processing conditions

The processability of a resin matrix system is usually evaluated by the processing time which is the time needed for the viscosity of the resin matrix system reaching to 1 Pa s as illustrated in Figure 4.27. As the influence on the polymerization and crystallization behavior from the preforming binder has been confirmed in the previous DSC investigations, its effect on the rheological behavior such as the processing time was investigated as illustrated in Figure 4.28. For the TEGOCAT256 catalyzed CBT500 matrix system, the addition of preforming binder leads to an ex-

tension of processing time. Compared with the reference matrix system without any preforming binder, the processing time was extended by 8 min for the sample filled with 7 wt.% EPIKOTE[®] preforming binder. This may be attributed to the low melting point (90 ± 15 °C) of EPIKOTE[®] preforming binder whose viscosity would become very low at 190 °C due to the thermoplastic nature of the EPIKOTE[®] resin system. On the other hand, the extension of processing time may also be ascribed to the limited crystallization rate of polymerized pCBT as indicated in Table 4.9 that the presence of preforming binder can impede to some extent the crystallization of pCBT polymer. The reason of this is that the amount of crystals presented in the simultaneous polymerizing matrix system could act as micro or nano fillers which can dramatically increase the viscosity of the matrix system.

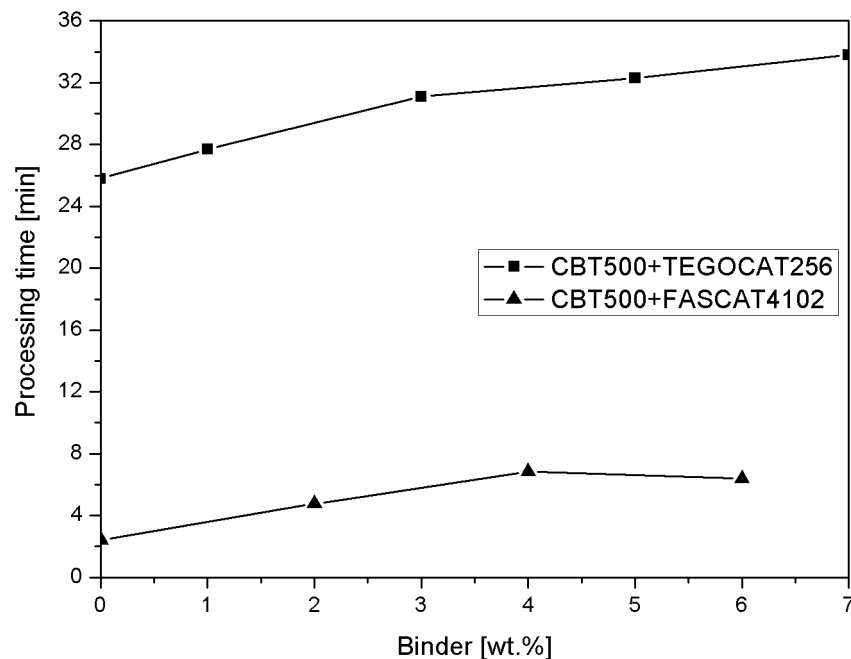


Figure 4.28.: Effect of binder on the processing time of CBT500 with various catalysts

The same trend of the effect on the processing time from preforming binder was observed for the FASCAT4102 catalyzed CBT500 matrix system as well. It is interesting to see that the processing time of FASCAT4102 catalyzed CBT500 matrix system with or without preforming binder is much shorter than the TEGOCAT256

catalyzed CBT500 matrix system. Compared with the TEGOCAT256 catalyzed CBT500 matrix system that has a processing time in the range of 25–35 min, the processing time of FASCAT4102 catalyzed CBT500 matrix system is only 2–7 min. This is much lower than the expected results which is about 10–15 min for the matrix system with 3 wt.% FASCAT4102 catalyst. The reason of the huge deviation may be attributed to the errors during preparation of the samples. As described in section 3.2.2, the samples for viscosity measurement is a circular plate with a diameter of 25 mm and a thickness of 1 mm. To prepare this kind of sample with CBT500 granulate and liquid FASCAT4102, the CBT500 was first fully melted at 180 °C in a aluminum cup, then the temperature of the resin melt was reduced and stabilized at 175 °C to add FASCAT4102 catalyst so that the polymerization rate can be decreased as much as possible. After mixing the matrix system with a magnet stirrer for 10 sec the samples were manufactured by resin casting with the help of a casting mold at the temperature of 120 °C. Whatever the operation speed (casting) is, there would be a certain extent of polymerization during mixing and the subsequent cooling of casted samples due to the fact that the catalyzed CBT oligomers can be polymerized even at lower temperatures as low as 160 °C [57, 87].

Summary

In this chapter, the effect of the compaction and preforming parameters on the FVF and RPT based on the Taguchi method and the preforming binder on the thermal and rheological properties of the catalyzed CBT oligomers were investigated. The main contributions of the chapter for further process development can be summarized as follows:

1. Based on the signal-to-noise ratio results, the optimal compaction and preforming parameters settings for fiber volume content and residual preform thickness are compaction temperature 190 °C, binder activation temperature 90 °C, binder content, 3 wt.%, binder activation time 0.5 min and compaction temperature 190 °C, binder activation temperature 90 °C, binder content 5 wt.%, binder activation time 0.5 min, respectively.

2. The compaction behavior of bindered textile preforms has been significantly influenced due to the presence of binder. Instead of the commonly applied three parameter model that correlates the fiber volume content and the compaction pressure during compaction of textile preforms under 0.1 MPa, a modified four parameter model was proposed to extend the modeling range up to 0.9 MPa. The fitted results have shown that the proposed modified four parameter model can make more accurate prediction of compaction and release response of the bindered textile preforms. Based on the proposed model the fiber volume content and residual preform thickness can be correlated well with the compaction and preforming parameters with the help of linear regression method.
3. Based on the analysis of variance results, the highly effective parameters on both the FVF and RPT were determined. Namely, the compaction temperature is the main factor that has the highest importance on the FVF and RPT. The preforming parameters binder activation temperature, binder content and binder activation time were confirmed to have little influence on FVF and RPT.
4. The presence of preforming binder has no distinct influence on the melting of catalyzed CBT oligomers. The crystallization of pCBT polymer during cooling, however, is confirmed to be significantly influenced by addition of preforming binder. The crystallization temperature and the crystallinity of pCBT polymer are both found to decrease with increased filling fraction of preforming binder.
5. The addition of preforming binder can influence the isothermal polymerization and crystallization process in terms of the starting time of crystallization, the crystallization rate and the crystal structures. The starting time of crystallization is found to be shifted to an earlier time due to the filling of preforming binder. The crystallization rate increases first with increasing preforming binder amount, which is then followed by a decreasing trend with further increased preforming binder.

6. A total of four typical phase transition zones can be observed during isothermal polymerizing of the catalyzed CBT oligomers, including the melting and stabilizing of the matrix, stabilized matrix system with purely viscous (Newtonian) fluid nature, reaction induced phase transition, and consolidated polymer matrix with nearly elastic solid nature. The processing time of the catalyzed oligomers during isothermal polymerization can be prolonged due to the presence of preforming binder.

Chapter 5

Key aspect II: Development of the manufacturing process

In this chapter, the development of the manufacturing process is demonstrated. Thermoplastic Vacuum Assisted Resin Infusion (T-VARI) manufacturing process was developed and evaluated by characterizing the thermal and mechanical properties of the manufactured textile reinforced pCBT composites. The proposed concept was achieved successfully with the developed T-VARI manufacturing process using bindered textile preforms. The influencing mechanism of the process parameters on the flexural properties of the textile reinforced pCBT composites were investigated using single factor analysis for further optimization intention on the T-VARI manufacturing process. The contributions from this chapter can be taken as the first milestone of the solution strategy of this dissertation research as shown in Figure 5.1.

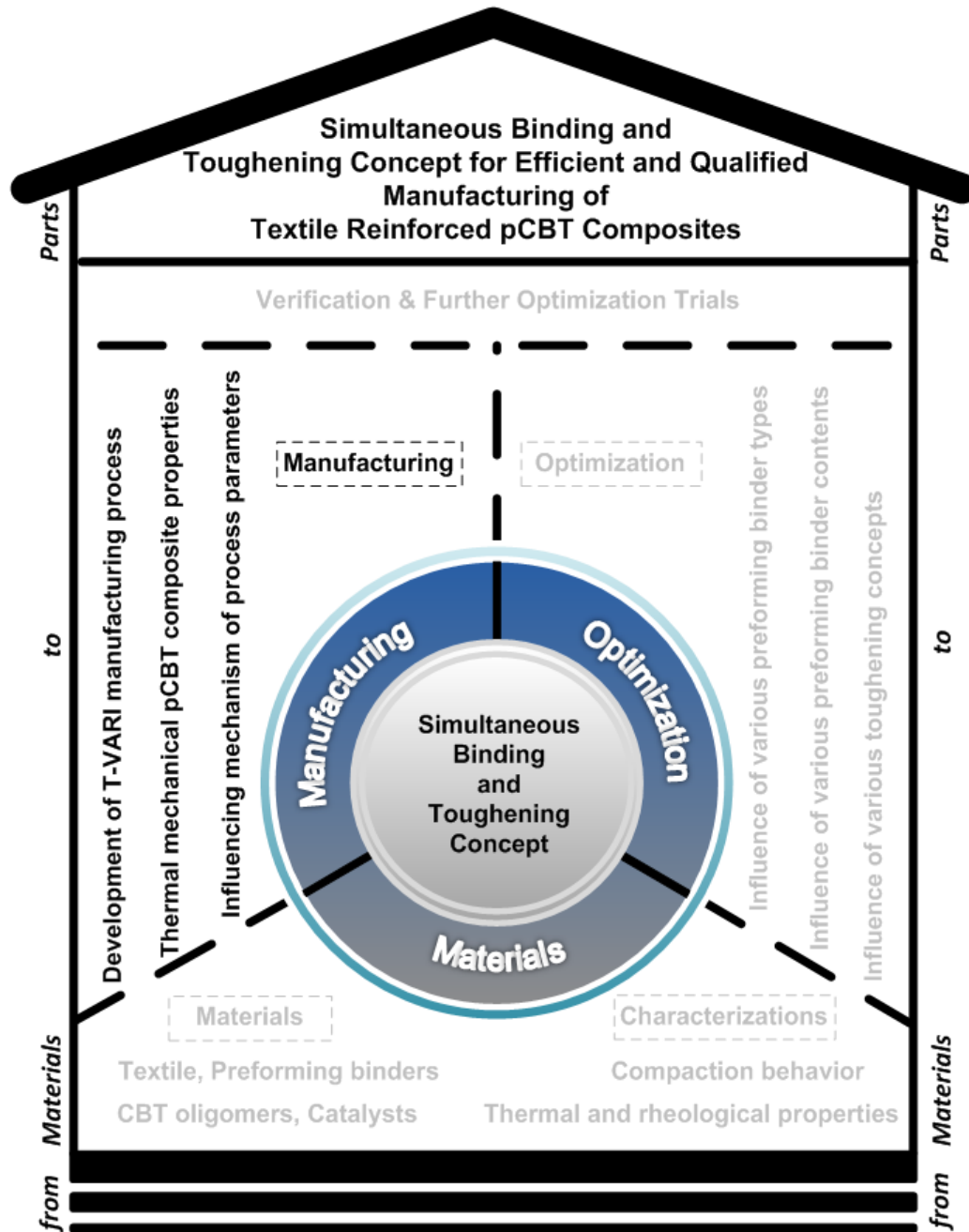
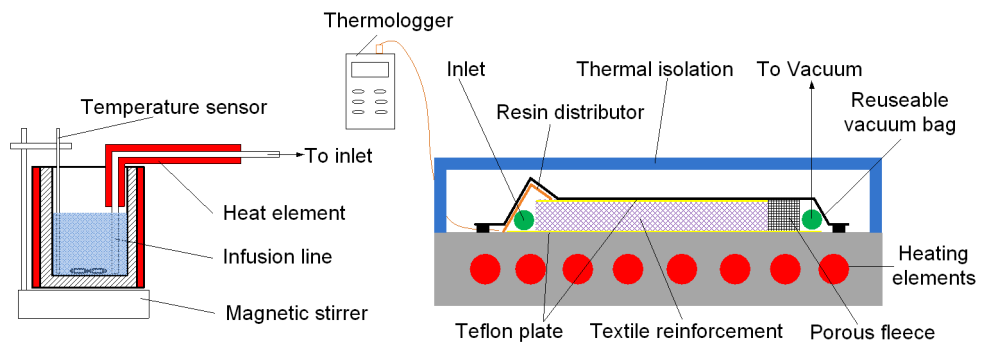


Figure 5.1.: Solution strategy: First milestone

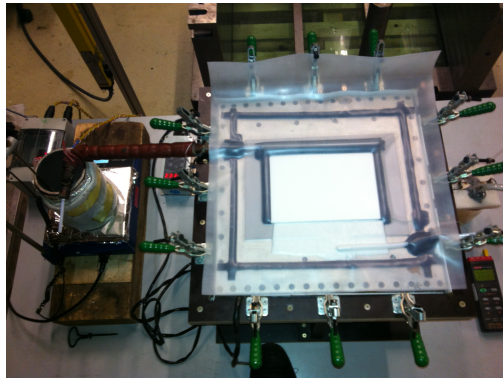
5.1. Realization of the manufacturing concept

5.1.1. Thermoplastic Vacuum Assisted Resin Infusion (T-VARI)

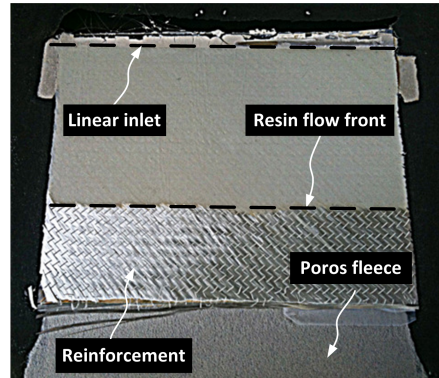
A schematic representation of the T-VARI system is shown in Figure 5.2(a). The CBT500 granulate is melted (175-185 °C) in a heated aluminum cup on a magnetic stirrer. After pouring the catalyst into the resin melt, the mixture is stirred by a rod rotating in the magnetic field for about 10 seconds. Then the resin infusion process is started with a defined vacuum pressure and mold temperature. The resin transfer tube (Silicon) goes through a heated L shape copper tube with a diameter greater than the resin transfer tube. The copper tube is sealed with iron powder filled between the silicon tube and copper tube in order to provide an isothermal temperature equal to the resin temperature so that the resin can neither be cooled nor overheated during transfer. A full vacuum of -850 mbar is applied during the polymerization reaction. The mold temperature is held constant for a certain time for the polymerization reaction. Two Teflon plates with a thickness of 1 mm are used in the experiment: one of them is between the laminate and the mold surface for easy de-molding and the other is between the laminate and the vacuum bag for improving the surface quality of the final plate. A reusable vacuum bag (Silicon film with a thickness of 1 mm) is applied to reduce the production cost. The porous fleece is used to stop the flow front timely, so that the vacuum could be held with a reusable unheated hose at the outlet side until the polymerization reaction is finished. Figure 5.2(b) and 5.2(c) show the developed processing system and a tri-axial glass fabric reinforced pCBT laminate manufactured with the processing system. The result indicates that the developed infusion process can achieve a good 1-dimensional infiltration of textile preforms, which is essential for analyzing the homogeneity of composite properties such as the variation of mechanical properties along the infiltration direction.



(a) Schematic representation



(b) Developed T-VARI processing system



(c) Manufactured textile reinforced pCBT laminate

Figure 5.2.: Development of T-VARI processing system

5.1.2. Characterization of the manufactured pCBT composites

Thermal properties

Figure 5.3 illustrates a typical heating trace of an unidirectional carbon fiber reinforced pCBT composites. A single melting peak was observed, indicating that the CBT oligomers can be polymerized and well crystallized without any small and defective crystals under isothermal processing conditions. The presence of textile reinforcement shows hardly any clear influence on the isothermal crystallization of pCBT polymer. A further observation was performed to examine the melting point and crystallinity along the infiltration direction. The results indicate that the flow distance has no distinct influence on the melting point and crystallinity. The investigated laminate has an average melting point of 224.8 ± 0.6 °C and an average crystallinity of 47.4 ± 2.6 %.

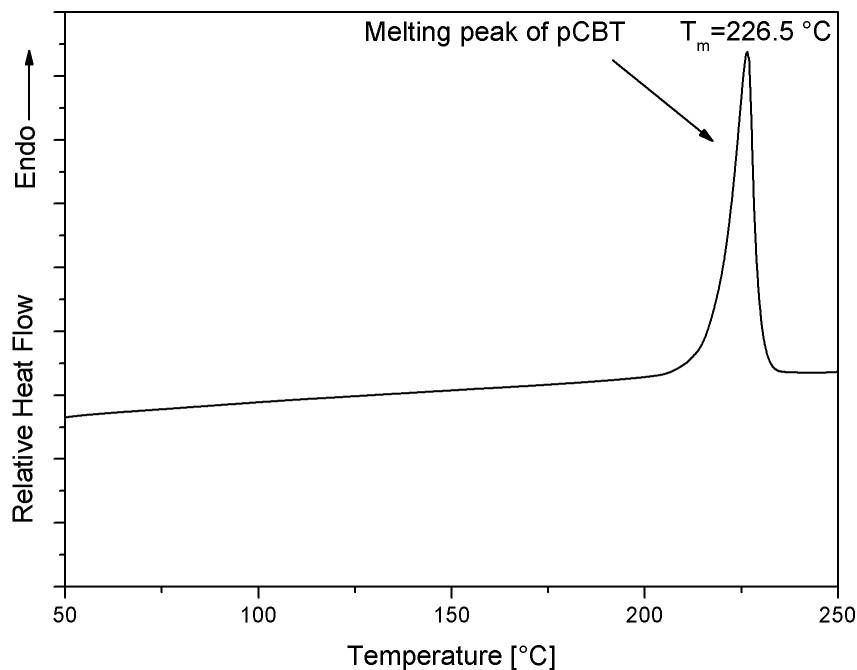


Figure 5.3.: Melting behavior of unidirectional carbon fiber reinforced pCBT laminate

The unidirectional carbon fiber reinforced pCBT sample was further investigated with TGA to determine the dynamic thermal stability of the composite laminate. As shown in Figure 5.4, a total weight loss of 38.6 % was observed until the temperature increases up to 500 °C, indicating that the composite sample has a fiber mass fraction of 61.4 %. Further observation was performed to determine the onset temperature of the composites along the infiltration direction. The results indicate that the flow distance has no distinct influence on the onset temperature. The investigated laminate has an average onset temperature of 372.6 ± 0.5 °C along the infiltration direction.

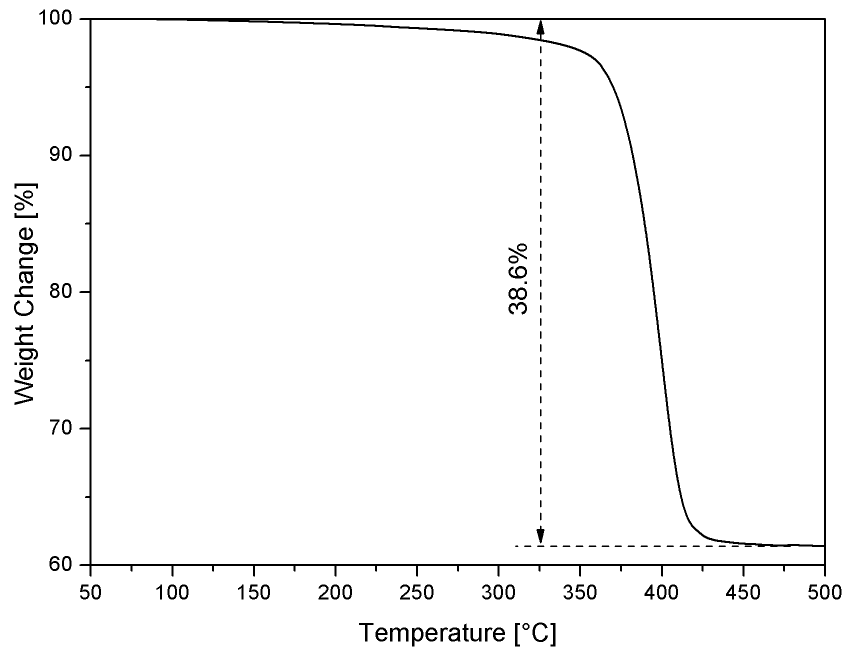


Figure 5.4.: Thermal stability of unidirectional carbon fiber reinforced pCBT laminate

Dynamic mechanical properties

Figure 5.5 shows the dynamic mechanical properties of a bi-axial carbon fiber fabric reinforced pCBT laminate. The influence of temperature on the storage modulus and loss modulus was illustrated with a temperature ramp of 2 °C/min starting from

-25 °C to 225 °C. The laminate sample has a initial storage modulus of 42.7 GPa, which is decreased to 26.2 GPa at onset point (206.3 °C) after glass transition, indicating a very good thermal durability of the materials. The value of the initial storage modulus in this study is about 25 % higher than the results from Shahzad et al. [88]. This may be ascribed to the high rigidity of carbon fibers and the difference of the reinforcement configuration which is $[0/90, \pm 45]_s$ in this study and $[0/90, \pm 45, 0/90, \pm 45, 0/90]_2$ in [88] respectively. On the other hand, the higher crystallinity of pCBT matrix at 190 °C than the pCBT matrix from Shahzad et al. [88] who conducted the isothermal production process at 200 °C could be another possible reason. In general, the results indicate that the developed T-VARI process and the manufactured composite materials in this study is comparable to the process used by Shahzad et al. [88].

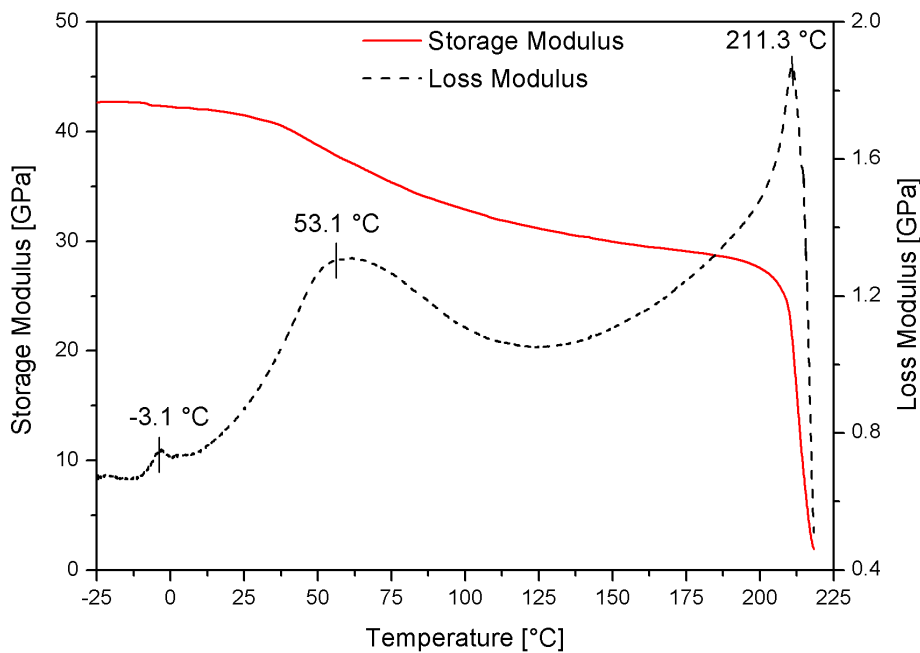


Figure 5.5.: Dynamic mechanical properties of a bi-axial carbon fiber fabric reinforced pCBT laminate

A total of three phase transition peaks were observed in the loss modulus curve. The first transition peak appears at -3.1 °C, which is a critical temperature that indicates the temperature dependence of storage modulus. Below this critical temperature

the storage modulus is essentially constant without temperature dependence. In contrast, the storage modulus starts to decrease with increasing temperature above this critical temperature. The second transition peak appears at 53.1 °C, which can be considered as the glass transition temperature of the composite sample. The composite laminate indicates a significant variation of storage modulus while passing through the glass transition span of temperature. With the same measurement conditions, the detected glass transition temperature is lower than the reported value of 61.2 °C for glass fiber reinforced pCBT composites by Shahzad [88]. This slight variation in glass transition temperature might be attributed to the difference of the reinforcement fibers (Carbon fiber versus Glass fiber) and the crystallization conditions in the two composite materials. The third transition peak near the onset point indicates that the energy dissipation reaches to a maximum and that the composite material reaches to its ultimate service temperature. After this temperature a dramatic decrease of the material rigidity would occur, followed by the melting of the polymer matrix in the composite materials.

Impregnation quality

The impregnation quality of the textile reinforced pCBT composites was observed under digital microscope using unidirectional fiber reinforced pCBT samples. An overview of the cross section of the sample with a magnification of 200× is illustrated in Figure 5.6. In general the unidirectional fibers are impregnated very well by the low viscous CBT resin, leaving only a few macro bubbles in the inter-ply region. Those macro bubbles may be caused by the dual scale flow effect during infiltration [32, 86]. Further observation in the fiber bundles was performed with a magnification of 1000× as shown in the upper left corner of Figure 5.6. Most of the fiber filaments are covered by pCBT matrix, indicating again a good fiber impregnation quality. However, a small amount of micro bubbles were observed among the fiber filaments as well. These bubbles may be included during the mixing of catalyst or infiltration because of the unbalance fast resin flow in the textiles [32, 86].

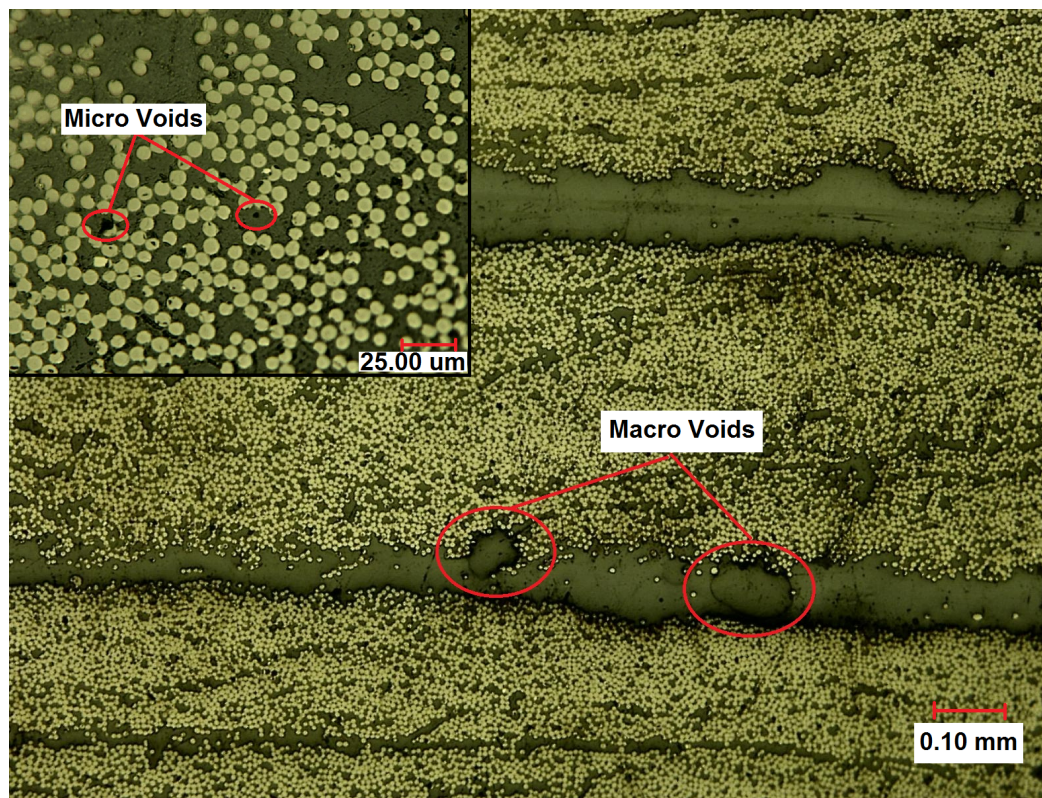


Figure 5.6.: Impregnation quality of unidirectional carbon fiber reinforced pCBT laminate

5.1.3. Simultaneous binding and toughening concept

After characterization of the materials (section 4.1 and 4.2) and the development of T-VARI manufacturing process (section 5.1.1), simultaneous binding and toughening concept proposed in section 1.2 was achieved in this step for textile reinforced pCBT composites. Bindered textile preforms were impregnated with the developed T-VARI manufacturing process as indicated in Figure 5.2. Flexural properties of the manufactured composite laminates were characterized according to the procedure as described in section 3.3.3.

Figure 5.7 indicates a typical flexural stress-strain relations of textile reinforced pCBT laminates prepared with or without applying simultaneous binding and toughening concept. Both of the two composite laminate shows a brittle failure before yielding as the curve 'a' illustrated in Figure 3.9. The brittle nature inherent in the composite laminate based on pCBT matrix was not completely eliminated. However, the composite laminate prepared with simultaneous binding and toughening concept exhibits a great improvement of flexural strain at break. Compared with the reference laminate, an increase of 74.2 % in flexural strain at break was observed for the textile reinforced pCBT laminate prepared with simultaneous binding and toughening concept. The expected simultaneous toughening of inter-ply region was achieved with EPIKOTE[®] Resin 05390 preforming binder. Most importantly, the toughening performance was obtained without impairing other mechanical properties. On the contrary, an increase of 69.6 % in flexural strength was observed in the case of simultaneous binding and toughening sample with the flexural modulus was not significantly influenced.

Further investigation focus on the effect of various toughening concepts on the toughening performance was analyzed according to the flexural test results, accompanied by the analysis of their influence on the mechanical properties. The toughening performance was evaluated by the value of flexural strain at break. While the flexural modulus and flexural strength results were taken for the mechanical analysis. Table 5.1 illustrates the flexural test results from a control laminate without any toughening effort, laminates prepared according to in-situ toughening concept in which the preforming binder was taken as toughening agent and directly mixed with

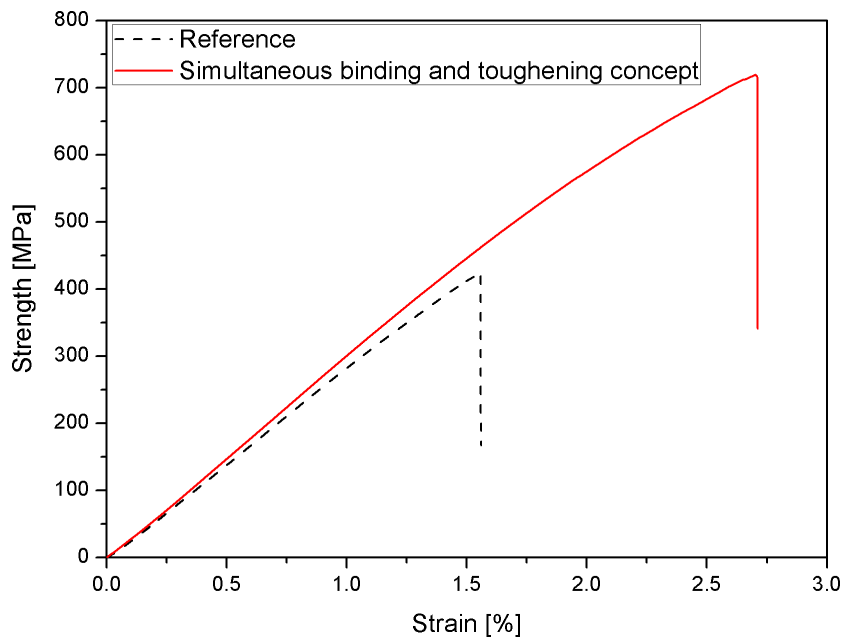


Figure 5.7.: Typical flexural stress-strain relations of textile reinforced pCBT laminate prepared with simultaneous binding and toughening concept

CBT resin before resin infiltration, and laminate prepared according to simultaneous binding and toughening concept (quasi as ex-situ toughening concept according to the description in section 1.3.3).

The results show that both in-situ and ex-situ toughening concept have great potential in toughening of textile reinforced pCBT composite. Compared with the control composite laminate, in-situ toughening with 2 or 4 wt.% leads to an improvement of about 18 % in flexural strain. Due to the presence of preforming binder the flexural strength was improved by about 26.7 % in the case of filling of 4 wt.% preforming binder. While the flexural modulus was nearly not changed. As for the ex-situ toughened variants, the toughening potential was only observed with 2 wt.% preforming binder in the inter-ply region, which illustrates an excellent toughening performance with an increase of 72.9 % in flexural strain, 69.1 % in flexural strength, and even 8.3 % in flexural modulus respectively. An increase of preforming binder up to 4 wt.% in the case of ex-situ toughening seems to have a negative influence on the toughening performance and mechanical properties. No significant

improvement of flexural strain was observed and both flexural modulus and flexural strength were greatly reduced compared with the control laminate.

Table 5.1.: Effect of simultaneous binding and toughening concept on the flexural properties of textile reinforced pCBT composite

Toughening concept	Binder content	Flexural modulus	Flexural strength	Flexural strain
	[wt.%]	[GPa]	[MPa]	[%]
—	0	26.5 ± 2.5	420.7 ± 21.1	1.59 ± 0.07
In-situ	2	25.1 ± 4.5	506.7 ± 54.7	1.94 ± 0.12
	4	26.4 ± 2.8	532.8 ± 25.1	1.99 ± 0.12
Ex-situ	2	28.7 ± 0.9	711.6 ± 31.4	2.75 ± 0.15
	4	21.5 ± 1.7	347.3 ± 11.1	1.69 ± 0.32

The toughening performance of both in-situ and ex-situ toughening concept for textile reinforced pCBT composites may be ascribed to the influence of preforming binder on the simultaneous polymerization and crystallization conditions of pCBT polymer matrix in the composite laminate. According to the findings in section 4.2.2 the pCBT polymer could be toughened by affecting of crystallization conditions through filling of preforming binder in both non-isothermal (Table 4.9) and isothermal conditions (Figure 4.21). For the in-situ toughening concept, the pCBT polymer matrix was toughened globally since the preforming binder was directly mixed with the CBT resin before infiltration. There will always be interactions between the preforming binder and the catalyzed CBT oligomers during manufacturing, including the infiltration and the followed isothermal polymerization and crystallization process. While in the case of ex-situ toughening concept, the pCBT polymer matrix was toughened locally since the preforming binder is mainly located in the inter-ply region of the composite laminate. The interaction between the preforming binder and the catalyzed CBT oligomers is limited in the inter-ply region and occurred primarily during isothermal polymerization and crystallization stage. This is because that the low viscous CBT oligomer melt tends to impregnate the intra-ply region first due to the lower flow resistance when compared with the inter-ply region which is partly blocked by the preforming binder.

This can be verified according to the results from Dickert et al. [29] in their study on the Influence of binder activation and fabric design on the permeability of non-crimp carbon fabrics. As shown in Figure 5.8, the preforming binder exhibits various states under different temperatures. For all of the investigated filling contents, the preforming binder starts to melt partly and forms agglomerates at the activation temperature of 90 °C in the inter-ply region, which is in accordance with Figure 1.5(a) described in section 1.2. Those agglomerates are fully melted at increased temperature of 110 °C. When the temperature is further increased up to 160 °C, the melted preforming binder indicates a reduced viscosity due to its thermoplastic nature and flows into the fiber bundles (Figure 1.5(b)). Therefore, the inter-ply region of the bindred textile preforms is blocked either by the partly melted preforming binder agglomerates at molding temperatures lower than 110 °C or by the fully melted preforming binder melt at molding temperatures higher than 110 °C (e.g. 185 °C in the present study)

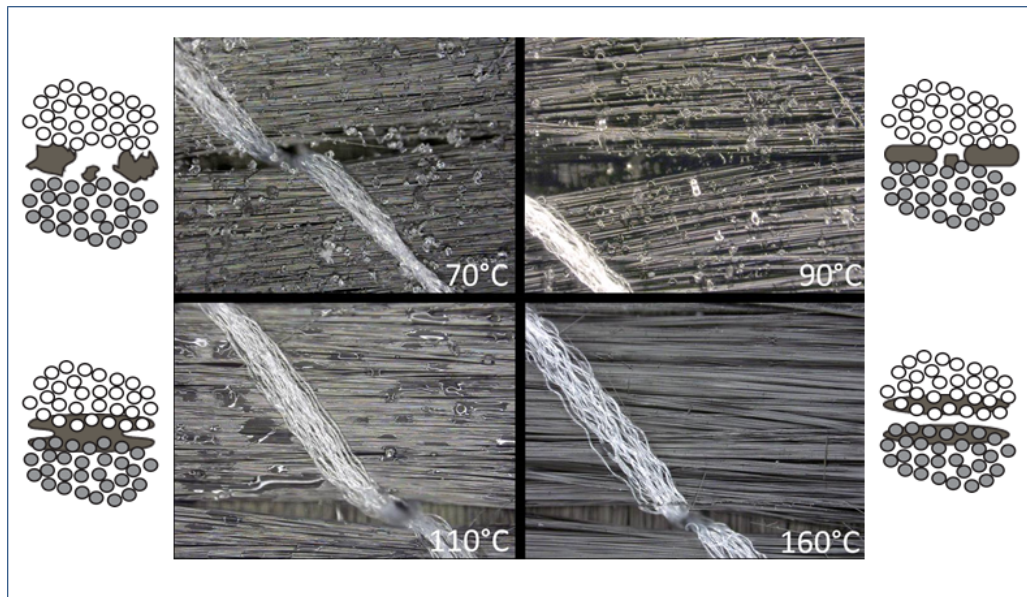


Figure 5.8.: Various preforming binder states under different activation temperatures according to Dickert et al. [29]

The difference interaction mechanism between the preforming binder and the catalyzed CBT oligomer melt leads to a completely different toughening performance of the two toughening concept. For the in-situ toughening concept the direct mixing of toughening agent may sacrifice the good flowability of CBT oligomer melt as stated in section 1.4. This would limit the availability of the appropriate toughening agents because they must fulfill an extra condition that the viscosity of oligomer melt should not be significantly influenced besides a good toughening performance. Moreover, the global toughening nature of in-situ toughening may lead to a limited toughening performance. The amount of toughening agent that can be filled with matrix resin is usually limited due to the fact that the excessively reduced crystallinity for good toughening performance may sacrifice the mechanical properties at the same time. As for the ex-situ toughening concept usually no extra requirement on the toughening agent is desired except for a good toughening performance. However, in this research an additional requirement of good adhesive properties is desired for a good binding of textiles. Since the preforming binder as toughening agent is located mainly in inter-ply regions, the interaction between preforming binder and CBT oligomers after resin infiltration can be considered that the inter-ply region is actually a highly filled resin matrix system with a high amount of toughening agent. In this way, the crystallinity in this area would be greatly decreased and the mechanical properties as well. However, the overall mechanical properties would not be influenced since it is primarily determined by the fiber reinforced intra-ply region where the pCBT matrix remains its high crystallinity nature because of the barely exists preforming binder.

5.2. Influence of process parameters

5.2.1. Analysis of related process parameters

Generally, there are four influential process parameters including catalyst amount, vacuum pressure, processing temperature, and reaction time in manufacturing of textile reinforced pCBT composites with T-VARI manufacturing process. For the proposed simultaneous binding and toughening concept, additional process param-

eters such as binder content may be introduced in the manufacturing process. As shown in Figure 5.9, the presence of preforming binder has confirmed that the material properties can be influenced as illustrated in section 4.1 and 4.2. However, its influence on the manufacturing process is not yet clear. The changed material properties can be transferred further to manufacturing process, resulting in a different process parameters as well. For example, the optimal vacuum pressure that could achieve a good balance of dual scale effect may be changed in the presence of preforming binder [32, 86]. This may be ascribed to the fact that the inter-ply region and the space between inter fiber bundles may partly be blocked by the preforming binder. Therefore, it is necessary to analyze the related process parameters during manufacturing of the textile reinforced pCBT composites. Possible effects due to the application of preforming binder on the process parameters are discussed as follows:

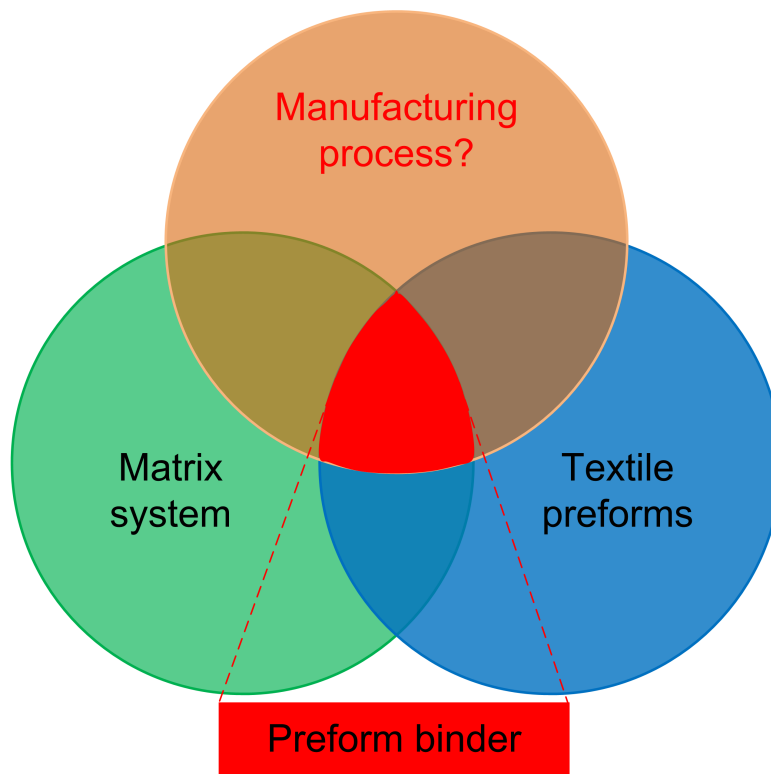


Figure 5.9.: Schematic description of the influence of preforming binder on the matrix system, textile preforms and manufacturing process

Catalyst amount

Since the catalyst amount may influence the processing time as the resin temperature, it is necessary that the catalyst amount should be tailored so as to fulfill the processing conditions. In addition, the catalyst amount can also influence the simultaneous polymerization and crystallization process during isothermal processing conditions, since the pCBT polymer can only crystallize with a sufficiently high molecular weight as discussed previously in section 4.2.2. The more amount of catalyst, the faster the polymerization of CBT oligomers to pCBT with a sufficiently high molecular weight. And the earlier the pCBT polymer starts to crystallize. This may further affect the mechanical properties of the textile reinforced pCBT composites.

Preforming binder

The preforming binder is another influential process parameter for manufacturing of textile reinforced pCBT composites with the proposed simultaneous binding and toughening concept. It has been confirmed that the preforming binder has a significant influence on the material behavior of the bindered textile preforms and CBT resin matrix system (section 4.1 and 4.2). Those influences may be further transferred to the manufacturing process and influence the production conditions.

In addition, the influence of binder on the properties of material component may be shifted to the composite system as well. As a typical example, DMA analysis as shown in Figure 5.5 for biaxial non crimp carbon fabric reinforced pCBT laminate ($[0/90^\circ, \pm 45^\circ]_s$) was extended by including a thermoplastic Polyamide (PA) fleece binder as indicated in Figure 5.10. The results in Figure 5.11 illustrate that the presence of the PA fleece binder in the inter-ply region has a significant influence on the thermal mechanical properties of textile reinforced pCBT composites. The composite laminate with PA fleece binder exhibited a higher initial storage modulus below room temperature (25 °C) but a lower storage modulus above room temperature until the inflection point. This may be attributed to the thermal mechanical properties of the PA fleece binder. For the temperatures below room temperature,

the thermoplastic PA fleece binder tends to become rigid and brittle (section 2.1.5). As a result, the fleece binder turns to a thermoplastic PA reinforcing fibers at lower temperatures so that the inter-ply region of the composite laminate is further reinforced, leading to a higher rigidity. However, as the temperature rises above room temperature, the reinforcing effect does not exist any more because of the softened PA fleece binder. What the worse is, the presence of softened PA fleece binder at higher temperatures leads to a reduced Fiber Volume Fraction, which is the main cause of reduced storage modulus.

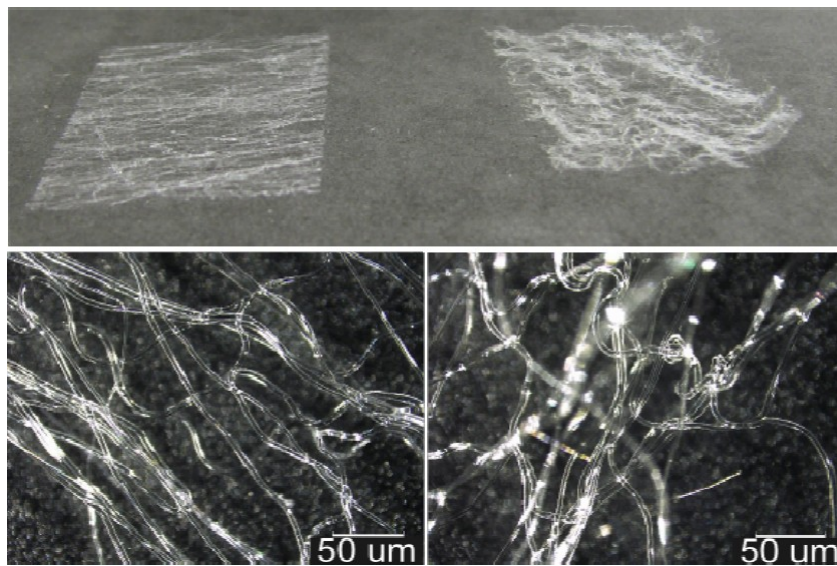


Figure 5.10.: Thermoplastic fleece binder [5]

Processing temperature

As indicated in section 4.1 and 4.2, processing temperature is one of the most influential process parameter that can affect both the compaction behavior of bindered textile preforms and the thermal rheological properties of catalyzed CBT oligomer system. These effects would further influence the whole manufacturing process from resin infiltration to the subsequent simultaneous polymerization and crystallization and to the final isothermal de-molding. For the resin infiltration process, too high processing temperature may lead to an accelerated reaction of infiltrated resin

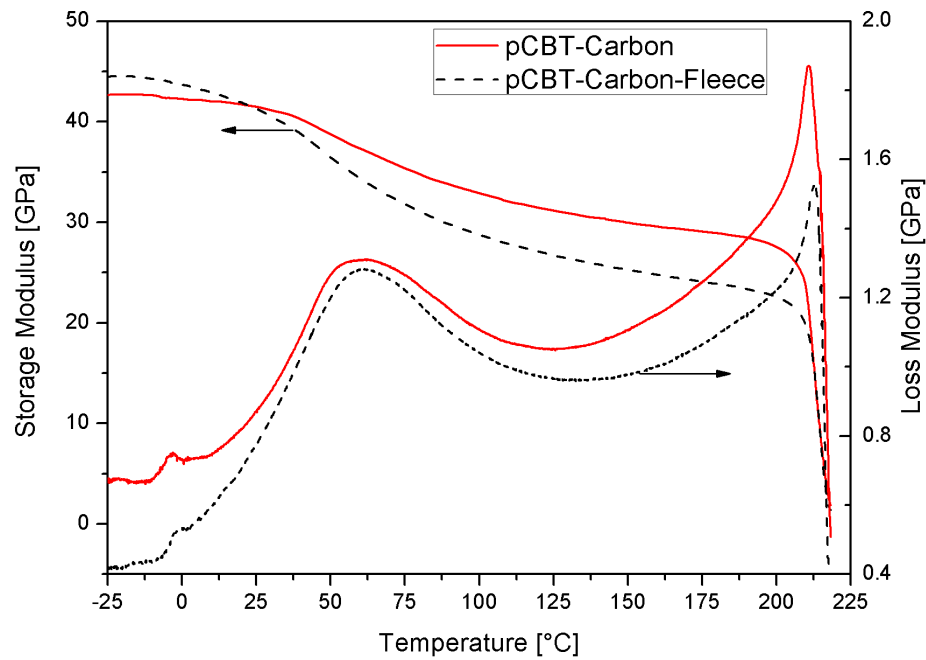


Figure 5.11.: Influence of binder on the dynamic mechanical properties of textile reinforced pCBT laminate

in the textile preform and a limited processing window (section 4.2.4), resulting a not fully infiltrated laminate. For the simultaneous polymerization and crystallization, the processing temperature can affect the conversion rate and the starting point of crystallization as the catalyst amount. As for the isothermal de-molding, the processing temperature can influence the rigidity of the manufactured laminate as illustrated in Figure 5.5. A temperature as high as the onset point (about 206 °C for pCBT matrix) can be considered as the maximum processing temperature for a non-destructive isothermal de-molding. Moreover, the processing temperature is also a process parameter that usually used for evaluation of the process economics, since the higher the processing temperature, the more energy consumption of the process and therefore the lower the process economics.

Vacuum pressure

For the very low viscous CBT oligomers melt, it is extremely important that the flow speed in the porous textile preforms should be controlled so that the dual scale effect could be balanced in an appropriate way [32, 86]. As stated before, this may be attributed to the partly blocked inter-ply region and the space among the fiber bundles. As a result, the macro flow speed in these areas is greatly limited. However, the micro flow which is caused by the strong capillary effect is not significantly influenced by the preforming binder. When the macro and micro flow during infiltration is not good balanced with appropriate vacuum pressure, macro or micro bubbles could be formed during infiltration, which would further influence the mechanical properties of the textile reinforced pCBT composites as well.

Reaction time

The reaction time is the time needed for simultaneous polymerization and crystallization process. It can be affected by the catalyst amount and the processing temperature. The more catalyst is added and the higher the processing temperature, the less time is required to finish the simultaneous polymerization and crystallization process. Not sufficient reaction time may lead to a limited conversion and crystallinity, resulting in a low mechanical performance of the manufactured textile reinforced pCBT composites.

In conclusion, the above mentioned five process parameters are so important that a parametric analysis is necessary to be performed in order to determine their influence on the toughening performance and the mechanical properties for textile reinforced pCBT composites manufactured with simultaneous binding and toughening concept. Therefore, in this section the influence of process parameters on the flexural properties of textile reinforced pCBT laminate were investigated. Special emphasis was put on the four process parameters, including the catalyst amount, preforming binder, processing temperature, and vacuum pressure due to their extremely importance on the material toughness and mechanical performance. The reaction time was taken as a constant parameter in this analysis due to its subor-

minated nature to other process parameters such as catalyst amount and processing temperature. The series experiments were designed according to single factor experiment method. The variation of the single process parameters including catalyst amount, binder filling content, processing temperature and vacuum pressure was based on a selected group of constant process parameters as illustrated in Table 5.2.

Table 5.2.: Process parameters for single factor experiment analysis

Process parameters	Unit	Investigated values			
Catalyst amount	[wt.%]	1	3	5	7
Binder filling content	[wt.%]	0	2	4	6
Processing temperature	[°C]	180	185	190	195
Vacuum pressure	[mbar]	−600	−700	−800	−900
Constant process parameter					
→ Catalyst amount: 5 wt.%;					
→ Binder content: 2 wt.%; Processing temperature: 185 °C;					
→ Vacuum pressure: -800 mbar; Reaction time: 90 min					

5.2.2. Effect of catalyst amount

Table 5.3 illustrates the variation of catalyst amount on the flexural properties of textile reinforced pCBT composite. Significant influences on the toughening performance and the mechanical properties was observed during the variation of catalyst amount. An obvious inflection point at 5 wt.% can be seen on the variation of catalyst amount from 1 wt.% to 7 wt.%. The flexural properties increases with increasing catalyst amount until the inflection point, followed by a falling trend with further increase of catalyst amount to 7 wt.%. A total improvement of 88.4 % in flexural strain, 172.1 % in flexural strength, and 61.1 % in flexural modulus were observed when the catalyst increases from 1 wt.% to 5 wt.%.

A catalyst amount of 5 wt.% leads to the optimum flexural properties of the textile reinforced pCBT composite. This may be ascribed to the moderate reaction speed which leads to a good impregnation of bindered textile preforms as a result of the modest increase of viscosity. On the other hand, good balance of the simultane-

ous polymerization and crystallization could probably be another reason, since the pCBT polymer polymerized with sufficiently high molecular weight is necessary for good rigidity and strength. The crystallization of pCBT is to some extent reduced by the preforming binder, leading to an improved composite toughness with a high flexural strain.

A lower amount of catalyst than 5 wt.% may lead to a poor impregnation quality because of the extension of resin processing time with very low viscosity, since the catalyst is insufficient for an appropriate viscosity increment. As a result, micro flow in fiber bundles due to the capillary effect is dominant during resin infiltration, resulting a lot of macro bubbles among fiber bundles [32, 86]. Furthermore, the conversion rate and crystallinity may not sufficient high enough for a good flexural properties due to the lack of catalyst. In contrast, excessive amount of catalyst may lead to a limited processing window because of the fast viscosity increment. This would further lead to a poor impregnation quality as well due to the high viscosity, since both macro and micro flow are both limited during resin infiltration in this case, resulting a poor impregnation quality in both scales.

Table 5.3.: Effect of catalyst amount on the flexural properties of textile reinforced pCBT composite

Toughening concept	Catalyst amount	Flexural modulus	Flexural strength	Flexural strain
	[wt.%]	[GPa]	[MPa]	[%]
Ex-situ	1	17.6 ± 2.1	261.6 ± 89.7	1.46 ± 0.23
	3	23.7 ± 3.1	389.7 ± 53.2	1.58 ± 0.24
	5	28.7 ± 0.9	711.6 ± 31.4	2.75 ± 0.15
	7	21.2 ± 1.3	410.9 ± 116.9	1.97 ± 0.40
Constant process parameter				
→ Binder content: 2 wt.%; Processing temperature: 185 °C				
→ Vacuum pressure: -800 mbar; Polymerization time: 90 min				

5.2.3. Effect of binder content

Table 5.4 illustrates the variation of binder on the flexural properties of textile reinforced pCBT composite. As illustrated in section 5.1.3 the application of preforming binder up to 2 wt.% lead to a significantly improved composite toughness such as the flexural strain and the mechanical properties like flexural modulus and flexural strength. The explanation of this improvement has been given in section 5.1.3. It is interesting to see that a further increase of binder filling content does not lead to a further improvement of both toughening performance and mechanical properties. On the contrary, both of them were negatively influenced with increasing binder filling content. A decrement of 38.5 % in flexural strain, 51.2 % in flexural strength, and 25.1 % in flexural modulus were observed when the binder filling content increases from 2 wt.% to 4 wt.%. There seems to be a recover of flexural properties when the binder filling content is further increased up to 6 wt.% compared to the variant with 4 wt.% preforming binder. However, the huge deviations in the flexural properties indicate that there is no point for further increase of binder filling content.

As illustrated in the material characterizations (section 4.1), the preforming binder can improve the compaction performance at high temperature such as 190 °C due to the lubricating effect of melted preforming binder. However, the porosity of the textile preforms may be greatly reduced due to the excessive binder which flows into the fabrics after melting at processing temperatures. This is probably the reason for the reduced flexural properties at higher binder filling contents, since the inter-ply region of pCBT laminate may actually become a low molecular binder rich area with barely existence of pCBT polymers. Another consequence of excessive preforming binder is the strong flow resistance during resin infiltration. As a result the resin infiltration speed is greatly limited with big difference of thermal history of pCBT polymer along infiltration direction. This would further lead to non-uniform properties such as the huge deviations presented in the manufactured laminate with 6 wt.% preforming binder.

Table 5.4.: Effect of binder content on the flexural properties of textile reinforced pCBT composite

Toughening concept	Binder content	Flexural modulus	Flexural strength	Flexural strain
	[wt.%]	[GPa]	[MPa]	[%]
Ex-situ	0	26.5 ± 2.5	420.7 ± 21.1	1.59 ± 0.07
	2	28.7 ± 0.9	711.6 ± 31.4	2.75 ± 0.15
	4	21.5 ± 1.7	347.3 ± 11.1	1.69 ± 0.32
	6	24.9 ± 3.9	478.4 ± 135.3	2.08 ± 0.48

Constant process parameter

→ Catalyst amount: 5 wt.%; Processing temperature: 185 °C

→ Vacuum pressure: -800 mbar; Polymerization time: 90 min

5.2.4. Effect of processing temperature

Table 5.5 illustrates the variation of processing temperature on the flexural properties of textile reinforced pCBT composite. The same variation trend of flexural properties was observed as in the case of preforming binder (Table 5.4). Both of the toughening performance and the mechanical properties are significantly influenced by the variation of processing temperature. An optimum performance of flexural performance exhibits at the processing temperature of 185 °C when the processing temperature increases from 180 °C to 195 °C. The flexural properties first increases with increasing processing temperature until 185 °C and then decreases with increasing processing temperature until 190 °C. Further increase of processing temperature up to 195 °C lead to a nearly unchanged flexural performance when the deviations are considered.

As explained for the effect of catalyst amount in section 5.2.2, processing temperature may influence the viscosity increment during infiltration and the simultaneous polymerization and crystallization as well. At processing temperatures as low as 180 °C, the reaction speed was greatly limited. The influence of processing temperature on the infiltration process and the subsequent simultaneous polymerization and crystallization can be interpreted the same as the insufficient catalyst amount (section 5.2.2). For higher processing temperatures as 190 or 195 °C, the effect

on the viscosity during infiltration is the same as excessive catalyst amount because of the accelerated reaction rate at higher processing temperatures. For the simultaneous polymerization and crystallization process, the polymerization of CBT oligomer to pCBT with a sufficiently high molecular weight is accelerated due to the higher processing temperature, leading to a longer time for crystallization of pCBT polymer. However, as the processing temperature approaching to the crystallization temperature of pCBT (Figure 4.20), a high amount of perfect crystals may be formed due to the fast crystallization process, leading to a worse toughening performance than the one with processing temperature of 185 °C. The flexural performance was therefore limited by the poor impregnation quality together with the high crystallinity of pCBT polymer.

Table 5.5.: Effect of processing temperature on the flexural properties of textile reinforced pCBT composite

Toughening concept	Processing temperature	Flexural modulus	Flexural strength	Flexural strain
	[°C]	[GPa]	[MPa]	[%]
Ex-situ	180	21.8 ± 2.5	331.4 ± 85.6	1.57 ± 0.24
	185	28.7 ± 0.9	711.6 ± 31.4	2.75 ± 0.15
	190	25.2 ± 4.6	444.9 ± 15.9	1.87 ± 0.12
	195	23.4 ± 3.2	436.4 ± 59.6	1.97 ± 0.27
Constant process parameter				
→ Catalyst amount: 5 wt.%; Binder content: 2 wt.%				
→ Vacuum pressure: -800 mbar; Polymerization time: 90 min				

5.2.5. Effect of vacuum pressure

Table 5.6 illustrates the influence of the variation of vacuum pressure on the flexural properties of textile reinforced pCBT composite. It is observed that both toughening performance and mechanical properties were influenced by the variation of vacuum pressure. As it has been demonstrated for the other process parameters, the flexural performance was first improved with increasing vacuum pressure to an optimum at -800 mbar, then it was impaired with further increased vacuum pressure of -900 mbar. A total improvement of 79.7 % in flexural strain, 109.2 % in flexural strength, and 25.3 % in flexural modulus was observed while the vacuum pressure increases from -600 mbar to -800 mbar. However, those improvements were completely lost when the vacuum pressure increases up to -900 mbar.

It is expected that the vacuum pressure would have those influences according to the dual scale flow effect [32, 86] as explained in the case of catalyst amount (section 5.2.2) and processing temperature (section 5.2.4). The resin infiltration speed would be only influenced by the vacuum pressure, when the catalyst amount and the processing temperature were given with a reasonable value so that the resin infiltration speed would not be influenced by the inappropriate resin viscosity because of the irrational reaction speed (section 5.2.2 and 5.2.4). At lower vacuum pressures such as -600 mbar and -700 mbar, the speed of macro flow among the fiber bundles is limited due to the insufficient pressure difference. However, the micro flow in the fiber bundles caused by the capillary effect remains unaffected, leading to the formation of macro bubbles among the fiber bundles [32, 86]. On the contrary, at higher vacuum pressure such as -900 mbar, the speed of macro flow among the fiber bundles is greatly accelerated and may even faster than the micro flow in the fiber bundles, leading to the formation of micro bubbles in the fiber bundles [32, 86].

Table 5.6.: Effect of vacuum pressure on the flexural properties of textile reinforced pCBT composite

Toughening concept	Vacuum pressure	Flexural modulus	Flexural strength	Flexural strain
	[mbar]	[GPa]	[MPa]	[%]
Ex-situ	-600	22.9 ± 2.1	340.1 ± 58.8	1.53 ± 0.38
	-700	26.5 ± 0.8	435.5 ± 125.6	1.71 ± 0.60
	-800	28.7 ± 0.9	711.6 ± 31.4	2.75 ± 0.15
	-900	20.2 ± 2.8	243.2 ± 24.2	1.27 ± 0.36

Constant process parameter

→ Catalyst amount: 5 wt.%; Binder content: 2 wt.%

→ Processing temperature: 185 °C; Polymerization time: 90 min

Summary

A Thermoplastic Vacuum Assisted Resin Infusion (T-VARI) manufacturing process was successfully developed to achieve the proposed concept with bindered textile preforms. The manufactured textile reinforced pCBT composites show a significantly increased toughness without impairing other mechanical properties such as flexural modulus and flexural strength. Single factor analysis was conducted taking the influencing mechanism of the key process parameters including the catalyst amount, binder filling fraction, processing temperature, and vacuum pressure into consideration. The results illustrate that the toughening performance and the mechanical properties both depend significantly on the investigated process parameters when the textile reinforced pCBT composites is prepared with the proposed concept. With other process parameters being held constant, each parameter indicates an optimum value that leads to the best flexural performance. **The key achievement of this chapter is that the proposed simultaneous binding and toughening concept is initially confirmed to be capable of manufacturing textile reinforced pCBT composite with increased material toughness.**

Chapter 6

Key aspect III: Optimization of the manufacturing process

The present chapter assesses various preforming binders and focuses on the inter-laminar fracture properties. Inter-laminar fracture toughness of textile reinforced pCBT composites was investigated under mode I and mode II deformation. A standard double cantilever beam (DCB) test and an end notched flexure (ENF) test based on a three-point bending test were applied to evaluate the mode I and mode II inter-laminar fracture toughness were evaluated by a standard double cantilever beam (DCB) test and an end notched flexure (ENF) test based on a three-point bending test, respectively. The effect of binder type, filling content and preparation concept on fracture properties under the mentioned two deformation modes were discussed on the basis of morphology analysis of fracture sections with scanning electric microscopy. Flexural properties of the textile reinforced pCBT laminate prepared using the optimized preforming binder were characterized for further verification of the performance of the proposed concept. A variant of the proposed concept was pointed out and tested for further optimization of the manufacturing process. The results of this chapter can be taken as the second milestone of the solution strategy of this dissertation research as shown in Figure [6.1](#)

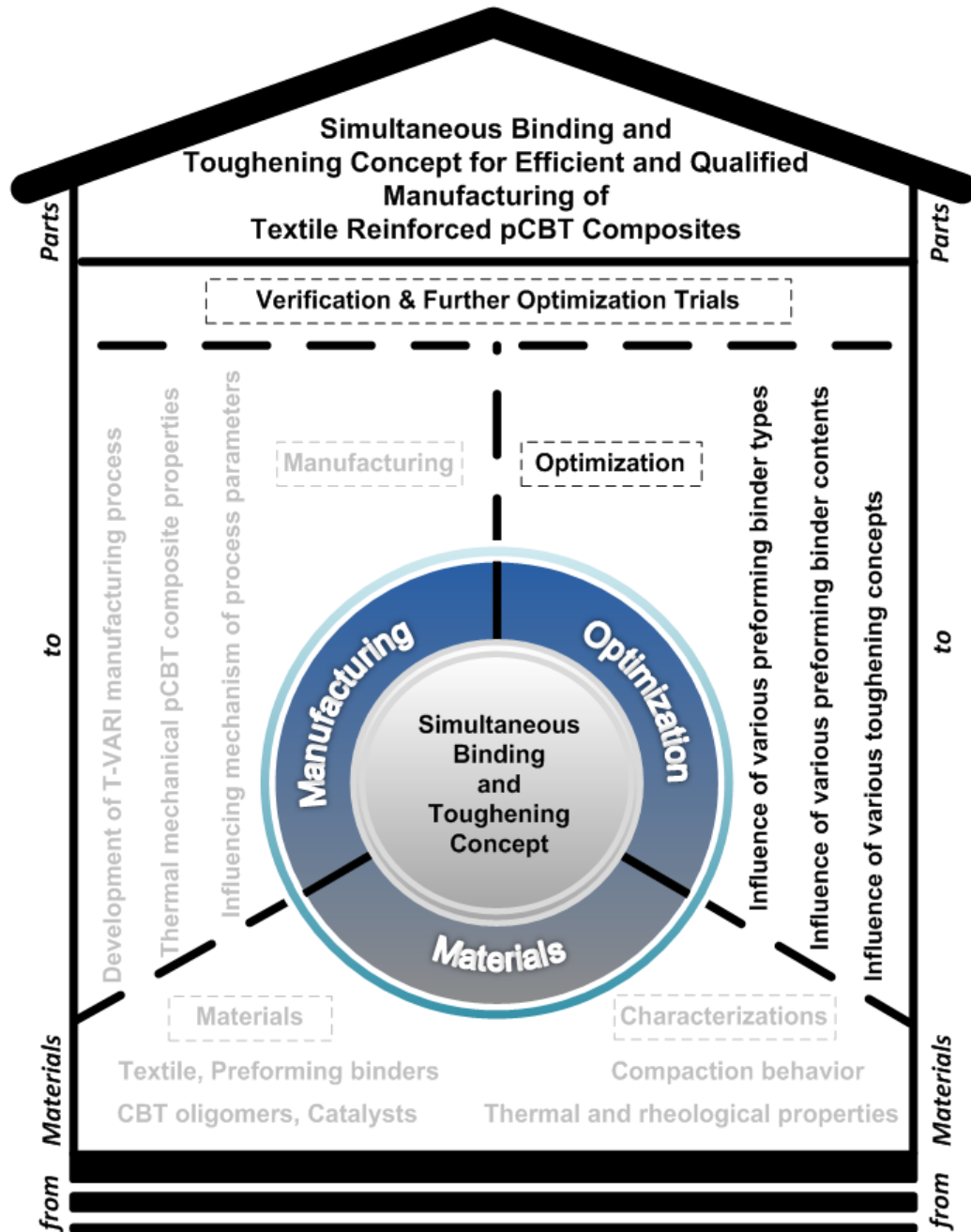


Figure 6.1.: Solution strategy: Second milestone

6.1. Mode I inter-laminar fracture properties

6.1.1. Effect of binder type and filling content

The relationship between applied load and crack opening displacement (COD) for the specimens are shown in Figure 6.2. The results indicate that the applied load and the COD are both influenced by the manufacturing and toughening concept. For the ex-situ toughened specimens the applied binders also show an effect on the applied load and especially for the COD. The specimen ex-situ toughened with PARALOID EXL® 2314 binder results the highest COD of all the tested specimens. As the stiffness is not significantly influenced by the ex-situ toughening, the increase of COD may indicate that the specimen has higher resistance to fracture and that the PARALOID EXL® 2314 binder might be the most appropriate binder for toughening of textile reinforced pCBT composites.

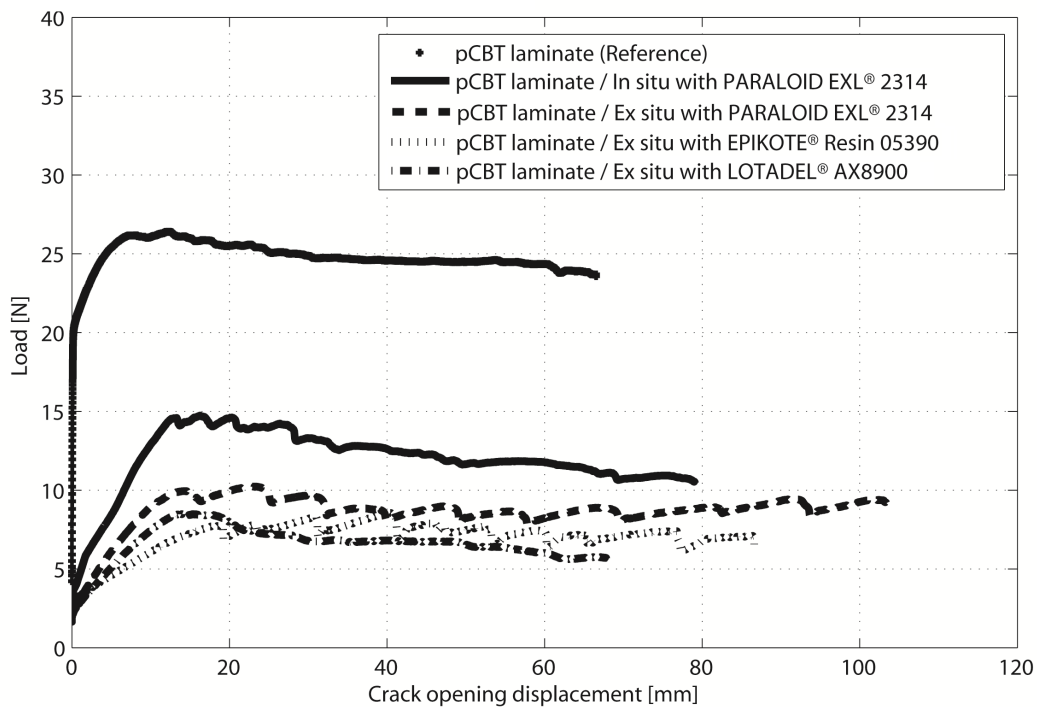


Figure 6.2.: Load displacement trace from DCB test

In order to make a better comparison, an overview of the results from all the tested specimens prepared with ex-situ toughening concept, including the final fracture toughness ($\Delta a = 40$)¹ and the sample thickness is shown in Figure 6.3. The first row of x-axis in the graph is the specimen number from 1 to 3 along with the resin infiltration direction. The second row of x-axis is the filling contents of the applied binders. And the third row indicates the applied binder type. The thickness of all the specimens is shown in the second y-axis to determine whether there is an influence from the thickness variation on the results of mode I fracture toughness. The results indicate that there is an intra-part thickness variation for all tested laminates and this variation does not result clearly a corresponding variation of mode I fracture toughness. Therefore, for the pre-selection of binders with DCB test, a repeatability test, which is very helpful due to the common inter-part thickness variation in VARI process, was not considered in this study.

As we can see in Figure 6.3, for the eighteen specimens with LOTADEL[®] AX8900 and EPIKOTE[®] Resin 05390 binder, the mode I fracture toughness is usually lower than 400 J/m² except for the 4 specimens marked with the arrows in the graph, each of which shows much higher mode I fracture toughness than the other two specimens which has very close results from the same laminate. Therefore, for the comparison these 4 specimens are excluded here because of the huge inter-specimen deviation which might be attributed to the error occurred during the specimen preparation. After comparing with the reference laminate whose mode I fracture toughness is in the range of 500-800 J/m² (Figure 6.3), the binders EPIKOTE[®] Resin 05390 and LOTADEL[®] AX8900 can be removed from the selection list due to the decreased mode I fracture toughness.

In this case, the PARALOID EXL[®] 2314 would be the only choice in the present study for the proposed simultaneous binding and ex-situ toughening concept. Actually, for the nine specimens with PARALOID EXL[®] 2314 binder, the mode I fracture toughness is indeed higher than its two counterparts. Except for the two specimens with 3 wt.% PARALOID EXL[®] 2314, which is still comparative with the best results available from the other two binders (Figure 6.3). This further confirms the initial conclusion that the PARALOID EXL[®] 2314 might be the most

¹ Δa is the crack length after initial crack as shown in Figure 3.10

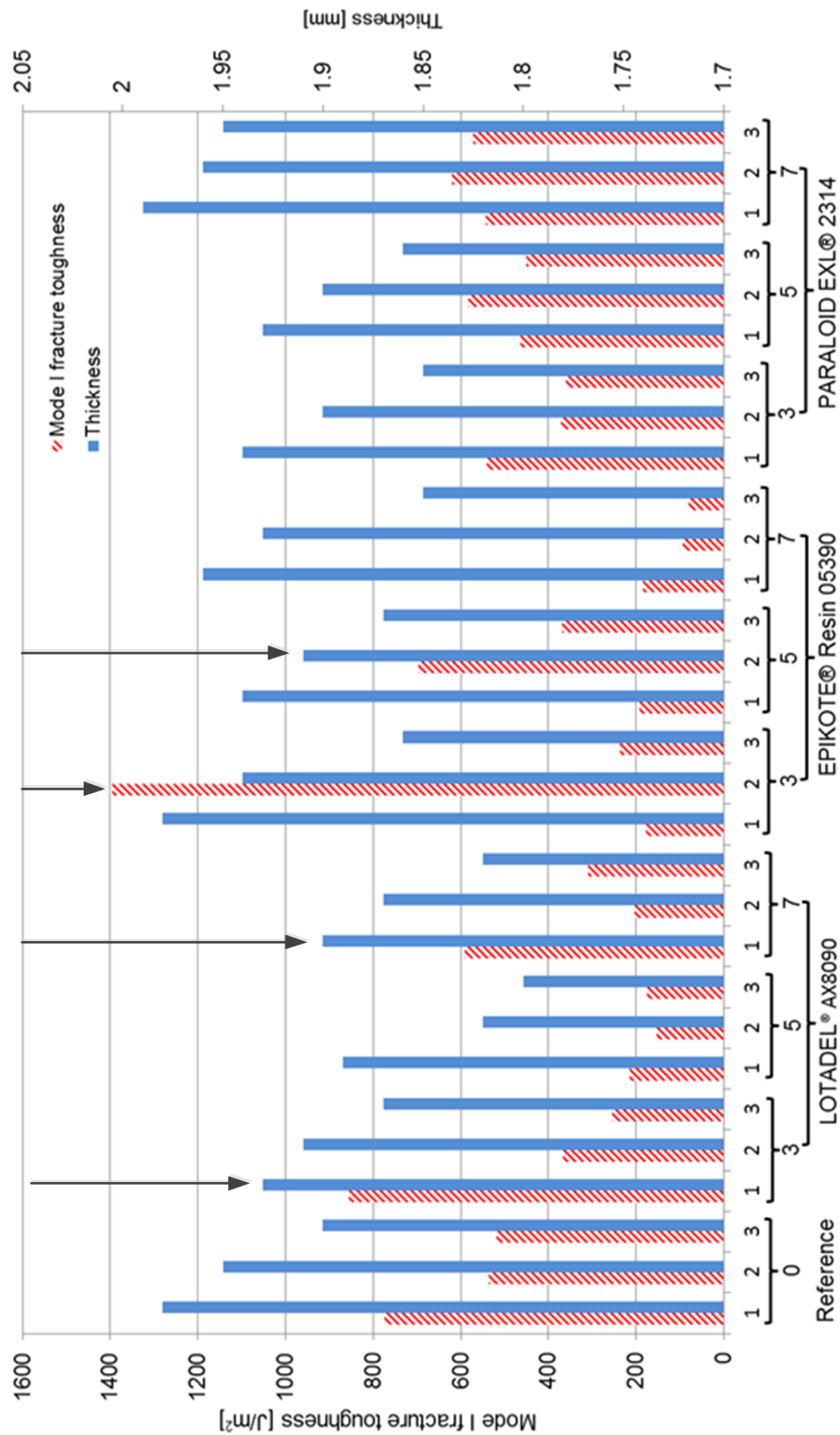


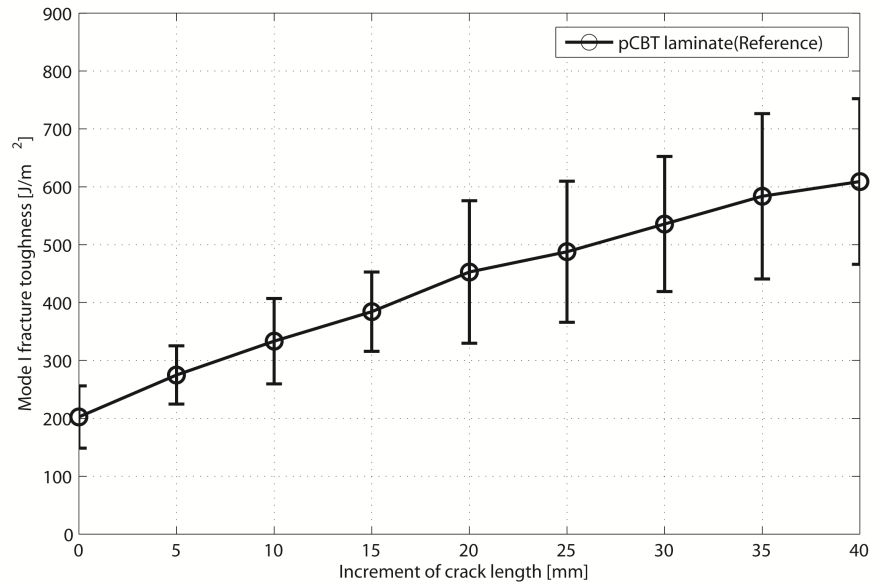
Figure 6.3.: The final mode I fracture toughness and thickness of all the tested specimens

appropriate binder according to Figure 6.2. Of all the three filling content for PARALOID EXL® 2314, the 7 wt.% specimen shows the best performance in the aspect of homogeneity. In addition, the specimens filled with 7 wt.% PARALOID EXL® 2314 also show more homogeneous mode I fracture toughness than the reference laminate.

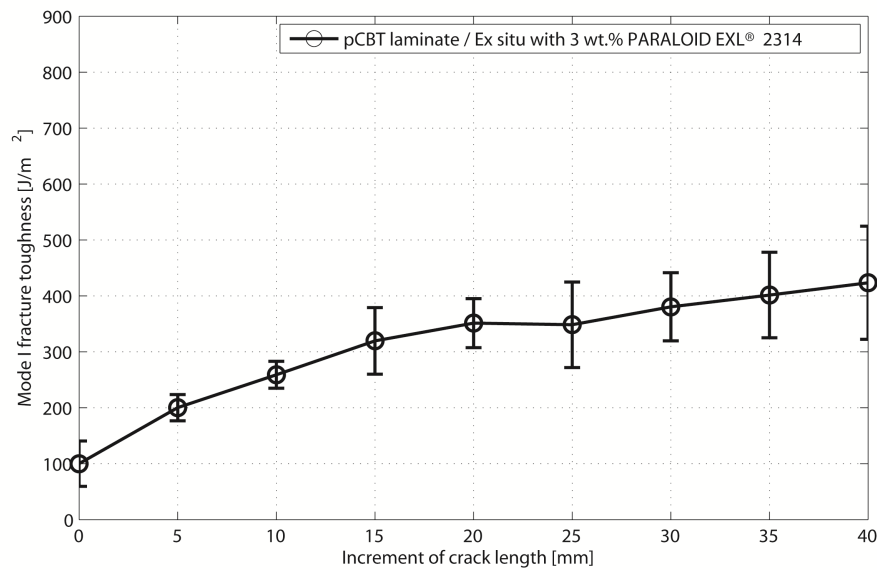
To make a quantitative comparison for the specimens from the reference laminate and the ex-situ toughened variant with 7 wt.% PARALOID EXL® 2314, the relationship between mode I fracture toughness and the increment of the crack length (*R*-curve), shown in Figure 6.4, was determined according to the visually determined increment of the crack length and the compliance of COD. In these graphs, the average mode I fracture toughness of three specimens is indicated at each increment of the crack length, and the standard deviations are indicated by the error bar. The mode I fracture toughness was found to increase with the propagation of crack length for all tested specimens as shown in the Figure 6.4. This increase in mode I fracture toughness can be attributed to the extensive fiber bridging effect on the fracture surface [7].

The homogeneity of the specimens filled with 7 wt.% PARALOID EXL® 2314, as shown in Figure 6.4(d), is further confirmed to be better than the reference laminate (Figure 6.4(a)) with smaller deviations. Compared with the reference laminate, the one with 7 wt.% PARALOID EXL® 2314 results in a final mode I fracture toughness ($\Delta a = 40$) decrease of only 5.1% (Figure 6.4(d)). The decrease of the final mode I fracture toughness may be ascribed to the fail of the preforming binder in the competition with the other toughening mechanism which is high temperature induced lower crystallinity. Considering the large deviations from the reference laminate, one could at least make a conclusion that the PARALOID EXL® 2314 binder could be an appropriate binder which has good compatibility with pCBT matrix and no significant influence on the final mode I fracture toughness.

A further observation on the effect of filling content of PARALOID EXL® 2314 binder on the mode I fracture toughness of the specimens is shown in Figure 6.5. The result indicates that the presence of PARALOID EXL® 2314 binder has generally a negative effect on the mode I fracture toughness. For all the specimens with



(a) Reference laminate



(b) Ex-situ with 3 wt.% PARALOID EXL® 2314

Figure 6.4.: Relation between mode I fracture toughness and the increment of crack length for textile reinforced reference laminate

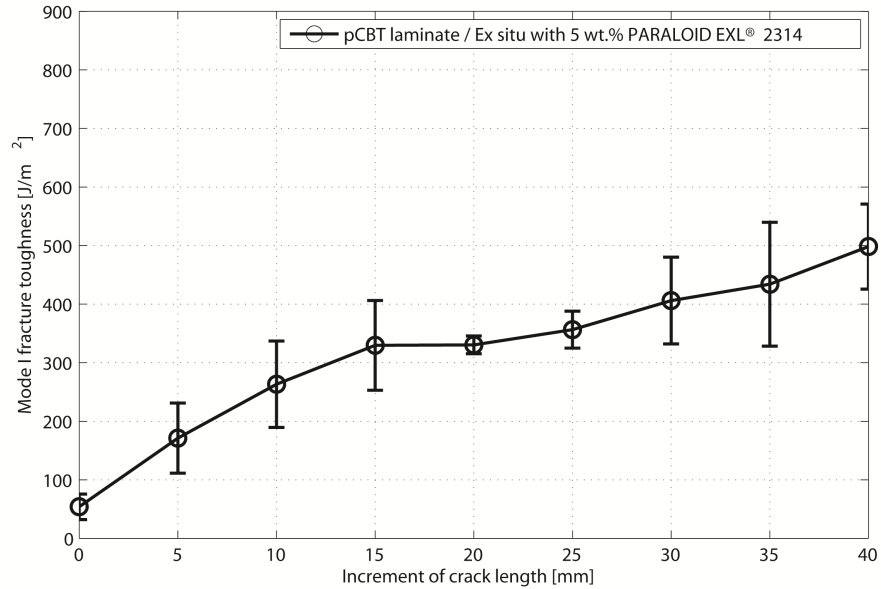
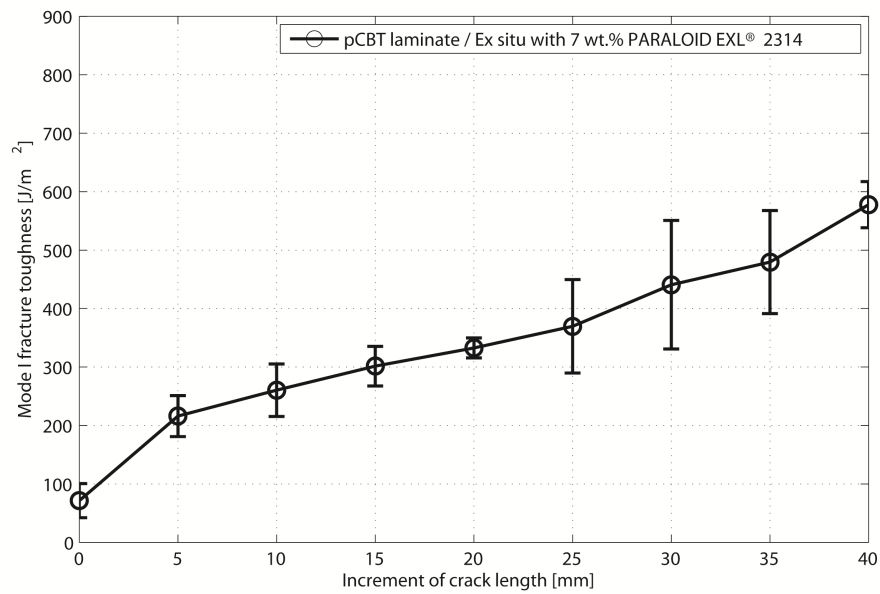
(c) Ex-situ with 5 wt.% PARALOID EXL[®] 2314(d) Ex-situ with 7 wt.% PARALOID EXL[®] 2314

Figure 6.4.: Relation between mode I fracture toughness and the increment of crack length for textile reinforced reference laminate

binder, the initial fracture toughness ($\Delta a = 0$) are decreased and the final fracture toughness ($\Delta a = 40$) has a limited decrease. The initial fracture toughness shows a decrease trend until a binder filling content of 5 wt.% and then a little bit increase at a binder filling content of 7 wt.%. The final fracture toughness, however, indicates a monotonic increase from 58.9 % up to 94.9 % of the final fracture toughness of the reference laminate, when the filling content of the binder increases from 3 wt.% up to 7 wt.% in the present study. The decrease of initial fracture toughness could be attributed to the errors such as the micro delamination near the end of the pre-crack, which can occur during cutting of the specimen from the composite laminate.

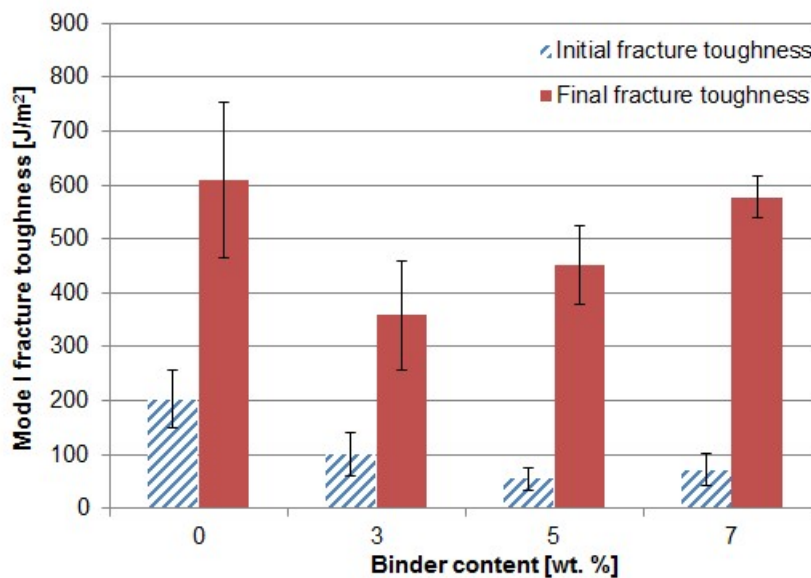


Figure 6.5.: Effect of binder content on the mode I fracture toughness of textile reinforced pCBT laminate

To investigate the effect of the production concept for textile reinforced pCBT composites, the PARALOID EXL® 2314 binder of 7 wt.% (refer to the resin amount) was mixed with the molten resin before resin infusion according to the in-situ toughening concept. The resulted specimens were then tested under the same procedure as the variants with ex-situ toughening concept. The result from the in-situ toughening concepts was compared with its ex-situ toughened variant with 7 wt.% PARALOID EXL® 2314 binder as shown in Figure 6.6. The mode I fracture toughness

shows a clear increasing trend with the increment of the crack length in both toughening concepts. And the magnitude of initial fracture toughness ($\Delta a = 0$) indicates also no distinct difference between the two toughening concepts. However, the increase trend of mode I fracture toughness is obviously stronger for the laminate prepared by ex-situ toughening concept. In addition, the ex-situ toughened specimens shows more homogeneous properties with much smaller deviations.

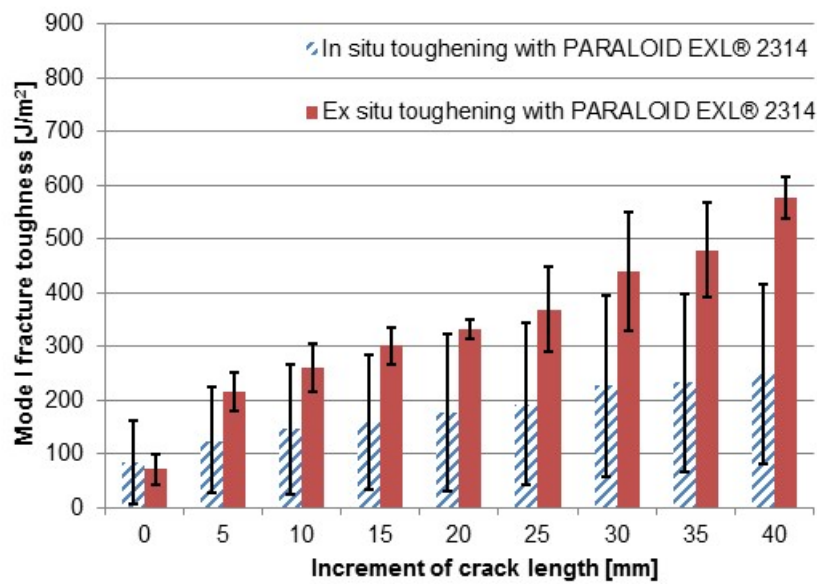


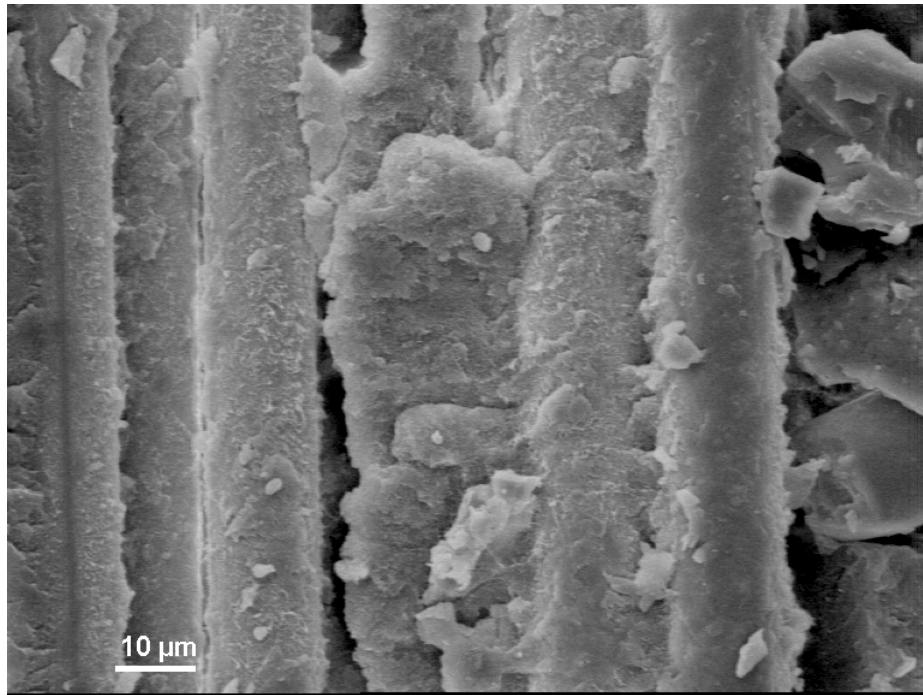
Figure 6.6.: Effect of the toughening concept on the mode I fracture toughness

In this context, the potential of the proposed simultaneous binding and ex-situ toughening concept for production of textile reinforced pCBT composites is confirmed when compared to in-situ toughening counterpart. The function of the PARALOID EXL® 2314 binder in the simultaneous binding and ex-situ toughening concept is only limited as binding for improving process efficiency. The expected simultaneous ex-situ toughening is not achieved for the mode I fracture toughness.

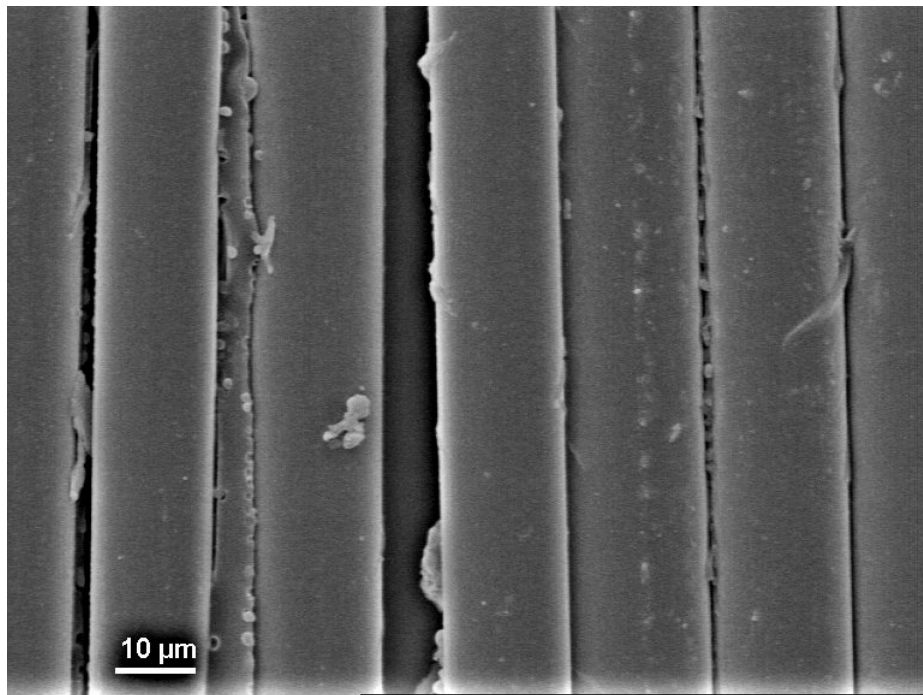
6.1.2. Fracture morphology of mode I deformation

Figure 6.7 shows the SEM image of the fracture surface on textile fiber reinforced pCBT laminates with various binders derived from DCB tests. As shown in Figure 6.7(a), the reference laminate indicates a typical brittle fracture from mode I deformation. The brittle pCBT matrix breaks into pieces around the fiber after mode I deformation. The effect of the three different binders on the mode I deformation are shown in Figure 6.7(b), 6.7(c) and 6.7(d). The fibers are nearly separated with the polymer in the case of pCBT/AX8090 laminate, indicating that the LOTADEL[®] AX8090 binder is not compatible with pCBT, such that the resulted matrix does not stick to the fibers very well (Figure 6.7(b)). Although the EPIKOTE[®] Resin 05390 shows a better compatibility with pCBT matrix compared with LOTADEL[®] AX8090, the toughness of the resulted matrix in the interface represents only incremental enhancements (Figure 6.7(c)). After comparing Figure 6.7(d) with Figure 6.7(a)-Figure 6.7(c), an obvious difference in the interface of the pCBT laminate with the PARALOID EXL[®] 2314 binder was observed. Not only a good adhesion between the fibers and the matrix is present, but the fracture surface indicates a clearly plastic deformation, meaning that the brittle pCBT matrix at the inter-layer of the pCBT laminate is greatly toughened by the introduction of PARALOID EXL[®] 2314 binder.

On the other hand, as shown in Figure 6.8, an obvious difference in the fracture sections was observed with different toughening concepts. The fracture surface of the laminate prepared with in-situ toughening concept shows nearly no plastic deformation of the matrix around the fibers (Figure 6.8(a)). While as shown in Figure 6.8(b), 6.8(c) and 6.8(d) this plastic deformation is quite clear for the laminate prepared with simultaneous binding and ex-situ toughening concept. The size and continuity of this plastic deformation zone seems to have an increase trend with increasing PARALOID EXL[®] 2314 content. Those variations in fracture surface appear to be related to the intensity of the fracture toughness as shown in Figure 6.5 and Figure 6.6.

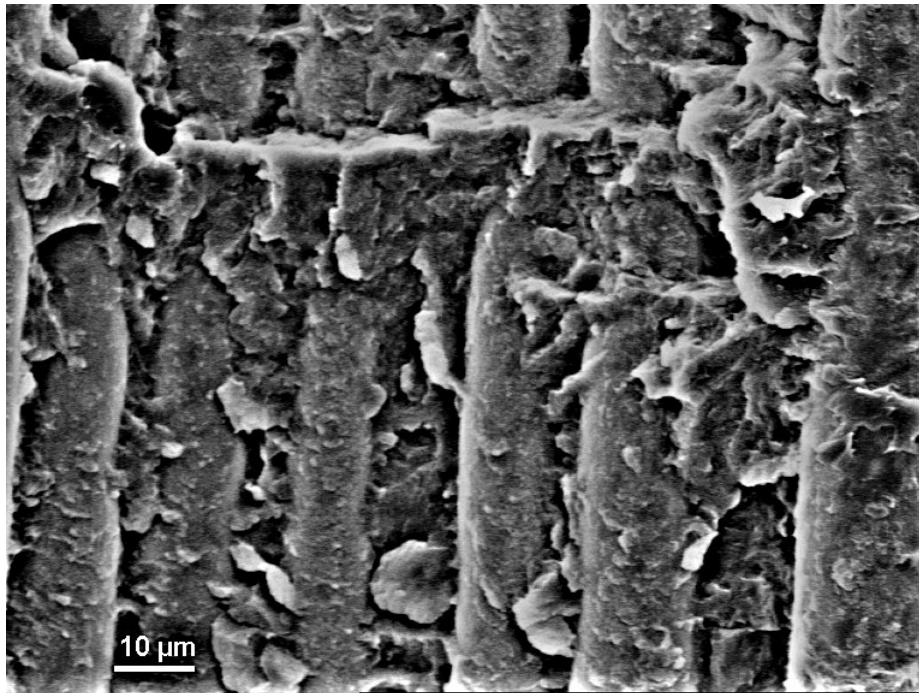


(a) Reference laminate

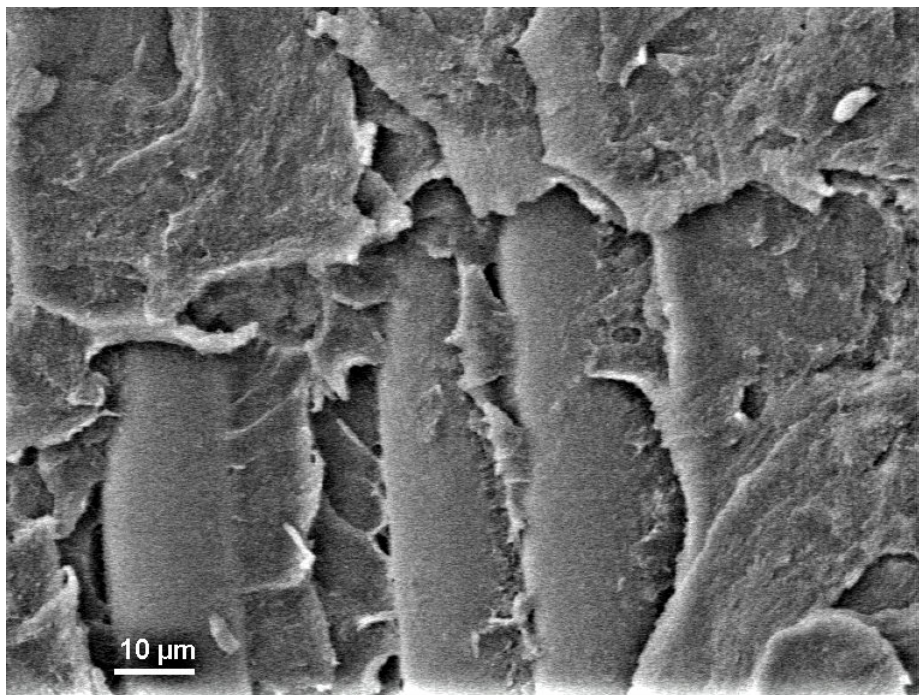


(b) pCBT/AX8090 3 %

Figure 6.7.: Scanning electron micro-graphs of the fracture surface under mode I loading of textile fiber reinforced pCBT laminates

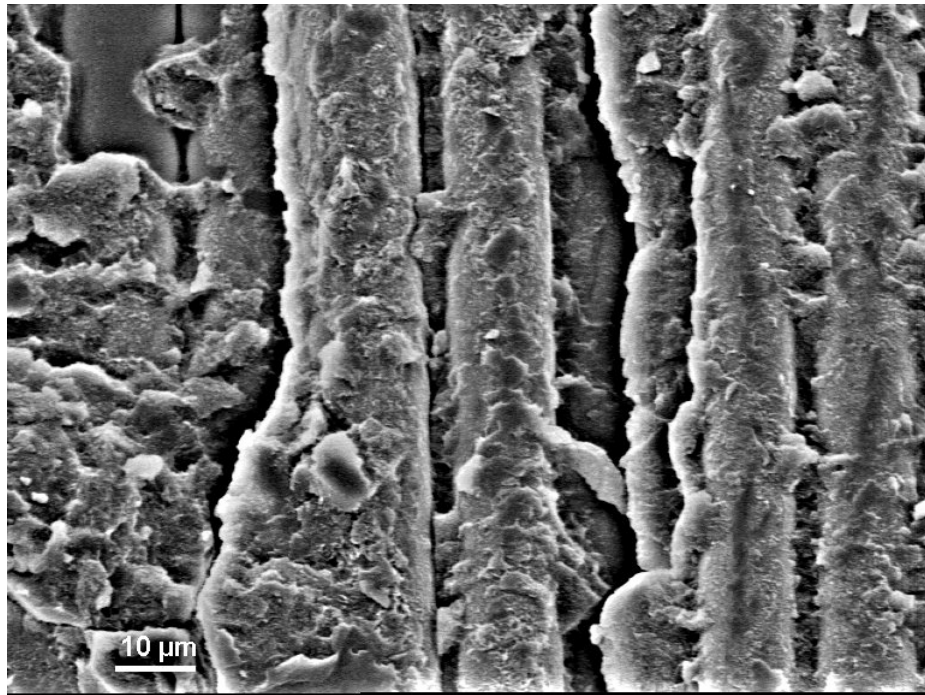


(c) pCBT/5390 3 %

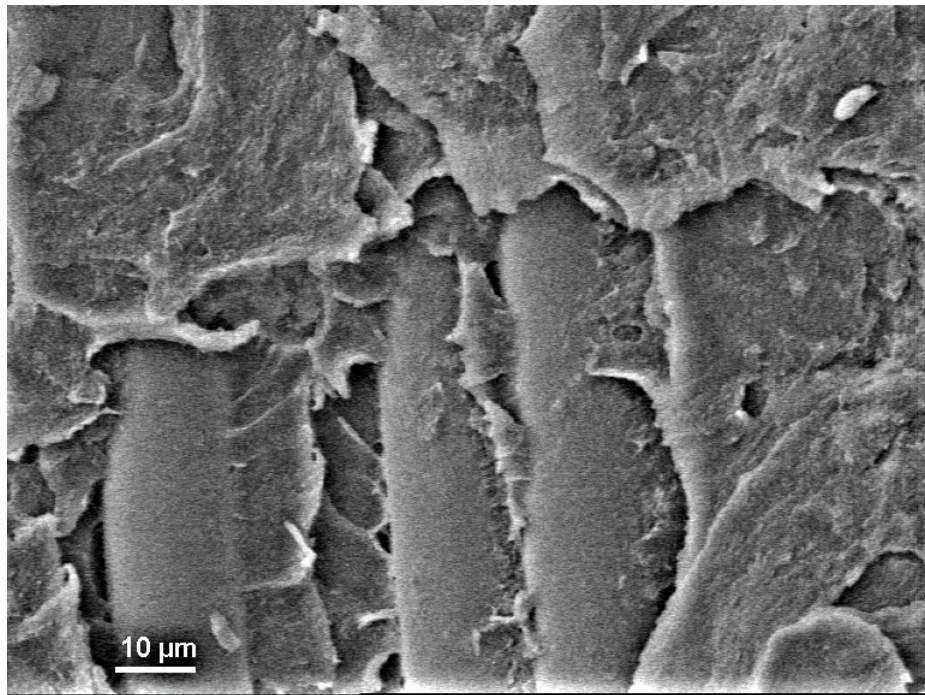


(d) pCBT/2314 3 %

Figure 6.7.: Scanning electron micro-graphs of the fracture surface under mode I loading of textile fiber reinforced pCBT laminates

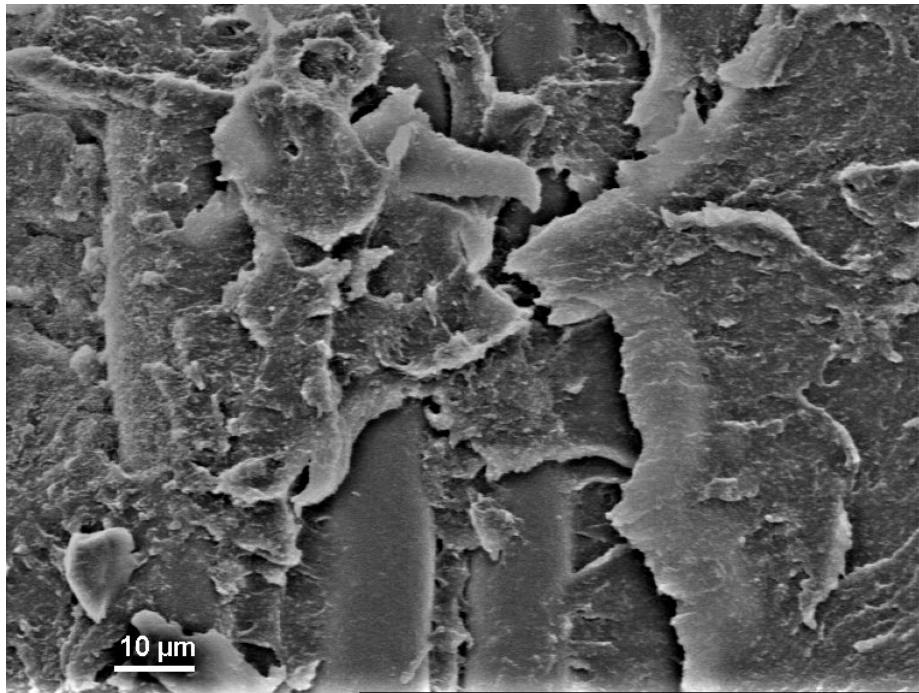


(a) In-situ, pCBT/2314 7 %

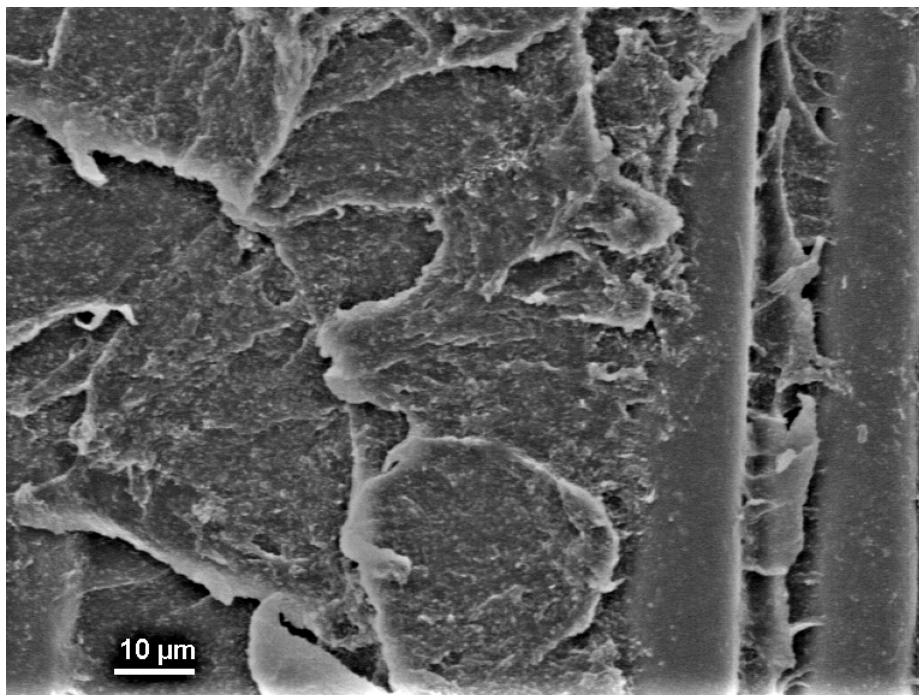


(b) Ex-situ, pCBT/2314 3 %

Figure 6.8.: Scanning electron micro-graphs of the fracture surface under mode I loading of pCBT/ PARALOID EXL[®] 2314 laminate



(c) Ex-situ, pCBT/2314 5 %



(d) Ex-situ, pCBT/2314 7 %

Figure 6.8.: Scanning electron micro-graphs of the fracture surface under mode I loading of pCBT/ PARALOID EXL[®] 2314 laminate

6.2. Mode II inter-laminar fracture properties

6.2.1. Effect of binder filling content

According to the proposed simultaneous binding and ex-situ toughening concept in Figure 1.5, the fracture resistance is supposed to have a gradient from the symmetric plane to each side of the specimen in the transverse direction because of the decentralized preforming binder. The symmetric plane which is also the inter-ply region has the highest fracture resistance due to the high amount of distributed preforming binder, while the intra-ply region in the fabric layer has lower fracture resistance due to the poor of preforming binder. As a result, shown in Figure 6.9, the delamination starts usually at the intra-ply region ($\pm 45^\circ$) for the ex-situ toughened specimens before the delamination progresses in the inter-ply region from the initial crack, though the three axial fiber bundles are knitted together with sewing thread. This phenomenon is in accordance with our expectation and can be understood preliminarily that the ex-situ toughening with preforming binder might be work for mode II fracture toughness of textile reinforced pCBT composite.

The relationship between applied load and load point displacement for the ENF test is shown in Figure 6.10 for textile reinforced pCBT laminate and its modified variants. It is obvious that the relationship between applied load and displacement is significantly influenced by not only the toughening concept but also the amount of toughening agent. Compared with the reference specimen, the ex-situ toughened specimens show increased central loading pin displacements at critical load, while for the in-situ toughened variant the outcome is reversed. The specimen ex-situ toughened with 7 wt.% PARALOID EXL[®] 2314 gives the highest critical load among the selected five specimens, indicating that ex-situ toughening with 7 wt.% PARALOID EXL[®] 2314 might be the most suitable solution in the present study for toughening of pCBT composites.

To study the effect of binder content on the fracture properties of pCBT composite, the mode II fracture toughness was calculated based on a total of five ENF tests for each variant and summarized in Figure 6.11 (initial experiment). The optimum

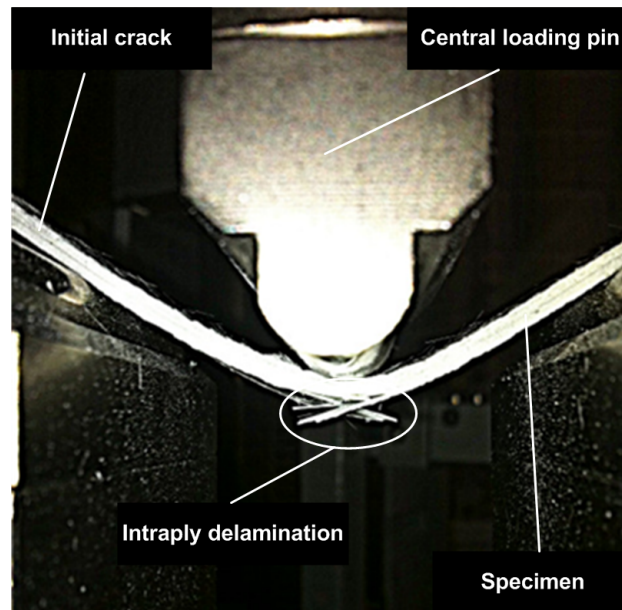


Figure 6.9.: Intra-ply delamination behavior of pCBT laminate under mode II deformation

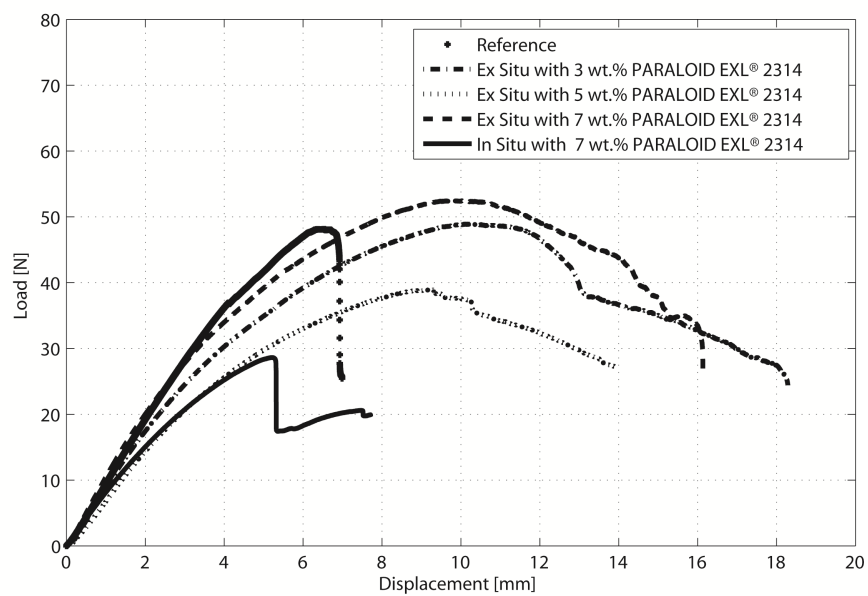


Figure 6.10.: Load vs. displacement curves of textile reinforced pCBT laminate obtained by ENF tests

value of the binder content, which gives the highest value of mode II fracture toughness for textile reinforced pCBT laminate, was confirmed to exist at a binder content of 7 wt.% in the present study. Compared with the reference laminate, the mode II investigation was confirmed to increase the mode II fracture toughness by approximately 151.6 % with the proposed simultaneous binding and toughening concept. In contrast to the fracture toughness in mode I, the increase of fracture toughness in mode II may be ascribed to the mechanical properties of the blend system consisting pCBT polymer and preforming binder in the inter-ply region. Although the amount of preforming binder is the same, the resulted blend system may have different performance in tensile (mode I) and shear (mode II) loading conditions.

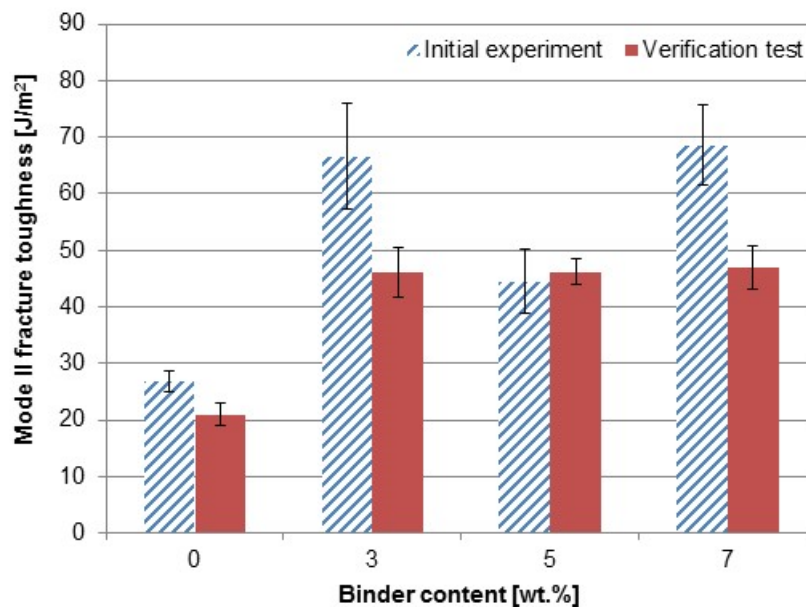


Figure 6.11.: Effect of binder content on the mode II fracture toughness of textile reinforced pCBT laminate

Furthermore, the results of mode II fracture toughness were compared in Figure 6.12 (initial experiment) in order to investigate the effect of the toughening concept on the fracture properties of textile reinforced pCBT laminate. The mode II fracture toughness of ex-situ toughened variants is about 2 times higher than their counterparts prepared with in-situ toughening concept and about 1.5 times higher than the reference specimens.

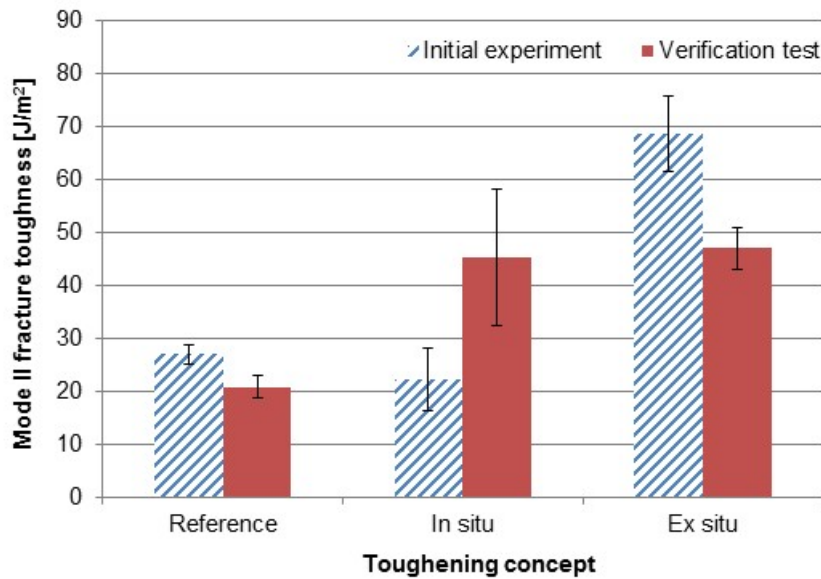


Figure 6.12.: Effect of the toughening concept on the mode II fracture toughness

From the initial experiment results, one may be curious about that the ex-situ toughened laminate with 5 wt. % PARALOID EXL® 2314 binder which behaves much differently than its other two counterparts with nearly the same mode II fracture toughness (Figure 6.11, initial experiment). The in-situ toughened laminate gives smaller mode II fracture toughness than the reference laminate (Figure 6.12), even though the binder has shown its toughening ability for pCBT matrix in the case of ex-situ toughened laminates. In order to explain those strange behavior from the initial experiment, a verification test was performed to verify the conclusions from the initial experiment. As shown in Figure 6.11 and 6.12 (verification test), the results from the verification test confirm first and importantly the potential of PARALOID EXL® 2314 binder for toughening of the textile reinforced pCBT laminate with the proposed simultaneous binding and toughening concept. And then the highest mode II fracture toughness was also presented at a binder content of 7 wt. %.

However, there are also two distinct differences between the initial experiment and the verification test. One of them is the ex-situ toughened laminates with the applied three binder contents result a mode II fracture toughness with little difference.

The binder content seems to have no significant influence on the mode II fracture toughness of ex-situ toughened textile reinforced pCBT laminate as shown in verification test. The strange behavior of the ex-situ toughened laminate with 5 wt.% PARALOID EXL[®] 2314 binder from the initial experiment may be attributed to the errors during specimens preparation, which may include: (1) the amount and distribution of the applied preforming binder; (2) temperature fluctuation of CBT resin melt after adding the liquid catalyst with room temperature, leading to a variation of resin temperature among experiments; and (3) different thermal history of bindered textile preform before resin infusion, which may affect the status of the preforming binder during reactivation. The other difference is the values of mode II fracture toughness from the verification test are generally lower than the one from the initial experiment except for the questionable specimens with 5 wt.% PARALOID EXL[®] 2314 binder. The increase of mode II fracture toughness of ex-situ toughened specimens compared to the reference specimens is reduced to 124.4 % in the verification test.

As the verification test was conducted about eight months after the initial experiment, the reduced value of mode II fracture toughness from the verification test might be attributed to the moisture absorption of the catalyst, which can interfere with the polymerization reaction and resulting a limited conversion rate from CBT to pCBT in the verification test according to the processing guide provided by Cyclics Europe. For the specimens prepared with in-situ toughening concept, the 7 wt.% PARALOID EXL[®] 2314 binder, which is to be mixed with molten CBT500 before impregnation, could be another source of moisture beside the catalyst. Therefore, in the verification test, the 7 wt.% PARALOID EXL[®] 2314 binder was dried first under the same conditions as CBT500 pellets before mixing with molten CBT500. The results indicate that the in-situ toughened specimens get much improvement in the mode II fracture toughness than the initial experiment (Figure 6.12, verification test). The mode II fracture toughness has been increased by 117.8 % when compared with the reference specimens. This increase of mode II fracture toughness from in-situ toughened specimens is nearly comparable to the ex-situ toughened variant (124.4 %). The shortcoming of in-situ toughened specimens is the large deviation, which can be attributed to the increase of viscosity of the

resin mixture, leading to a poor impregnation quality and therefore inhomogeneous material properties along the infiltration direction as shown in Figure 6.13.

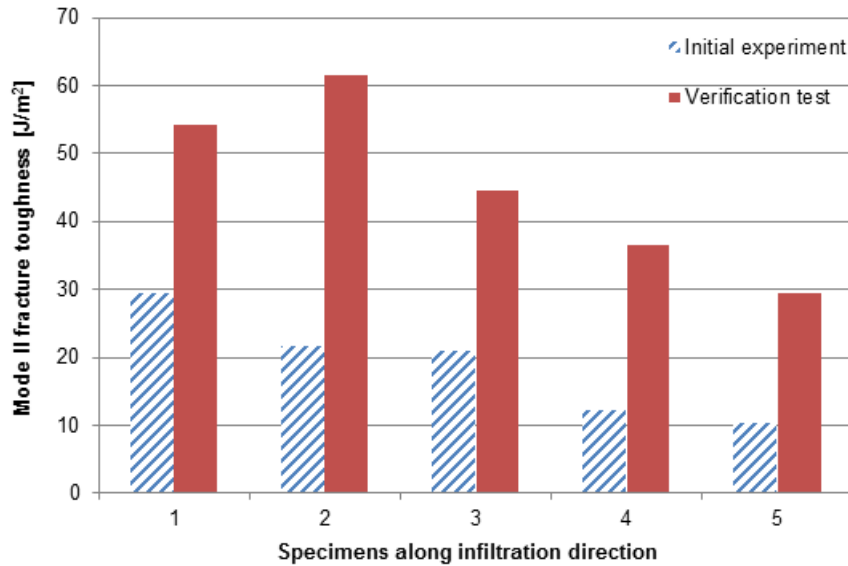


Figure 6.13.: Effect of the impregnation length on mode II fracture toughness of in-situ toughened laminate

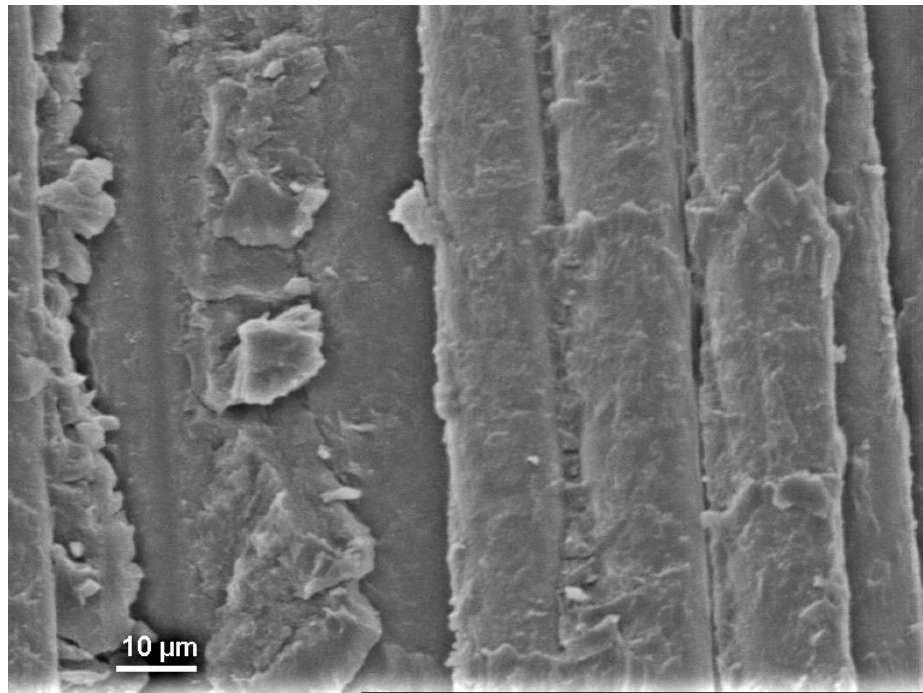
In this context, the potential of the proposed simultaneous binding and toughening concept for production of textile reinforced pCBT composites is further confirmed when compared to in-situ toughening concept. The expected function of the pre-forming binder as binding for improved process efficiency and toughening for improved inter-laminar fracture properties is achieved simultaneously with the acrylic modifier based PARALOID EXL[®] 2314 binder.

6.2.2. Fracture morphology of mode II deformation

Figure 6.14 shows the SEM image of the fracture surface after ENF tests for textile fiber reinforced pCBT laminates from the initial experiment with various preparation concepts. It is obvious to see that the fracture surface is greatly influenced by the toughening method. Compared with the reference laminate (Figure 6.14(a)), the fracture surface for the samples fabricated with in-situ toughening concept does not

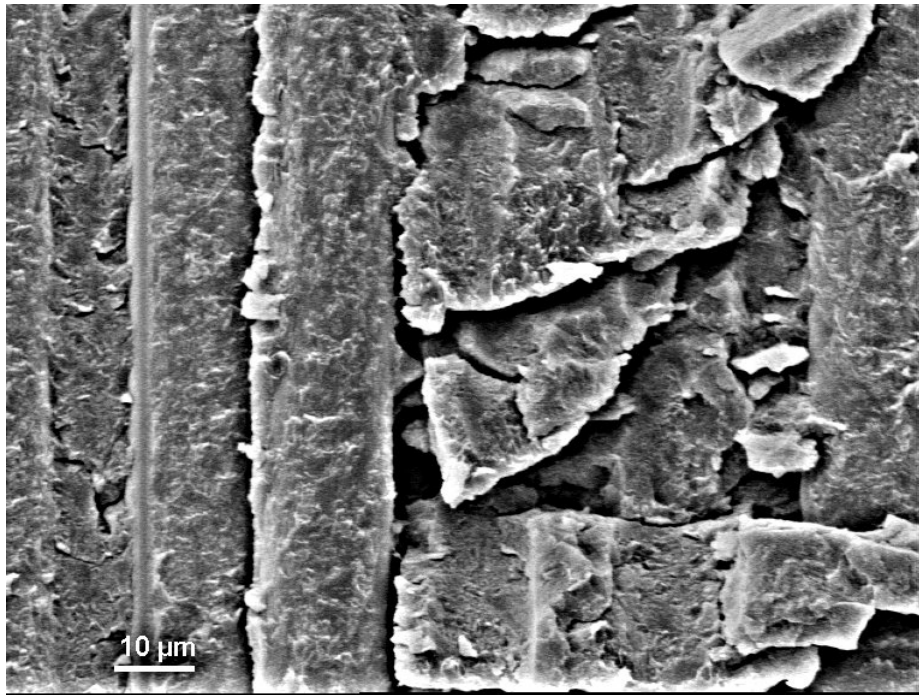
show any improvement of the toughness (Figure 6.14(b)). While as shown in Figure 6.14(c) a totally different fracture surface with more toughness of the resulted matrix is achieved with ex-situ toughening concept.

As shown in Figure 6.15, the fracture surface is also influenced by the weight percentage of the toughening agent in the ex-situ toughening process. Compared with the fracture surface with 5 weight percent of PARALOID EXL® 2314 (Figure 6.15(b)), the fracture surface in Figure 6.15(a) and 6.15(c) indicates a matrix with more fracture toughness. The fracture surface with a high amount of continuous matrix rich area observed in Figure 6.15(c) indicates that a higher fracture toughness was achieved with 7 weight percent of PARALOID EXL® 2314. Those variations in fracture surface appear to be related to the intensity of the fracture toughness as shown in Figure 6.11 and 6.12 (initial experiment).

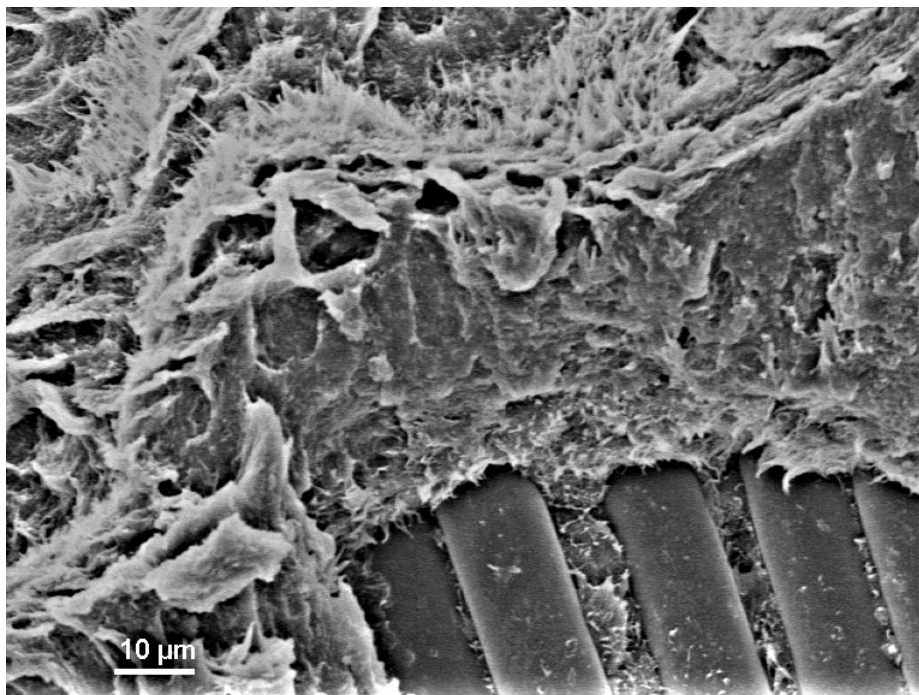


(a) Reference laminate

Figure 6.14.: Scanning electron micro-graphs of the fracture surface under mode II loading of textile fiber reinforced pCBT laminates

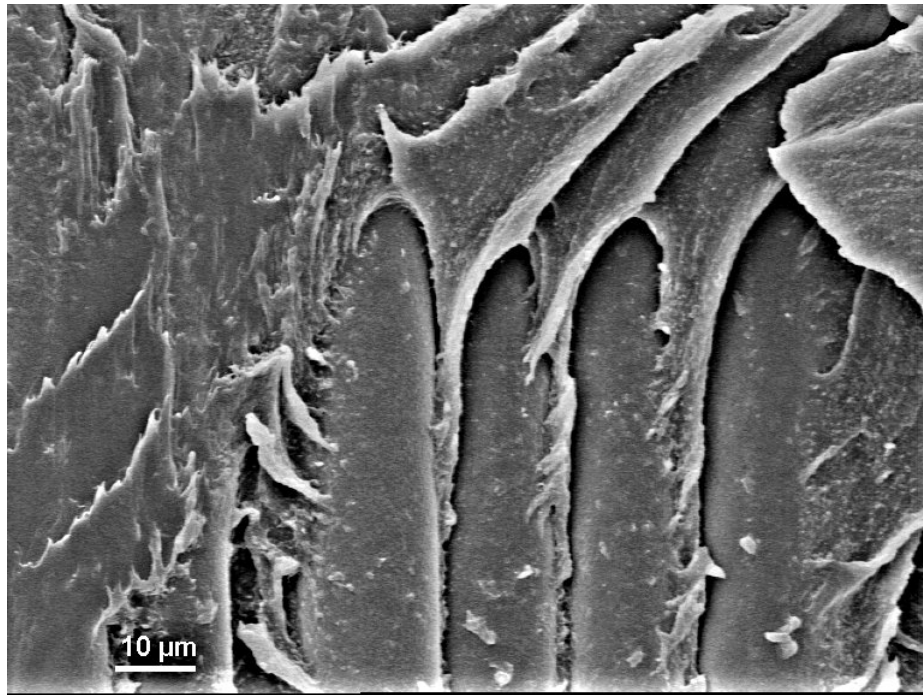


(b) In-situ, pCBT/2314 7 %

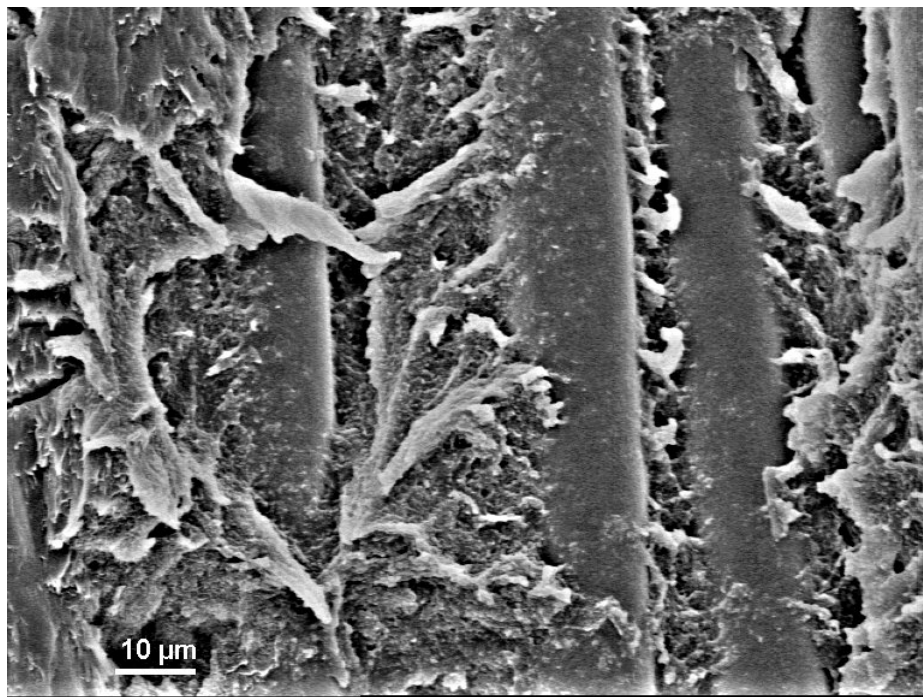


(c) Ex-situ, pCBT/2314 7 %

Figure 6.14.: Scanning electron micro-graphs of the fracture surface under mode II loading of textile fiber reinforced pCBT laminates

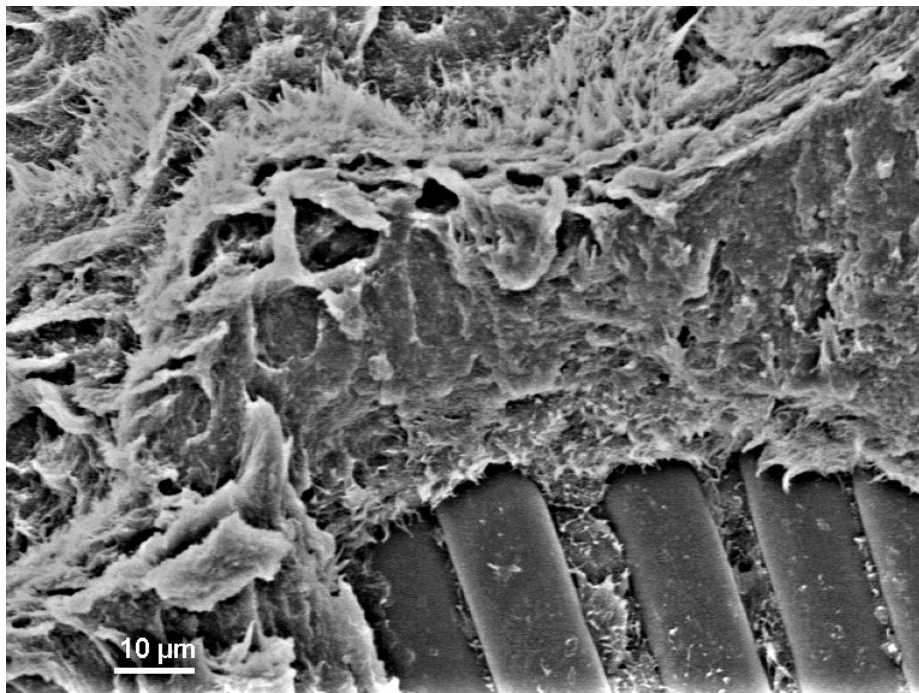


(a) Ex-situ, pCBT/2314 3 %



(b) Ex-situ, pCBT/2314 5 %

Figure 6.15.: Scanning electron micro-graphs of the fracture surface under mode II loading of pCBT/ PARALOID EXL[®] 2314 laminate



(c) Ex-situ, pCBT/2314 7 %

Figure 6.15.: Scanning electron micro-graphs of the fracture surface under mode II loading of pCBT/ PARALOID EXL® 2314 laminate

6.3. Verification experiments

6.3.1. Verification of the optimized preforming binder

According to the results from subsection 5.2, the optimum process parameter for good toughening performance and mechanical properties was found with the initially selected constant process parameters for single factor experiment analysis. In this step, this group of process parameter was further applied to verify the PARALOID® EXL2314 binder which has been confirmed to have optimum performance in Mode I and Mode II inter-laminar fracture properties (section 6.1 and 6.2).

Table 6.1 illustrates the effect of binder type on the flexural properties of textile reinforced pCBT composites. The optimized PARALOID® EXL2314 binder system indicates significantly better toughening performance than the original used EPIKOTE® Resin 05390 binder. A total improvement of 110.1 % in flexural strain was observed with the PARALOID® EXL2314 binder when compared with reference laminae without any binder. While the improvement from the EPIKOTE® Resin 05390 binder is only 72.9 %. Moreover, the mechanical performance of the laminate with optimized PARALOID® binder illustrates better results as well. Compared with the reference laminate, the laminate indicates an improvement of 90.5 % in flexural strength when manufactured with simultaneous binding and toughening concept applying PARALOID® binder. While the improvement from the EPIKOTE® Resin 05390 binder is only 69.1 %. The flexural modulus, which shows an average improvement of about 6 % in case of both binders, can be considered as unaffected with the presence of preforming binder due to the deviations.

The better performance of PARALOID® EXL2314 binder in the manufacturing of textile reinforced pCBT composite with simultaneous binding and toughening concept may be attributed to its well defined rubber particle size which is not significantly influenced during binder activation and resin infiltration process. Together with its reactive functionality in the shell, the binder particles in the inter-ply region could have a good interaction with infiltrated resin and remain homogeneously

distributed during isothermal crystallization of pCBT polymers, leading to a good toughened inter-ply region of pCBT laminate.

A further investigation was performed to study the influence on the flexural properties of pCBT laminate from the filling content of PARALOID® EXL2314 binder. As illustrated in Table 6.2, the binder filling content indicates influences both on the toughening performance and the mechanical properties. The flexural strain shows a similar variation trend as illustrated in Table 5.4 when the binder filling content increases from 1 wt.% to 4 wt.%. While the mechanical properties indicate a different variation trend. The flexural strength decreases with increasing binder filling content. And the flexural modulus remain nearly unchanged when the deviations are taken into consideration.

It is interesting to see that a better toughening performance and mechanical properties than the laminate with 2 wt.% EPIKOTE® Resin 05390 binder can be achieved with only 1 wt.% PARALOID® EXL2314 binder. This is a further indication that the PARALOID® EXL2314 binder is better than EPIKOTE® Resin 05390 binder. The decrement of flexural strength with increasing PARALOID® EXL2314 binder may be ascribed to the infiltration conditions as a results of excessive binder in the inter-ply region as explained in subsection 5.2.3.

Table 6.1.: Effect of binder type on the flexural properties of textile reinforced pCBT composite

Preforming binders	filling content	Flexural modulus	Flexural strength	Flexural strain
Ex-situ	[wt.%]	[GPa]	[MPa]	[%]
NONE	0	26.5 ± 2.5	420.7 ± 21.1	1.59 ± 0.07
EPIKOTE® 05390	2	28.7 ± 0.9	711.6 ± 31.4	2.75 ± 0.15
PARALOID® 2314	2	28.1 ± 2.3	801.6 ± 25.9	3.34 ± 0.29
Constant process parameter				
→ Catalyst amount: 5 wt.%; Processing temperature: 185 °C				
→ Vacuum pressure: -800 mbar; Polymerization time: 90 min				

Table 6.2.: Effect of PARALOID® binder content on the flexural properties of textile reinforced pCBT composite

Toughening concept	Binder content	Flexural modulus	Flexural strength	Flexural strain
	[wt.%]	[GPa]	[MPa]	[%]
Ex-situ	1	31.0 ± 1.9	831.5 ± 59.2	3.18 ± 0.15
	2	28.0 ± 2.3	801.6 ± 25.9	3.34 ± 0.29
	3	31.1 ± 1.8	650.8 ± 48.4	2.67 ± 0.23
Constant process parameter				
→ Catalyst amount: 5 wt.%; Processing temperature: 185 °C				
→ Vacuum pressure: -800 mbar; Polymerization time: 90 min				

6.3.2. Further optimization trials

It is confirmed that both in-situ and ex-situ toughening can be effective in some respects. Specifically, in-situ toughening concept has the advantage of global toughening of the whole matrix system, accompanied by the shortcomings like the increase of resin viscosity and the decrease of mechanical properties. While the advantage of ex-situ toughening concept is the local toughening specially for the vulnerable inter-ply region, leading to an unchanged (sometimes improved) mechanical performance. Due to the local toughening nature of ex-situ toughening concept, the improvement of composite toughness is limited in this study (i.e. 72.9 % and 110.1 % in flexural strain with EPIKOTE® Resin 05390 binder and PARALOID® EXL2314 binder respectively). Therefore, it is necessary to find more possibilities for further improvement of the toughness of pCBT composite.

In a further attempt, a combination of in-situ toughening concept and ex-situ toughening concept was tried in order to achieve a tailored global toughening performance. Specifically, a small amount of binder used additionally as in-situ toughening agent which is directly mixed with CBT oligomers melt in order to toughen the pCBT matrix in the intraply region. The amount of binder as in-situ toughening agent should be as low as possible so that the flow properties of the matrix resin and the mechanical properties composite would not be negatively influenced.

The bindered textile preforms with 2 wt.% preforming binder was still applied for toughening of inter-ply region. Table 6.3 illustrates the results of the modified simultaneous binding and toughening concept. The two binders, EPIKOTE® Resin 05390 and PARALOID® EXL2314, were applied in the experiments with 0.5 and 1.0 wt.% of each binder as in-situ toughening agent.

The results indicate that the flexural modulus from the four modified variants remains nearly unchanged as before. However, different performance in flexural strength and flexural strain were observed for the two binders with modified concept. For the PARALOID® EXL2314 binder, both the flexural strength and flexural strain were found to decrease when the in-situ toughening part of binder increases from 0.5 wt.% to 1 wt.%. The flexural strength and flexural strain results from the two modified variants are 12 % and 16.7 % lower than the pure ex-situ toughening variant. For the EPIKOTE® Resin 05390 binder, an addition of 0.5 wt.% binder as in-situ toughening agent leads to nearly the same flexural strength and flexural strain in comparison with the pure ex-situ toughening variant. Further increase of in-situ toughening agent up to 1 wt.% results to a decrease of flexural strength and flexural strain as well.

The different performance of the two binder in the modified concept may be attributed to the difference of the two binders. The EPIKOTE® Resin 05390 is a low melting point epoxy resin which have a good compatibility with CBT oligomers at lower filling content so that the infiltration behavior is not significantly influenced. Therefore, a filling content of 0.5 wt.% with in-situ concept gives almost the same results as the pure ex-situ toughening variant. The PARALOID® EXL2314 binder is a rubber powder with well defined particle size which remains unchanged during in-situ mixing with CBT oligomer melt according to the product description. As a result, only a little amount as low as 0.5 wt.% can already increase the viscosity of the mixture, leading to a poor impregnation quality.

Table 6.3.: Effect of simultaneous binding and toughening concept variants on the flexural properties of textile reinforced pCBT composite

Preforming binders	Toughening concepts	Flexural modulus [GPa]	Flexural strength [MPa]	Flexural strain [%]
NONE	—	26.5 ± 2.5	420.7 ± 21.1	1.59 ± 0.07
PARALOID [®] 2314	Ex-situ	28.1 ± 2.3	801.6 ± 25.9	3.34 ± 0.29
	CombI*	31.2 ± 1.3	705.4 ± 55.1	2.78 ± 0.27
	CombII**	32.7 ± 1.7	689.5 ± 68.1	2.39 ± 0.22
EPIKOTE [®] 05390	Ex-situ	28.7 ± 0.9	711.6 ± 31.4	2.75 ± 0.15
	CombI	30.8 ± 1.5	715.8 ± 11.7	2.77 ± 0.26
	CombII	30.9 ± 3.6	657.0 ± 59.9	2.28 ± 0.21

*CombI: Ex-situ 2 wt.% plus In-situ 0.5 wt.%
**CombII: Ex-situ 2 wt.% plus In-situ 1 wt.%
Constant process parameter
→ Catalyst amount: 5 wt.%; Processing temperature: 185 °C
→ Vacuum pressure: -800 mbar; Polymerization time: 90 min

Summary

Three kinds of preforming binders were first compared under mode I deformation regarding to their influence on the mode I fracture toughness. From all the selected binders, the acrylic modifier based binder PARALOID EXL[®] 2314 shows the best performance in terms of the homogeneity of the pCBT laminate and the magnitude of the final fracture toughness. The potential of simultaneous binding and toughening was limited to as binding for improving process efficiency at higher processing temperature (e.g. 205 °C) due to the fact that the mode I fracture toughness was not significantly altered compared to the reference laminate. However, further investigations with PARALOID EXL[®] 2314 binder under mode II deformation completely demonstrate the advantage of simultaneous binding and ex-situ toughening. The mode II fracture toughness is improved by 124.4 % - 151.6 % compared to the reference laminate without binder. Moreover, in both of the two deformation modes, the simultaneous binding and ex-situ toughening concept ex-

hibits better results than its in-situ toughening counterpart. Finally, the effectiveness of the proposed concept was further verified by the optimized PARALOID EXL[®] 2314 binder with significantly improved flexural properties. The flexural strain of the composites laminate is greatly improved without impairing the flexural strength and modulus, indicating a great toughening potential by using preforming binder. Further studies on the modification of the proposed concept indicate that the combination of the in-situ toughening and the proposed concept leads to comparable results to the proposed concept alone as long as the amount of the in-situ toughening agent is very low, meaning that further improvement of the toughening performance of the proposed concept is still possible. **To summarize, the toughening of textile reinforced pCBT composites has been successfully achieved with simultaneously improved process efficiency by introducing simultaneous binding and toughening concept.**

Chapter 7

Conclusions and future work

7.1. Conclusions

A new concept consisting of binding and toughening simultaneously has been proposed for an efficient and qualified manufacturing of textile reinforced pCBT composites. Specifically, textile preforms with preforming binder are prepared first for enhanced handling stability and improved process efficiency. After impregnation of the bindered textile preforms with catalyzed CBT oligomers, toughening of pCBT at the inter-laminar region is achieved simultaneously as a result of the presence of preforming binder. In the present dissertation, research efforts have been put into the following three aspects: (1) Material characterization focusing on the effect of preforming binder on the material behavior of textile preforms and catalyzed CBT oligomers; (2) Process development including T-VARI manufacturing process and parametric analysis of the processing conditions; and (3) Process optimization in terms of the performance of various preforming binders and the manufacturing concept.

For the material characterizations: The influence of an epoxy resin based preforming binder on the compaction behavior of the bindered textile preforms and the thermal and rheological properties of the catalyzed CBT oligomers were studied. The effect of compaction and preforming parameters on the Fiber Volume Fraction

(FVF) and the Residual Preform Thickness (RPT) of bindered textile preforms during a compaction experiment was investigated by using Taguchi method. Thermal and rheological investigations were conducted respectively with Differential Scanning Calorimetry (DSC) and plate-plate rheometry.

The results reveals that the compaction behavior of bindered textile preforms has been significantly influenced due to the presence of binder. Instead of the commonly applied three parameter model that correlates the fiber volume content and the compaction pressure during compaction of textile preforms under 0.1 MPa, a modified four parameter model, which can extend the modeling range up to 0.9 MPa, has been proposed in this study. The fitted results have shown that the proposed modified four parameter model can make more accurate prediction of compaction and release response of the bindered textile preforms. In addition, the compaction temperature was found to be the most influential process parameter that can significantly affect the compaction behavior of bindered textile preforms.

The results from the thermal and rheological investigation illustrate that the presence of preforming binder has no distinct influence on the melting of catalyzed CBT oligomers. The crystallization of pCBT polymer during cooling, however, is confirmed to be significantly influenced by addition of preforming binder. The crystallization temperature and the crystallinity of pCBT polymer are both found to decrease with increased filling fraction of preforming binder. The addition of preforming binder can influence the isothermal polymerization and crystallization process in terms of the starting time of crystallization, the crystallization rate and the crystal structures. The starting time of crystallization is found to be shifted to an earlier time due to the filling of preforming binder. The crystallization rate increases first with increasing preforming binder amount, which is then followed by a decreasing trend with further increased preforming binder. The processing time of the catalyzed oligomers during isothermal polymerization can be prolonged due to the presence of preforming binder.

For the process development: Thermoplastic Vacuum Assisted Resin Infusion (T-VARI) manufacturing process was developed and evaluated by characterizing the thermal and mechanical properties of the manufactured textile reinforced pCBT

composites. The proposed concept was achieved successfully with the developed T-VARI manufacturing process using bindered textile preforms. The influencing mechanism of the process parameters on the flexural properties of the textile reinforced pCBT composites were investigated using parametric analysis for further optimization intention on the T-VARI manufacturing process.

The results indicate that A Thermoplastic Vacuum Assisted Resin Infusion (T-VARI) manufacturing process was successfully developed to achieve the proposed concept with bindered textile preforms. The manufactured textile reinforced pCBT composites show a significantly increased toughness without impairing other mechanical properties such as flexural modulus and flexural strength. Single factor analysis was conducted taking the influencing mechanism of the key process parameters including the catalyst amount, binder filling fraction, processing temperature, and vacuum pressure into consideration. The results illustrate that the toughening performance and the mechanical properties both depend significantly on the investigated process parameters when the textile reinforced pCBT composites is prepared with the proposed concept. With other process parameters being held constant, each parameter indicates an optimum value that leads to the best flexural performance. It is initially confirmed to be capable of manufacturing textile reinforced pCBT composite with increased material toughness.

For the process optimization: Three kinds of preforming binders were evaluated concerning on their influence on the interlaminar fracture properties of textile reinforced pCBT composites. Inter-laminar fracture toughness of the specimens was investigated under mode I and mode II deformation. A standard double cantilever beam (DCB) test and an end notched flexure (ENF) test based on a three-point bending test were applied to evaluate the mode I and mode II inter-laminar fracture toughness were evaluated by a standard double cantilever beam (DCB) test and an end notched flexure (ENF) test based on a three-point bending test, respectively. The effect of binder type, filling content and preparation concept on fracture properties under the mentioned two deformation modes were discussed on the basis of morphology analysis of fracture sections with scanning electric microscopy. Flexural properties of the textile reinforced pCBT laminate prepared using the optimized preforming binder were characterized for further verification of the performance of

the proposed concept. A variant of the proposed concept was pointed out and tested for further optimization of the manufacturing process.

The results illustrate that the acrylic modifier based binder PARALOID EXL[®] 2314 shows the best performance in terms of the homogeneity of the pCBT laminate and the magnitude of the final fracture toughness. The potential of simultaneous binding and toughening was limited to as binding for improving process efficiency at higher processing temperature (e.g. 205 °C) due to the fact that the mode I fracture toughness was not significantly altered compared to the reference laminate. However, further investigations with PARALOID EXL[®] 2314 binder under mode II deformation completely demonstrate the advantage of simultaneous binding and ex-situ toughening. The mode II fracture toughness is improved by 124.4 % - 151.6 % compared to the reference laminate without binder. Moreover, in both of the two deformation modes, the simultaneous binding and ex-situ toughening concept exhibits better results than its in-situ toughening counterpart. Finally, the effectiveness of the proposed concept was further verified by the optimized PARALOID EXL[®] 2314 binder with significantly improved flexural properties. The flexural strain of the composites laminate is greatly improved without impairing the flexural strength and modulus, indicating a great toughening potential by using preforming binder. Further studies on the modification of the proposed concept indicate that the combination of the in-situ toughening and the proposed concept leads to comparable results to the proposed concept alone as long as the amount of the in-situ toughening agent is very low, meaning that further improvement of the toughening performance of the proposed concept is still possible.

In conclusion, the toughening of textile reinforced pCBT composites has been successfully achieved with simultaneously improved process efficiency by introducing simultaneous binding and toughening concept.

7.2. Future works

It has been demonstrated that the proposed simultaneous binding and toughening concept can realize an efficient and qualified manufacturing of textile reinforced pCBT composites. For serial production of high performance textile reinforced pCBT composites applications such as Organo Sheet, composite panels and curved structures etc., however, there are still several issues to be addressed in the future as shown in Figure 7.1. The details of those issues are discussed in the following sections.

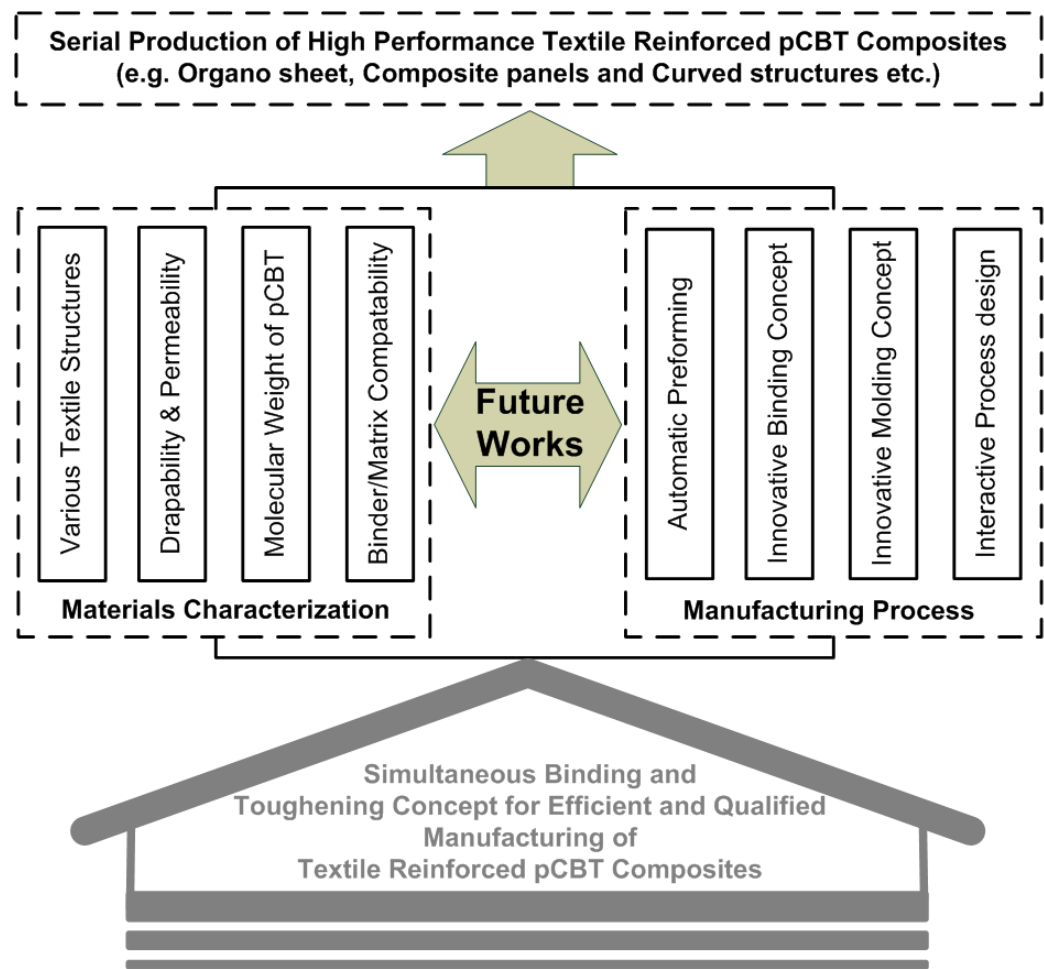


Figure 7.1.: Future works for serial production of high performance textile reinforced pCBT composites

Materials characterization

For material properties of textile preforms, the characterization and modeling of compaction behavior of binder textile preform in this research are limited for a tri-axial glass fiber Non Crimp Fabrics. It is necessary to extend this study for various kinds of textile reinforcements so that **the influence mechanisms depending on the textile structures** can be understood and the applicability of the developed compaction model can be determined. In addition, **the influences from preforming binder on the drapability and permeability** should also be investigated for a better process design with bindered textile preforms.

For the characterization of CBT resin matrix system, the development of new preforming binders should be considered. As illustrated in section 6.3.2, the combination of in-situ toughening with the ex-situ toughening concept included in the proposed simultaneous binding and toughening has the possibility to achieve a tailored global toughening performance. For further investigation, it is essential that **the compatibility of CBT resin matrix and preforming binder should be investigated in order to find an appropriate preforming binder with both good compatibility with CBT resin matrix and good toughening capability**. Moreover, the effect preforming binder on the polymerization of CBT oligomers, especially **the molecular weight should be studied for a better understanding of the influence mechanism**.

Manufacturing process

The preparation of the bindered textile preforms in this research involving a lot of hand work such as cutting textiles and applying binder. Especially for the binder application, huge deviations could be encountered in the aspect of the applied amount and homogeneity if not properly handled. Thus, **an automatic preforming setup with a certain degree of automation is recommended for future researches**. For serial production applications, the Preforming Center developed by ITA RWTH [33] can be considered for a highly automated manufacturing of bindered textile preforms.

In addition, besides the further endeavors on developing appropriate preforming binders, the effect of various binding type should be considered as well. An area binding, where the preforming binder was applied the whole area of inter-ply region, was mainly used in this research. Advantage of this kinds of binding including good stability of the preforms and fully toughened inter-ply region. However, due to the complexity of various composite structures, the area binding may limit the drapability of the bindered textile preforms. Therefore, **innovative binding type such as point or linear binding should be considered as well for manufacturing of curved structures.**

For the developed T-VARI manufacturing process, **further improvements can be achieved with innovative molding concept such as the various reusable vacuum bagging systems developed by Torr Technologies [1] and the on-line mixing equipment developed by Tartler GmbH [58].** With the reusable vacuum bagging system, the application of tacky tape could be eliminated as much as possible for further reduction of production cost and improvement of the process efficiency. Furthermore, the on-line mixing equipment can give a reproducible matrix formulation and achieve a continuous production process. For the process parameter for the simultaneous binding and toughening concept, the catalyst amount, processing temperature and polymerization time indicates a strong interaction among each other according to the analysis in section 5.2. Therefore, **an interactive experiment design with Taguchi method should be considered for a more effective process design.**

Appendix A

Curriculum Vitae

Personal Information

Family name:	Wu
Given name:	Wangqing
Date of Birth	August 21 st , 1983
Citizenship	P. R. China
Marital Status	Married, no children

Education

Oct. 2008 to July 2013	PhD Program Materials Engineering Institute of Polymer Materials and Plastics Engineering Clausthal-Zellerfeld, Germany
July 2013	Graduated as Doctor of Engineering (Dr.-Ing.)
Sep. 2005 - June, 2008	Master program Mechanical Manufacture and Automatic Engineering Central South University Changsha, P.R.China
June 2008	Graduated as Master of Science (M.Sc.)

Sep. 2001 - June 2005 **Bachelor program**
Mechanical and Electrical Engineering
 Central South University
 Changsha, P.R.China

June 2005 Graduated as **Bachelor of Science (B.Sc.)**

Profession

Dec. 2009 - May 2013 **Scientific Co-Worker**
Composite Materials Group
 Institute of Polymer Materials and Plastics Engineering
 Clausthal University of Technology
 Clausthal-Zellerfeld, Germany

Publications

1. **W. Wu**, F. Klunker, L. Xie, B. Jiang, G. Ziegmann. Simultaneous binding and ex situ toughening concept for textile reinforced pCBT composite: Influence of preforming binders on interlaminar fracture properties, In: *Composite Part A: Applied Science and Manufacturing* 53 (2013), S. 190-203
2. **W. Wu**, L. Xie, B. Jiang, G. Ziegmann. Simultaneous binding and toughening concept for textile reinforced pCBT composite: Manufacturing and flexural properties, In: *Composite Structures* 105 (2013), S. 279-287
3. **W. Wu**, L. Xie, B. Jiang, G. Ziegmann. Influence of textile preforming binder on the thermal and rheological properties of the catalyzed cyclic butylene terephthalate oligomers, In: *Composite Part B: Engineering* 55 (2013), S. 453-462
4. **W. Wu**, B. Jiang, L. Xie, F. Klunker et al.. Effect of Compaction and Preforming Parameters on the Compaction Behavior of Bindered Textile Preforms for Automated Composite Manufacturing, In: *Applied Composite Materials* (2013), doi: <http://dx.doi.org/10.1007/s10443-012-9308-1>

Bibliography

- [1] <http://www.torrtech.com/Pages/Systems.htm>
- [2] ABT, T ; SANCHEZ-SOTO, M ; LLARDUYA, AM de: Toughening of in situ polymerized cyclic butylene terephthalate by chain extension with a bifunctional epoxy resin. In: *Euro Polymer Journal* 48 (2012), S. 163–71
- [3] ABT, Tobias ; SANCHEZ-SOTO, Miguel ; ILLESCAS, Silvia: Toughening of in situ polymerized cyclic butylene terephthalate by addition of tetrahydrofuran. In: *Polymer International* 60 (2010), S. 549–556
- [4] ARAI, Masahiro ; NORO, Yukihiro ; SUGIMOTO, Koh ichi: Mode I and mode II interlaminar fracture toughenss of CFRP laminates toughened by carbon nanofiber interlayer. In: *Composite Science and Technology* 68 (2008), S. 516–525
- [5] ARANDA, S. ; KLUNKER, F. ; ZIEGMANN, G.: Compaction response of fiber reinforcements depending on processing temperature. In: *Proceedings of ICCM17 conference, 2009*
- [6] ARANDA, S. ; KLUNKER, F. ; ZIEGMANN, G.: Influence of the binding system in the compaction behavior of NCF carbon fiber reinforcement. In: *Proceedings of ICCM18 conference, 2011*

- [7] ASTM-D5528: *Standard Test Method for Mode I Interlaminar Fracture Toughness of Unidirectional Fibre-Reinforced Polymer Matrix Composites*. 1994
- [8] ASTM-D790: *Standard Test Methods for Flexural Properties of Unreinforced and Reinforced Plastics and Electrical Insulating Materials*. 2003
- [9] BAETS, J. ; DEVAUX, J. ; VERPOEST, I.: Toughening of basalt fiber-reinforced composites with a cyclic butylene terephthalate matrix by a non-isothermal production method. In: *Advances in Polymer Technology* 29 (2010), S. 70–79
- [10] BAETS, J. ; DUTOIT, M. ; DEVAUX, J.: Toughening of glass fiber reinforced composites with a cyclic butylene terephthalate matrix by addition of polycaprolactone. In: *Composites: Part A* 39 (2008), S. 13–18
- [11] BAETS, J. ; GODARA, A. ; DEVAUX, J.: Toughening of polymerized cyclic butylene terephthalate with carbon nanotubes for use in composites. In: *Composites: Part A* 39 (2008), S. 1756–1761
- [12] BAETS, J. ; GODARA, A. ; DEVAUX, J.: Toughening of isothermally polymerized cyclic butylene terephthalate for use in composite. In: *Polymer Degradation and Stability* 95 (2010), S. 346–352
- [13] BAETS, Joris: *Toughening of in-situ polymerized cyclic butylene terephthalate for use in continuous fiber reinforced thermoplastic composites*, Katholieke Universiteit Leuven, Diss., 2008
- [14] BAHLOUL, W. ; BOUNOR-LEGARE, V. ; FENOUILLOT, F.: EVA/PBT nanostructured blends synthesized by in situ polymerization of cyclic CBT (cyclic butylene terephthalate) in molten EVA. In: *Polymer* 50 (2009), S. 2527–2534
- [15] BARRINGTON, Normann ; BLACK, Malcolm ; IMAMURA, Tugio ; BARBAUX, Yann ; CANTOR, Brian (Hrsg.) ; ASSENDER, Hazel (Hrsg.) ; GRANK, Patrick (Hrsg.): *Aerospace Materials*. IOP Publishing Ltd, 2001

- [16] BARTCZAK, Z. ; ARGON, A.S. ; COHEN, R.E.: Toughness mechanism in semi-crystalline polymer blends: II. High-density polyethylene toughened with calcium carbonate filler particles. In: *Polymer* 40 (1999), S. 2347–2365
- [17] BARTCZAK, Z. ; ARGON, A.S. ; COHEN, R.E. ; WEINBERG, M.: Toughness mechanism in semi-crystalline polymer blends: I. High-density polyethylene toughened with rubbers. In: *Polymer* 40 (1998), S. 2331–2346
- [18] BESSELL, T.J. ; HULL, D. ; SHORTALL, J.B.: Effect on polymerization conditions and crystallinity on the mechanical properties and fracture of spherulitic nylon 6. In: *Journal of Materials Science* 10 (1975), S. 1127–9880
- [19] BICKERTON, S ; BUNTAIN, MJ ; SOMASHEKAR, AA: The viscoelastic compression behavior of liquid composite molding preforms. In: *Composite Part A: Applied Science and Manufacturing* 34 (2003), S. 431–444
- [20] BRUNELLE, DJ ; BRADT, JE ; SERTH-GUZZO, J ; TAKEKOSHI, T ; EVANS, RA ; PEARCE, EJ: Semicrystalline polymers via ring-opening polymerization: preparation and polymerization of alkylene phthalate cyclic oligomers. In: *Macromolecules* 31 (1998), S. 4782–90
- [21] BRUNELLE, D.J. ; BURNT, H.: *Method for polymerizing macrocyclic polyester oligomers*. 1996
- [22] BRUNELLE, DJ ; SERTH-GUZZO, J: Titanate-catalyzed ring-opening polymerization of cyclic phthalate ester oligomers. In: *Polym Preprints, Am Chem Soc, Div Polym Chem* 40 (1999), S. 566–7
- [23] BRUNELLE, et a.: *Titanate esters useful as polymerization initiators for macrocyclic polyester oligomers*. 1997
- [24] BUCKNALL, CB ; GILBERT, AH: Toughening of tetrafunctional epoxy resins using polyetherimide. In: *Polymer* 30 (1989), S. 213
- [25] CHENG, Qunfeng ; FANG, Zhengping ; YI, Xiao-Su: "Ex Situ" concept for toughening the RTMable BMI Matrix Composites, Part I: Improving the

- Interlaminar fracture toughness. In: *Journal of Applied Polymer Science* 109 (2008), S. 1625–1634
- [26] CHIU, HJ ; SHU, WH ; HUANG, JM: Crystallization kinetics of poly(trimethylene terephthalate)/poly(ether imide) blends. In: *Polymer Engineering and Science* 46 (2006), S. 89–96
- [27] CYCLIC-CORPORATION: *CBT® Composites Processing Guide*
- [28] DEKKER, Marcel ; ARENDS, C.B. (Hrsg.): *Polymer toughening*. CRC Press, 1996
- [29] DICKERT, M. ; BERG, D.C. ; ZIEGMANN, G.: Influence of binder activation and fabric design on the permeability of non-crimp carbon fabrics. In: *FPCM Auckland*, 2012
- [30] DOYLE, Nathan ; DEANS, Fred: Advances in thermoplastic composites using CBT / Cyclics Corp. and Allied Composite Technologies, LLC. 2009. – Forschungsbericht
- [31] EDER, R. ; WINCHLER, S.: Processing of advanced thermoplastic composites using cyclic thermoplastic polyester. In: *International SAMPE Europe Conference Proceedings*, 2001
- [32] GEORGE, Andrew: *Optimization of Resin Infusion Processing for Composite Materials: Simulation and Characterization Strategies*, University of Stuttgart, Diss., 2011
- [33] GREB, C. ; SCHNABEL, A. ; LINKE, M.: Neuartige Technologie und Prozessketten für die Großserienfertigung textiler Preforms. In: *17. SAMPE Deutschland e.V.: Faserverbundwerkstoffe, Hochleistung und Großserie*, 2011
- [34] HAKME, C ; STEVENSON, I ; MAAZOUZ, A ; CASSAGNAU, P ; BOITEUX, G ; SEYTRE, G: In situ monitoring of cyclic butylene terephthalate polymerization by dielectric sensing. In: *Journal of Non- Crystalline Solids* 353 (2007), S. 4362–65

- [35] HARNISCH, K ; MUSCHIK, H: Determination of the Avrami exponent of partially crystallized polymers by DSC-(DTA-) analysis. In: *Colloid & Polymer Science* 261 (1983), S. 908–13
- [36] HARTNESS, Timothy: Thermoplastic Powder Technology for Advanced Composites Systems. In: *Journal of Thermoplastic Composite Materials* 1 (1988), S. 210–220
- [37] HAY, JN: Application of the modified avrami equations to polymer crystallisation kinetics. In: *British Polymer Journal* 3 (1971), S. 74–82
- [38] HENNING, K. ; GRIES, T. ; FLACHSKAMPF, P.: Wirtschaftliche Herstellung von Faserverbundbauteilen mit Hilfe automatisiert hergestellter textiler Pre-forms / Lehrstuhls Informatik im Maschinenbau. 2008. – Forschungsbericht
- [39] HODGE, P ; COLQUHOUN, HM ; WILLIAMS, DJ: From macrocycles to macromolecules - and back. In: *Chem Ind* (1998), S. 162–7
- [40] ISHAK, Z.A. M. ; LEONG, Y.W. ; STEEG, M.: Mechanical properties of woven glass fabric reinforced in situ polymerized poly(butylene terephthalate) composites. In: *Composite Science and Technology* 67 (2007), S. 390–398
- [41] ISHAK, Z.A. M. ; SHANG, PP ; KARGER-KOCSIS, J: A modulated DSC study on the in situ polymerization of cyclic butylene terephthalate oligomers. In: *J Therm Anal Cal* 84 (2006), S. 637–41
- [42] JENKINS, MJ ; CAO, Y ; KUKUREKA, SN: The effect of molecular weight on the crystallization kinetics and equilibrium melting temperature of poly(tetramethylene ether glycol). In: *Polymers for Advanced Technologies* 17 (2006), S. 1–5
- [43] KARGER-KOCSIS, J. ; SHANG, P.P. ; ISHAK, Z.A. M.: Melting and crystallization of in-situ polymerized cyclic butylene terephthalate with and without organoclay: a modulated DSC study. In: *Polymer Letters* 1 (2007), S. 60–68
- [44] KELLY, PA ; UMER, R ; BICKERTON, S: Viscoelastic response of dry and wet fibrous materials during infusion processes. In: *Composite Part A: Applied Science and Manufacturing* 37 (2006), S. 868–873

- [45] KLUNKER, F. ; ARANDA, S ; ZIEGMANN, G.: Permeability and compaction models for non crimped fabrics to perform 3D filling simulations of vacuum assisted resin infusion. In: *The 9th International Conference on Flow Processes in Composite Materials*, 2008
- [46] LEHMANN, B ; KARGER-KOCSIS, J: Isothermal and non-isothermal crystallization kinetics of pCBT and PBT. In: *Journal of Thermal Analysis and Calorimetry* 95 (2009), S. 221–227
- [47] LI, Hongyun: An innovative technology for toughening carbon fiber reinforced composite / Beijing Institute of Aeronautical Materials. 2009. – Forschungsbericht
- [48] LIN, TR: Optimisation technique for face milling stainless steel with multiple performance characteristics. In: *Int J Adv Manuf Technol* 19 (2002), S. 330–335
- [49] LUO, Y. ; VERPOEST, I.: Compressibility and relaxation of a new sandwich textile preform for liquid composite molding. In: *Polymer Composites* 20 (1999), S. 179–191
- [50] MADHUKAR, MS ; DRZAL, LT: Fiber-matrix adhesion and its effect on composite mechanical properties: I. Inplane and interlaminar shear behavior of graphite/epoxy composites. In: *Journal of Composite Materials* 25 (1991), S. 932–957
- [51] MADHUKAR, MS ; DRZAL, LT: Fiber-matrix adhesion and its effect on composite mechanical properties: II. Longitudinal (0°) and Transverse (90°) tensile and flexure properties of graphite/epoxy composites. In: *Journal of Composite Materials* 25 (1991), S. 958–991
- [52] MADHUKAR, MS ; DRZAL, LT: Fiber-matrix adhesion and its effect on composite mechanical properties: IV. Mode I and Mode II fracture toughness of graphite/epoxy composites. In: *Journal of Composite Materials* 26 (1992), S. 936

- [53] MAIRTIN, PO ; McDONELL, P ; CONNOR, MT ; EDER, R ; BRADAIGH, CMO: Process investigation of a liquid PA-12/Carbon fiber moulding system. In: *Composite Part A: Applied Science and Manufacturing* 32 (2001), S. 915–923
- [54] McGRAIL, CB ; SEFTON, MS ; ALMEN, GR ; WILKINSON, SP: *Polymer composition*. 1989
- [55] MICHAELI, W. ; KOSCHMIEDER, M. ; KELLY, Anthony (Hrsg.) ; ZWEBEN, Carl (Hrsg.): *Comprehensive composite materials*. Pergamon Pr, 2000
- [56] MICHAUD, V. ; ZINGRAFF, L. ; VERREY, J. ; BOURBAN, P-E. ; MANSON, J-AE.: Resin transfer molding of anionically polymerized polyamide 12. In: *Proceedings of 7th international conference on flow processes in composite materials (FPCM-7)*, 2003
- [57] MILLER, S: *Macrocyclic polymer from cyclic oligomers of polybutylene terephthalate*, University of Massachusetts, Diss., 1998
- [58] MITSCHANG, P.: Prozessvariable Entwicklung von Faser-Kunststoff-VeFaser auf PBT-Basis / IVW-Schriftenreihe Band 91. 2010. – Forschungsbericht
- [59] MURAKAMI, K. ; ONO, K. ; BOHDANECKY, M. ; KOVAR, J. ; WYPYCH, J. ; MARTUSCELLI, E. (Hrsg.) ; MUSTO, P. (Hrsg.) ; RAGOSTA, G. (Hrsg.): *Advances routes for polymer toughening*. Elsevier, 1996
- [60] NAFFAKH, M. ; DUMON, M. ; GERARD, J.F.: Study of reactive epoxy-amine resin enabling in situ dissolution of thermoplastic films during resin transfer moulding for toughening composite. In: *Composite Science and Technology* 66 (2006), S. 1376–1384
- [61] NALBANT, M ; GOKKAYA, H ; SUR, G: Application of Taguchi method in the optimization of cutting parameters for surface roughness in turning. In: *Mater. Des.* 28 (2007), S. 1379–1385

- [62] OUAGNE, P. ; BIZET, L. ; BALEY, C. ; BREARD, J.: Analysis of the film stacking processing parameters for PLLA/flax fiber biocomposites. In: *Journal of Composite Materials* 44(10) (2010), S. 1201–1215
- [63] PARTON, H ; BAETS, J ; LIPNIK, P ; DEVAUS, J ; VERPOEST, I: Liquid moulding of textile reinforced thermoplastics. In: *Proceedings of 11th European conference on composite materials (ECCM-11)*. Rhodos Greece, 2004
- [64] PARTON, Hilde: Characterization of the in-situ polymerisation production process for continuous fiber reinforced thermoplastics / Department of Metallurgy and Materials Engineering, Katholieke Universiteit Leuven. 2006. – Forschungsbericht
- [65] PARTON, Hilde ; BAETS, Joris ; LIPNIK, Pascale: Properties of poly(butylene terephthalate) polymerized from cyclic oligomers and its composites. In: *Polymer* 46 (2005), S. 9871–9880
- [66] PARTON, Hilde ; VERPOEST, Ignaas: In situ polymerization of thermoplastic composites based on cyclic oligomers. In: *Polymer Composites* 26 (2005), S. 60–65
- [67] PEARSON, RA ; YEE, AF: Toughening mechanisms in elastomer-modified epoxies. In: *Journal of Materials Science* 24 (1989), S. 2571–2580
- [68] PELTONEN, P. ; LAHTENKORVE, K. ; PAAKKONEN, E.J. ; JARVELA, P.K. ; TORMALA, P.: The influence of melt impregnation parameters on the degree of impregnation of a polypropylene/glass fiber prepreg. In: *Journal of thermoplastic composite materials* 5(4) (1992), S. 313–343
- [69] PILLAY, Selvam ; VAIDYA, Uday K. ; JANOWSKI, Gregg M.: Liquid Molding of carbon fabric-reinforced nylon matrix composites laminates. In: *Journal of Thermoplastic Composite Materials* 18 (2005), S. 509–527
- [70] PUNGOR, Erno ; HORVAL, G: *A Practical Guide to Instrumental Analysis*. CRC Press, 1994. – 181–191 S.
- [71] QI, Y ; CHEN, T ; XU, J: Synthesis of cyclic precursor of poly(ether ether ketone). In: *Polym Bull* 42 (1999), S. 245–9

- [72] RIGHETTI, MC ; LORENZO, ML: Melting process of poly(butylene terephthalate) analyzed by temperature-modulated differential scanning calorimetry. In: *Journal of Polymer Science Part B: Polymer Physics* 42 (2004), S. 2191–201
- [73] RIJSWIJK, K. van: *Vacuum infusion technology for anionic polyamide-6 composites*, Delft University of Technology, Diss., 2007
- [74] RIJSWIJK, K. van ; BERSEE, H. E. ; JAGER, W.F.: Optimisation of anionic polyamide-6 for vacuum infusion of thermoplastic composites. In: *Composites: Part A* 37 (2006), S. 949–956
- [75] RIJSWIJK, K. van ; BERSEE, H.E.N.: Reactive processing of textile fiber-reinforced thermoplastic composites - An overview. In: *Composites: Part A* 38 (2007), S. 666–681
- [76] RIJSWIJK, K. van ; BERSEE, H.E.N. ; BEUKERS, A.: Optimisation of anionic polyamide-6 for vacuum infusion of thermoplastic composites: Influence of polymerisation temperature on matrix properties. In: *Polymer Testing* 25 (2006), S. 392–404
- [77] RIJSWIJK, K. van ; GEENEN, A.A. van ; BERSEE, H.E.N.: Textile fiber reinforced anionic polyamide-6 composites: Part II: Investigation on interfacial bond formation by short beam shear test. In: *Composites: Part A* 40 (2009), S. 1033–1043
- [78] RIJSWIJK, K. van ; TEUWEN, J.J.E. ; BERSEE, H.E.N.: The interface of reactive- and melt processed polyamide-6 composites. In: *ICCM 16 16th International Conference on Composite Materials*, 2007
- [79] RIJSWIJK, K. van ; TEUWEN, J.J.E. ; BERSEE, H.E.N.: Textile fiber-reinforced anionic polyamide-6 composites. Part I: The vacuum infusion process. In: *Composites: Part A* 40 (2009), S. 1–10
- [80] ROBITAILLE, F. ; GAUVIN, R.: Compaction of textile reinforcements for composite manufacturing. I. Review of experimental results. In: *Polymer Composites* 19 (1998), S. 198–216

- [81] ROBITAILLE, F. ; GAUVIN, R.: Compaction of textile reinforcements for composites manufacturing. II. Compaction and relaxation of dry and H₂O-saturated woven reinforcements. In: *Polymer Composites* 19 (1998), S. 553–557
- [82] ROBITAILLE, F. ; GAUVIN, R.: Compaction of textile reinforcements for composites manufacturing. III. Reorganization of fiber network. In: *Polymer Composites* 20 (1999), S. 48–61
- [83] ROSS, PJ ; MCGRAW-HILL (Hrsg.): *Taguchi technique for quality engineering*. 1998
- [84] ROSSO, Patrick ; FRIEDLICH, Klaus ; WOLLNY, Andreas: A novel polyamide 12 polymerization system and its use for a LCM-process to produce CFRP. In: *Journal of Thermoplastic Composite Materials* 18 (2005), S. 77–90
- [85] ROY, RK ; REINHOLD, Van N. (Hrsg.): *A primer on Taguchi method*. 1990
- [86] RUDD, C. D. ; LONG, A.C. (Hrsg.) ; KENDALL, K. N. (Hrsg.) ; MANGIN, C. (Hrsg.): *Liquid moulding technologies: resin transfer moulding, structural reaction injection moulding and related processing techniques*. Woodhead Publishing, 1997
- [87] SAMSUDIN, Sani A.: *The thermal behavior and isothermal crystallization of cyclic poly(butylene terephthalate) and its blends*, University of Birmingham, Diss., 2010
- [88] SHAHZAD, Muhammad A. ; STEEG, Markus ; MITSCHANG, Peter: Development and characterization of glass fiber reinforced in-situ polymerized thermoplastic matrix composite material. In: *SAMPE 2010 Seattle*, 2010
- [89] SHAJI, S ; RADHAKRISHNAN, V: Analysis of process parameters in surface grinding with graphite as lubricant based on the Taguchi method. In: *J. Mater. Process. Technol.* 141 (2003), S. 51–59
- [90] STEEG, M: *Prozesstechnologie für Cyclic Butylene Terephthalate im Faser-Kunststoff-Verbund*, TU Kaiserslautern, Diss., 2009

- [91] STEEG, M. ; MITSCHANG, P. ; CHAKRABORTY, P.: Modeling the viscosity and conversion of in-situ polymerizing PBT using empirical data. In: *ICCM-17 17th International Conference on Composites Materials*, 2009
- [92] STEENKAMER, DA ; SULLIVAN, JL: On the recyclability of a cyclic thermoplastic composite material. In: *Composite Part B: Engineering* 29B (1998), S. 745–52
- [93] TAGUCHI, G: *Introduction to Quality Engineering: Designing Quality into Products and Processes*. Asian Productivity Organization, 1990
- [94] TAKEKOSHI, T. ; PEARCE, E.J.: *Titanate esters useful as polymerization initiators for macrocyclic polyester oligomers*. 1995
- [95] TALBOTT, Margaret F. ; SPRINGER, George S. ; BERGLUND, Lars A.: The effects of crystallinity on the mechanical properties of PEEK polymer and graphite fiber reinforced PEEK. In: *Journal of Composite Materials* 21 (1987), S. 1056–1081
- [96] TANOGLU, M ; SEYHAN, AT: Investigating the effects of polyester pre-forming binder on the mechanical and ballistic performance of E-glass fiber reinforced polyester composites. In: *International Journal of Adhesion and Adhesives* 23 (2003), S. 1–8
- [97] TEUWEN, Julie J. ; RIJSWIJK, K. van ; JONCAS, Simon: Vacuum infusion thermoplastic composite for wind turbine blades / Delf University of Technology. 2008. – Forschungsbericht
- [98] TEUWEN, Julie J. ; RIJSWIJK, Kjelt van ; BERSEE, Harald E.: Effect of fiber textile reinforcement on anionic polyamide-6 composites properties. In: *ICCM 16 16th International Conference on Composite Materials*, 2007
- [99] TRIPATHY, A. R. ; CHEN, W. ; KUKURAKA, S. N.: Novel poly(butylene terephthalate)/poly(vinyl butyral) blends prepared by in situ polymerization of cyclic poly(butylene terephthalate) oligomers. In: *Polymer* 44 (2003), S. 1835–1842

- [100] TRIPATHY, Amiya R. ; ELMOUMNI, Aadil ; WINTER, H. H.: Effects of catalyst and polymerization temperature on the in-situ polymerization of cyclic poly(butylene terephthalate) oligomers for composite applications. In: *Macromolecules* 38 (2005), S. 709–715
- [101] TRIPATHY, Amiya R. ; MACKNIGHT, William J. ; KUKURAKA, Stephen N.: In-Situ copolymerization of cyclic poly(butylene terephthalate) oligomers and ε-caprolactone. In: *Macromolecules* 37 (2004), S. 6793–6800
- [102] VAIDYA, U.K. ; CHAWLA, K.K.: Processing of fibre reinforced thermoplastic composites. In: *International Materials Reviews* 53 (2008), S. 185–218
- [103] VERPOEST, Ignaas: Thermoplastic composites: challenges for an even brighter future / Department of Metallurgy and Materials Engineering, Katholieke Universiteit Leuven. 2008. – Forschungsbericht
- [104] VERREY, J. ; MICHAUD, V ; MANSON, J-AE.: Capillary effects in liquid composite moulding with non-crimp fabric. In: *Proceedings of 14th international conference on composite materials (ICCM-14)*, 2003
- [105] WANG, Y-F ; HAY, AS: Macrocyclic arylene ether ether sulfide oligomers: new intermediates for the synthesis of high-performance poly(arylene ether ether sulfide)s. In: *Macromolecules* 30 (1997), S. 182–197
- [106] WEI, LONG ; YA-HONG, XU ; XIAO-SU, YI: Preliminary study on resin transfer molding of highly-toughened graphite laminates by ex-situ method. In: *Journal of Materials Science* 39 (2004), S. 2263–2266
- [107] WEST, B.P. van ; PIPES, R. B. ; ADVANI, S.G.: The consolidation of commingled thermoplastic fabrics. In: *Polymer Composites* 12(6) (1991), S. 417–427
- [108] WU, Chang-Mou ; JIANG, Chi-Wea: Crystallization and Morphology of polymerized cyclic butylene terephthalate. In: *Journal of Polymer Science Part B: Polymer Physics* 48 (2010), S. 1127–1134

- [109] WU, G.M. ; SCHULTZ, J.M.: Processing and properties of solution impregnated carbon fiber reinforced polyethersulfone composites. In: *Polymer Composites* 21(2) (2000), S. 223–230
- [110] WU, W. ; JIANG, B. ; XIE, L. ; KLUNKER, F. ; ARANDA, S. ; ZIEGMANN, G.: Effect of Compaction and Preforming Parameters on the Compaction Behavior of Binded Textile Preforms for Automated Composite Manufacturing. In: *Applied Composite Materials* DOI: 10.1007/s10443-012-9308-1 (2013)
- [111] XIE, F. ; ZHOU, C. ; YU, W.: Study on the reaction kinetics between PBT and epoxy by a novel rheological method. In: *European Polymer Journal* 41 (2005), S. 2171–2175
- [112] YANG, J. ; XIAO, J. ; ZENG, J. ; JIANG, D. ; PENG, C.: Compaction behavior and part thickness variation in vacuum infusion molding process. In: *Applied Composite Materials* DOI 10.1007/s10443-011-9217-8 (2011)
- [113] YANG, WH ; TARNG, YS: Design optimization of cutting parameters for turning operations based on the Taguchi method. In: *J. Mater. Process. Technol* 84 (1998), S. 122–129
- [114] YI, Xiao-Su ; AN, Xuefeng: Development of high-performance composites by innovation ex situ concept for aerospace application. In: *Journal of Thermoplastic Composite Materials* 22 (2009), S. 29–49
- [115] YOKOUCHI, Mitsuru ; SAKAKIBARA, Yoshio ; CHATANI, Yozo: Structures of two crystalline forms of poly(butylene terephthalate) and reversible transition between them by mechanical deformation. In: *Macromolecules* 9 (1976), S. 266–273
- [116] ZHANG, JL: Study of poly(trimethylene terephthalate) as an engineering thermoplastics materials. In: *Journal of Applied Polymer Science* 91 (2004), S. 1657–1666

